SEPARATION OF TRIVALENT ACTINIDES AND LANTHANIDES WITH SULFUR DONOR LIGANDS AND EXTRACTANTS

by

Nathan Patrick Bessen

A thesis submitted to the Faculty and the Board of Trustees of the Colorado School of Mines in partial fulfillment of the requirements for the degree of Doctor of Philosophy (Chemistry).

Golden, Colorado

Date:_____

Signed:_____

Nathan Bessen

Signed:_____

Dr. Jenifer C. Shafer

Golden, Colorado

Date:_____

Signed:_____

Dr. Thomas Gennett

Professor and Head

Department of Chemistry

ABSTRACT

The separation of trivalent actinides and lanthanides in the processing of used nuclear fuel is challenging due to the similar sizes, charges, and redox properties of the two classes of metals. Typical separations procedures rely on ligands or extractants that can coordinate the metals with polarizable soft donor atoms such as nitrogen or sulfur. These soft donor atoms display a preference for coordinating the actinides which can be utilized to provide selectivity in this separation. Among the different ligands and extractants used for this separation, the sulfur containing dithiophosphinic acids have shown some of the highest reported selectivities, with separation factors of up to 100,000 for the separation of americium and europium. However, the extraction mechanism for the dithiophosphinic acids are not fully defined, especially for the transcurium actinides. The most commonly studied dithiophosphinic acid, bis(2,4,4-trimethylpentyl)dithiophosphinic acid (HC301), is known to extract metals as several different complexes dependent upon both the extracted metal and the conditions used. A more complete understanding this behavior will promote the optimization of HC301-based separation procedures and possibly the development of extractants with even greater selectivity. Additionally, HC301 is susceptible to degradation by radiolysis, oxidation, and hydrolysis which both reduces the amount of HC301 in the system and forms new species that can impact the separation.

In this work, the current knowledge in the use of sulfur donating extractants, including the dithiophosphinic acids and HC301, for the separation of lanthanides and actinides is summarized and two new developments in the use of HC301 are reported. The first development is a novel method to quickly determine concentrations of HC301 by a colorimetric permanganometric titration to enable more effective monitoring of a potential separation process. The second project is a characterization of the extraction of the transplutonium actinides, Am-Es, by HC301 to determine how extensively these metals are extracted and what complexes are extracted. Additionally, the use of more degradation resistant and water-soluble sulfur donating ligands as an alternative to dithiophosphinic acids is examined. Overall, both HC301 and the aqueous sulfur donating ligands display selectivity for all the actinides tested. This selectivity seems to be greatly influenced by the formation of different complexes between the lanthanide and actinide series. The actinides tend to form complexes where the metal is more completely

coordinated by sulfur and the metal-sulfur bonds are shorter whereas the lanthanides tend to have less coordination by sulfur and longer metal-sulfur bonds.

TABLE OF CONTENTS

ABSTRACT…….. iii

LIST OF FIGURES…… ix

LIST OF TABLES……..... xvii

ACKNOWLEDGEMENTS…….. xxi

CHAPTER 1 INTRODUCTION……..……. 1

1.1 Motivation……..…… 1

1.2 Solvent Extraction…….…… 2

1.3 Soft Donor Selectivity……. 4

1.4 Approaches……..…..... 4

1.4.1 UV-Visible Spectroscopy…….…… 4

1.4.2 Distribution Measurements…… 5

1.4.3 Formation Constants……..... 5

1.4.3.1 Spectrophotometric Titration…… 6

1.4.3.2 Potentiometric Titration…….. 7

1.4.4 Extended X-ray Absorption Fine Structure Spectroscopy..... 8

1.4.5 Density Functional Theory…… 8

1.5 Research Purpose and Outline……. 9

CHAPTER 2 SULFUR DONATING EXTRACTANTS FOR THE SEPARATION OF TRIVALENT ACTINIDES AND LANTHANIDES…….. 10

2.1 Abstract……..... 10

2.2 Introduction…….…… 10

2.3 Origin or Selectivity……..... 12

2.4 Sulfur Donating Extractants…… 13

2.4.1 Carbamoylmethylphosphine Sulfide……..……. 15

2.4.2 Di- and Mono-thiophosphoric Acids……..…..…… 17

2.4.3 Dithiophosphinic Acids……..... 19

2.4.3.1 Synthesis……..…… 20

2.4.3.2 Effect of Varying Alkyl and Aryl Groups…….…. 22

2.4.3.3 Mechanisms…… 26

2.4.3.4 Degradation Studies…… 32

2.4.4 Miscellaneous Sulfur Containing Extractants…….. 34

2.5 Conclusion…….….. 36

2.6 Acknowledgements…….. 37

CHAPTER 3 PERMANGANOMETRIC QUANTIFICATION OF CYANEX 301 IN *N*-DODECANE…… 38

3.1 Abstract……..... 38

3.2 Introduction…….…… 38

3.3 Experimental…….……..... 40

3.3.1 Solution Preparation……...……...…… 40

3.3.2 UV-vis Spectroscopy……...…...…….…… 41

3.4 Results and Discussion……..... 41

3.4.1 Permanganate Stability…….……...…… 42

3.4.2 Quantification of HC301.....…...…….. 43

3.5 Conclusions…….. 46

3.6 Acknowledgements…….…… 47

CHAPTER 4 EXTRACTION OF THE TRIVALENT TRANSPLUTONIUM ACTINIDES AMERICIUM THROUGH EINSTEINIUM BY PURIFIED CYANEX 301……. 48

4.1 Abstract……... 48

4.2 Introduction…….……. 48

4.3 Experimental…….……..... 50

4.3.1 Radiotracer Distribution Studies…...…….....…… 51

4.3.2 Lanthanide Distribution Studies.…….……. 51

4.3.3 Computational Details…….……. 52

4.4 Results and Discussion……..... 52

4.4.1 Carrier Metal…….…….……...…… 52

4.4.2 Transplutonium Actinide Extraction…….……... 53

4.4.3 Nitrate Dependency…….……. 55

4.5 Conclusions...…….…. 59

4.6 Acknowledgements…….……. 60

CHAPTER 5 LANTHANIDE & ACTINIDE COMPLEXES WITH AQUEOUS SULFUR DONATING LIGANDS…….…… 61

5.1 Abstract…….……... 61

5.2 Introduction…….……. 62

5.3 Experimental……..... 64

5.3.1 Potentiometric Titrations……...……...……...…… 64

5.3.2 Spectrophotometric Titrations…..…….……... 65

5.3.3 Extended X-ray Absorption Fine Structure …….…… 65

5.3.4 Computational Details……..…… 66

5.4 Results and Discussion…….……..... 67

5.4.1 Ligand Acid Dissociation Constants…… 67

5.4.2 Metal Complex Formation Constants…… 68

5.4.3 Extended X-ray Absorption Fine Structure …… 72

5.4.4 Computational Results…… 75

5.4.5 Coordination Chemistry & Selectivity Discussion…… 78

5.5 Conclusions…… 80

5.6 Acknowledgements…… 80

CHAPTER 6 CONCLUDING STATEMENTS…… 82

6.1 Permanganometric Quantification of Cyanex 301…… 82

6.2 Extraction of Transplutonium Actinides with Cyanex 301…… 83

6.3 Aqueous Sulfur Donor Ligands…… 83

6.4 Future Directions…… 84

REFERENCES…… 85

APPENDIX A CHAPTER FOUR SUPPLEMENTARY INFORMATION…… 99

APPENDIX B CHAPTER FIVE SUPPLEMENTARY INFORMATION…… 103

APPENDIX C COPYRIGHT PERMISSIONS…… 147

LIST OF FIGURES

Figure 1.1 The hazard index of used nuclear fuel after removal of a) none of its components and b) the U, Np, Pu, Am, and Cm. A hazard index of 1 corresponds to the same level of radioactivity as the non-irradiated fuel[1,2]……..… 1

Figure 1.2 An example of a spectrophotometric titration of $^{248}Am^{3+}$ with the ligand 2,2'-thiodiactic acid (TDA)……... 7

Figure 1.3 An example of a potentiometric titration of Nd^{3+} with the ligand 2,2'-thiodiactic acid (TDA)……... 8

Figure 2.1 Phosphinic, monothiophosphinic, and dithiophosphinic acid functional groups[3]……..... 15

Figure 2.2 Structures of a generic carbamoylmethylphosphine oxide and carbamoylmethylphosphine sulfide. R_1 = methyl, t-butyl, t-pentyl. R_2 = t-butyl, t-pentyl[4]……... 15

Figure 2.3 Synthetic procedure for the preparation of CMPS[4]. As tested, R_1 and R_2 were combinations of methyl, *t*-butyl, and *t*-pentyl groups and n=1,2[4]…… 16

Figure 2.4 Structure of HDEHP, HDEHTP, HDEHDTP, and TBP[5]…….. 17

Figure 2.5 Synthetic procedure for dithiophosphinic acids as done by Tian et al[6]……. 20

Figure 2.6 Synthetic procedure for dithiophosphinic acids as done by Klaehn et al. and Peterman et al[7,8]…….. 21

Figure 2.7 Synthesis procedure of dithiophosphinic acids from 1,1-dichloro-N,N-diethylphosphanamine as done by Klaehn et al.[7]……..... 21

Figure 2.8 Proposed structures of the complexes extracted in Equations 2.9 to 2.11[3,9]. R=2,4,4-trimethylpentyl…… 27

Figure 2.9 Speculative structures of the complexes postulated by Tian et al[10,11]. R=2,4,4-trimethylpentyl…… 28

Figure 2.10 Speculative structures of the complexes postulated by Zhu et al[12]. R=2,4,4-trimethylpentyl…… 29

Figure 2.11 Speculative structures of the Am and Eu complexes extracted in Equations 2.12 and 2.13. R=2,4,4-trimethylpentyl and R'=*n*-butyl……... 31

Figure 2.12 a) ^{31}P NMR spectra of purified HC301 at various doses of radiation and b) ^{31}P NMR spectra of commercial HC301 at various doses of radiation[13]…….. . 33

Figure 2.13 Structure of a bis(thiophosphoryl)disulfane and bis(thiophosphinyl)disulfane ……..…….. 34

Figure 2.14 Generic structure of a dialkylammonium dithiocarbamate. R= butyl, octyl, phenyl, or benzyl……...…… 35

Figure 2.15 Tetrakis(phosphane sulfide) cavitand……..…….. 35

Figure 2.16 Structure of thenoyltrifluoroacetone, thiothenoyltrifluoroacetone, and tri-iso-butylphosphine sulfide…….……..…….. 36

Figure 3.1 Structure of HC301 (bis(2,4,4-trimethylpentyl)dithiophosphinic acid)…... 39

Figure 3.2 Calibration curves of $KMnO_4$ in water (λ = 526 nm) and acetone (λ = 528 nm)……. 42

Figure 3.3 Left: The spectra of $KMnO_4$ in acetone. The initial spectra are shown in blue and the final spectra are shown in red. Right: Stability of $KMnO_4$ in water, acetone, and a mixture of 40.024 mM 18-crown-6 and 5.046 mM bis(2-ethylhexyl)phosphoric acid in benzene……..…….. 43

Figure 3.4 Left: Spectra of $KMnO_4$ in acetone after addition of HC301. Spectra with less HC301 added are shown in blue and those with more HC301 are shown in red. Right: The amount of MnO_4^- dissolved in acetone consumed as a function of the amount of HC301 added……..……. 45

Figure 3.5 Comparison of the amount of HC301 measured by LOOCV and the known amount of HC301 that was added. The dashed line represents the ideal relationship between the known and measured amount (i.e. LOOCV measured amount is equal to the known amount or y = x)……..…….. 46

Figure 4.1 Structure of HC301 (bis(2,4,4-trimethylpentyl)dithiophosphinic acid…..… 50

Figure 4.2 The distribution ratio of Eu at pH 4.66 with varying aqueous concentrations of Eu (red squares) or Lu (black circles)……... 53

Figure 4.3 Left: The distribution ratios of Eu, Am, Cm, Bk, Cf, and Es as a function of pC_{H+} with 0.5024 M HC301 in dodecane at an ionic strength of 1 M. Right: The distribution ratios for the extraction of the actinides Am, Cm, Bk, Cf, and Es and the lanthanides at pH 4.50 as a function of ionic radii with 0.50 M HC301 in dodecane at an ionic strength of 1 M. Distribution ratios for the radiotracers were extrapolated from the graph on the left. Error bars are shown at 3 σ uncertainty…… 54

Figure 4.4 The UV-vis spectra of aqueous Nd^{3+} (black) and the organic phase resulting from the extraction of Nd^{3+} by 0.5024 M HC301 in dodecane from an aqueous phase containing 0.5 M Nd^{3+} and 1.5 to 5.00 M NO_3^- at a pH of 4.20. …… 56

Figure 4.5 The distribution ratio for the lanthanides Pr, Nd, Eu, and Lu at pH 4.50 and the actinides Am (pH 3.23), Cm (pH 2.51), Bk (pH 2.93), and Es (pH 2.93) with 0.5024 M HC301…… 57

Figure 4.6 Left: The structure of the $Am(C301)_3$ complex. Right: The structure of the $Am(C301)_2(NO_3)$ complex…… 59

Figure 5.1 Structures of bis(2,4,4-trimethyl-pentyl) dithiophosphinic acid (HC301) and bis[o-(trifluoro-methyl)phenyl]dithiophosphinic acid…… 63

Figure 5.2 Structures of 2,2'-thiodiacetic acid (TDA), (2R,5S)-tetrahydrothiophene-2,5-dicarboxylic acid (THTPA), and 2,5-thiophenedicarboxylic acid (TPA)…… 64

Figure 5.3 Potentiometric titrations of (left) TDA and (right) TPA protonation at 25.0 ± 0.1 °C and ionic strength of 1.00 ± 0.1 M. For the TDA titration , V_{init} = 24.911 mL, C_{TDA} = 19.99 mM, $C_{H+,total}$ = 49.78 mM. For the TPA titration, V_{init} = 24.837 mL, C_{TDA} = 8.56 mM, $C_{H+,total}$ = 8.90 mM. The titrant for both ligands contained 0.507 M NaOH and 0.500 M $NaClO_4$. (•) Experimental pC_{H+}, (dashed red line) calculated pC_{H+}, (black solid line) H_2L, (red solid line) HL^-, and (blue solid line) L^{2-}…… 67

Figure 5.4 Nd and Eu Potentiometric Titrations with TDA and TPA at 1.00 ± 0.01 M $NaClO_4$ and 25 °C. (•) Experimental pC_{H+}, (red dashed line) calculated pC_{H+}, (black solid line) Eu, (red solid line) ML^+ (blue solid line) ML_2^-. a) Nd/TDA. For this titration, Vinit = 25.349 mL, C_{TDA} = 19.25 mM, C_{Nd} = 7.806 mM, and C_{H+},total = 48.73 mM. The titrant contained 0.507 M NaOH and 0.500 M $NaClO_4$. b) Eu/TDA. For this titration, V_{init} = 25.261 mL, C_{TDA} = 19.70 mM, C_{Eu} = 6.634 mM, and $C_{H+,total}$ = 49.03 mM. The titrant contained 0.507 M NaOH and 0.500 M $NaClO_4$. b) Nd/TPA. For this titration, Vinit = 25.447 mL, C_{TPA} = 8.375 mM, C_{Nd} = 10.15 mM, and $C_{H+,}$total = 8.939 mM. The titrant contained 0.507 M NaOH and 0.500 M $NaClO_4$. d) Eu/TPA For this titration, V_{init} = 25.494 mL, C_{TPA} = 8.374

mM, C_{Eu} = 10.18 mM, and $C_{H+,total}$ = 9.021 mM. The titrant contained 0.507 M NaOH and 0.500 M $NaClO_4$…….. 69

Figure 5.5 Spectrophotometric titrations of Nd, Am, and Cm with TDA and molar absorptivities calculated using HypSpec2014 at room temperature and an ionic strength of 1.00 ± 0.01 M. The spectra changes from blue to red over the course of the titration. a) Nd/TDA titration, V_{init} = 0.803 mL, C_{Nd} = 10.15 mM, and pC_{H+} ,initial = 3.08. The titrant contained C_{TDA} = 150.1 mM, C_{Nd} = 10.12 mM and after the addition of 0.792 mL of titrant, the $pC_{H+,final}$ = 5.17. b) Molar absorptivity of Nd, $NdTDA^+$, and $Nd(TDA)_2^-$. c) Am/TDA titration, V_{init} = 0.795 mL, C_{Am} = 0.844 mM, and $pC_{H+,initial}$ = 2.581. The titrant contained C_{TDA} = 10.03 mM, C_{Am} = 0.832 mM and after the addition of 0.793 mL of titrant, the $pC_{H+,final}$ = 3.676. d) Molar absorptivity of Am, $AmTDA^+$, and $Am(TDA)_2^-$. e) Cm/TDA titration, V_{init} = 0.795 mL, C_{Cm} = 0.937 mM, and $pC_{H+,initial}$ = 3.182. The titrant contained C_{TDA} = 0.137 M, C_{Cm} = 0.939 mM and after the addition of 0.731 mL of titrant, the $pC_{H+,final}$ = 3.707. f) Molar absorptivity of Cm, $CmTDA^+$, and $Cm(TDA)_2^-$……..……. 70

Figure 5.6 Spectrophotometric titrations of Nd, Am, and Cm with TPA and molar absorptivities calculated using HypSpec2014 at room temperature and an ionic strength of 1.00 ± 0.01 M. The spectra changes from blue to red over the course of the titration. a) Nd/TPA titration, V_{init} = 0.803 mL, C_{Nd} = 10.14 mM, and $pC_{H+,initial}$ = 3.12. The titrant contained C_{TPA} = 50.32 mM and after the addition of 0.792 mL of titrant, the $pC_{H+,final}$ = 4.21. b) Molar absorptivity of Nd and $NdTPA^+$. c) Am/TPA titration, V_{init} = 0.795 mL, C_{Am} = 1.914 mM, and $pC_{H+,initial}$ = 2.404. The titrant contained C_{TPA} = 49.79 mM and after the addition of 0.796 mL of titrant, the $pC_{H+,final}$ = 4.007. d) Molar absorptivity of Am and $AmTPA^+$. e) Cm/TPA titration, V_{init} = 0.795 mL, C_{Cm} = 1.746 mM, and $pC_{H+,initial}$ = 3.282. The titrant contained C_{TPA} = 49.79 mM and after the addition of 0.796 mL of titrant, the $pC_{H+,final}$ = 4.296. f) Molar absorptivity of Cm and $CmTPA^+$……..…... 71

Figure 5.7 Data and fit results for the $Cf(TDA)_x$ sample, assuming N(Cf-C)=4. The left panel shows the data and results in k-space. The right panel shows the Fourier transform (FT), where the outer envelope is the complex transform amplitude and the modulating line is the real part. The data were transformed between 2.5 and 10 $Å^{-1}$, and narrowed with a Gaussian window with width 0.3 $Å^{-1}$. The fit range is from 1.5 to 3.5 Å. Individual fit components are arbitrarily offset vertically for display……..…….. 73

Figure 5.8 The structures of a) TDA, b) THTPA, c) TPA Bi (two coordinating oxygens in one carboxylate group), and d) TPA OS (one oxygen and one sulfur coordinating) complexes. The purple atom represents the metal ion, red represents oxygen, yellow represents sulfur, black represents carbon, and white represents hydrogen……..…… 76

Figure 5.9 Structures of iminodiacetic acid (IDA) and 2,6-pyridinedicarboxylic acid (DPA)……..……... 79

Figure A.1 The pH corrected distribution ratio of the lanthanides Pr, Nd, Sm, Eu, Gd, Dy, Ho, Er, Tm, Yb, and Lu with 0.5024 M HC301 at an average pC_{H+} of 4.46. The value for n_{H+} (1.13) was obtained from radiotracer experiments with Eu……...…… 99

Figure A.2 The slope of the nitrate dependency of the pH corrected distribution ratio vs. $Log_{10}[NO_3^-]$ for the lanthanides and the actinides Am, Cm, Bk, and Es with 0.5024 M HC301 at an average pC_{H+} of 4.46 for lanthanides and 3.07 for actinides……..……..…… 100

Figure B.1 Nd and Eu Isothermal Titration Calorimetry with TDA. Three TDA isothermal titration calorimetry trials at 1.00 ± 0.01 M $NaClO_4$ and 25 °C. Left) Nd. For this titration, V_{init} = 965 µL, C_{Nd} = 3.00 mM, pC_{H+} = 4.00. The titrant contained 0.1492 M TDA at a pC_{H+} of 4.03. Right) Eu. For this titration, V_{init} = 965 µL, C_{Eu} = 3.00 mM, pC_{H+} = 4.01. The titrant contained 0.1492 M TDA at a pC_{H+} of 4.03……..…… 103

Figure B.2 Nd and Eu Potentiometric Titrations with TDA. TDA potentiometric titrations with Nd or Eu at 1.00 ± 0.01 M $NaClO_4$ and 25 °C. Top) Nd. For this titration, Vinit = 25.349 mL, C_{TDA} = 19.25 mM, C_{Nd} = 7.806 mM, and C_{H+},total = 48.73 mM. The titrant contained 0.507 M NaOH and 0.500 M $NaClO_4$. (•) Experimental pC_{H+}, (red dashed line) calculated pC_{H+}, (black solid line) Nd, (red solid line) NdTDA+. Bottom) Eu. For this titration, V_{init} = 25.261 mL, C_{TDA} = 19.70 mM, C_{Eu} = 6.634 mM, and $C_{H+,total}$ = 49.03 mM. The titrant contained 0.507 M NaOH and 0.500 M $NaClO_4$. (•) Experimental pC_{H+}, (red dashed line) calculated pC_{H+}, (black solid line) Eu, (red solid line) $EuTDA^+$, (blue solid line) $EuTDA_2^-$……..…….. 104

Figure B.3 Nd and Eu Potentiometric Titrations with TPA. TPA potentiometric titrations with Nd or Eu at 1.00 ± 0.01 M $NaClO_4$ and 25 °C. Top) Nd. For this titration, Vinit = 25.447 mL, C_{TPA} = 8.375 mM, C_{Nd} = 10.15 mM, and $C_{H+,}$total = 8.939 mM. The titrant contained 0.507 M NaOH and 0.500 M $NaClO_4$. (•) Experimental $pC_{H+,}$ (red dashed line) calculated $pC_{H+,}$ (black solid line) Nd, (red solid line) Nd_{TPA}^+. Bottom) Eu. For this titration, V_{init} = 25.494 mL, C_{TPA} = 8.374 mM, C_{Eu} = 10.18 mM, and $C_{H+,total}$ = 9.021 mM. The titrant contained 0.507 M NaOH and 0.500 M $NaClO_4$. (•) Experimental pC_{H+}, (red dashed line) calculated pC_{H+}, (black solid line) Eu, (red solid line) $EuTPA^+$……..... 105

Figure B.4 Spectrophotometric Titrations of Nd, Am, and Cm with TDA**.** Spectrophotometric titration of a metal and TDA at room temperature and an ionic strength of 1.00 ± 0.01 M. The spectra changes from blue to red over the course of the titration. Top) For the Nd titration, V_{init} = 0.803 mL, C_{Nd} = 10.15 mM, and $pC_{H+,initial}$ = 3.08. The titrant contained C_{TDA} = 150.1 mM, C_{Nd} = 10.12 mM and after the addition of 0.792 mL of titrant, the $pC_{H+,final}$ = 5.17. Middle) For the Am titration, V_{init} = 0.795 mL, C_{Am} = 0.844 mM, and $pC_{H+,initial}$ = 2.581. The titrant contained C_{TDA} = 10.03 mM, C_{Am} = 0.832 mM and after the addition of 0.793 mL of titrant, the $pC_{H+,final}$ = 3.676. Bottom) For the Cm titration, V_{init} = 0.795 mL, C_{Cm} = 0.937 mM, and $pC_{H+,initial}$ = 3.182. The titrant contained C_{TDA} = 0.137 M, C_{Cm} = 0.939 mM and after the addition of 0.731 mL of titrant, the $pC_{H+,final}$ = 3.707…….…….. 106

Figure B.5 Molar absorptivity of Nd, Am, and Cm complexes with TDA. Molar absorptivity of Nd (top), Am (middle), and Cm (bottom) complexes with TDA calculated from the spectra shown in Figure B.4 using HypSpec2014. These spectra were collected at room temperature and an ionic strength of 1.00 ± 0.01 M……..……... 107

Figure B.6 Spectrophotometric Titrations of Nd, Am, and Cm with TPA. Spectrophotometric titration of a metal and TPA at room temperature and an ionic strength of 1.00 ± 0.01 M. The spectra changes from blue to red over the course of the titration. Top) For the Nd titration, V_{init} = 0.803 mL, C_{Nd} = 10.14 mM, and $pC_{H+,initial}$ = 3.12. The titrant contained C_{TPA} = 50.32 mM and after the addition of 0.792 mL of titrant, the $pC_{H+,final}$ = 4.21. Middle) For the Am titration, V_{init} = 0.795 mL, C_{Am} = 1.914 mM, and $pC_{H+,initial}$ = 2.404. The titrant contained C_{TPA} = 49.79 mM and after the addition of 0.796 mL of titrant, the $pC_{H+,final}$ = 4.007. Bottom) For the Cm titration, V_{init} = 0.795 mL, C_{Cm} = 1.746 mM, and $pC_{H+,initial}$ = 3.282. The titrant contained C_{TPA} = 49.79 mM and after the addition of 0.796 mL of titrant, the $pC_{H+,final}$ = 4.296…….…….. 108

Figure B.7 Molar absorptivity of Nd, Am, and Cm complexes with TPA. Molar absorptivity of Nd (top), Am (middle), and Cm (bottom) complexes with TPA calculated from the spectra shown in Figure B.6 using HypSpec2014. These spectra were collected at room temperature and an ionic strength of 1.00 ± 0.01 M……..……... 109

Figure B.8 EXAFS results of $Cm(TDA)_2^-$ complex with N(Cm-C) = 4. EXAFS data for the $Cm(TDA)_2^-$ complex. For this sample, C_{Cm} = 0.79 mM, C_{TDA} = 0.15 M, pH = 3.50, and the ionic strength was adjusted to 1.00 M by addition of sodium perchlorate…….……... 110

Figure B.9 EXAFS results of $Cm(TDA)_2^-$ complex with N(Cm-C) = 8. EXAFS data for the $Cm(TDA)_2^-$ complex. For this sample, C_{Cm} = 0.79 mM, C_{TDA} = 0.15 M, pH = 3.50, and the ionic strength was adjusted to 1.00 M by addition of sodium perchlorate…….……..... 111

Figure B.10 EXAFS results of $Bk(TDA)_2^-$ complex with N(Bk-C) = 4. EXAFS data for the $Bk(TDA)_2^-$ complex. For this sample, C_{Bk} = 0.79 mM, C_{TDA} = 0.02 M, pH = 3.50, and the ionic strength was adjusted to 1.00 M by addition of sodium perchlorate…….…… 112

Figure B.11 EXAFS results of $Bk(TDA)_2^-$ complex with N(Bk-C) = 8. EXAFS data for the $Bk(TDA)_2^-$ complex. For this sample, C_{Bk} = 0.79 mM, C_{TDA} = 0.02 M, pH = 3.50, and the ionic strength was adjusted to 1.00 M by addition of sodium perchlorate…….…… 113

Figure B.12 EXAFS results of $Cf(TDA)_2^-$ complex with N(Cf-C) = 4. EXAFS data for the $Cf(TDA)_2^-$ complex. For this sample, C_{Cf} = 0.79 mM, C_{TDA} = 0.02 M, pH = 3.50, and the ionic strength was adjusted to 1.00 M by addition of sodium perchlorate……...…….. 114

Figure B.13 EXAFS results of $Cf(TDA)_2^-$ complex with N(Cf-C) = 8. EXAFS data for the $Cf(TDA)_2^-$ complex. For this sample, C_{Cf} = 0.79 mM, C_{TDA} = 0.02 M, pH = 3.50, and the ionic strength was adjusted to 1.00 M by addition of sodium perchlorate……...…….. 115

Figure B.14 EXAFS results of $Eu(TDA)_2^-$ complex with N(Eu-C) = 4. EXAFS data for the $Eu(TDA)_2^-$ complex. For this sample, C_{Eu} = 3.00 mM, C_{TDA} = 0.15 M, pH = 3.50, and the ionic strength was adjusted to 1.00 M by addition of sodium perchlorate…….…… 116

Figure B.15 EXAFS results of $Eu(TDA)_2^-$ complex with N(Eu-C) = 8. EXAFS data for the $Eu(TDA)_2^-$ complex. For this sample, C_{Eu} = 3.00 mM, C_{TDA} = 0.15 M, pH = 3.50, and the ionic strength was adjusted to 1.00 M by addition of sodium perchlorate…….…… 117

Figure B.16 EXAFS results of $Tb(TDA)_2^-$ complex with N(Tb-C) = 4. EXAFS data for the $Tb(TDA)_2^-$ complex. For this sample, C_{Tb} = 3.00 mM, C_{TDA} = 0.15 M, pH = 3.50, and the ionic strength was adjusted to 1.00 M by addition of sodium perchlorate…….…… 118

Figure B.17 EXAFS results of $Tb(TDA)_2^-$ complex with N(Tb-C) = 8. EXAFS data for the $Tb(TDA)_2^-$ complex. For this sample, C_{Tb} = 3.00 mM, C_{TDA} = 0.15 M, pH = 3.50, and the ionic strength was adjusted to 1.00 M by addition of sodium perchlorate…….…… 119

Figure B.18 EXAFS results of $Cm(TPA)^+$ complex with N(Cm-C) = 4. EXAFS data for the $Cm(TPA)^+$ complex. For this sample, C_{Cm} = 0.79 mM, C_{TPA} = 0.05 M, pH = 3.90, and the ionic strength was adjusted to 1.00 M by addition of sodium perchlorate…… 120

Figure B.19 EXAFS results of $Cm(TPA)^+$ complex with N(Cm-C) = 8. EXAFS data for the $Cm(TPA)^+$ complex. For this sample, C_{Cm} = 0.79 mM, C_{TPA} = 0.05 M, pH = 3.90, and the ionic strength was adjusted to 1.00 M by addition of sodium perchlorate…… 121

Figure B.20 EXAFS results of $Eu(TPA)^+$ complex with N(Eu-C) = 4. EXAFS data for the $Eu(TPA)^+$ complex. For this sample, C_{Eu} = 3.00 mM, C_{TPA} = 0.05 M, pH = 3.90, and the ionic strength was adjusted to 1.00 M by addition of sodium perchlorate……..……... 122

Figure B.21 EXAFS results of $Eu(TPA)^+$ complex with N(Eu-C) = 8. EXAFS data for the $Eu(TPA)^+$ complex. For this sample, C_{Eu} = 3.00 mM, C_{TPA} = 0.05 M, pH = 3.90, and the ionic strength was adjusted to 1.00 M by addition of sodium perchlorate……..……... 123

Figure B.22 EXAFS results of $Tb(TPA)^+$ complex with N(Tb-C) = 4. EXAFS data for the $Tb(TPA)^+$ complex. For this sample, C_{Tb} = 3.00 mM, C_{TPA} = 0.05 M, pH = 3.90, and the ionic strength was adjusted to 1.00 M by addition of sodium perchlorate……..……... 124

Figure B.23 EXAFS results of $Tb(TPA)^+$ complex with N(Tb-C) = 8. EXAFS data for the $Tb(TPA)^+$ complex. For this sample, C_{Tb} = 3.00 mM, C_{TPA} = 0.05 M, pH = 3.90, and the ionic strength was adjusted to 1.00 M by addition of sodium perchlorate……..……... 125

LIST OF TABLES

Table 2.1 Various mono- and di-thiophosphinic acids and their separation factors for tracer amounts of Am and Eu from nitric acid media. None of the extractants have been saponified prior to extraction……..……... 24

Table 3.1 Molar absorption coefficient (ε) measured at λ_{max} and intercept for $KMnO_4$ in water, acetone, and benzene……..……... 42

Table 3.2 Known amounts of HC301 added and the amount measured by LOOCV along with the difference between these two values…….…… 46

Table 4.1 The separation factors of Am, Cm, Bk, Cf, and Es from Eu with 0.50 M HC301 in dodecane at an ionic strength of 1 M and pC_{H+} = 4.00…..…..... 55

Table 4.2 Calculated thermodynamic parameters for the reaction $M(C301)_3 + NO_3^- \rightleftharpoons M(C301)_2(NO_3) + C301^-$. ΔG is calculated at a temperature of 298.15 K……..….. 59

Table 5.1 Formation constants of trivalent lanthanides and actinides with TDA at 25.0 ± 0.1 °C and 1.00 ± 0.01 M ionic strength……... 68

Table 5.2 Formation constants of trivalent lanthanides and actinides with TPA at 25.0 ± 0.1 °C and 1.00 ± 0.01 M ionic strength……... 69

Table 5.3 Fit results assuming σ^2(M-S) = 0.008 $Å^2$ and N(M-C) = 4. Note that with these constraints, the absolute error on N(M-S) is estimated to be as large as 30%. For full details and for fits with N(M-C) = 8, see Appendix B…... 74

Table 5.4 Bond lengths of the computed Cm, Eu, and Gd complexes with TDA, THTPA, and TPA. Coordinating water molecules were added to maintain a coordination number of nine for all complexes. TPA Bi binds to the metal center using both oxygens from one carboxylate group. TPA OS binds to the metal by one oxygen and the sulfur……... 76

Table 5.5 Energy of formation (ΔE, kJ/mol) for geometry optimized 1:1 complexes with sufficient coordinated water molecules to maintain a coordination number of nine for Cm, Eu, and Gd with TDA, THTPA, and TPA. The denticity (d) of each ligand is also included……..… 78

Table 5.6 Calculated values of β_{An}/β_{Eu}. The upper and lower bounds at 1σ uncertainty of this value are shown in parenthesis……..….. 78

Table A.1 Emission wavelengths of lanthanides used in ICP-OES……..…. 99

Table B.1 Thermodynamic parameters for Nd and Eu complexes with TDA as determined by isothermal titration calorimetry……..... 103

Table B.2 Details of EXAFS fitting. Fourier transform and fit ranges, together with the associated number of independent data points, N_{ind}[14,15], and fit degrees of freedom, ν, after fitting. These are followed with the figures and tables for all the fit parameters for each fit, using both N(M-C)=4 and N(M-C)=8. Important! σ^2(M-S) is fixed at 0.008 $Å^2$ for all fits; therefore, the reported errors on N(M-S) are for comparisons between these samples only. Absolute errors are estimated to be as large as 30% on N(M-S). Note that the M-C shell is included to account for overlap with the M-S shell. Likewise, the M-C shell likely overlaps with further shells, and so the results from the M-C shell should be viewed with skepticism…….. 110

Table B.3 EXAFS results of $Cm(TDA)_2^-$ complex with N(Cm-C) = 4. EXAFS fit for the $Cm(TDA)_2^-$ complex. For this sample, C_{Cm} = 0.79 mM, C_{TDA} = 0.15 M, pH = 3.50, and the ionic strength was adjusted to 1.00 M by addition of sodium perchlorate. Note that the Cm-C shell is split……..... 111

Table B.4 EXAFS results of $Cm(TDA)_2^-$ complex with N(Cm-C) = 8. EXAFS fit for the $Cm(TDA)_2^-$ complex. For this sample, C_{Cm} = 0.79 mM, C_{TDA} = 0.15 M, pH = 3.50, and the ionic strength was adjusted to 1.00 M by addition of sodium perchlorate. Note that the Cm-C shell is split……... 112

Table B.5 EXAFS results of $Bk(TDA)_2^-$ complex with N(Bk-C) = 4. EXAFS fit for the $Bk(TDA)_2^-$ complex. For this sample, C_{Bk} = 0.79 mM, C_{TDA} = 0.02 M, pH = 3.50, and the ionic strength was adjusted to 1.00 M by addition of sodium perchlorate……. 113

Table B.6 EXAFS results of $Bk(TDA)_2^-$ complex with N(Bk-C) = 8. EXAFS fit for the $Bk(TDA)_2^-$ complex. For this sample, C_{Bk} = 0.79 mM, C_{TDA} = 0.02 M, pH = 3.50, and the ionic strength was adjusted to 1.00 M by addition of sodium perchlorate……. 114

Table B.7 EXAFS results of $Cf(TDA)_2^-$ complex with N(Cf-C) = 4. EXAFS fit for the $Cf(TDA)_2^-$ complex. For this sample, C_{Cf} = 0.79 mM, C_{TDA} = 0.02 M, pH = 3.50, and the ionic strength was adjusted to 1.00 M by addition of sodium perchlorate……..... 115

Table B.8 EXAFS results of $Cf(TDA)_2^-$ complex with N(Cf-C) = 8. EXAFS fit for the $Cf(TDA)_2^-$ complex. For this sample, C_{Cf} = 0.79 mM, C_{TDA} = 0.02 M, pH = 3.50, and the ionic strength was adjusted to 1.00 M by addition of sodium perchlorate……. 116

Table B.9 EXAFS results of $Eu(TDA)_2^-$ complex with N(Eu-C) = 4. EXAFS fit for the $Eu(TDA)_2^-$ complex. For this sample, C_{Eu} = 3.00 mM, C_{TDA} = 0.15 M, pH = 3.50, and the ionic strength was adjusted to 1.00 M by addition of sodium perchlorate……..…….. 117

Table B.10 EXAFS results of $Eu(TDA)_2^-$ complex with N(Eu-C) = 8. EXAFS fit for the $Eu(TDA)_2^-$ complex. For this sample, C_{Eu} = 3.00 mM, C_{TDA} = 0.15 M, pH = 3.50, and the ionic strength was adjusted to 1.00 M by addition of sodium perchlorate……..…….. 118

Table B.11 EXAFS results of $Tb(TDA)_2^-$ complex with N(Tb-C) = 4. EXAFS fit for the $Tb(TDA)_2^-$ complex. For this sample, C_{Tb} = 3.00 mM, C_{TDA} = 0.15 M, pH = 3.50, and the ionic strength was adjusted to 1.00 M by addition of sodium perchlorate……...…….. 119

Table B.12 EXAFS results of $Tb(TDA)_2^-$ complex with N(Tb-C) = 8. EXAFS fit for the $Tb(TDA)_2^-$ complex. For this sample, C_{Tb} = 3.00 mM, C_{TDA} = 0.15 M, pH = 3.50, and the ionic strength was adjusted to 1.00 M by addition of sodium perchlorate……...…….. 120

Table B.13 EXAFS results of $Cm(TPA)^+$ complex with N(Cm-C) = 4. EXAFS fit for the $Cm(TPA)^+$ complex. For this sample, C_{Cm} = 0.79 mM, C_{TPA} = 0.05 M, pH = 3.90, and the ionic strength was adjusted to 1.00 M by addition of sodium perchlorate……..…….. 121

Table B.14 EXAFS results of $Cm(TPA)^+$ complex with N(Cm-C) = 8. EXAFS fit for the $Cm(TPA)^+$ complex. For this sample, C_{Cm} = 0.79 mM, C_{TPA} = 0.05 M, pH = 3.90, and the ionic strength was adjusted to 1.00 M by addition of sodium perchlorate……..…….. 122

Table B.15 EXAFS results of $Eu(TPA)^+$ complex with N(Eu-C) = 4. EXAFS fit for the $Eu(TPA)^+$ complex. For this sample, C_{Eu} = 3.00 mM, C_{TPA} = 0.05 M, pH = 3.90, and the ionic strength was adjusted to 1.00 M by addition of sodium perchlorate…….……... 123

Table B.16 EXAFS results of $Eu(TPA)^+$ complex with N(Eu-C) = 8. EXAFS fit for the $Eu(TPA)^+$ complex. For this sample, C_{Eu} = 3.00 mM, C_{TPA} = 0.05 M, pH = 3.90, and the ionic strength was adjusted to 1.00 M by addition of sodium perchlorate…….……... 124

Table B.17 EXAFS results of $Tb(TPA)^+$ complex with N(Tb-C) = 4. EXAFS fit for the $Tb(TPA)^+$ complex. For this sample, C_{Tb} = 3.00 mM, C_{TPA} = 0.05 M, pH = 3.90, and the ionic strength was adjusted to 1.00 M by addition of sodium perchlorate……..……... 125

Table B.18 EXAFS results of $Tb(TPA)^+$ complex with N(Tb-C) = 8. EXAFS fit for the $Tb(TPA)^+$ complex. For this sample, C_{Tb} = 3.00 mM, C_{TPA} = 0.05 M, pH = 3.90, and the ionic strength was adjusted to 1.00 M by addition of sodium perchlorate……..……... 126

ACKNOWLEDGEMENTS

I would like to thank my advisor and mentor, Dr. Jenifer Shafer, for her leadership and support throughout this experience. Without her support, I would not have been able to have this amazing experience.

I would also like to thank all of the collaborators that I have had the privilege of working with over the past several years for their immeasurable contributions to this work. To my committee, Dr. Andrew Osborne, Dr. Mark Jensen, Dr. Brian Trewyn, and Dr. Shubham Vyas, thank you for your guidance and feedback.

Po Ki, thank you for all of your support and companionship. I would like to thank my family for helping me get here. To my grandfather, Dr. Irwin Bessen, thank you for inspiring me to be curious about how the world works and to rigorously pursue answers.

CHAPTER 1: INTRODUCTION

1.1 Motivation

The trivalent transplutonium actinides are present in used nuclear fuel where they contribute significantly to the long-term radioactivity and heat load of the material, which drastically limits the quantity that can be stored in a given repository. The fission products, despite accounting for most of the initial radioactivity, decay on a shorter timescale and pose a lesser challenge to their safe disposal. Figure 1.1A shows that the used fuel without any components removed, will be more radioactive than the unirradiated fuel for approximately 4,000,000 years. The removal of the actinides U, Np, Pu, Am, and Cm dramatically reduces the time required for used fuel to decay to about 1000 years as shown in Fig 1.1B.

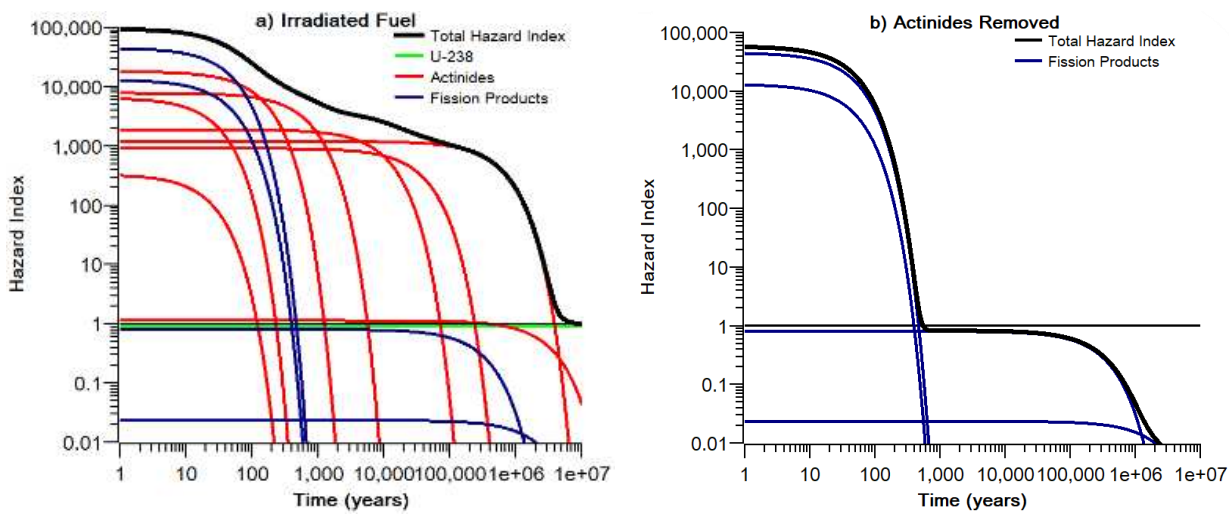

Figure 1.1 The hazard index of used nuclear fuel after removal of a) none of its components and b) the U, Np, Pu, Am, and Cm. A hazard index of 1 corresponds to the same level of radioactivity as the non-irradiated fuel[1,2].

After the actinides are separated from the fuel, one approach to handling them is to fission them in a specialized nuclear reactor where they will be converted into less hazardous fission products by nuclear fission.[16] For this approach to be effective, the actinides to be destroyed must be reasonably free of neutron absorbing impurities as their presence would cause the process to be inefficient by reducing the number of neutrons available to destroy the actinides. Methods have been developed for the removal of many elements from the

transplutonium, trivalent actinide waste stream,[17] but the efficient separation from the trivalent lanthanides capable of working on an industrial scale is elusive.

To separate the trivalent actinides and lanthanides, a system that is selective for either the lanthanides or actinides is necessary. In many separations, differences in the ionic radii, charges, or charge densities are used for the separation of metal ions, but they are too similar for the trivalent actinides and lanthanides to provide a significant separation. This requires other differences between the two classes of metals to be exploited for the separation, such as different abilities to form covalent bonds. The actinides have shown the ability to bond more covalently with soft donors than the actinides, thus enabling a separation.[18–23] Most work has been focused on nitrogen based soft donor ligands for the separation, but the even softer sulfur donors show greater covalency with the actinides[24–26] and have provided large separation factors.[8,12,27,28] The greater covalency of the actinides manifests as shorter and stronger bond between the metal and sulfur donor than the bond between a comparable lanthanide and the sulfur donor.[24–26] Further research on the interactions between the lanthanides and actinides with soft, sulfur donor ligands for this challenging separation will not only provide insight on the fundamental chemistry of the little studied heavy actinides, but will assist in the development of effective separations relevant to processing used nuclear fuel.

1.2 Solvent Extraction

For the separation of lanthanides and trivalent actinides, liquid-liquid extraction is the most widely considered process as it is can be scaled up to provide the high throughput necessary for an industrial scale separation while giving an acceptable purity. These separations consist of two immiscible liquid phases, an aqueous phase containing the metals to be separated and some amount of acid in contact with an organic phase consisting of an extractant dissolved in an organic diluent. The goal of this type of system in a separation is to retain one type of metal (e.g. the lanthanides) in the aqueous phase while another type of metal is extracted into the organic phase, thus providing a separation. The selectivity in this separation may arise from the presence of selective ligands in the aqueous phase or selective extractants in the organic phase or some combination thereof. In many separation schemes for metal ions, the extractants provide the source of selectivity. There are two main methods by which extractants function, solvation of the metal ion or cation exchange.

Solvating extractants are organic soluble species that are neutral and polar. They are capable of solvating the charge dense metal ions in the organic phase with enough counterions to maintain the overall neutrality of the species. Equation 1.1 shows a generic mechanism for the solvating extractant, E. As the extraction of metal requires the coextraction of counterions, conditions where high concentrations of anions are present in the aqueous phase are used to promote the extraction of metal. This is most commonly achieved by using high concentrations of acid to provide the necessary counteranions, although salts have also been used. To strip the extracted metal from the organic phase, a low concentration of counteranions is used in the aqueous phase.

$$M^{4+} + 4NO_3^- + 2E_{org} \rightleftharpoons M(NO_3)_4E_{2,org} \tag{1.1}$$

Cation exchange extractants are acidic organic soluble species. They extract metals by exchanging their acidic protons initially in the organic phase for metal ions from the aqueous phase. Equation 1.2 shows this process for the cation exchange extractant HA. These extractants do not require counteranions to maintain neutrality, unlike the solvating extractants. These extractants extract the most strongly when the acid concentration in the aqueous phase is low as the addition of the protons to the aqueous phase is more favorable. Higher acid concentrations in the aqueous phase lessen the effectiveness of the extractant and if high enough, will strip metal from the organic phase.

$$M^{3+} + 3HA_{org} \rightleftharpoons MA_{3,org} + 3H^+ \tag{1.2}$$

In addition to liquid-liquid extraction methods where only one extractant is used, a mixture of extractants can be used in some cases. Typically, one of the extractants is a cation exchanger and the other is a solvating extractant. When two extractants are used and a more complete extraction is observed than for either of the extractants by themselves at the same concentration, a synergistic extraction is occurring.[29,30] The mechanism by which this occurs is typically complex and poorly understood, but is typically caused by the formation of more lipophilic metal complexes.[29,30] The increase in lipophilicity can happen by the addition of another extractant molecule to the complex, typically by increasing the coordination number of the metal ion, opening a chelate ring, or displacing bound water molecules.[29,30] Besides the basic mechanism given here, synergistic extractants can alter other components of the system by affecting aggregation and micelle formation or by changing interfacial properties.[29]

1.3 Soft Donor Selectivity

To enable a solvent extraction system to selectively extract a particular metal over other species requires either an extractant or ligand that provides selectivity by preferentially interacting with one type of metal. In the separation of the trivalent actinides and lanthanides, this selectivity arises from soft donor ligands or extractants. Soft atoms are atoms that are polarizable such as nitrogen or sulfur.[18] Hard atoms which are smaller and not as polarizable, such as oxygen and fluorine, are not generally considered to provide selectivity for this separation. This soft donor selectivity was first observed by Street and Seaborg who found that chloride preferentially bonded with the actinides and could be utilized for separating them from lanthanides.[19] Subsequent studies by many investigators have found the actinides form shorter and stronger bonds with soft atoms[24–26] that may be utilized to provide selectivity in a separation process.

Computational studies have found that soft donors are able to interact more strongly with the actinides by forming bonds of a more covalent nature.[31,32] Further analysis has revealed that this covalent interaction is caused by the 5f orbitals of the actinides and orbitals of soft donor atom having similar energies which promotes covalent bonding.[33–35] The 4f orbitals of the lanthanides are unable to engage is such bonding causing a difference between the lanthanides and actinides that can be exploited for a separation of these metals. The selectivity of soft donors for the actinides is more thoroughly examined in Chapter Two.

1.4 Approaches

A variety of methods can be used for examining the behavior and selectivity of different ligands and extractants. Several of the most common are explained below.

1.4.1 UV-Visible Spectroscopy

UV-vis spectroscopy uses ultraviolet and visible light to probe electronic transitions within an atom or molecule by measuring the absorption of light. The absorption of light can be related to the concentration of the absorbing species by Beer's Law, Equation 1.3, where the absorbance of a sample (A) can be related to the concentration of an absorbing species (c) and pathlength (ℓ) by the molar absorption coefficient (ε). Additionally, the spectra of metal ions, especially certain actinides and lanthanides, can be quite sensitive to the coordination

environment of the metal and can provide information about the number and type of ligands coordinating the metal ion.

$$A = \varepsilon \ell c \tag{1.3}$$

1.4.2 Distribution Measurements

As solvent extraction systems are being studied for the separation of trivalent actinides and lanthanides, it is important to be able to quantify the extraction and separation of metals within these systems. The extraction of metal can be quantified by the distribution ratio (D), Equation 1.4. The distribution ratio is the ratio of the concentration of metal in the organic phase to the concentration in the aqueous phase. Since radioactive isotopes of the metals are often being studied here, the radioactivity (A) of each phase is used in place of concentration as radioactivity is proportional to the amount of the isotope present. To compare the extraction of different metals in a separation process, the separation factor (SF) is used, Equation 1.5. The separation factor is the ratio of the distribution ratios of the metals being separated. A separation factor of unity indicates no separation while a value significantly greater or less than one is an effective separation.

$$D = \frac{[M]_{org}}{[M]_{aq}} = \frac{A_{org}}{A_{aq}} \tag{1.4}$$

$$SF_{An/Ln} = \frac{D_{An}}{D_{Ln}} \tag{1.5}$$

1.4.3 Formation Constants

When considering the formation of complexes between a metal and ligand, a useful approach to quantifying the strength of this interaction is the formation constant (β). The general equation for the formation of a complex with M metal ions, no acidic protons, and L ligands is shown in Equation 1.6. When this formula is applied to the reaction with one metal and one ligand, as shown in Equation 1.7, the formation constant β_{101} can be determined using Equation 1.8. When considering the reaction of one metal with two ligands, Equation 1.9, the formation constant β_{102} can be determined from Equation 1.10.

$$\beta_{M0L} = \frac{[M_M L_L]}{[M^{3+}]^M [L^{2-}]^L} \tag{1.6}$$

$$M^{3+} + L^{2-} \rightleftharpoons ML^+ \tag{1.7}$$

$$\beta_{101} = \frac{[ML^+]}{[M^{3+}][L^{2-}]} \tag{1.8}$$

$$M^{3+} + 2L^{2-} \rightleftharpoons ML_2^- \tag{1.9}$$

$$\beta_{102} = \frac{[ML_2^-]}{[M^{3+}][L^{2-}]^2} \tag{1.10}$$

There are a number of different experimental approaches to determining formation constants including spectrophotometric and potentiometric titrations, isothermal titration calorimetry, nuclear magnetic resonance, and competitive extraction. Spectrophotometric and potentiometric titrations are explained below as these techniques were used to determine formation constants in the work shown here.

1.4.3.1 Spectrophotometric Titration

One method for determining formation constants is to titrate a metal solution with a solution containing a ligand and to measure the spectra of the metal after each addition. An example of the spectra collected from this type of titration is shown in Figure 1.2 which shows the spectra collected from the titration of Am^{3+} with the ligand 2,2'-thiodiacetic acid (TDA). If the metal has spectral features that change upon complexation, the number of species and their formation constants may be determined by analyzing the spectra. In Figure 1.2, it can be observed that the addition of TDA causes the absorption peak of Am to redshift in two distinct steps corresponding to the two complexes formed, $AmTDA^+$ and $Am(TDA)_2^-$. This can be further analyzed to determine formation constants either manually or using software such as HypSpec2014.[36]

This method of determining formation constants is quite useful, but it requires having metals, or in some cases, ligands, that have spectra that change upon complexation. Fortunately, many lanthanides and actinides have either UV-vis or fluorescence features that meet this criterion. Additionally, this method usually requires macroscopic quantities of metals that may prohibit studies with certain actinides due to the low quantities available or high amount of radiation emitted.

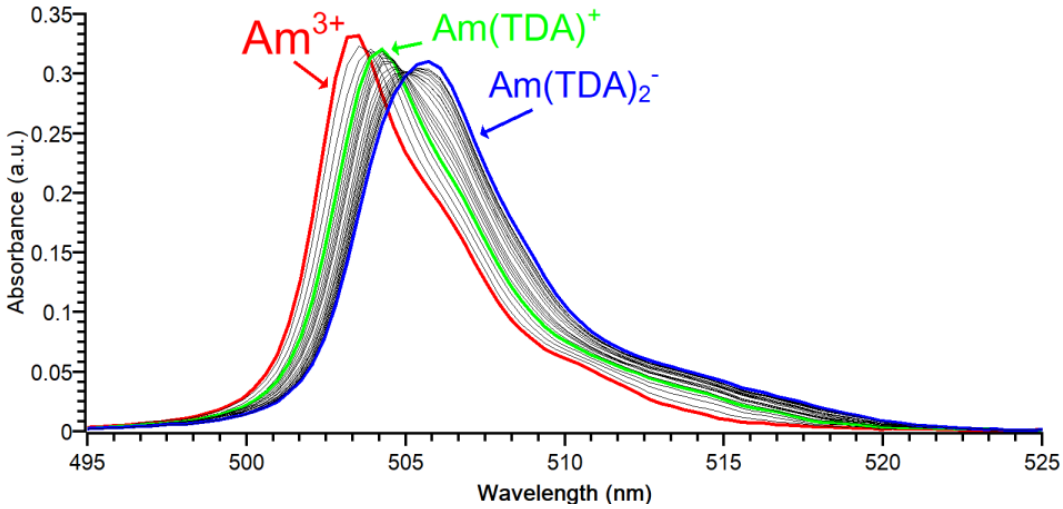

Figure 1.2 An example of a UV-vis spectrophotometric titration of $^{248}Am^{3+}$ with the ligand 2,2'-thiodiactic acid (TDA).

1.4.3.2 Potentiometric Titration

Formation constants can also be determined by potentiometric titrations. In a potentiometric titration, a solution containing a metal, ligand, and occasionally an acid is titrated with a base and the resulting pC_{H+} response is recorded, typically with a glass pH electrode. An example of the potentiometric titration of Nd^{3+} with the ligand 2,2'-thiodiactic acid (TDA) is shown in Figure 1.3. In this example, it can be seen that the presence of metal causes the solution to have a lower pC_{H+} (more acidic) than the sample with no metal as acidic protons are released upon the formation of a complex. This perturbation to the pC_{H+} can be related to the formation constant either manually or by software such as Hyperquad2013.[36]

This approach to determining formation constants is somewhat more versatile than spectrophotometric titrations as it does not require a metal or ligand to have any spectral features. However, this method does require the ligand to have acidic protons that are displaced upon complexation, so not all systems can be quantified using this technique. Additionally, macroscopic quantities of metals are required, so it can be difficult to use with certain actinides.

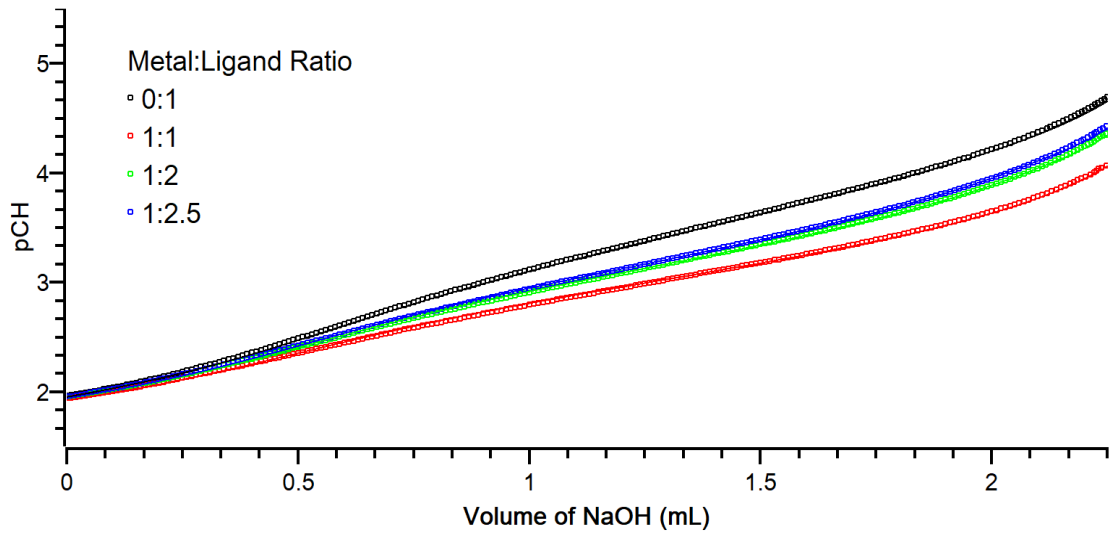

Figure 1.3 An example of a potentiometric titration of Nd^{3+} with the ligand 2,2'-thiodiactic acid (TDA).

1.4.4 Extended X-ray Absorption Fine Structure Spectroscopy

Extended x-ray absorption fine structure (EXAFS) spectroscopy is a synchrotron-based technique that looks at the absorption of x-rays at energies higher than the absorption edge. The photoelectrons ejected by the x-rays are scattered by the surrounding atoms and the resulting backscatter interacts with the forward propagating wave.[37] This results in an oscillation in the absorption spectra at energies greater than the absorption edge.[37] The oscillation can be used to calculate the number, type, and distances of atoms surrounding the atom absorbing the x-rays via the EXAFS equation, Equation 1.11.[37] This is useful as these criteria are important to understanding the structure of complexes.

$$\chi(k) = \sum_j \frac{N_j S_0^2}{kR_j^2} F_j(k) e^{-2R_j/\lambda_j(k)} e^{-2k^2\sigma_j^2} \sin[2kR_j + \Phi_j(k)] \tag{1.11}$$

1.4.5 Density Functional Theory

Density functional theory (DFT) is a computational method to model small to moderately sized chemical systems. In this method, a functional is applied to the electron density of a molecule, complex, or structure to determine many of its properties. Among the many properties that can be studied by DFT, the optimized structures, electronic structure, vibrational spectra (IR spectra), thermodynamic parameters, and excitation spectra (UV-vis) were used in this work.

Many additional corrections can be made for factors including relativistic effects of heavier elements and solvation.

1.5 Research Purpose and Outline

The purpose of this research is to gain a better understanding of why sulfur donating ligands are selective for the trivalent actinides over the lanthanides and to develop actinide selective sulfur-based ligands with greater stability. In addition to reviewing the current understanding of sulfur containing extractants, a novel method for quantifying the most common sulfur containing extractant, HC301, by permanganometric titration is reported and the mechanism for the extraction of transcurium actinides by HC301 is studied. Additional efforts to develop more stable alternatives to dithiophosphinic acid extractants are also detailed.

CHAPTER 2

SULFUR DONATING EXTRACTANTS FOR THE SEPARATION OF TRIVALENT ACTINIDES AND LANTHANIDES

Adapted with permission from *Coordination Chemistry Reviews*

Nathan P. Bessen,[1] Jessica A. Jackson,[1,2] Mark P. Jensen,[1,2] Jenifer C. Shafer[1,2]

The following chapter has been adapted from the published review article.

2.1 Abstract

The effective separation of trivalent actinides and lanthanides is capable of reducing the long term radiation hazard associated with used nuclear fuel. This class of separation exploits the tendency of ligands containing large and polarizable soft donor atoms to preferentially bind to the trivalent actinides instead of the lanthanides. Among the soft donors, nitrogen and sulfur based ligands have received the most attention with sulfur donors generally having greater selectivity for the actinides. Herein, the speciation, mechanism, and selectivity for the extraction of lanthanides and actinides from aqueous media into an organic phase by various sulfur containing extractants is reviewed.

2.2 Introduction

The significant and scalable approach for actinide/lanthanide group separations centers on the principle that actinides may be able to interact more strongly with soft donors, such as chloride, nitrogen and sulfur, relative to lanthanides of comparable charge density. This is most broadly explained on the basis of Pearson's Hard Soft Acid Base chemistry, where softer, more polarizable metals interact preferentially with softer, more polarizable ligand donors[18]. This stronger interaction with soft donors was first discovered by Street and Seaborg by examining the preferential interaction of chloride and americium relative to lanthanides, such as promethium[19]. The stronger interaction between actinides and soft donors relative to the lanthanides is generally thought to be caused by the actinides increased ability to interact more

[1] Department of Chemistry, Colorado School of Mines, 1500 Illinois St, Golden, CO 80401, United States
[2]Nuclear Science and Engineering, Colorado School of Mines, 1500 Illinois St, Golden, CO 80401, United States

covalently with soft donors[38]. Although heavy actinides were long thought to lack any covalency due relativistic effects encouraging the contraction of the 5f orbitals within the core electronic structure[39], recent work with berkelium, californium and einsteinium show their ability to bond with some degree of covalency with dipicolinic acid[40–43] and borates[42,44–46].

The origins of the actinide covalency in the literature are frequently debated, as is the extent to which covalency is responsible for controlling trivalent actinide/lanthanide group separations. An emerging idea is that, due to the multiplicity of available orbitals and varying orbital energies across the actinide series, the specifics of actinide-ligand covalency are likely dependent on the given actinide and ligand involved[40–44,46]. This idea more closely mirrors transition metal chemistry, where a given metal-ligand pairing can show unique chemistry across a series of 5f elements. A general class of separations that has limited review in the literature are those based on sulfur-actinide interactions.

While separations centering on selective sulfur-actinide interactions are demonstrated to be the most efficient single-stage trivalent lanthanide-actinide separations, sulfur has generally received little attention relative to nitrogen donating ligands[9,20,22–24,40,47–50]. Some of this lack of attention is due to complications arising from sulfur contamination in high-level waste streams[51], the poor radiation resistance of sulfur ligands[13,52], and the difficulty of extractant synthesis and purification[6–8]. Despite these potential issues, sulfur containing ligands provide remarkably high separation factors that could be utilized in more efficient separation processes than nitrogen based separations[7,8,12,28]. Bis(2,4,4-trimethylpenthy)dithiophosphinic acid, Cyanex 301 (HC301) in Figure 2.1, has reported separation factors between Am and Eu, $\mathrm{SF}_{\mathrm{Eu}}^{\mathrm{Am}} = \mathrm{D}_{\mathrm{Am}}/\mathrm{D}_{\mathrm{org}}$ where $\mathrm{D}_{\mathrm{M}} = [\mathrm{M}]_{\mathrm{org}}/[\mathrm{M}]_{\mathrm{aq}}$, of greater than 5,000[12]. See Section 2.4.3 for a more complete description. Trifluoromethyl substituted aryl dithiophosphinates have the highest $\mathrm{SF}_{\mathrm{Eu}}^{\mathrm{Am}}$ever reported using any approach at greater than 100,000[7]. More explanation regarding separation factors and distribution ratios, D, is provided in Section 2.4.3 (*vide infra*). The purpose of this review is to summarize the work done with various sulfur containing ligands for the separation of actinides from lanthanides.

2.3 Origin of Selectivity

The preference that soft donors have for actinides over lanthanides is thought to stem from greater covalency encouraging shorter and stronger actinide-soft donor bonds, though reports exist that suggest some covalent actinide-ligand interactions have longer, weaker bonds[53]. It has been shown that U(III) and Pu(III) both form shorter bonds with sulfur than with lanthanides of nearly the same ionic radii, La(III) and Ce(III) when using thiophosphorylphosphinothioic amides, $N(SPR_2)_2$, (R = Ph, *i*Ph, and H)[24] and arylthiolate ligands[25]. In computational modelling of the same complexes, the shorter bond lengths were also observed an interpreted to indicate increased covalency[24,25]. Although complexes of thiophosphorylphosphinothioic amides with both U(III) and Pu(III) showed shorter bond lengths than with similar lanthanides, the Pu-S bond length, although shorter than the U-S bond, was not a short as expected based on the different crystallographic radii of U and Pu. Therefore, it was concluded that the Pu-S interactions had a degree of covalence intermediate between that of the U-S bonds and the lanthanide-S bonds[24]. This lead Gaunt et al. to conclude that the light actinides bond more covalently with sulfur, but this effect decreases along the series, possibly terminating at Am or Cm[24].

This hypothesis has been difficult to test as only small amounts of the actinides heavier than Pu are available and their high specific activities make them challenging to handle. Another consequence of the high specific activity of transuranic actinides is the damage to crystal structures by self-irradiation. Despite the associated challenges, single crystals of $(NBu_4)Am[S_2P(tBu_2C_{12}H_6)]_4$ have been synthesized and analyzed along with the analogous Nd and Eu crystals[26]. Single crystal XRD has shown that the Am-S bond (2.921(9) Å) is shorter than with Nd (2.941(8) Å), a lanthanide with a similar ionic radius[26]. Although the uncertainty at the 68% confidence interval associated with these measurements makes it difficult to say with confidence that Am and Nd have different metal-sulfur bond lengths, UV-vis spectroscopy and luminescence spectra of the same crystals show that for Am, the ligand field has a far greater influence on the metal's electronic structure, as reflected in the f-f electronic transitions, than for either Nd or Eu[26]. In crystals of Am, Cm, and Cf dithiocarbamates, the heavier actinides showed shorter metal-sulfur bonds than the similarly sized lanthanides when accounting for changes in the metal's ionic radii[54]. This suggests Am and heavier actinides have greater interactions with

soft, sulfur donating ligands than lanthanides. The greater interactions of sulfur donating ligands with the actinides may manifest as stronger bonds and different speciation that may enable an effective method of separating lanthanides and actinides.

The selectivity that the above sulfur donors display towards actinides is thought to be due to the ability of actinides to bond more covalently than lanthanides. The source of this greater covalency is thought to arise from energy degeneracy or orbital overlap between the metal and ligand or some combination of both[55]. Density functional theory (DFT) experiments have shown that the 5f orbitals of Am overlap with orbitals in dithiophosphinic acids in a bonding manner while the same ligand orbitals are antibonding to the 4f orbitals of Eu[33,34]. Across the heavy actinides, covalency was found to increase as due to greater energy degeneracy between the actinides and dithiophosphinic acid[35]. Additional DFT studies have shown that the bonding of a dithiophosphinic acid to Am is energetically more favorable than bonding with Eu[31,32].

The more favorable bonding of dithiophosphinic acid to Am than Eu has not only suggests the formation of stronger bonds, but also brings the possibility of different speciation for lanthanides and actinides. Bhattacharyya et al. found that with HC301, Am would form complexes of the form $Am(C301)_3$ whereas Eu could form two complexes $Eu(C301)_3$ and $Eu(C301)_2(NO_3)$[32]. These differences between lanthanides and actinides can cause selectivity in an extraction system due to the greater extractability of the actinide[31,35] or differences in the speciation of the metals that have different extractabilities in the organic phase[32].

2.4 Sulfur Donating Extractants

Many different types of sulfur containing extractants have been studied for their application in the organic phase of a liquid-liquid extraction system. Sulfur containing extractants would preferentially extract actinides to the organic phase while the lanthanides primarily remain in the aqueous phase. Systems that use sulfur containing extractants are already used industrially for the separation of cobalt and nickel from magnesium and manganese[56]. These extractants have yet to be developed into a technologically feasible means for the separation of lanthanides and actinides. Lab scale experiments have shown great promise regarding the selectivity of sulfur donor extractants in actinide/lanthanide separation, but barriers to their implementation due to the limited chemical and radiolytic stability of the extractants and the impact of sulfate, a decomposition product, on waste processing remain[51].

Two main mechanisms exist by which these extractants function, solvation and cation exchange. Solvating extractants are neutral, polar molecules that solvate metal ions in the organic phase when the metal is bound by the appropriate anions to maintain a neutral charge[57]. Solvating extractants usually extract most efficiently at higher acid concentrations and metals can be stripped from them at low acid concentrations[57]. Cation exchange extractants have acidic functional groups capable of exchanging a hydrogen ion initially bound to the extractant in the organic phase with a metal ion from the aqueous phase[57]. Unlike solvating extractants, cation exchange extractants extract most strongly at low acid conditions and can be stripped at high acid concentrations[57].

Synergism can occur when a mixture of extractants is used and the resulting extraction of the metal is greater than the summed metal recovery by each individual extractant, at the same concentration. Although synergism is a complex process, several mechanisms exist through which synergistic extraction can occur[30,58]. Synergism can be caused by the opening of a chelate ring and the addition of a lipophilic adduct on the newly vacant site, the replacement of coordinated waters with a more lipophilic group, or an increase in the coordination number of the metal ion allowing additional lipophilic molecules to bond to the complex[30,58]. Additionally, the addition of a synergic agent can alter other aspects of the extraction system by causing changes in interfacial properties, or effecting aggregation and micelle formation[58].

In liquid-liquid extractions, the amount of metal extracted is quantified by the distribution ratio (D). The distribution ratio is defined as the concentration of analyte in the organic phase divided by the concentration of analyte in the aqueous phase, as shown in Equation 2.1. When extracting radioactive materials, the radioactivity of each phase is often substituted for the concentration as radioactivity is proportional to the concentration and is typically easier to measure than the concentration. To quantify the efficacy of a separation using liquid-liquid extraction, the separation factor (SF) is evaluated. The separation factor is the ratio of the distribution ratios of the species being separated as shown in Equation 2.2. In this paper, the distribution ratio of the actinide is the numerator while the ratio for the lanthanide is the denominator. Therefore, a SF greater than unity indicates that actinides are extracted more readily than lanthanides and a separation factor of one indicates no separation.

$$D = \frac{[M]_{org}}{[M]_{aq}} = \frac{A_{org}}{A_{aq}} \tag{2.1}$$

$$SF_{An/Ln} = \frac{D_{An}}{D_{Ln}} \tag{2.2}$$

Among the many types of sulfur bearing extractants, a general trend is found. When comparing phosphinic, monothiophosphinic, and dithiophosphinic acids, the extraction strength decreases with increasing sulfur in the extractant, but the separation factor increases in the same order. This is true for phosphoric and phosphonic acids as well[3,59,60].

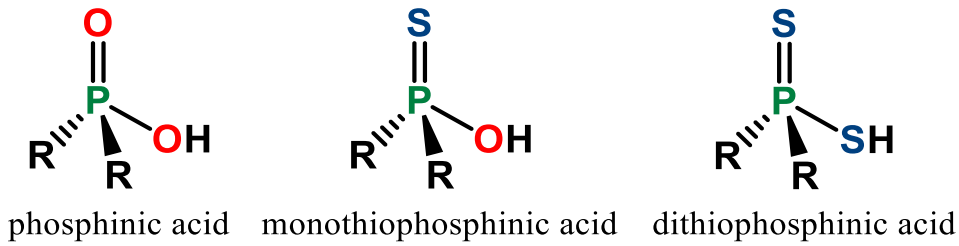

Figure 2.1 Phosphinic, monothiophosphinic, and dithiophosphinic acid functional groups[3].

2.4.1 Carbamoylmethylphosphine Sulfide

Carbamoylmethylphosphine oxides (CMPO) have been widely studied for their ability to non-selectively extract the trivalent lanthanides and actinides from highly acidic media as in the transuranic extraction (TRUEX) process. Since the actinides show a preference for soft donors, Matloka et al. studied softer, sulfide versions of CMPO, carbamoylmethylphosphine sulfide (CMPS) for the separation of lanthanides and actinides[4].

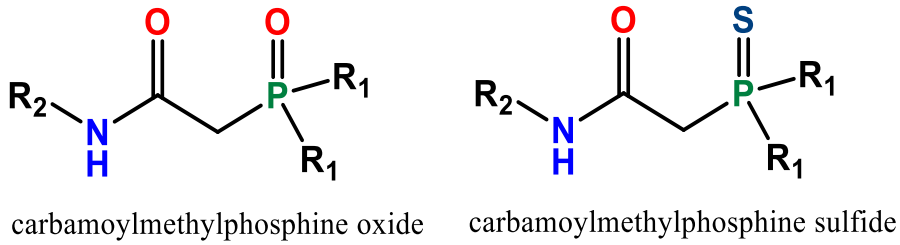

Figure 2.2 Structures of a generic carbamoylmethylphosphine oxide and carbamoylmethylphosphine sulfide. R_1 = methyl, t-butyl, t-pentyl. R_2 = t-butyl, t-pentyl[4].

Matloka et al. prepared the various types of CMPS they used by the condensation of 2-(diphenylphosphorothioyl)acetic acid with the appropriate amine containing substituent as shown in Figure 2.3[4].

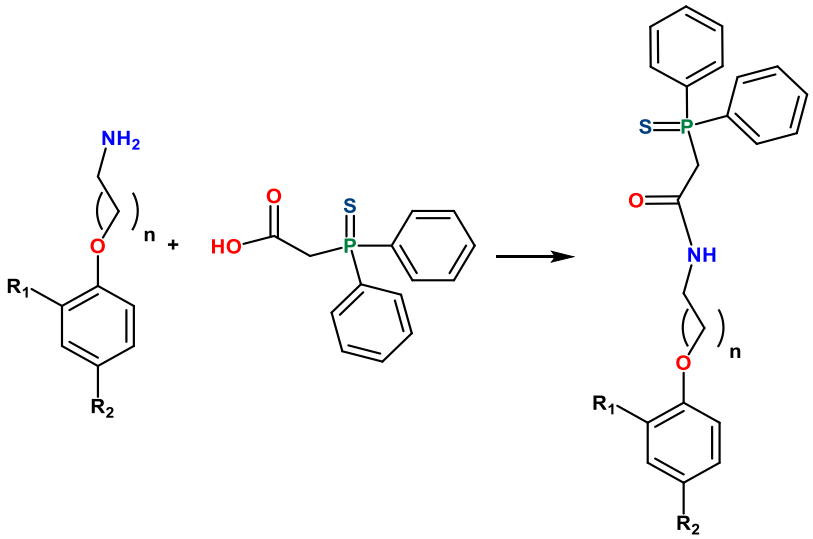

Figure 2.3 Synthetic procedure for the preparation of CMPS[4]. As tested, R_1 and R_2 were combinations of methyl, *t*-butyl, and *t*-pentyl groups and n=1,2[4].

All CMPS varieties are solvating extractants. They were found to extract lanthanides and americium poorly from 1 M nitric acid with no measurable separation in distribution experiments with ^{241}Am and ^{152}Eu when CMPS was dissolved in methylene chloride - the only solvent tested[4]. Unlike typical experiments with CMPO, these systems did not include phase modifiers to improve the solubility of the extracted metal-ligand complex[17,58,61–63]. With CMPO, phase modifiers are used to prevent the formation of a third phase[58]. A third phase occurs when the single organic phase splits into two distinct organic phases, commonly due to a high concentration of metal ions or acid in the organic phase. It remains to be seen if third phases form as readily with CMPS as with CMPO. Additionally, when single crystals of the terbium CMPS complex were studied by XRD, no Tb-S bonding was seen[4]. Assessment of this system with phase modifiers might be appropriate, since these are crucial for metal extraction in the CMPO system.

Although the CMPS sulfide does not seem to interact with the lanthanides or actinides, CMPS has been shown to form metal-sulfur bonds with softer metals. Aleksenko et al. synthesized and studied several different CMPS and CMPO derivatives with Pd(II) and Re(I)[64]. Pd and Re both formed metal-sulfur and metal-oxygen bonds with the CMPS and the expected metal-oxygen bonds with CMPO[64].

2.4.2 Di- and Mono- Thiophosphoric Acids

Di- and mono- thiophosphoric acids are the sulfur analogs of the widely used cation exchange extractant bis-(2-ethylhexyl)phosphoric acid (HDEHP). For this reason, the extractants bis-(2-ethylhexyl)monothiophosphoric acid (HDEHTP) and bis-(2-ethylhexyl)dithiophosphoric acid (HDEHDTP) have been the most studied extractants in this class.

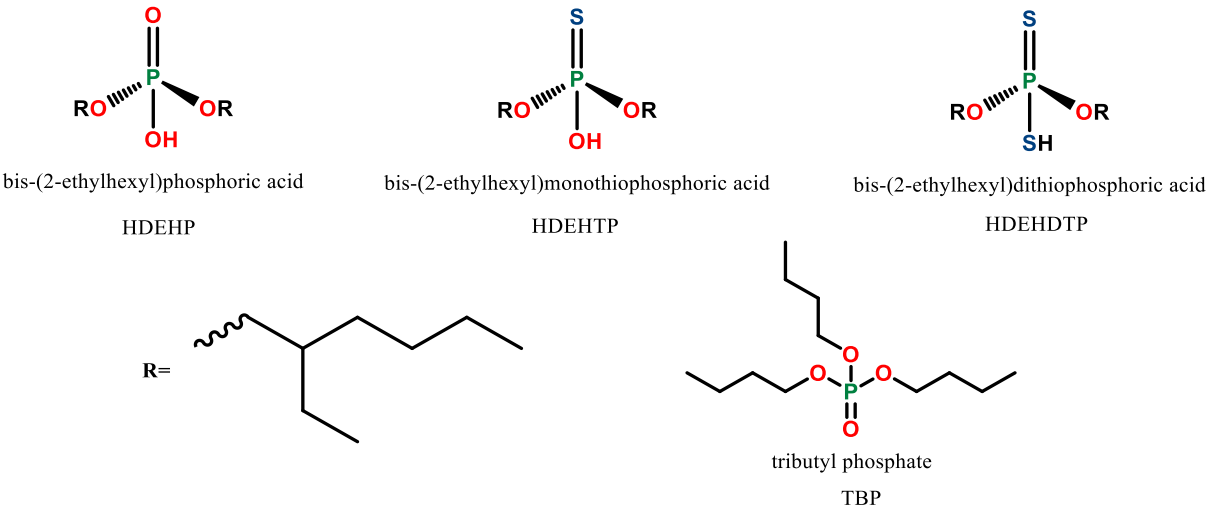

Figure 2.4 Structure of HDEHP, HDEHTP, HDEHDTP, and TBP[5].

Dithiophosphoric acids are typically synthesized by the reaction of phosphorus pentasulfide with the appropriate anhydrous alcohol[65,66]. Unfortunately, hydrogen sulfide evolves during the course of the reaction. This reaction is sensitive to moisture, as water will cause the formation of the triprotic inorganic acid instead of the desired monoprotic diester[65]. This sensitivity to water does complicate the synthesis, but reasonable yields can be achieved with the proper attention to reaction conditions.

Pattee et al. was one of the first groups to extract lanthanides and trivalent actinides with a thiophosphoric acid. They found that although HDEHDTP extracts Am and Eu far more weakly than HDEHTP, HDEHDTP gives larger separation factors (SF=2.55) than HDEHTP (SF=0.89) in nitric acid[5]. These separation factors were found to be consistent over a range of approximately pH 1.7 to 3.6 for HDEHDTP and 0.8 to 1.9 for HDEHTP[5]. HDEHP gives a separation factor of approximately 0.06[67]. Xu et al. have confirmed these results in perchloric acid media, by observing the same trend in extractant efficiency and selectivity with HDEHDTP and HDEHTP[60]. They measured similar separation factors of 2.43 (pH 3.13) and 0.68 (pH 2.87)

for HDEHDTP and HDEHTP respectively[60]. These separation factors are considerably lower than those for the dithiophosphinic acids discussed in Section 2.4.3. Small amounts of strongly extracting and non-selective impurities may be present, as was observed with some dithiophosphinic acids[68]. Pattee et al. also considered both fully protonated HDEHDTP in cyclohexane and fully saponified HDEHDTP (i.e. NaDEHDTP) in benzene and observed conventional extraction of Am and Eu in discrete HDEHDTP complexes whereas reverse micelles containing up to 25 water molecules per metal ion were observed for the saponified system[69]. It remains unclear as to whether metal is extracted as discrete complexes, reverse micelles; or some combination of both at intermediate degrees of saponification.

Extracted complex stoichiometry has been found through slope analysis experiments, where the distribution of the metal of interest is measured as a function of extractant concentration and pH. In these studies, one metal atom was found to be extracted by 3 HDEHDTP or HDEHTP molecules according to Equations 2.3 through 2.6[5] and by 6 HDEHP according to Equations 2.7 and 2.8[67]. The authors also suggest that some quantity of water is present in the extracted complex[5], but do not report an attempt to quantify the number of water molecules in the complex. As HDEHTP is ambidentate, it is possible that it may coordinate metal ions with either the oxygen or sulfur site, or both. Although coordination of lanthanides by HDEHTP is unknown, it is plausible that the oxygen coordinates more strongly due to its greater electronegativity. It is likely that the sulfur site is weaker for the coordination of these hard acid cations as demonstrated by the weaker extraction of lanthanides by HDEHDTP than HDEHTP or HDEHP[5]. Co(III) complexes with monothiophosphoric acid been observed with both the sulfur and oxygen coordinating the metal[70]. Although not a monothiophosphoric acid, the monothiophosphinic acid Cyanex 302 (HC302), prefers to coordinate An and Ln ions through the oxygen atoms. EXAFS studies of the Cm, Sm, and Nd complexes of Cyanex 302 indicated each metal was coordinated with 4 oxygen atoms and 1 sulfur atom with a proposed composition of $M(C302)_3(H_2O)$ where the metal was coordinated by all three oxygens from the HC302 and one sulfur out of the three available[9]. The differences between the formulas for HDEHDTP and HDEHTP arise from the tendency for HDEHTP to dimerize much like HDEHP while HDEHDTP is less likely to aggregate due to weaker hydrogen bonding ability brought on by sulfur being less prone to hydrogen bonding than oxygen and more acidic[5,20]. The authors also suggest that some quantity of water is present in the extracted complex[5], but do not report an

attempt to quantify the number of water molecules in the complex. The weakness of the S-H-S hydrogen bond in HDEHDTP is reflected in its aggregation constant, which is reported to be K_3 = 0.145 for formation of $(HDEHDTP)_3$ in benzene[69]. This is also consistent with the work of Zucal et al., who found no evidence for dimerization of short chain (ethyl, propyl, and butyl) dithiophosphoric acids in carbon tetrachloride[71].

$$Am^{3+} + 3HDEHDTP_{org} + xH_2O \rightleftharpoons Am(DEHDTP)_3 \bullet xH_2O_{org} + 3H^+ \quad (2.3)$$

$$Eu^{3+} + 3HDEHDTP_{org} + xH_2O \rightleftharpoons Eu(DEHDTP)_3 \bullet xH_2O_{org} + 3H^+ \quad (2.4)$$

$$Am^{3+} + 1.5HDEHTP_{2,org} + yH_2O \rightleftharpoons Am(DEHTP)_3 \bullet yH_2O_{org} + 3H^+ \quad (2.5)$$

$$Eu^{3+} + 1.5HDEHTP_{2,org} + yH_2O \rightleftharpoons Eu(DEHTP)_3 \bullet yH_2O_{org} + 3H^+ \quad (2.6)$$

$$Am^{3+} + 3HDEHP_{2,org} \rightleftharpoons Am(H(DEHP)_2)_{3,org} + 3H^+ \quad (2.7)$$

$$Eu^{3+} + 3HDEHP_{2,org} \rightleftharpoons Eu(H(DEHP)_2)_{3,org} + 3H^+ \quad (2.8)$$

In addition to the research done with thiophosphoric acids as the sole extracting species, work has been done with synergistic mixtures of thiophosphoric acids with a neutral organophosphorus species. When tributyl phosphate (TBP) is added to the organic phase, less water is extracted than by HDEHDTP alone and the Am/Eu separation factor significantly increases to 25[5]. Pattee et al. proposed this is caused by TBP coordinating to the metal in place of water which causes a decrease in the metal-sulfur bond length and this decrease enhances the covalency of the bond between actinides and sulfur[5].

2.4.3 Dithiophosphinic Acids

Dithiophosphinic acids, Figure 2.1, have been the most widely studied sulfur bearing class of ligands for the separation of lanthanides and actinides with bis(2,4,4-trimethylpentyl)dithiophosphinic acid (HC301), commercially available as Cyanex 301, being of particular interest. This class of extractants have given some of the highest separation factors observed at this time - up to 100,000[7,8,12,28]. As stronger Lewis Bases, the dithiophosphinic acids also have a greater affinity for metals than their dithiophosphoric acid counterparts if the pH is high enough to enable binding[72]. The selectivity that dithiophosphinic acids display towards actinides due to the ability of actinides to bond more covalently than lanthanides due to energy degeneracy, orbital overlap, or some combination of both. This covalency could cause selectivity by enabling stronger bond with the actinides[9,55] or by forming complexes with different structures and extractabilities[10]. For some cases, the extracted complexes of lanthanides and

actinides are the same except for the metal which suggests that stronger interactions between the extractant and actinide drives the observed selectivity[9]. However, in other cases the complexes are different which points to different speciation as the driver of selectivity[10,11]. It may also be possible that both causes can occur simultaneously.

2.4.3.1 Synthesis

Most dithiophosphinic acids are not commercially available necessitating their synthesis at the laboratory scale. Many synthetic schemes have been developed to produce different types of thiophosphinic acids. Due to the number of different synthesis, only the more widely used procedures that require few unusual or difficult steps will be given here.

For symmetric dithiophosphoric acids, diethylphosphite can be reacted with the Grignard reagent of the desired alkyl chain[6]. The resulting dialkylphosphine oxide is then reduced to a dialkylphosphine by a strong reducing agent such as lithium aluminum hydride[6]. The dialkylphosphine is reacted with sulfur in aqueous ammonia to yield the crude dialkyldithiophosphinic acid, Figure 2.5[6]. Due to the simplicity of the procedure, this is the most commonly used method. This is the method used by Tian et al. and Xu et al[6,59,60]. A similar procedure for this synthesis uses phosphorus trichloride as an alternative to diethylphosphite as a starting material and forms a chlorodialkylphosphane as an intermediate instead of a dialkylphosphine as shown in Figure 2.6[7,8]. Although normally used for the synthesis of symmetric dialkyldithiophosphinic acids, with careful control of the stoichiometry this method has been used to create asymmetric dithiophosphinic acids[8].

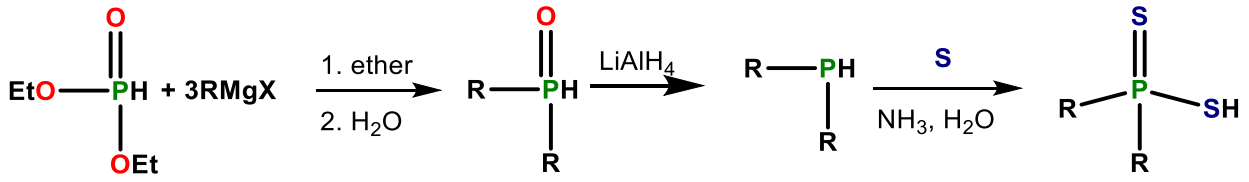

Figure 2.5 Synthetic procedure for dithiophosphinic acids as done by Tian et al.[6]

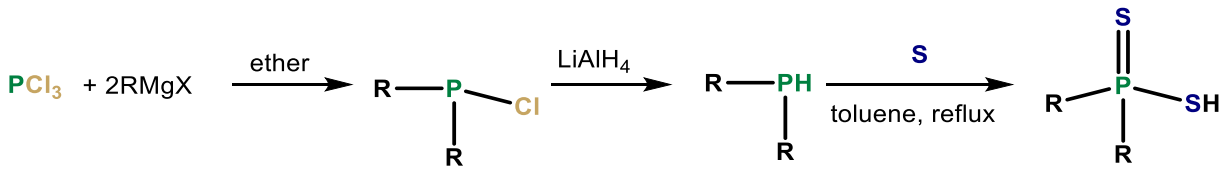

Figure 2.6 Synthetic procedure for dithiophosphinic acids as done by Klaehn et al. and Peterman et al[7,8].

Another procedure for this synthesis uses 1,1-dichloro-N,N-diethylphosphanamine and a Grignard reagent to prepare N,N-diethyldialkylphosphanamine, which is converted into a chlorodialkylphosphane[8]. The chlorodialkylphosphane is reduced to a dialkylphosphine and reacted with elemental sulfur in toluene to prepare the dithiophosphinic acid, Figure 2.7[8].

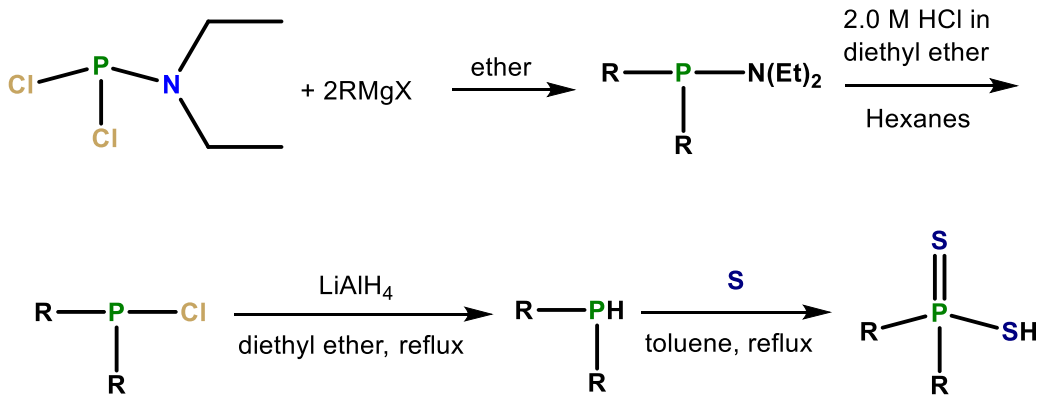

Figure 2.7 Synthesis procedure of dithiophosphinic acids from 1,1-dichloro-N,N-diethylphosphanamine as done by Klaehn et al.[7].

Preparing monothiophosphinic acids is somewhat more difficult than dithiophosphinic acids, but can be done by several means. The dialkylphosphinothioic chloride can be reacted with sodium hydroxide, or the more common treatment of dialkylphosphinic chloride with sodium sulfide, to prepare a monothiophosphinic acid[73].

Throughout the synthesis, storage, and use of these thiophosphinic acids, it is important to be mindful of the formation of impurities. In particular, more oxygenated impurities can have a large impact on the extraction strengths and selectivity of the extractants as these impurities are often stronger extractants and lack selectivity. The effects of these impurities are particularly pronounced when using tracer or small quantities of metals.

2.4.3.2 Effect of Varying Alkyl and Aryl Groups

Many mono- and di-thiophosphinic acids have been tested for their ability to separate f-elements and to determine the impact of the alkyl or aryl group on the separation. Despite the number of different extractants tested, providing a definitive assignment to the role of the alkyl or aryl group on selectivity remains difficult. The thiophosphinic acids evaluated to date and their separation factors for tracer amounts of Am and Eu are shown in Table 2.1. If the pH at which the separation factor was measured has been published, the pH has been included in Table 2.1.

Xu et al. have synthesized and evaluated thiophosphinic acids substituted with many different straight chain and branched alkyl groups and several aryl groups. To evaluate the extraction behavior of these thiophosphinic acids, tracer amounts of Am and Eu in 0.1 M $NaClO_4$ were contacted with a solution of the extractant in xylene[59,60]. Alkyl group substituted extractants were found to provide a lower selectivity for Am over Eu than with branched chain substituted extractants[59,60]. Aryl group substituted extractants typically gave better separations than alkyl group substituted extractants[59] and, by being more acidic, they will likely have stronger extraction from more acidic media[6,59,74].

Tian et al. also synthesized several dialkyldithiophosphinic acids and came to a different conclusion regarding the impact of the alkyl chain on selectivity. They found the separation factors for Am and Eu were nearly unaffected by varying the alkyl group between octyl, 1-methylheptyl, 2-ethylhexyl, and 2,4,4-trimethylpenthyl[6]. The separation factors found by Xu et al. and Tian et al. have a difference of several orders of magnitude, with those found by Tian et al. being much closer to other reported separation factors for dithiophosphinic acids[6,12,59,60,75]. This could be due to difference in pH, which were not reported by Xu et al., or traces of impurities in the organic phase. However, these discrepancies cast some doubt on the findings of Xu et al. as the separation factors they found are substantially different.

The effect of electron donating and withdrawing groups on aryl dithiophosphinic acids was also tested. With electron withdrawing groups, separation factors were increased and with electron donating groups, the separation factors decrease, but extractant strength is increased[59]. Klaehn et al. and Peterman et al., in addition to developing novel synthetic pathways for dithiophosphinic acids, have tested several aromatic dithiophosphinic acids with trifluoromethyl

group on different sites on the benzene rings using phenyltrifluoromethylsulfone (FS-13) as a solvent and a 1 M sodium nitrate aqueous phase. They found that location of the trifluoromethyl group has a profound impact on the selectivity[7,8]. With bis(*o*-trifluoromethylphenyl)dithiophosphinic acid, the remarkably high separation factor of 100,000[7] was observed. For the isomeric bis(*m*-trifluoromethylphenyl)dithiophosphinic acid, the separation factor was two orders of magnitude less[8].

Daly et al. examined this system with sulfur K-edge x-ray absorption spectroscopy and time-dependent DFT. They found that when substituents were present in the *ortho* position, the symmetry of the ligands was reduced to C_2 from C_{2v} due to steric effects and the electron delocalization increased on the aromatic rings[55]. These changes cause the energy of the highest occupied molecular orbital (HOMO) to increase, thus decreasing the HOMO-LUMO gap and creating a softer ligand which promotes greater selectivity for actinides[55]. Pu et al. also found that the steric effects of the trifluoromethyl group greatly impact the extractant's properties[76]. The decreased symmetry may also be responsible for the greater selectivity possessed by branched alkyldithiophosphinic acids as observed by Xu et al. Another possible explanation for the high selectivity of bis(*o*-trifluoro-methylphenyl)dithiophosphinic acid is that that the trifluoromethyl groups are effective at displacing water molecules from the metal center thus raising the entropic contribution to complex formation and increasing selectivity[77].

Overall, the effect of the alkyl or aryl group on selectivity remains unclear. In many cases, little more than the separation factor is known. If more information were available, a more comprehensive explanation for the effect may be determined. Of particular interest would be the structure and coordination of the extracted complexes for extractants other than HC301. This will likely require extended x-ray absorption fine structure (XAFS) as the long alkyl groups of many extractants likely prevent the formation of crystals necessary for single crystal XRD.

Table 2.1 Various mono- and di-thiophosphinic acids and their separation factors for tracer amounts of Am and Eu from nitric acid media. None of the extractants have been saponified prior to extraction.

Phosphinic Acid	$SF_{Am/Eu}$	Solvent	Aqueous pH	Reference
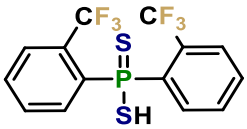	100,000	FS-13	2.5	7
	10,000	FS-13	~2.3	8
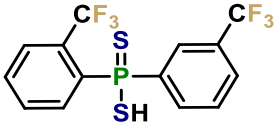	40,000	FS-13	~2.3	8
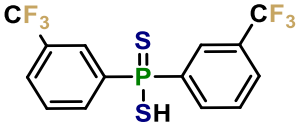	1,000	FS-13	~2.1	8
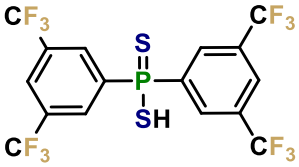	20	FS-13	2.5	7
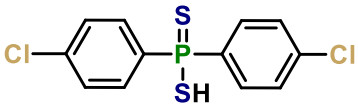	21	Xylene	Not Reported	59
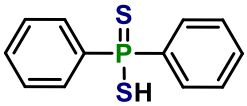	4.4	Xylene	Not Reported	59
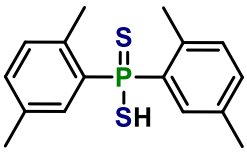	1.8	Xylene	Not Reported	59
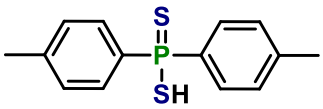	1.3	Xylene	Not Reported	59
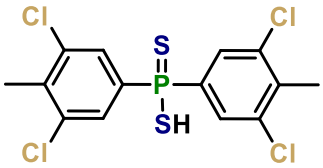	1.0	Xylene	Not Reported	59
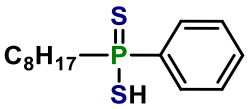	3.0	Xylene	Not Reported	59

Table 2.1 Continued

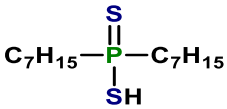	2.1	Xylene	2.82	59,60
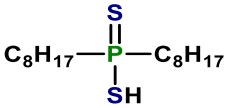	1.4	Xylene	3.51	59,60
	9,700	Toluene	Not Reported	6
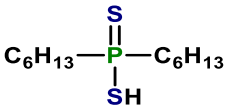	0.71	Xylene	4.90	59,60
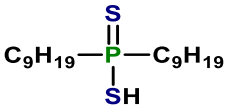	0.3	Xylene	1.94	59,60
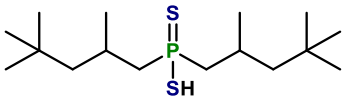	5,900	Kerosene	~2.8-4.4	12
	6,000	Dodecane	3.4	75
	9,800	Toluene	Not Reported	6
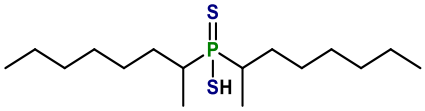	8.3	Xylene	4.12	60
	10,000	Toluene	Not Reported	6
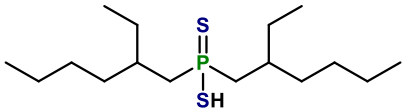	4.2	Xylene	2.36	59,60
	10,000	Toluene	Not Reported	6
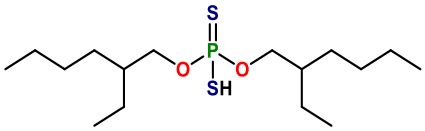	1.3	Xylene	Not Reported	59
	2.43	Xylene	3.13	60
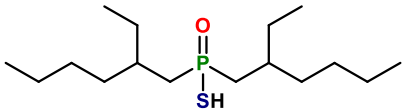	0.8	Xylene	Not Reported	59
	0.96	Xylene	0.86	60
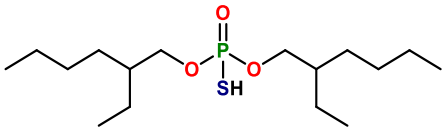	0.3	Xylene	Not Reported	59
	0.68	Xylene	2.87	60

In addition to the above thiophosphinic acids being considered as the sole extractant, dithiophosphinic acids have been studied in combination with neutral, organophosphorus extractants in a synergistic extraction system. Modolo and Odoj have characterized bis(phenyl)-,

bis(fluorophenyl)-, and bis(chlorophenyl)-dithiophosphinic acids with many synergic, solvating extractants. They found the extractant strength increases in the order of phenyl < fluorophenyl < chlorophenyl, but as the extractant strength increases, the separation factor decreases[78,79]. Xu et al. also observed that an increase in extractant strength corresponds to a decrease in selectivity, even though no synergists were used in Xu's work[59].

2.4.3.3 Mechanisms

The precise mechanism by which dithiophosphinic acids extract lanthanide and actinide ions is not universally agreed upon, but it is generally accepted that dithiophosphinic acids are cation exchange extractants that exchange protons for metal ions in the extraction process. A more complete understanding of the mechanism by which these acids extract could lead an improvement of the separation of lanthanides and actinides. However, uncertainty remains about the effect of extractant aggregation, stoichiometry of the extracted complexes, impact of saponification, and effect of solvents.

In solution, purified HC301 has been found to weakly dimerize in deuterated *n*-heptane (K_2=0.67)[3] and toluene (K_2=0.78)[80]. Therefore, under typical extraction conditions, both HC301 monomers and dimers are present and able to impact the extraction of metal. In contrast, the monothiophosphinic acid analog, bis(2,4,4-trimethylpentyl)monothiophosphinic acid (HC302), (K_2=20)[81] and its phosphinic acid analog, bis(2,4,4-trimethylpentyl)phosphinic acid (HC272), (K_2=1.0 x 10^3)[82] are substantially dimerized.

When Jensen and Bond conducted distribution experiments in dodecane and accounted for changes in the concentration of extractant dimers, slope analysis showed three molecules of purified HC301 or HC302 are necessary for the extraction of one trivalent lanthanide or actinide as per Equations 2.9-2.10, but the more strongly dimerized HC272 extracts trivalent metals using three dimers of $H(C272)_2^-$, Equation 2.11[3,9]. The complexes that are proposed to be formed from these reactions are shown in Figure 2.8. This behavior was further confirmed by SANS studies of the Cyanex 301 solutions[83,84]. Later XAFS studies of the coordination environments of Cm, Sm, and Nd extracted by HC301 were best fit with 6 sulfur atoms which corresponds to three molecules of HC301[9]. XAFS also showed similar bond lengths for lanthanides and actinides with HC301, and metal-sulfur distances consistent with hexacoordination[9]. Since XAFS shows the same number of sulfur atoms coordinating to both the lanthanides and actinides with HC301, yet

selectivity is observed, they proposed that the selectivity must be due to greater covalency with actinides under their extraction conditions[9].

$$M^{3+} + 3HC301_{org} \rightleftharpoons M(C301)_{3,org} + 3H^+ \quad (2.9)$$

$$M^{3+} + 3HC302_{org} + H_2O \rightleftharpoons M(C302)_3(H_2O)_{org} + 3H^+ \quad (2.10)$$

$$M^{3+} + 3HC272_{2,org} \rightleftharpoons M(H(C272)_2)_{3,org} + 3H^+ \quad (2.11)$$

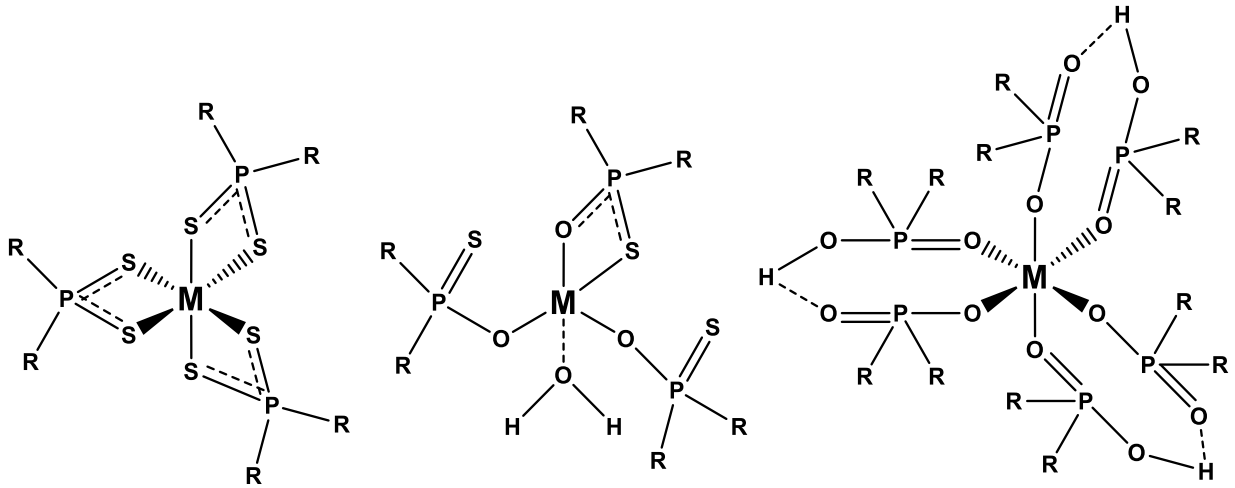

$M(C301)_3$ $M(C302)_3(H_2O)$ $M(H(C272)_2)_3$

Figure 2.8 Proposed structures of the complexes extracted in Equations 2.9 to 2.11[3,9]. R=2,4,4-trimethylpentyl.

Xu et al. and Pu et al. studied the reaction of lanthanides with the ammonium salts of HC301[85] and aromatic dithiophosphinic acids[77] in ethanol. UV-vis and calorimetric titrations showed the step-wise addition of dithiophosphinates to the metal center ultimately leading to complexes of one metal coordinated by three dithiophosphinates[77,85]. Formation constants and thermodynamic parameters were determined this data and enable the calculation of speciation for most of the lanthanides with HC301 in ethanol[85]. Although this system is not directly comparable to the solvent extraction system used by Jensen and Bond[9], it is worth noting that the same complex was observed at the endpoint of the titrations and from solvent extraction.

The extraction mechanisms shown in Equations 2.9-2.11 are not the only proposed mechanisms. Tian et al. used XAFS to characterize the complexes formed when purified HC301 extracts Am in hydrogenated kerosene[11] and La, Nd, and Eu in toluene[10]. They found seven sulfur atoms and the oxygen from a water molecule are coordinated to the lanthanides and eight

sulfur atoms and no oxygens are coordinated to Am, suggesting that 4 molecules of HC301 participate in the extraction as shown in Figure 2.9[10,11]. These results were also obtained by a mass spectrometry experiment[10]. Due to the difference in the coordination environments of lanthanides and actinides in these results, they propose that differences in the hydration of the metal are responsible for the selectivity observed with HC301.

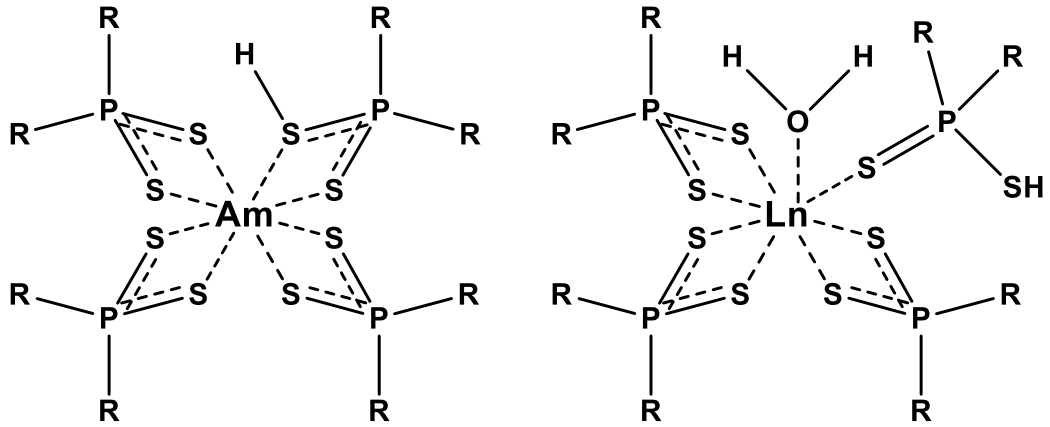

$Am(H(C301)_4)$ $M(H(C301)_4)(H_2O)$

Figure 2.9 Speculative structures of the complexes postulated by Tian et al[10,11]. R=2,4,4-trimethylpentyl.

Zhu et al. have also studied the extraction of lanthanides and actinides with purified HC301 in kerosene using slope analysis distribution studies. They found four HC301 molecules are required for the extraction of one trivalent actinide or lanthanide when they assumed that all HC301 is dimerized in the slope analysis[12]. This group has also reported the widely cited Am and Eu separation factor of 5900 for purified HC301 with no additional synergistic reagents[12]. This group's studies that show four HC301 moieties used in the extraction of lanthanides also show consistent coordination environments with single crystal XRD studies of dithiophosphinic acids with smaller alkyl groups[26,86,87]. Single crystals of metal complexes with dithiophosphinic acids with more sterically demanding alkyl groups, such as cyclohexyl groups, show three dithiophosphinic acids[84].

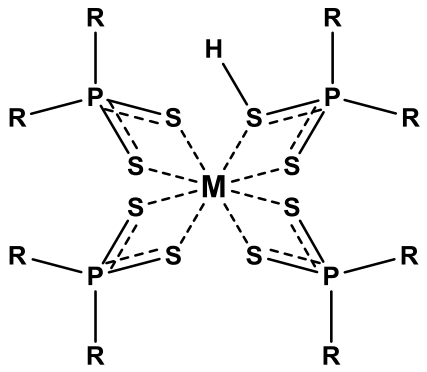

$M(H(C301)_4)$

Figure 2.10 Speculative structures of the complexes postulated by Zhu et al[12]. R=2,4,4-trimethylpentyl.

A third mechanism for lanthanide extraction by HC301 has also been identified for the heavy lanthanides. While light lanthanides form inner sphere complexes with the Cyanex 301 anion in organic phases, lanthanides heavier than Eu are extracted as fully hydrated cations with the extractant in the outer coordination sphere when extracted from a 0.1 M solution of the lanthanide nitrate adjusted to pH 3.5 with NaOH or HNO_3[88]. XAFS, UV-vis, and fluorescence measurements of the extracted complexes of heavy lanthanides with 30% saponified HC301 in toluene show only water in the coordination sphere and are similar to the aqua ions whereas the light lanthanides show sulfur and phosphorus from HC301 in the coordination sphere and are quite different than for the aqua ions[88]. Computational studies have also suggested that heavy actinides more prone to be extracted as outer sphere complexes[89]. At higher degrees of saponification, further extraction of water with both light and heavy lanthanides due to the formation of water-in-oil micelles is observed[90,91].

Under the narrow pH ranges tested without saponification of the extractant, slope analysis suggests a consistent metal-to-ligand ratio[3,12]. However, at a higher pH or with a saponified extractant, it is possible that different extracted complexes or micelles may form. Therefore, it is possible that the different mechanisms observed by Tian et al. and Zhu et al., as compared to the mechanism found by Jensen and Bond, arise from saponification of the extractant. Jensen and Bond did not saponify their organic phases for their studies[3,9], whereas Tian et al. and Zhu et al. added a base to partially neutralize the HC301 and promote greater metal uptake[10–12]. Therefore, the differences in the observed mechanisms may both be correct for the different conditions used, but further research is needed to verify this.

In addition to the previous studies, where purified HC301 is considered, the commercially supplied form of HC301 has been studied. HC301 as supplied has been found to contain HC301 is 75-83% of the desired dithiophosphinic acid, 5-8% is neutral phosphine sulfides, 3-6% is the monothiophosphinic acid, and the remainder is unknown[92]. Zhu et al. have tested HC301 as supplied by the manufacturer and found that the separation depends on the concentration of lanthanide in the aqueous phase. With higher lanthanide concentrations and tracer amounts of Am, the separation factor increased[68]. They propose that at low concentrations of lanthanides, the impurities which are not selective extract metals, particularly lanthanides, more strongly than bis(2,4,4-trimethylpentyl)dithiophosphinic acid. The lack of selectivity provided by the impurities are responsible for the low separation factors[68]. As the concentration of lanthanides increases, the impurities become saturated with metal leaving bis(2,4,4-trimethylpentyl)dithiophosphinic acid as the only ligand still capable of extraction, which it does selectively[68].

Dithiophosphinic acids have also been considered in conjunction with other neutral, oxygen donor extractants in synergistic mixtures. Hill et al. have studied lanthanide and actinide separations with synergistic mixtures of purified HC301 and TBP. Using slope analysis of distribution experiment results, they found Am and Eu are extracted through the formation of different complexes as shown in Equations 2.12 and 2.13[75]. Structures of the complexes extracted in Equations 2.10 and 2.11 are shown in Figure 2.11. A maximum separation factor of this HC301 and TBP synergistic mixture was observed at 10% TBP (SF≈6,000), where the separation factor was greater than that of only HC301 (SF≈3,500)[75]. In addition to testing synergistic mixtures of HC301 and TBP, Hill et al. tested mixtures of HC301 with either triphenylphosphate (TPP) or diphenylsulfoxide (DPSO) and were able to modulate the distribution values and separation factors with the use of other synergic agents[75]. Ionova et al. have continued studying synergistic effects of neutral, oxygen donating extractants. They found that for both HC301 and bis(chlorophenyl)dithiophosphinic acid with TBP, tri-*tert*-butylphosphate (T*t*BP), TPP, trioctylphosphine (TOPO), and CMPO, the distribution ratio of Am and Eu is linearly related to both the effective charge on the oxygen of the neutral extractant and the chemical shift of the molecule with ^{31}P NMR[72,93].

$$Am^{3+} + 2HC301_{2,org} + TBP_{org} \rightleftharpoons AmH(C301)_4TBP_{org} + 3H^+ \quad (2.12)$$

$$Eu^{3+} + NO_3^- + HC301_{2,org} + 2TBP_{org} \rightleftharpoons EuNO_3(C301)_2TBP_{2,org} + 2H^+ \quad (2.13)$$

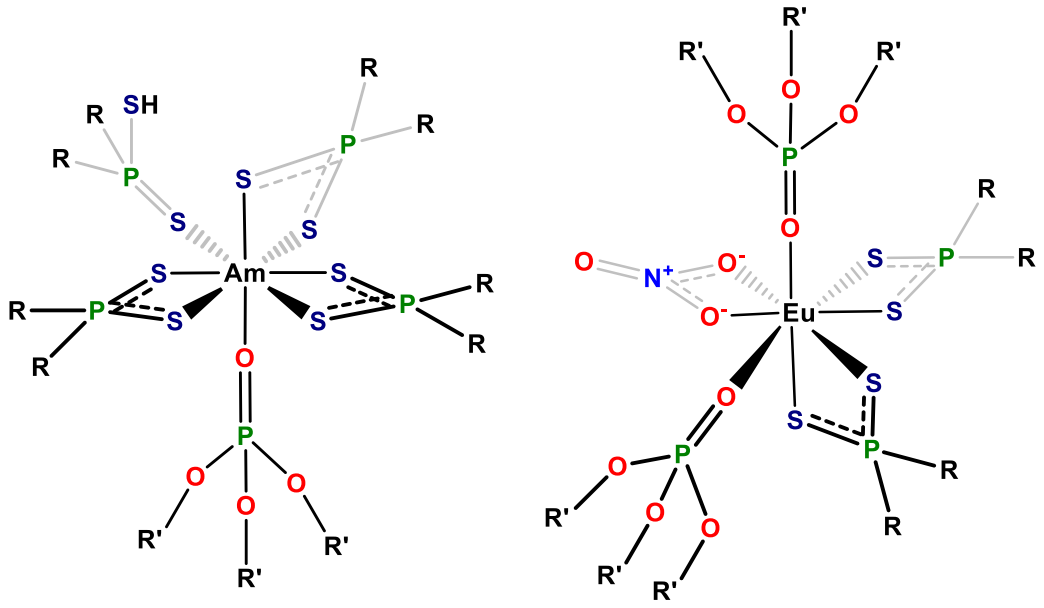

Figure 2.11 Speculative structures of the Am and Eu complexes extracted in Equations 2.12 and 2.13. R=2,4,4-trimethylpentyl and R'=*n*-butyl.

The synergistic effect of TBP or other synergic agents likely arises from the increased coordination of the metal ion by lipophilic moieties[30,58]. In the mechanisms for the extraction of metal solely by HC301 as proposed by Jensen and Bond, three HC301 molecules are coordinated to a metal ion[3]. With all of the sulfur from the HC301 and no water molecules coordinating the metal, as supported by XAFS[9], the metal would be under coordinated with a coordination number of six. Being incompletely coordinated allows the coordination of a TBP molecule or similar moiety causing the entire complex to become more lipophilic and thus more readily extracted. This effect would increase the distribution ratio, but it does not fully explain the increase of the separation factor from 3,500 to 6,000 or the different complexes extracted in Equations 2.12 and 2.13 observed by Hill et al[75].

The greater separation factor with TBP or similar synergic agents may be explained by competition between HC301 and the neutral, solvating extractant. Since the lanthanides are bound less strongly than actinides by HC301, the HC301 bound to a lanthanide can be replaced by TBP more easily as evidenced by the Eu complex from Equation 2.11 having two TBP molecules and only two $C301^-$ species versus the three $C301^-$ from Jensen and Bond's findings.

The substitution of an anionic $C301^-$ with a neutral TBP species requires the coordination of another anion to maintain the charge neutrality required for organic phase solubility.

In the work done by Hill et al., this anion was nitrate which is not lipophilic and therefore poorly extracted. The extraction of nitrate roughly balances the increased lipophilicity resulting from the coordination of TBP to the complex. This crude balance causes the distribution ratio of Eu to change only slightly with the addition of TBP[75]. For Am, the lipophilicity would increase by the addition of a TBP and the retention of HC301. In this case, Am extraction increases with the addition of TBP[75]. This increase in the Am distribution ratio, while the Eu distribution ratio remains relatively unchanged, has been argued to generate the separation factor to increase shown by Hill et al[75].

The solvent effects on the synergistic extraction by a mixture of bis(chlorophenyl)dithiophosphinic acid and TOPO has been briefly studied. Ionova et al. tested the effect of using toluene, xylene, *t*-butylbenzene, or tri-*i*-propylbenzene as the diluent for this extraction and found that the distribution ratio of Am greatly increases as the polarizability of the diluent increases. The degree of increase in the Eu distribution ratio reduces as the bulkiness of a solvent molecule increases[93]. As a result, the separation factor increases from 23.5 for toluene to 45.6 for tri-*i*-propylbenzene [93].

2.4.3.4 Degradation Studies

One concern about the use of dithiophosphinic acids for separating the components of used nuclear fuel is their radiolytic stability. Chen et al. have studied the effects of irradiating both commercial and purified HC301 in an open glass tube with a ^{60}Co γ-source in the absence of an aqueous phase[13]. From NMR spectra of the irradiated extractants, they found both decompose to the monothiophosphinic acid and phosphinic acid, sulfuric acid, and an unidentified, neutral phosphorus containing molecule as shown in Figure 2.12[13]. Initially, both the purified and commercial HC301 are primarily the dithiophosphinic acid with a ^{31}P NMR peak at 65 ppm[13]. As the radiation dose increases, an ingrowth of peaks occurs corresponding to the monothiophosphinic acid (93.5 ppm), phosphinic acid (59.8 ppm), and other phosphorus compounds. Photodegradation of HC301 also produces the monothiophosphoinic and phosphinic acids plus an unknown compound[94]. Accompanying the decomposition of the HC301, the separation factors also markedly decrease[13]. Although both the commercial and purified HC301

decompose, the purified HC301 is more robust, being able to effectively separate tracer amounts of Am and Eu after $1x10^5$ Gy whereas the commercial HC301 only retains that ability up to $1x10^4$ Gy[13].

Despite the radiolysis, Chen et al. propose that under typical process conditions, purified HC301 would be capable of the industrial separation of lanthanides and actinides for approximately 10 hours[13]. Modolo and Odoj have also studied the radiolytic stability of purified HC301 and confirmed the findings of Chen et al. Modelo and Odoj have also found that after irradiation, the separation factor between Am and Eu more sensitive to pH[52]. In addition to HC301, Modelo and Odoj found the irradiation characteristics of bisphenyldithiophosphinic acid and bis(chlorophenyl)dithiophosphinic acid to be much more resistant than HC301[78]. At a dose of $1x10^6$ Gy, 82% of the HC301 had decomposed[52], but under the same conditions, <2% decomposition was observed for the aromatic dithiophosphinic acids[78]. Although not discussed by Modolo and Odoj, these dithiophosphinic acids likely decompose into their monothiophosphinic and phosphinic acid analogues similarly to how HC301 decomposes[13]. Modolo and Seekamp further examined the radiolysis and hydrolysis of bis(chlorophenyl)dithiophosphinic acid. They found that both radiolysis and hydrolysis produce the monothiophosphinic acid and phosphinic acid and that the nitrous acid scavengers amidosulfuric acid, hydrazine, and urea prevent hydrolysis[95]. Although untested, further decreases in radiolysis may be possible by adding a radical scavenger to the organic solution. The greater stability of the aromatic dithiophosphinic acids, in combination with the higher separation factors they provide, is promising for the use of such extractants for the industrial separation of actinides and lanthanides.

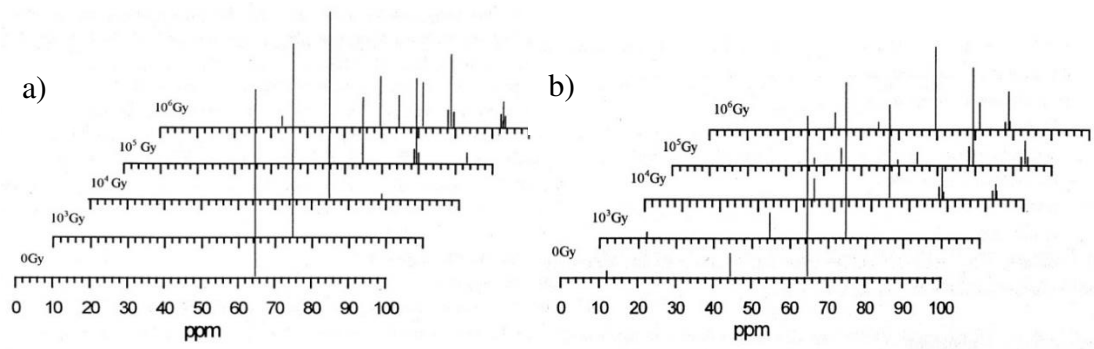

Figure 2.12 a) ^{31}P NMR spectra of purified HC301 at various doses of radiation and b) ^{31}P NMR spectra of commercial HC301 at various doses of radiation[13].

HC301 was also found to be susceptible to degradation by nitric acid[96–98], but not sulfuric acid[96]. As seen with radiolysis and photolysis of HC301, this degradation results in the formation of the monothiophosphinic and phosphinic acids[96]. An intermediate that consists of two HC301 molecules linked by a disulfide bridge has been observed[97,98]. This disulfide intermediate is produced more quickly at higher nitric acid concentrations[97] and therefore should be less of a problem at the low nitric acid concentrations typically used for separations.

The stability of bis(*o*-trifluoromethylphenyl)dithiophosphinic acid has also been tested when in contact with aqueous nitric acid during irradiation. Klaehn et al. found that after 140 days of being in contact with 0.01 M nitric acid, 68% of the dithiophosphinic acid remained and when no acid was present, 81% remained[7]. When the high radiolytic stability of similar bisphenyldithiophosphinic acids is also considered, bis(*o*-trifluoromethylphenyl)dithiophosphinic acid is likely to be quite stable under typical reprocessing conditions.

2.4.4 Miscellaneous Sulfur Containing Extractants

In addition to the sulfur containing extractants detailed above, other reagents have been considered. Zalupski et al. have tested the cation exchange extractant P,P'-di(2-ethylhexyl)-methylenebisthiophosphonic acid and its oxygen analog, P,P'-di(2-ethylhexyl)methylenebisphosphonic acid. They found the bisthiophosphonic acid has lower extractant strength for both Am and Eu than for the phosphonic acid, but has higher selectivity for Am[99]. This increase in selectivity does not enable an effective separation, as Am and Eu are extracted with nearly the same strength, whereas the phosphonic acid extracts Eu more strongly[99]. This behavior is similar to that of monothiophosphinic acids such as HC302, where lanthanides and actinides are extracted to approximately the same degree[3]. Bisdithiophosphonic acids have not been tested for the separation of trivalent actinides and lanthanides although they may be expected to display more selectivity due to additional sulfur sites. They have been observed to extract Gd^{3+} poorly though they hydrolyze below pH 2 and above 11 to 12[100].

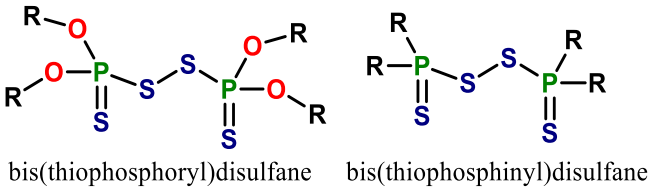

Figure 2.13 Structure of a bis(thiophosphoryl)disulfane and bis(thiophosphinyl)disulfane.

Another class of extractants that may merit more study are the bis(thiophosphoryl)disulfanes and bis(thiophosphinyl)disulfanes. They have been used as extractants for soft, transition metal cations and their complexes with several lanthanides have been characterized[101–104]. Although they have yet to be studied in the context of lanthanide/actinide separations, they may have implications on the use of dithiophosphinic or dithiophoshoric acids as they can form bis(thiophosphinyl)disulfanes or bis(thiophosphoryl)disulfanes by the formation of a disulfide bond in oxidizing conditions[101].

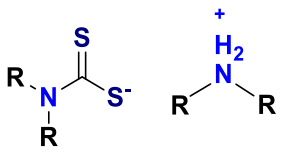

Figure 2.14 Generic structure of a dialkylammonium dithiocarbamate. R= butyl, octyl, phenyl, or benzyl.

Dithiocarbamates have shown high separation factors of up to 32,000. Miyashita et al. have prepared dialkylammonium dialkyldithiocarbamates *in situ* where the alkyl groups were butyl, octyl, phenyl, or benzyl and tested their ability to separate Am and Eu in different organic solvents[105–107]. They act as cation exchange extractants that extract metal as complexes with one trivalent metal ion and three dithiocarbamates to form a neutral complex[105–107]. To avoid the rapid hydrolysis of these extractants when contacted with an acidic aqueous phase, they were synthesized *in situ* by combining carbon disulfide and the appropriate disubstituted amine[106].

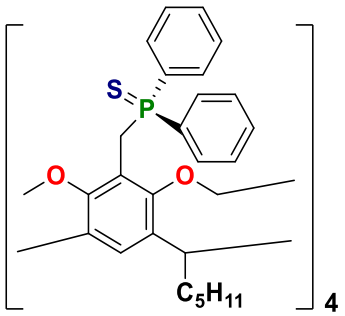

Figure 2.15 Tetrakis(phosphane sulfide) cavitand.

Tetrakis(phosphane sulfide) cavitands have been synthesized and their efficacy for separations has been tested[108]. They were found to extract both Am^{3+} and Eu^{3+} very weakly if at all and with a SF of 1.7[108]. These cavitands were also tested in the presence of the synergists

TBP and TOPO. Although the distribution ratios of both Am^{3+} and Eu^{3+} were increased, almost no selectivity was observed with SFs ranging from 1.1 to 1.2[108].

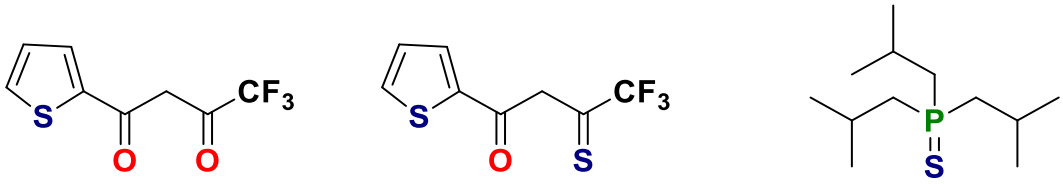

thenoyltrifluoroacetone thiothenoyltrifluoroacetone tri-iso-butylphosphine sulfide

Figure 2.16 Structure of thenoyltrifluoroacetone, thiothenoyltrifluoroacetone, and tri-iso-butylphosphine sulfide.

Thenoyltrifluoroacetone (HTTA) is often used as an extractant for f-block metals that has been tested in conjunction with the sulfur donating synergist tri-iso-butylphosphine sulfide (TBPS) for the separation of Am^{3+} and Eu^{3+}[109]. In extractions from perchlorate media, metal was weakly extracted as complexes of the form $M(TTA)_2(ClO_4)(TBPS)$ in cyclohexane[109]. The SF for this separation is approximately 0.59[109]. A sulfur donating version of HTTA was also prepared, thiothenoyltrifluoroacetone (HSTTA)[109]. It was found to extract trivalent metals as complexes of the form $M(STTA)_2(ClO_4)(HSTTA)$[109]. The addition of TBP caused the formation of $M(STTA)_3(TBP)$ and $M(STTA)_3(TBP)_2$ complexes while increasing the distribution ratio and selectivity for Am^{3+}[109].

2.5 Conclusions

Soft, sulfur donating ligands have shown remarkable success for the difficult, laboratory scale separation of lanthanides and trivalent actinides. Although many of the sulfur containing ligands have not yielded usable separations, several molecules show promise for an efficient industrial scale separation. Generally, extractants that contain anionic sulfur donors and can form chelate rings, such as the dithiophosphinic acids, dithiophosphoric acids, and dithiocarbamates display the best selectivity for actinides. Of these three extractants, dithiophosphinic acids have shown the most promise as the dithiophosphoric acids give lower separation factor and are weaker extractants while the dithiocarbamates rapidly hydrolyze at low pH. Extractants that have neutral sulfur donor sites are much weaker extractants and require the ability to form chelate rings to extract lanthanides or actinides as the sole extractant as seen with the phosphane sulfide cavitands and STTA. Yet extractants with neutral sulfur sites that cannot form chelates can increase selectivity as a synergist, such as TBPS. Perhaps the best example of a successful sulfur

based extractant is bis(*o*-trifluoromethylphenyl)dithiophosphinic acid as this extractant has a high Am/Eu separation factor[7,8] and usable stability[7]. Other sulfur containing extractants, even those that do not show great separations, indicate what drives trivalent actinide/lanthanide selectivity and can help guide the design of better molecules for this challenging separation.

There are several benefits and drawbacks that would be associated with the implementation of one of these extractants on a scale suitable for processing large quantities of used nuclear fuel. There are several extractants with high separation factors[7,8,12] that would enable a more compact and efficient process flowsheet for the separation of actinides and lanthanides. However, these sulfur based extractants will introduce sulfur to the waste stream which adds an additional waste treatment challenge[51] and the synthesis and purification of these extractants is not trivial[6–8]. More research is needed to develop this class of extractants into a useful, scalable separation process.

While many unknown facets of this type of chemistry still exist, the most pressing question relevant to this and other soft donor work is the precise cause of the selectivity that sulfur and other soft donors have for the actinides over the lanthanides. It has been shown that sulfur sometimes forms shorter bonds with the actinides than the lanthanides[24–26], but the cause of this bond shortening remains unknown and may contribute to the observed selectivity of some sulfur donating ligands. Work on structure-function relationships for this class of extractants is needed and would assist in assessing the source of sulfur's selectivity towards the actinides, ultimately leading to improvements in the challenging separation of trivalent actinides and lanthanides.

2.6 Acknowledgements

This work was supported by the U.S. Department of Energy Office of Science, Office of Basic Energy Sciences, Heavy Elements Chemistry Program at Colorado School of Mines under Award Number DE-SC0020189.

CHAPTER 3

PERMANGANOMETRIC QUANTIFICATION OF CYANEX 301 IN *N*-DODECANE

Nathan P. Bessen,[1] Erin R. Bertelsen,[2] Jenifer C. Shafer[1]

3.1 Abstract

The organic soluble extractant bis(2,4,4-trimethylpentyl)dithiophosphinic acid (HC301) has shown selectivity for preferentially extracting trivalent actinides over the lanthanides in the treatment of used nuclear fuel. To maintain control and efficiency of a separation process using this extractant, it is necessary to accurately know specific parameters of the system, including the concentration of HC301 in the organic phase, at any given time. Here, the ability to quickly determine the concentration of HC301 in *n*-dodecane was tested by a one-step permanganometric titration using a double beam UV-vis spectrophotometer. Potassium permanganate ($KMnO_4$) was found to have reduced stability relative to water in both acetone and a mixture of 18-crown-6 and benzene. The addition of HC301 in *n*-dodecane to any of the solutions of $KmnO_4$ was found to decolorize the $KmnO_4$ solutions, but the HC301 was quantified best by the amount of decolorization in solutions of $KmnO_4$ in acetone. Cross validation of a calibration curve relating the amount of $KmnO_4$ consumed to the amount of HC301 added was able to reproduce the known amount of HC301 added with a relative difference of 4.03% or less.

3.2 Introduction

The extractant bis(2,4,4-trimethylpentyl)dithiophosphinic acid, commercially available as Cyanex 301 (HC301), Figure 3.1, is used industrially for the extraction of cobalt and nickel[110] and has shown promise for selectively extracting actinides during the difficult separation of trivalent actinides and lanthanides found in used nuclear fuel[12,111], as have other related dithiophosphinic acids[8,27,76,78,93]. Generally, the separation procedure comprises an organic phase containing the chosen dithiophosphinic acid dissolved in a hydrocarbon diluent, possibly with the addition of a second, synergistic extractant[29,30,78,93]. This organic phase would selectively

[1] Department of Chemistry, Colorado School of Mines, 1500 Illinois St, Golden, CO 80401, United States
[2]University of Massachusetts Lowell, 220 Pawtucket St, Lowell, MA 01854, United States

extract actinides from an aqueous phase containing the metals to be separated and adjusted to a defined pH. To maximize the efficiency and maintain stability of such a process, it is necessary to frequently and quickly determine and adjust various process conditions such as extractant concentration, pH, and phase ratios. Of interest here is the determination of the HC301 concentration in the organic phase as it decreases due to oxidation and hydrolysis[96–98] or radiolysis[13,52,78].

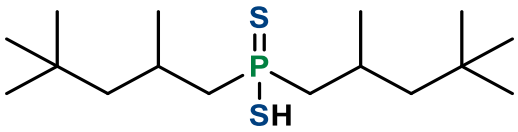

Figure 3.1 Structure of HC301 (bis(2,4,4-trimethylpentyl)dithiophosphinic acid).

Permanganometry is a type of colorimetric redox titration in which the strongly colored and oxidizing permanganate anion (MnO_4^-) as potassium permanganate ($KmnO_4$) is used to quantify the amount of an oxidizable species in a sample. HC301 has reduced sulfur sites that are capable of being oxidized by nitric acid[96–98], so the more powerfully oxidizing MnO_4^- would also be capable of this oxidation—making permanganometry and ideal candidate for HC301 quantification. Additionally, due to the intense visible absorption bands of MnO_4^-, even at low concentrations, its concentration can be quickly determined by UV-vis spectroscopy. As MnO_4^- reacts with HC301, and the concentration of MnO_4^- before and after the reaction can be easily and quickly determined spectroscopically, MnO_4^- seems well suited to be developed into a method to quickly determine the concentration of HC301.

One problem with permanganometry is that permanganometry is traditionally used to analyze oxidizable species in aqueous solution whereas HC301 is dissolved in an organic diluent, frequently *n*-dodecane or kerosene. Therefore, the ability to conduct a permanganometric titration in two different organic phases was studied. The first organic phase was based on purple benzene, where a phase transfer catalyst, in this case 18-crown-6, is used to solubilize $KmnO_4$ in benzene[112,113], and bis(2-ethylhexyl)phosphoric acid was used to solubilize reduced Mn species. $KmnO_4$ was expected to have high stability in this benzene-based solvent, but, due to the hazards associated with benzene, acetone was also considered despite likely being able to react with $KmnO_4$[114]. The stability of $KmnO_4$ in these two organic solvents and water was tested as was the ability to quantify the concentration of purified HC301 in *n*-dodecane via permanganometry with these different $KmnO_4$ solutions.

3.3 Experimental

Potassium permanganate (ACS grade) was obtained from Alfa Aesar and dried in vacuo prior to use. Bis(2-ethylhexyl)phosphoric acid (97%) was purchased from Sigma-Aldrich and purified by the third-phase method published by Hu et al[115]. Benzene (HPLC grade), anhydrous dodecane (≥99%), and anhydrous hexanes (≥99%) were obtained from Sigma-Aldrich and used as supplied. The 18-crown-6 (99%) was purchased from Acros organics. Ethanol (200 proof) and acetone (ACS grade) was purchased from Pharmco by Greenfield Global. Concentrated nitric acid (ACS grade) was purchased from Mallinckrodt Chemicals and hydrochloric acid (ACS grade) was supplied from Macron Fine Chemicals. Sodium sulfate (ACS grade) and ammonium sulfate (ACS grade) were obtained from Fisher Chemical. Neodymium oxide (99.995%) was purchased from Treibacher Industrie AG and converted to the nitrate by dissolution in nitric acid.

Cyanex® 301 GN extractant (HC301) was obtained from Solvay and purified as follows[116]. The crude HC301 was converted to the ammonium salt by bubbling with excess dry ammonia gas generated from the reaction between ammonium sulfate and sodium hydroxide. The precipitate of NH_4C301 was filtered and washed with hexanes then dissolved in a mixture of ethanol in water with 6.8% ethanol and sodium hydroxide was added to achieve a pH of 10. To this, hexane and 0.005 equivalents of neodymium nitrate were added and mixed for several minutes. Once the phases separated, the hexane phase was removed, and this process was repeated for a total of 15 times. Then the remaining aqueous phase was acidified with hydrochloric acid to reprotonate the HC301 which was extracted with fresh hexane. This hexane phase was removed and dried with anhydrous sodium sulfate before evaporation of the hexane to recover the purified HC301. The resulting purity was found to exceed 99.9% by ^{31}P NMR.

3.3.1 Solution Preparation

Solutions of $KmnO_4$ in both water and acetone were prepared by dissolving the required quantity of $KmnO_4$ in the appropriate solvent. Solutions in benzene were prepared by dissolving $KmnO_4$ in a solution containing 40 mM 18-crown-6 and 5.0 mM bis(2-ethylhexyl)phosphoric acid. HC301 solutions were prepared by dissolving the required quantity of purified HC301 in *n*-dodecane.

3.3.2 UV-vis Spectroscopy

UV-vis spectra were collected with a Cary 300 Bio UV-Visible Spectrophotometer. Quartz cuvettes with a 1 cm pathlength were used for all samples. The reference cell was loaded with the same solvent as used in the sample except for the quantification of HC301 in dodecane using potassium permanganate dissolved in acetone. Due to the limited stability of MnO_4^- in acetone, the same $KmnO_4$ solution was used in both the sample and reference cell and the HC301 sample to be quantified was added to the sample cell.

3.4 Results and Discussion

To determine the concentration of $KmnO_4$ by UV-vis, the value for the molar absorption coefficient is required for each solvent. Equation 3.1 shows the formula for Beer-Lambert Law by which the absorbance of a sample (A) is related to the concentration of an absorbing species (c) and pathlength (ℓ) by the molar absorption coefficient (ε). These were determined by preparing samples with different concentrations of $KmnO_4$ in water or acetone and immediately measuring their UV-vis spectrum, Figure 3.2. If the absorbance at a single wavelength (λ) is plotted against the concentration of the absorbing species and the pathlength is constant, the slope of the resultant line is the molar absorption coefficient and the y-intercept should approximate zero barring no other interferences. As $KmnO_4$ was found to be much less soluble in the benzene solvent and more difficult for permanganometry, the molar absorption coefficient was less rigorously determined. The molar absorption coefficient was estimated from the slope between the origin and the absorbance of a single point, 0.058 mM $KmnO_4$ in benzene. This concentration is also the concentration at which this benzene-based solvent is saturated with $KmnO_4$. All of the molar absorption coefficients and related information is shown in Table 3.1.

$$A = \varepsilon \ell c \tag{3.1}$$

The plots of absorbance as a function of $KmnO_4$ concentration in water and acetone, Figure 3.2, are both linear and intercept the y-axis at close to zero as would be expected from the Beer-Lambert Law. From these plots, the molar absorption coefficient was determined with the maximum relative standard deviation being 3%. The molar absorption coefficients are found to increase with the decreasing polarity of the solvent.

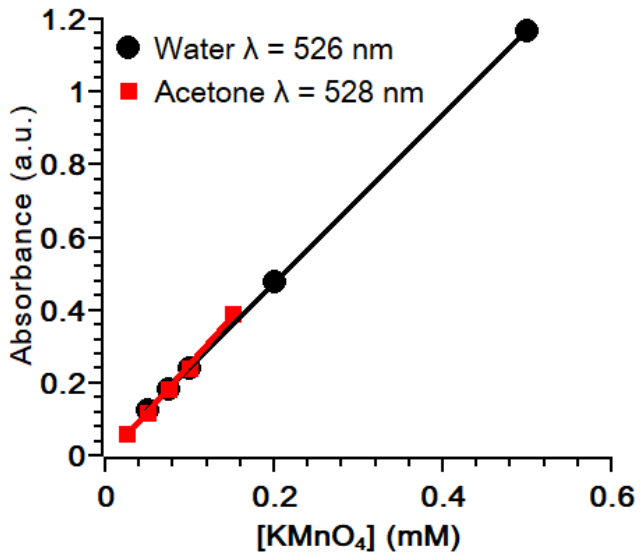

Figure 3.2 Calibration curves of $KmnO_4$ in water (λ = 526 nm) and acetone (λ = 528 nm).

Table 3.1 Molar absorption coefficient (ε) measured at λ_{max} and intercept for $KmnO_4$ in water, acetone, and benzene.

Solvent	λ_{max} (nm)	ε ($mM^{-1}\cdot cm^{-1}$)	y-Intercept	r^2
Water	526	2.323 ± 0.005	0.011 ± 0.001	0.99998
Acetone	528	2.62 ± 0.08	-0.010 ± 0.007	0.997
Benzene	525	13.6		

3.4.1 Permanganate Stability

The stability of $KMnO_4$ was observed in water, acetone, and benzene by UV-vis and the results are shown in Figure 3.3. The $KMnO_4$ in water is stable and no decrease in its concentration was observed during 1200 minutes of observation. The stability is greatly reduced in both organic solvents and negligible quantities of $KMnO_4$ remain after approximately 300 minutes. The stability of $KMnO_4$ in the benzene solution is higher than for acetone, as the rate at which the MnO_4^- concentration decreases is slower in benzene than acetone. Although the stability was lowest in acetone among the organic solvents tested, $KMnO_4$ is more soluble in acetone than the benzene mixture. The ability to dissolve greater quantities of $KMnO_4$ partly offset the reduced stability and appears to offer a reasonable working time of approximately 200 minutes if considerations are taken for the decreasing concentration of $KMnO_4$. This possibility

is beneficial as it is desirable to eliminate the use of benzene when possible for a less hazardous solvent like acetone. Toluene or xylene could also be considered as less hazardous alternatives to benzene but would have similar low solubility for $KMnO_4$ while being less oxidation resistant than benzene[117].

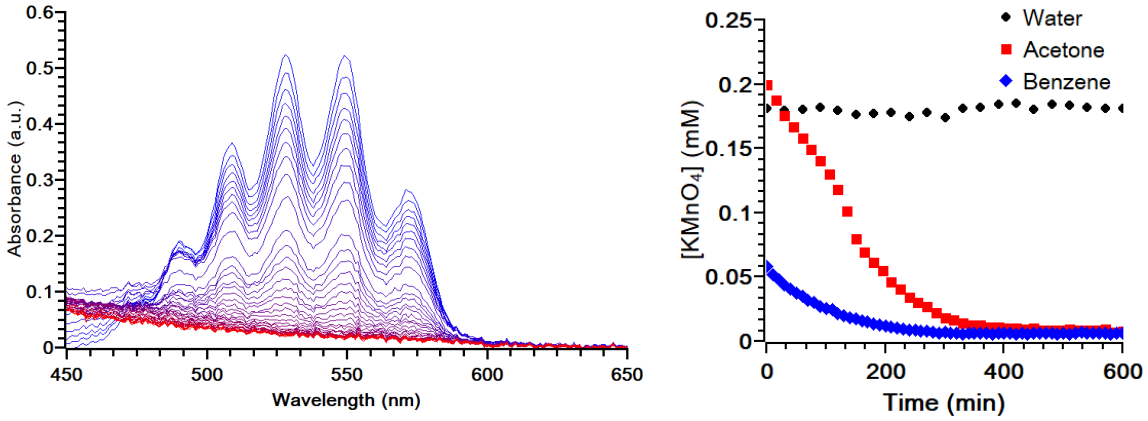

Figure 3.3 Left: The spectra of $KMnO_4$ in acetone. The initial spectra are shown in blue and the final spectra are shown in red. Right: Stability of $KMnO_4$ in water, acetone, and a mixture of 40.024 mM 18-crown-6 and 5.046 mM bis(2-ethylhexyl)phosphoric acid in benzene.

3.4.2 Quantification of HC301

To quantify the concentration of HC301 as quickly as reasonably possible, it is desirable to not have to conduct a full titration to the endpoint to determine the concentration while maintaining accuracy and precision. Instead of titrating to the endpoint, an aliquot of the HC301 containing sample can be added to a solution containing a known, sizable excess of $KMnO_4$ and allowed to react. After this reaction, the concentration of $KMnO_4$ remaining can be determined by UV-vis and the difference between the initial and final amount of $KMnO_4$ will be proportional to the amount of HC301 contained within the aliquot of sample.

This one-step titration was first tried with aqueous $KMnO_4$. Upon addition and mixing of an HC301 containing sample, but not a sample containing solely *n*-dodecane, an immediate lightening of the $KMnO_4$ solution's color was observed indicating a reaction between the $KMnO_4$ and HC301 as the reduced sulfur of HC301 is oxidized, presumably to sulfate considering the high reduction potential of MnO_4^-. Despite the successful reaction, attempts to quantify the HC301 by this method were largely unsuccessful as the UV-vis spectra collected after the addition were unusually variable. This was likely due to the formation of droplets of negligibly water-soluble *n*-dodecane and oxidized HC301 suspended in the aqueous bulk as a

result of mixing the two phases. These droplets would be capable of scattering light and causing the poorly reproducible UV-vis spectra observed.

As $KMnO_4$ and HC301 were observed to react with each other in water, but the insolubility of *n*-dodecane and oxidized HC301 in water prevented the reproducible quantification of the remaining $KMnO_4$ by UV-vis, this reaction was tested in acetone. Either the acetone or benzene-based solvents could have been used as *n*-dodecane and HC301 are soluble in both, but acetone was chosen as it could dissolve more $KMnO_4$ and is less hazardous than benzene. A major drawback of using either of these organic solvents is the reduced stability of the MnO_4^- anion. To avoid this instability from affecting the determination of HC301, the same solution containing an excess of $KMnO_4$ was put into both the sample and reference cell of the double beam spectrophotometer. With this approach, although the $KMnO_4$ is continuously degrading in the sample cell, it is degrading at the same rate in the reference cell too. Therefore, if nothing else is added to either of the cells and the spectra is recorded over time, the baseline spectra should be recorded at all time points. Indeed, when the same solution of $KMnO_4$ in acetone was placed in the sample and reference cell, stable baseline spectra are observed over at least three hours. When an oxidizable species is added to the sample cell, such as HC301, the concentration of $KMnO_4$ in the sample cell will decrease relative to the reference cell and a negative absorption peak that is proportional to the amount of oxidizable species added should be detected. Upon addition of an aliquot containing HC301 to the sample cell, a negative absorbance peak was observed and had a consistent absorbance from immediately after mixing to 30 minutes later.

Since issues arising from the instability of $KMnO_4$ in acetone were avoided by using the same $KMnO_4$ solution in both the sample and reference cell, this system was assessed for its ability to quantify HC301. Figure 3.4 shows the spectra resulting from the addition of HC301 and the amount of MnO_4^- consumed as a function of HC301 added. During this reaction, no solid products were observed, suggesting that neither $MnO_{2(s)}$ or $S_{(s)}$ form. The amount of HC301 added was calculated from the molar absorption coefficient previously determined. The first nine spectra show a continuous decrease which, when converted to the graph on the right, show a consistent linear response to the addition of HC301 with a y-intercept of nearly zero, $-6 \pm 1 \times 10^{-6}$. This linear portion of the graph can serve as a calibration curve to relate the amount of HC301 added to the amount of $KMnO_4$ reduced. The later spectra and points did not have

sufficient $KMnO_4$ to react with all the HC301 added which causes this linear response upon addition of HC301 to cease.

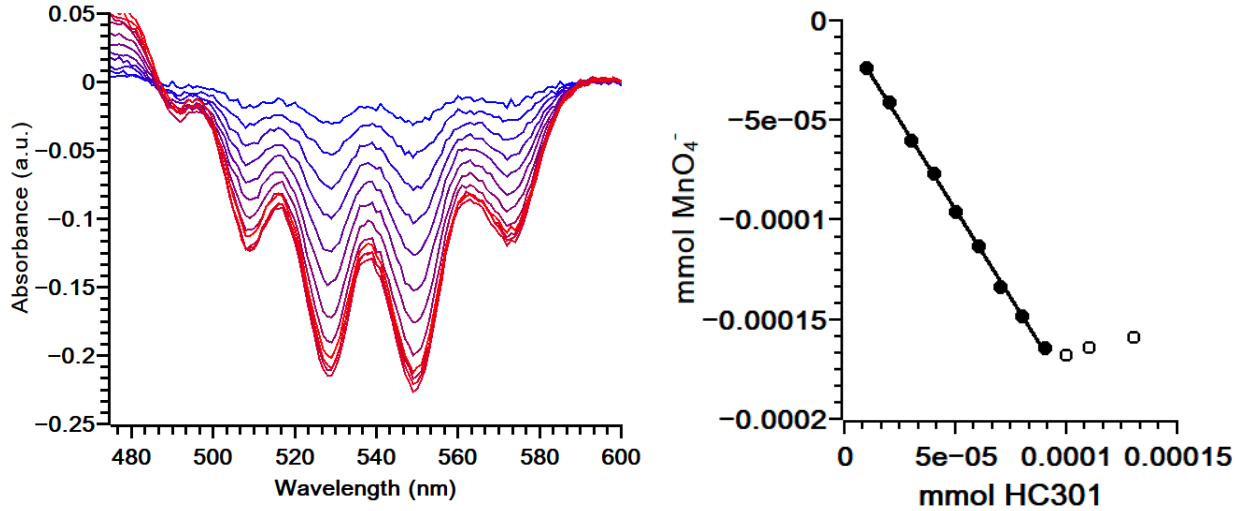

Figure 3.4 Left: Spectra of $KMnO_4$ in acetone after addition of HC301. Spectra with less HC301 added are shown in blue and those with more HC301 are shown in red. Right: The amount of MnO_4^- dissolved in acetone consumed as a function of the amount of HC301 added.

As the reduction $KMnO_4$ remaining was found to have a linear relationship to the amount of HC301 added, it has the potential to quantify the amount of HC301 that has been added. To test this, Leave-One-Out Cross-Validation[118] (LOOCV) was applied to the linear portion of the relationship between the reduction in $KMnO_4$ and the amount of HC301 added. In this method of cross-validation, a single data point is removed from the data set and a calibration curve is created from the remaining points. This new calibration curve is then used to determine the amount of HC301 added for the data point that was removed from the data set. The value resulting from the new calibration curve can be compared to the known value, Figure 3.5 and Table 3.2. The amount of HC301 measured by the LOOCV method is close to the known amount, with the first data point having the largest relative difference from the known value (4%). When greater amounts of HC301 were added, the LOOCV result had smaller relative differences, especially for points in the middle of the series where the relative difference was frequently within ± 1%. Overall, the average of the absolute value of the relative differences was 1.73%. If the calibration curve is accurate, the slope of the relationship between the LOOCV measured value and known value will equal one. The slope determined for this data set is 1.00 ± 0.01 and therefore this method of quantifying HC301 is accurately reproducing the known quantity.

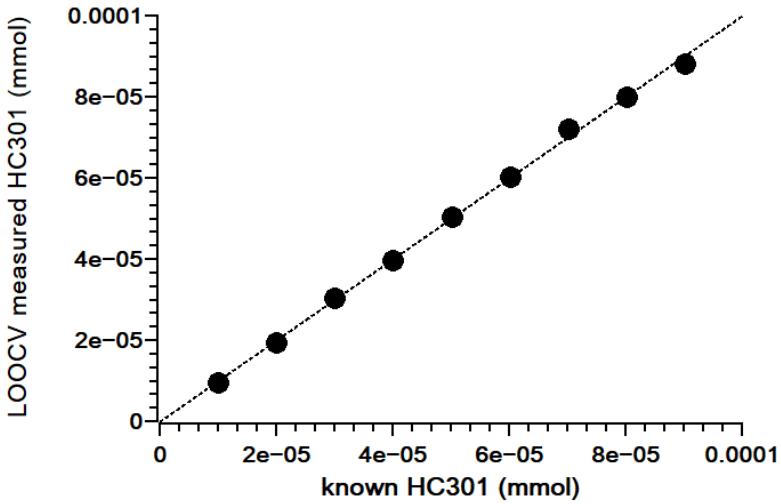

Figure 3.5. Comparison of the amount of HC301 measured by LOOCV and the known amount of HC301 that was added. The dashed line represents the ideal relationship between the known and measured amount (i.e. LOOCV measured amount is equal to the known amount or y = x).

Table 3.2 Known amounts of HC301 added and the amount measured by LOOCV along with the difference between these two values.

Known HC301 (mmol)	LOOCV Measured HC301 (mmol)	Difference (mmol)	Difference (%)
1.00×10^{-5}	9.62×10^{-6}	4×10^{-7}	4
2.00×10^{-5}	1.94×10^{-5}	6×10^{-7}	3
3.00×10^{-5}	3.04×10^{-5}	-4×10^{-7}	-1
4.00×10^{-5}	3.98×10^{-5}	2×10^{-7}	1
5.01×10^{-5}	5.05×10^{-5}	-4×10^{-7}	-1
6.01×10^{-5}	6.03×10^{-5}	-2×10^{-7}	0
7.01×10^{-5}	7.22×10^{-5}	-2.1×10^{-6}	-3.0
8.02×10^{-5}	8.00×10^{-5}	2×10^{-7}	0
9.02×10^{-5}	8.81×10^{-5}	2.1×10^{-6}	2.3

3.5 Conclusions

The ability to quantify the amount of HC301 in *n*-dodecane by permanganometry was tested here. Traditional aqueous permanganometry was found to be unsuitable for this fast,

spectrophotometric titration due to light scattering from droplets of the water insoluble *n*-dodecane and oxidized HC301. To avoid the formation of droplets within the cuvette, two solvents which can dissolve *n*-dodecane and HC301 were tested, an 18-crown-6 and benzene based solvent mixture and acetone. The stability of $KMnO_4$ was found to be reduced in both organic solvents relative to water, particularly for acetone, but can be accounted for by using the same solution of $KMnO_4$ in both the reference and sample cell of the spectrophotometer. By adding aliquots containing a known quantity of HC301 to the sample cell, a linear calibration curve can be obtained relating the amount of MnO_4^- consumed to the amount of HC301 added until all $KMnO_4$ is consumed. Cross validating this calibration curve by LOOCV shows that this technique was able to determine the known amount of HC301 with reasonable accuracy. The average of the absolute value of the difference between the amount of HC301 calculated by LOOCV and the known value is 1.73%. The largest relative difference was 4%, with other points having smaller relative differences. Although this system has shown the ability to quantify purified HC301 in a pure solvent, additional studies are needed to determine how suitable this method is to quantify HC301 within a solvent extraction system as the presence of HC301 degradation products, acid, oxidizable metal species, solvents, anions, and other impurities could interfere.

3.6 Acknowledgements

This work was supported by the U.S. Department of Energy Office of Science, Office of Basic Energy Sciences, Heavy Elements Chemistry Program at Colorado School of Mines under Award Number DE-SC0020189.

CHAPTER 4

EXTRACTION OF THE TRIVALENT TRANSPLUTONIUM ACTINIDES AMERICIUM THROUGH EINSTEINIUM BY PURIFIED CYANEX 301

Nathan P. Bessen,[1] Ning Pu,[2] Jing Chen,[2] Taoxiang Sun,[2] Chao Xu,[2] Jenifer C. Shafer[1]

4.1 Abstract

In the extraction of lanthanides by the purified Cyanex 301 (HC301, bis(2,4,4-trimethylpentyl)dithiophosphinic acid), a transition in the coordination mode of extracted complexes has been observed between Eu and Gd. The light lanthanides La–Eu tend to be extracted as inner sphere complexes with HC301 directly coordinating the metal whereas the second half of the series Gd–Lu have a tendency to be extracted as outer sphere complexes. Without extended actinide studies, spanning the transplutonium actinides, it was unclear if a similar change in the extraction mechanism occurs in the actinide series. To assess this, solvent extraction studies were completed examining the slope dependence of the actinides in the presence of varied nitrate and acid concentrations. Significant variation in the slope dependences was not observed for either the actinides or the lanthanides as pH varied, however, the nitrate dependence and neodymium spectroscopy data suggest that the formation of outer sphere complexes is suppressed by higher nitrate concentrations. This suppression of outer sphere complexes enhanced the extraction of lanthanides, but not the actinides and suggests that the actinides form inner sphere complexes. Therefore, the HC301 separations chemistry observed thus far suggest differences in the chemistry of the actinides and lanthanides continues to persist deep into the actinide series.

4.2 Introduction

One of the most challenging separations for the processing and disposal of used nuclear fuel is the separation of trivalent actinides and lanthanides due to the similar sizes, charges and chemistries of the two types of metals. Of the proposed processes for this separation, those using

[1] Department of Chemistry, Colorado School of Mines, 1500 Illinois St, Golden, CO 80401, United States
[2]Institute of Nuclear and New Energy Technology, Tsinghua University, Beijing 100084, China

dithiophosphinic acids have shown some of the greatest selectivity for the actinides relative to the trivalent lanthanides[8,12,27,111]. In particular, bis(2,4,4-trimethylpentyl)dithiophosphinic acid (HC301), Figure 4.1, has received the most attention due to having the most significant commercial availability relative to other dithiophosphinates and reported separation factors as large as 5000 between trivalent lanthanides and actinides[111].

Despite the volume of research on HC301, a multitude of questions about its extraction characteristics remain - including how it extracts the heavier actinides. In the current literature, the heaviest actinide studied with HC301 and no other ligands was Cm by Jensen and Bond[3]. The lanthanides in this system have been more thoroughly studied and an interesting change in the extraction mechanism is observed half-way through the series[88,89,111]. When HC301 has not been saponified by the addition of sodium hydroxide, the first half of the lanthanide series tend to be extracted as inner sphere complexes with distinct metal-sulfur bonds while the heavier metals from Gd to Lu are typically extracted as outer sphere complexes where water is directly solvating the metal ion[88,89,111]. This transition from inner- to outer-sphere complexes is gradual with some formation of both types of complexes occurring simultaneously[89,111,119]. A high degree of saponification of the HC301 leads to all of the metals being extracted within reverse micelles that likely contain multiple metal ions and additional water[90,91]. In an extraction system using HC301 as supplied, no saponification, and the strongly coordinating ligand 3,4,3-LI(1,2-HOPO) in the aqueous phase, there were significant changes in the extraction of the actinides from Am to Cf, but this was attributed to changes in the stability of the aqueous complex and oxidation of Bk to the tetravalent state instead of any changes in the extraction mechanism for the different actinides[120]. Additionally, to mimic industrially anticipated conditions, this manuscript did not purify the HC301 and much of the metal-extractant interactions under radiotracer conditions were probably controlled by the oxo-extractant impurity, Cyanex 272. In systems containing only purified, non-saponified HC301 as the extractant and no aqueous ligands, all of the actinides studied have been lighter than Bk, so it was unknown if the actinide series has the same change in extraction mechanism as the lanthanides or if they continue to be extracted as the inner sphere complexes that have been observed with the light lanthanides, Am, and Cm[3,9–12,85,111].

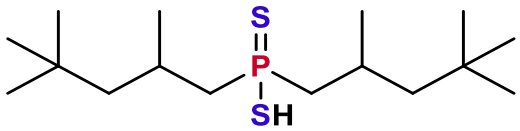

Figure 4.1 Structure of HC301 (bis(2,4,4-trimethylpentyl)dithiophosphinic acid).

In this work, the extraction of the trivalent actinides Am–Es and most of the lanthanides from an aqueous, sodium nitrate media by purified, non-saponified HC301 was examined to determine if the extracted complexes of actinides with HC301 undergo a change from inner sphere to outer sphere complexes with the heavier members of the series as is observed within the lanthanide series. Based on slope analysis of the previous extraction results, the impact of nitrate anions in the aqueous phase on the extraction was also tested for these metals.

4.3 Experimental

Sodium nitrate (ACS grade), anhydrous dodecane (≥99%), anhydrous hexanes (≥99%), and 50% sodium hydroxide solution were obtained from Sigma-Aldrich and used as supplied. Ethanol (200 proof) was purchased from Pharmco by Greenfield Global. Concentrated nitric acid (ACS grade) was purchased from Mallinckrodt Chemicals and hydrochloric acid (ACS grade) were supplied from Macron Fine Chemicals. Sodium sulfate (ACS grade) and ammonium sulfate (ACS grade) were obtained from Fisher Chemical. Lanthanum oxide (99.99%), neodymium oxide (99.995%), samarium oxide (99.99%), europium oxide (99.99%), gadolinium oxide (99.99%), dysprosium oxide (99.9%), erbium oxide (99.995%), ytterbium oxide (99.995%), and lutetium oxide (99.95%) was purchased from Treibacher Industrie AG. Praseodymium oxide (99.9%), holmium oxide (99.99%), and thulium oxide (99.99%) was purchased from Yick-Vic Chemicals and Pharmaceuticals. All lanthanide oxides were converted to the nitrate by dissolution in nitric acid.

Cyanex® 301 GN extractant (HC301) was obtained from Solvay and purified as follows[116]. The crude HC301 was dissolved in hexanes and converted to the ammonium salt by bubbling with dry ammonia gas generated from the reaction between ammonium sulfate and sodium hydroxide. The solid NH_4C301 salt was filtered, washed, dissolved in a 6.8% solution of ethanol in water, and adjusted to pH 10 by addition of sodium hydroxide. To this, hexane and 0.005 equivalents of neodymium nitrate were added and shaken for two minutes. After the phases disengaged, the hexane phase was removed, and this process was repeated 14 more times.

The remaining aqueous phase was acidified with hydrochloric acid and the regenerated HC301 was extracted with hexane. This hexane phase was removed and dried over anhydrous sodium sulfate before evaporation of the hexane to recover the purified HC301 (18.9% yield). The resulting purity was found to exceed 99.9% by ^{31}P NMR.

4.3.1 Radiotracer Distribution Studies

Distribution measurements were made with $^{152/154}Eu$, ^{241}Am, ^{244}Cm, ^{249}Bk, ^{249}Cf, and $^{253/254}Es$ radiotracers using an organic phase of 0.5024 M HC301 dissolved in dodecane that had been pre-equilibrated with the appropriate aqueous phase prior to the introduction of metal. The aqueous phase contained 5 mM $Lu(NO_3)_3$ and the appropriate concentration of sodium nitrate. The desired pH was obtained by addition of nitric acid or sodium hydroxide. Equal volumes (0.750 mL) of the aqueous phase and pre-equilibrated organic phase were combined in a glass vial and the appropriate volume (4–8 μL) of the desired lanthanide or actinide (Eu, Am–Es, dissolved in 0.001 M nitric acid) was added. Samples were shaken for 30 min at room temperature and subsequently centrifuged for 2 min. The activity (***A***) of a 0.300 mL sample of each phase was counted on a HIDEX 300 SL liquid scintillation counter. Ultima Gold AB scintillation cocktail was used for experiments that require discrimination between two radioisotopes (one α emitter and one β^- emitter). When α/β discrimination was not needed, Ecoscint A scintillation cocktail was used. The pC_{H+} (which is $-\log_{10}[H^+]$ on the molar concentration scale) of the remaining, post-contact aqueous phase was measured with an Orion 8103BNUWP Ross Ultra pH probe. The distribution ratio (*D*) for a given radioisotope was calculated by $D = A_{org}/A_{aq}$. To quantify the separation between an actinide and Eu, the separation factor (*SF*) was calculated by the formula: $SF_{An/Eu} = D_{An}/D_{Eu}$.

4.3.2 Lanthanide Distribution Studies

The distribution ratios of the non-radioactive lanthanides were collected from a system much like that used for the radiotracer experiment, except for the aqueous phase which contained a set of four or five lanthanides (either La, Pr, Nd, Sm, and Lu, or Eu, Gd, Dy, and Lu, or Ho, Er, Tm, Yb, and Lu) at a concentration 5 mM of each metal, the appropriate amount of sodium nitrate, and the pC_{H+} was adjusted to 4.46. An aliquot of the aqueous phase was taken and diluted in 3% nitric acid for analysis in a Varian Liberty Series II inductively coupled plasma-atomic

emission spectrometer (ICP-OES). The emission wavelengths used for each metal are shown in Table A.1. As only the concentration of metal in the aqueous phase was measured, the distribution ratio (D) was calculated by $D = ([M_{initial}] - [M_{aq}])/[M_{aq}]$. The mass balance of a Eu radiotracer within this systems was found to be within 100 ± 3%.

4.3.3 Computational Details

Geometry optimizations and frequency calculations of $M(C301)_3$ and $M(C301)_2(NO_3)$ complexes were done using density functional theory (DFT) using a PBE functional with scalar relativity[121–123] and triple-ζ plus one polarization function (TZP) with a small frozen core approximation[124] in ADF 2019.104[125]. The 2,4,4-trimethylpentyl groups of HC301 were truncated to methyl groups to reduce the computational time. The calculations used COSMO solvation with hexane and the atomic radii were set to the Allinger radii divided by 1.2[126]. Coordinates of the optimized structures can be found in Appendix A.

4.4 Results and Discussion

The extraction of lanthanides and actinides by HC301 was tested under varying concentrations of carrier metals, pC_{H+}, and aqueous phase nitrate concentration. The results of these studies are presented below.

4.4.1 Carrier Metal

The distribution ratio of Eu at a constant pC_{H+} of 4.66 was found to be dependent upon the concentration of metal in the aqueous phase, Figure 4.2. At higher concentrations of metal, the distribution ratio of Eu decreased. This is consistent with the findings of Zhu et al. who found that higher concentrations of lanthanides increase separation factors by decreasing the extraction of lanthanides[68]. Lutetium was found to be more effective than Eu in this regard as it suppressed the extraction of Eu at lower concentrations than Eu. With Lu the distribution ratio of Eu stabilized at approximately 3 mM or greater Lu in the aqueous phase whereas this occurred with Eu around 5 mM. It is expected that Lu would be more effective at masking the impurities than Eu as Lu is the most readily extracted lanthanide by both Cyanex 272 and Cyanex 302[127,128] which are common extracting impurities and degradation products found in HC301[92,94,96–98]. For these reasons, all subsequent experiments were conducted with an aqueous phase containing 5 mM $Lu(NO_3)_3$ to ensure that the strongly extracting impurities were fully masked.

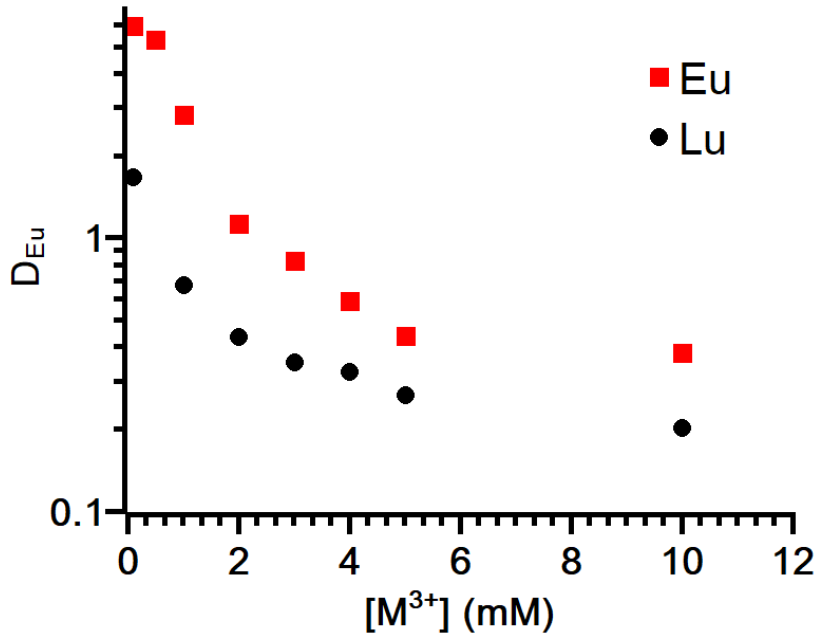

Figure 4.2 The distribution ratio of Eu at pC_{H+} 4.66 with varying aqueous concentrations of Eu (red squares) or Lu (black circles).

4.4.2 Transplutonium Actinide Extraction

The distribution ratios of Eu and the actinides Am through Es at varying pC_{H+} are shown in Figure 4.3. The distribution ratios of the actinides are closely grouped with slopes ranging from 2.4 ± 0.1 (Bk) to 2.57 ± 0.07 (Am), Figure 4.3. Europium is more weakly extracted compared to any of the actinides tested and has a lower slope of 1.13 ± 0.08. These slopes are flatter than those observed by both Zhu et al.[12] and Jensen and Bond[3], particularly for Eu. These flatter slopes may be due to examining a wider range of pC_{H+} here and the presence of the 5 mM Lu carrier. As Lu is more readily extracted by HC301 than Eu[119], the addition of Lu can suppress the extraction of Eu and cause the flatter slope. The greater extraction of the actinides, particularly at higher pC_{H+} gives rise to a separation factor that increases with pC_{H+} (Table 4.1). Separation factors at pC_{H+} 4 range from 700 for Es to 6300 for Am. The separation factor for Am is comparable to the value of 5900 seen by Zhu et al[12]. and 6000 seen by Hill et al[75].

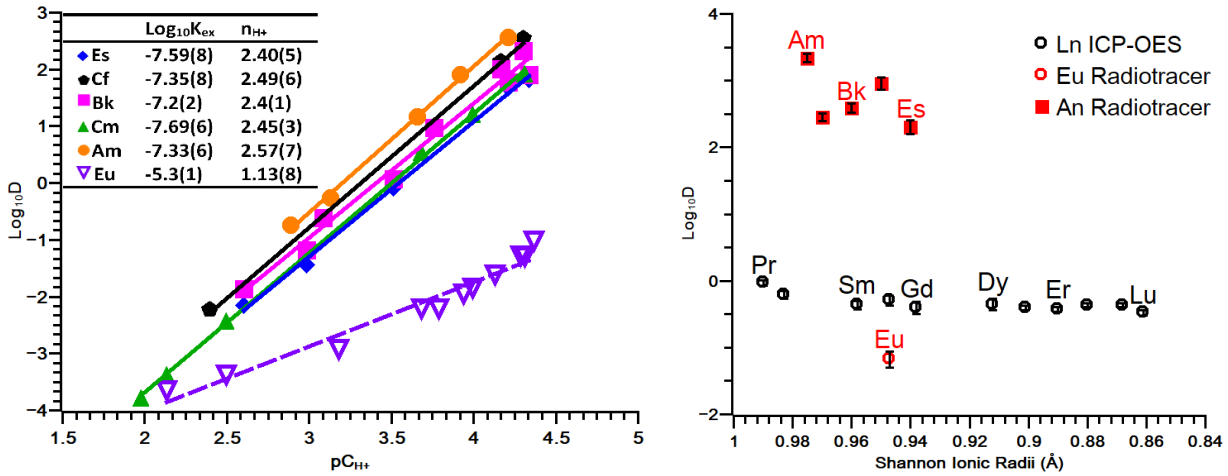

Figure 4.3. Left: The distribution ratios of Eu, Am, Cm, Bk, Cf, and Es as a function of pC_{H+} with 0.5024 M HC301 in dodecane at an ionic strength of 1 M. Right: The distribution ratios for the extraction of the actinides Am, Cm, Bk, Cf, and Es and the lanthanides at pC_{H+} 4.50 as a function of ionic radii with 0.50 M HC301 in dodecane at an ionic strength of 1 M. Distribution ratios for the radiotracers were extrapolated from the graph on the left. Error bars are shown at 3 σ uncertainty.

The distribution ratios at pC_{H+} 4.50 are shown in Figure 4.3. The distribution ratios for the actinides and lanthanide tested each form their own group with actinides being more strongly extracted and the lanthanides more weakly. The distribution for Eu measured by the radiotracer is lower than for the ICP-OES method. It is unclear if this is from different metal concentrations in the aqueous phase or extrapolation of the radiotracer distribution ratios to pC_{H+} 4.50. Across the lanthanide series, it can be seen that the distribution ratio for the lanthanides initially decreases slightly, then remains relatively consistent for the heavier lanthanides even though they are extracted as outer sphere complexes under these conditions[88,89,111]. Also, an emulsion is observed at the interface between the aqueous and organic phases for the heavier lanthanides at higher pC_{H+} but not the lighter lanthanides. All radiotracer studies had mass balances within 100 ± 3%. This trend in the distribution ratios of the lanthanides is also consistent with the distribution ratios observed by He et al[88].

Table 4.1. The separation factors of Am, Cm, Bk, Cf, and Es from Eu with 0.50 M HC301 in dodecane at an ionic strength of 1 M and pC_{H+} = 4.00.

Metal	SF
Am	6300
Cm	930
Bk	1400
Cf	2800
Es	700

The similarity of the distribution ratios within both the lanthanide and actinide series suggests that the change from inner sphere to outer sphere coordination does not have a large impact on the quantity of metal extracted and therefore the consistency of distribution ratios for the actinides is not necessarily indicative of changing coordination modes within that series. The similar distribution ratios and slopes among the actinides shown in Figure 4.3 do not conclusively suggest either a consistent extraction mechanism across the series or a change from inner- to outer-sphere complexes. This is different from the behavior within the lanthanide series where there is a change in the mechanism across the series[88,89,111]. Without saponification of the HC301, the first half of lanthanide series tend to be extracted as inner sphere complexes with bonds between the metal and HC301, while the heavier lanthanides tend to form outer sphere complexes[88,89,111]. Due to the presence of the Lu carrier and the co-extraction of water within its outer sphere complexes, there is some possibility that this could impact the speciation of the actinides. At higher pC_{H+} values than tested here, saponification of the HC301 will be more extensive and may cause the actinides to be extracted within reverse micelles as has been observed with the lanthanides[90,91].

4.4.3 Nitrate Dependency

As the slopes shown in Figure 4.3 for the distribution ratio as a function of pC_{H+} are less than the value of three that would be expected to maintain a neutral extracted complex, the effect of changing the concentration of the nitrate anion (as sodium nitrate) in the aqueous phase was tested. Figure 4.4 shows the UV-vis spectra of Nd^{3+} in the organic phase after extraction from an aqueous phase containing between 1.50 and 5.00 M nitrate as compared to the spectrum of Nd^{3+}

in 5.00 M aqueous nitrate media. All the organic phase spectra are different from the aqueous spectrum and they continue to change with changing nitrate concentrations. This is especially clear in the hypersensitive transitions from 560 to 610 nm. These changes in the organic Nd^{3+} spectra indicate that the coordination environment of Nd is changing with the aqueous nitrate concentration. The spectra can be further interpreted via the nephelauxetic effect[129]. The nephelauxetic effect causes a redshift of a metal ion's spectra upon complexation by ligands with a tendency to form covalent bonds, such a HC301. Indeed, a redshift of the Nd spectra upon coordination by HC301 has been previously observed[85,130]. Coordination of nitrate causes a redshift of a much smaller magnitude[131,132] and coordination of water causes a blueshift approaching the spectra of the hydrated Nd ion[90]. Therefore, as the spectra is redshifted at higher nitrate concentrations, it suggests that more sulfur from HC301 is coordinating Nd at higher nitrate concentrations. This greater coordination by sulfur could be due to a salting out effect reducing the concentration of water in the organic phase thereby preventing the formation of complexes with water coordinating the Nd center. Principle component analysis (PCA) of these spectra shows two significant components which is consistent with the existence of inner and outer sphere complexes.

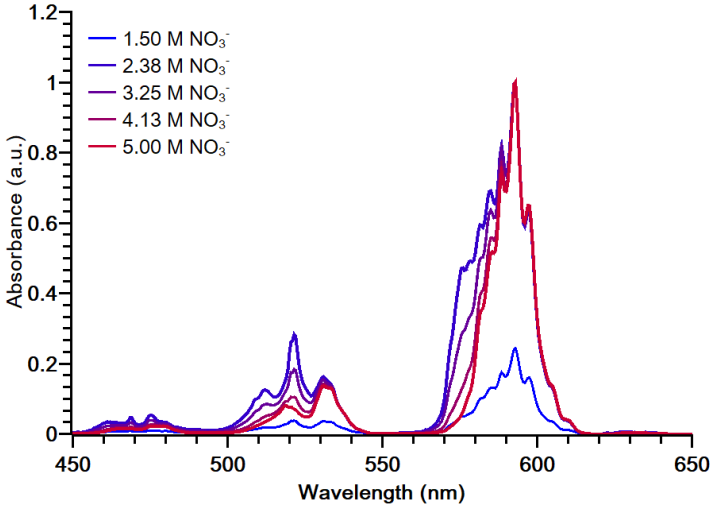

Figure 4.4 The UV-vis spectra of aqueous Nd^{3+} (black) and the organic phase resulting from the extraction of Nd^{3+} by 0.5024 M HC301 in dodecane from an aqueous phase containing 0.5 M Nd^{3+} and 1.5 to 5.00 M NO_3^- at a pH of 4.20.

As the coordination of Nd^{3+} changes with nitrate concentration, the spectra alone provide limited information about how the distribution ratios of Nd or other metals are affected. To look more closely at this, distribution ratios were measured for most lanthanides and the actinides

Am, Cm, Bk, and Es at different nitrate concentrations. The results for the actinides and lanthanides are shown in Figure 4.5 and A.1. The actinides were minimally affected by the changing nitrate concentration as the slope with a flat or slightly negative slope. However, the lanthanides have increased extraction at higher nitrate concentrations and this trend becomes more pronounced along the lanthanide series.

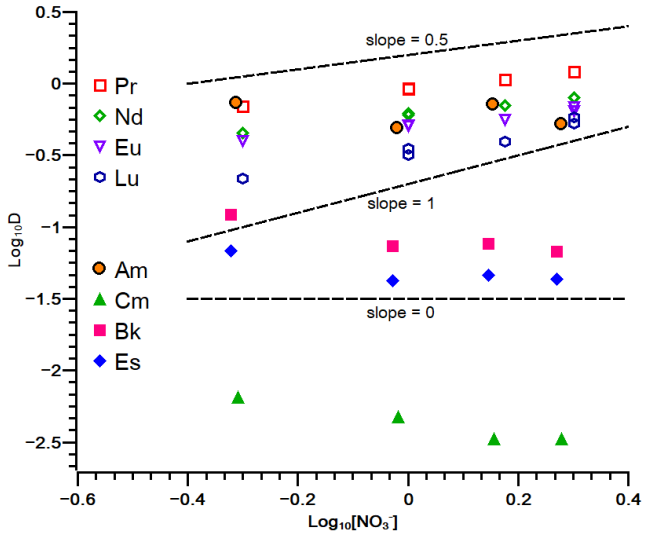

Figure 4.5 The distribution ratio for the lanthanides Pr, Nd, Eu, and Lu at pC_{H+} 4.50 and the actinides Am (pC_{H+} 3.23), Cm (pC_{H+} 2.51), Bk (pC_{H+} 2.93), and Es (pC_{H+} 2.93) with 0.5024 M HC301.

As the slope of the distribution ratio plotted against the nitrate concentration is approximately zero or slightly negative, nitrate does not appear to have an effect on the extraction of these actinides. The lanthanides show a much greater dependence on nitrate concentration where higher nitrate concentrations promote extraction, especially for the heavier lanthanides. One possible reason for the enhanced extraction is due to the salting out effect at higher nitrate concentrations. As the concentration of nitrate in the aqueous phase increases, the quantity of water extracted will decrease. With less water in the organic phase, the formation of outer sphere complexes or complexes that have water coordinating the metal will be limited. As the actinides Am and Cm have previously been observed to form inner sphere complexes with no coordinating water molecules[3,9], it is unsurprising that this limitation on the formation of outer sphere complexes has no great impact on the extraction of Am and Cm. As the extraction of Bk and Es was also minimally affected, it suggests that these actinides continue to form inner sphere complexes as with Am and Cm. The lanthanides, which are seen to be more affected by the aqueous nitrate concentration and have been shown to produce both inner- and outer-sphere

complexes[89,111,119], would have their extraction mechanism more affected because the formation of outer sphere complexes is limited. As the extraction of inner sphere complexes was observed to be more favorable than outer sphere complexes in Figure 4.3, it follows that preventing outer sphere complexes from forming with higher nitrate concentrations promotes the extraction of the lanthanides seen in Figure 4.5.

Another possible explanation is the co-extraction of nitrate in heteroleptic complexes of the form $Ln(C301)_2(NO_3)$. Bhattacharya observed Eu complexes of this form at lower concentrations (<0.3 M) of HC301 than used here[133] and computationally observed that the formation of $M(C301)_2(NO_3)$ and $M(C301)_3$ complexes with Am, La, Eu, and Lu were close to the same reaction energy[32]. Therefore, it is plausible that these heteroleptic complexes have favorable or nearly equal reaction energies for all the lanthanides and a mixture of the $M(C301)_3$ and $M(C301)_2(NO_3)$ are extracted.

To test this hypothesis, the substitution of a C301 anion for a nitrate anion, Equation 4.1, was modeled using DFT calculations and the resulting thermodynamic parameters are shown in Table 4.2. Examples of the complexes modeled are shown in Figure 4.6. The uncertainty of the calculated Gibbs free energy (ΔG) is estimated to be approximately 1-2 kcal/mol[40,134]. Although this reaction is the system modeled by Bhattacharya, the metal centers are somewhat undercoordinated with a coordination number of six and all complexes are assumed to be inner sphere. These simplifications may limit the application of this modeling to this system, especially for the heavier lanthanides that form outer sphere complexes. The calculated ΔG of this reaction is endergonic for all the metal studied which indicates that this substitution is unfavorable, but it is less endergonic for the lanthanides, particularly the heavier lanthanides. Several of the metals examined have values of ΔG that are slightly higher or lower than would be expected given the ΔG of neighboring metals and the general trend observed, but these variances are well within the estimated uncertainty of these calculations. Overall, this trend suggests that if the heteroleptic complex does form, it will do so most readily with the lanthanides, particularly the heaviest lanthanides. As this substitution of C301 anion for a nitrate anion is endergonic for all metals considered and does not account for the nephelauxetic effect seen in Figure 4.4, it seems that the formation of this heteroleptic complex is less important to extraction of the lanthanides or actinides than the salting out effect.

$$M(C301)_3 + NO_3^- \rightleftharpoons M(C301)_2(NO_3) + C301^- \quad (4.1)$$

Figure 4.6 Left: The structure of the $Am(C301)_3$ complex. Right: The structure of the $Am(C301)_2(NO_3)$ complex.

Table 4.2 Calculated thermodynamic parameters for the reaction $M(C301)_3 + NO_3^- \rightleftharpoons M(C301)_2(NO_3) + C301^-$. ΔG is calculated at a temperature of 298.15 K.

Lanthanide	ΔG (kcal/mol)	ΔH (kcal/mol)	ΔS (cal/mol·K)	Actinide	ΔG (kcal/mol)	ΔH (kcal/mol)	ΔS (cal/mol·K)
Ce	3.78	4.44	2.21	Am	4.55	5.22	2.22
Pr	3.1	3.7	2.01	Cm	4.45	5.38	3.11
Pm	3.92	5.01	3.65	Bk	5.55	6.97	4.79
Sm	3.06	7.48	14.81	Cf	5.04	6.47	4.80
Eu	4.67	7.4	9.13	Es	5.69	7.42	5.81
Tb	4.13	7.49	11.26				
Dy	3.64	6.32	8.98				
Ho	1.97	7.4	18.23				
Er	1.65	6.5	16.24				
Tm	1.07	7.49	21.55				
Lu	1.66	6.26	15.46				

4.5 Conclusions

The extraction of Eu and the trivalent actinides Am through Es with HC301 has been investigated. The distribution ratios and pH dependency of the actinides is similar from Am to Es. This alone cannot fully justify a claim of either consistent inner sphere or a change from

inner- to outer-sphere coordination within the actinide series occurs as it does with the lanthanide series[88,89,111].

The aqueous nitrate concentration dependency was also probed, and the extraction of the actinides was found to be less dependent on the nitrate concentration than the lanthanides, particularly the later members of the series. This nitrate dependency may be due to the suppression of outer sphere complexes at higher nitrate concentrations resulting in the formation of more strongly extracted inner sphere complexes. As all actinides tested were minimally impacted by this suppression of outer sphere complexes, it suggests that the actinides exclusively form inner sphere complexes under the conditions tested.

4.6 Acknowledgements

The work at Colorado School of Mines was supported by the U.S. Department of Energy Office of Science, Office of Basic Energy Sciences, Heavy Elements Chemistry Program at Colorado School of Mines under Award Number DE-SC0020189. The Bk-249 and Cf-249 used in this and prior research by this PI were supplied by the United States Department of Energy Office of Science by the Isotope Program in the Office of Nuclear Physics.

CHAPTER 5

LANTHANIDE & ACTINIDE COMPLEXES WITH AQUEOUS SULFUR DONATING LIGANDS

Nathan P. Bessen,[1] Ivan A. Popov,[2] Colt R. Heathman,[3] Travis S. Grimes,[3] Peter R. Zalupski,[3] Liane M. Moreau,[4] Kurt F. Smith,[4] Corwin H. Booth,[4] Rebecca J. Abergel,[4] Enrique R. Batista,[2] Ping Yang,[2] Jenifer C. Shafer[1]

5.1 Abstract

The separation of trivalent lanthanides and actinides is challenging due to their similar sizes and charge densities. Sulfur donating extractants have shown significant selectivity for trivalent actinides over the lanthanides, with single stage americium/lanthanide separation efficiency for some thiol-based extractants reported at >99.999%. While such separations could transform the nuclear waste management landscape, these systems are often limited by the hydrolytic and radiolytic stability of the extractant. Progress away from thiol-based systems is limited by the poorly understood and complex interactions of these extractants in organic phases, where molecular aggregation and micelle formation obfuscates assessment of the metal-extractant coordination environment. Since sulfur-donating thioethers are generally more resistant to hydrolysis and oxidation, and the aqueous phase coordination chemistry is anticipated to lack complications brought on by micelle formation, we have considered three thioethers, 2,2'-thiodiacetic acid (TDA), (2R,5S)-tetrahydrothiophene-2,5-dicarboxylic acid (THTPA), and 2,5-thiophenedicarboxylic acid (TPA), as possible trivalent actinide selective reagents. Formation constants, extended X-ray absorption fine structure (EXAFS) spectroscopy, and computational studies were completed for thioether complexes with a variety of trivalent lanthanides and actinides. TPA was found to have moderately higher selectivity for the actinides due to the ability to bind actinides in a different manner than lanthanides, but the utility of TPA is limited by poor water solubility and high rigidity. While significant competition with water for

[1] Department of Chemistry, Colorado School of Mines, 1500 Illinois St, Golden, CO 80401, United States
[2]Theoretical Division, Los Alamos National Laboratory, Los Alamos, NM 87545, United States
[3]Idaho National Laboratory, 2525 Fremont Ave, Idaho Falls, ID 83402, United States
[4] Lawrence Berkeley National Laboratory, 1 Cyclotron Rd, Berkeley, CA 94720, United States

the metal center limits the efficacy of aqueous-based thioethers for separations, the characterization of these solution-phase, sulfur-containing lanthanide and actinide complexes is among the most comprehensive available in the literature to date. This is due to the breadth of lanthanides and actinides considered as well as the techniques deployed, and serves as a platform for further development of sulfur-containing reagents for actinide separations. Additionally, this manuscript reports on the first bond lengths for californium and berkelium with a neutral sulfur donor.

5.2 Introduction

Much of the long-term radiotoxicity and decay heat associated with used nuclear fuel originates from transplutonium actinides produced by neutron capture and β-decay[135]. To reduce the potential hazards of storing used nuclear fuel, these elements could be removed from the used fuel and fissioned into nuclides that pose less long-term risk[135]. This process is complicated by the presence of other elements that could capture neutrons, thereby reducing the efficiency of the fission process. The lanthanides pose a particular challenge as they tend to have large neutron capture cross sections[135–137] and are difficult to separate from the transplutonium actinides due to their similar sizes, charge densities, and oxidation states[138].

To allow the separation between trivalent actinides and lanthanides, slight differences between their Lewis acidities have been exploited using soft-donor[18] ligands. These ligands contain polarizable soft-donor atoms, such as N or S, which are thought to allow for greater interaction with the more radially extended 5*f* orbitals of the actinides. These soft-donor ligands have shown to preferentially bind with actinides, enabling a separation to proceed[19,38,43,138]. Of the soft-donor atom candidates in the literature, sulfur-based extractants, particularly dithiophosphinic acids, have shown considerable selectivity for trivalent actinides over trivalent lanthanides[8,12,27,28,105–107,111]. Unfortunately, the dithiophosphinic acids tend to degrade through radiolysis[13,52], oxidation[96–98], and hydrolysis[105–107] to form stronger phosphinic acid extractants with poorer selectivity[3,13]. Development of separation methods that retain the selectivity of dithiophosphinic acids but are more resistant to degradation is therefore desirable.

Such separations development must address the instability of the dithiophosphinates and leverage more complete understanding of f-element interactions with sulfur donating reagents in the solution phase. Recent reports have indicated solution phase chemistry for these systems is

complex. For example, the coordination chemistry of bis(2,4,4-trimethylpentyl)dithiophosphinic acid (HC301, Figure 5.1) with f-elements changes from an inner-sphere complex, either $M(C301)_3$ or $M(C301_3 \cdot HC301)$[3,9,10,12,83,84], at lower aqueous pH, to a reverse micelle complex,[90,91] at higher pH. Entropic metal-ligand binding contributions for bis[o-(trifluoromethyl)phenyl]dithiophosphinate, Figure 5.1, drive both the binding efficiency and trivalent actinide/lanthanide selectivity[77]. Therefore, while the functional groups are central to the design of a sulfur-containing extractant for trivalent f-element separations, the solution phase speciation cannot be ignored. To date, few reports exist that consider systematic impacts of changes to sulfur containing ligands on trivalent lanthanide and actinide binding. This work consistently considers associated effects with a series of metal ions including the trivalent actinides, americium, curium, berkelium and californium, as well as the lanthanides neodymium and europium with several sulfur donating ligands.

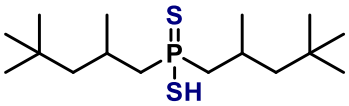

HC301

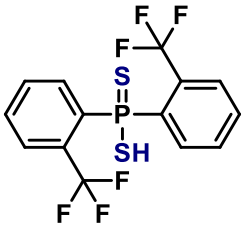

bis[o-(trifluoromethyl)phenyl]dithiophosphinic acid

Figure 5.1 Structures of bis(2,4,4-trimethyl-pentyl) dithiophosphinic acid (HC301) and bis[o-(trifluoro-methyl)phenyl]dithiophosphinic acid.

Of the possible sulfur containing functional groups, thioethers are suspected to be more stable due to the C-S bond being stronger than the P-S bond while still maintaining the ability to coordinate metal ions with the sulfur site[139]. Oxidation of the sulfur in a thioether generally requires strong oxidizing agents[140]. Additionally, computational studies have suggested that thioethers have selectivity for trivalent actinides over lanthanides[141]. Herein, two thioethers (Figure 5.2), 2,2'-thiodiacetic acid (TDA), and 2,5-thiophenedicarboxylic acid (TPA) were chosen to test their selectivity for americium and curium interactions over the lanthanides, as well as to assess their solution phase, metal-ligand coordination environment. An additional

thioether, (2R,5S)-tetrahydrothiophene-2,5-dicarboxylic acid (THTPA), which has an intermediate molecular structure, between those of TDA and TPA, was examined computationally. Because these ligands have modest water solubility, they would be suitable for a solvent extraction separation system comparable to TALSPEAK (Trivalent Actinide Lanthanide Separation with Phosphorus-reagent from Aqueous Komplexes),[62,142] in which the actinide is selectively retained in the aqueous phase while the lanthanide is preferentially extracted.

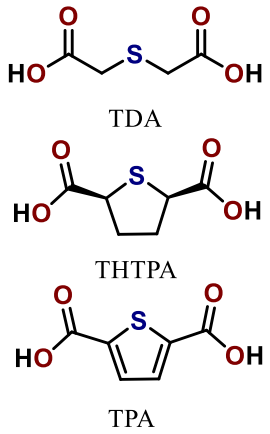

Figure 5.2 Structures of 2,2'-thiodiacetic acid (TDA), (2R,5S)-tetrahydrothiophene-2,5-dicarboxylic acid (THTPA), and 2,5-thiophenedicarboxylic acid (TPA).

5.3 Experimental

The ligands TDA (98%) and TPA (99%) were supplied by Sigma-Aldrich and used as supplied. Sodium perchlorate (ACS grade) was obtained from Sigma-Aldrich and purified by recrystallization from water three times. A 50% sodium hydroxide solution was obtained from Sigma-Aldrich and used as supplied. Perchloric acid (ACS grade) was used from Macron Fine Chemicals. Neodymium oxide (99.995%) and europium oxide (99.99%) was purchased from Treibacher Industrie AG. The lanthanide oxides were converted to perchlorate salts by dissolution in perchloric acid.

5.3.1 Potentiometric Titrations

Solutions of TDA or TPA, with and without Nd or Eu, were titrated with sodium hydroxide to determine the acid dissociation constants (pK_a) of the ligands and metal-ligand formation constants (β_{MHL}). All solutions were adjusted to an ionic strength of 1 M by addition of sodium perchlorate. A Mettler Toledo T-90 Graphix Autotitrator with a Ross Orion semimicro

glass electrode filled with 3 M NaCl was used for all titrations. The electrode was calibrated by Gran analysis[143] on a solution of perchloric acid with sodium hydroxide. The titration occurred in a water jacketed titration beaker maintained at 25.0 ± 0.1 °C under a hydrated nitrogen gas blanket to avoid CO_2 absorption. The resulting titration curves were fit using Hyperquad2013 from Hyperquad[36] to determine the appropriate pK_a and β_{MHL} values.

5.3.2 Spectrophotometric Titrations

Absorbance spectra of ^{243}Am and ^{248}Cm were collected in a quartz cuvette with an Ocean Optics Flame-S-Vis-NIR-ES Spectrometer connected to an Ocean Optics DH-2000-BAL light source by 2 m UV-vis-NIR fiber optic cables. The titrand contained the Am or Cm at a pC_{H+} of 2.49 or 3.23, respectively. For TDA, the titrant contained TDA and the same concentration of metal as the titrand. Due to solubility issues, the titrant for the TPA studies contained TPA with no metal present. The ionic strengths of both the titrand and titrant were adjusted to 1 M using sodium perchlorate. The contents of the cuvette were thoroughly mixed after each addition of the titrant and the spectra was recorded. An identical titration was carried out in parallel for the measurement of the increasing pC_{H+} after each addition. The resulting spectra and pC_{H+} values were fit using HypSpec2014 from Hyperquad[36] to determine the β_{MHL} values.

5.3.3 Extended X-ray Absorption Fine Structure

Solutions for EXAFS spectroscopic analysis were prepared with either Eu or Tb at 3 mM, ^{248}Cm was prepared at 0.79 mM. In all of these experiments, the TDA concentration used was 0.15 M and the pC_{H+} was adjusted to 3.50. Under these conditions, ≥95% of the metals exist as complexes of the form $M(TDA)_2^-$ based on calculations made using formation constants for Eu and Cm in HySS2009. ^{249}Bk and ^{249}Cf samples both were prepared with 0.79 mM metal and 0.02 M TDA at pC_{H+} 3.50. The predominant species was expected to be $M(TDA)^+$ based on HySS2009 calculations using the formation constants determined for Cm. For TPA, the same concentrations of Eu, Tb, or Cm were used with 0.05 M TPA at pC_{H+} 4. Due to the limited solubility and reduced thermodynamic favorability for metal complexation of TPA, the relative abundance of the $M(TPA)^+$ species was estimated to range from 44% to 57%. For all solutions, the ionic strength was adjusted to 1 M by the addition of sodium perchlorate. Lanthanide solutions were stored in polyvinylidene fluoride (PVDF) sample holders with Kapton windows. Cm solutions were stored in triply contained PVDF sample holders with Kapton windows.

X-ray absorption data were collected on beamline 11-2 of the Stanford Synchrotron Radiation Lightsource at the L_{III}-edge of the metal. Energy selection was achieved with a Si(220) double-crystal monochromator. Harmonic rejection was accomplished by detuning the monochromator by 50%. Further rejection for the lanthanide data was accomplished with a Rh-coated mirror using a cutoff energy of approximately 10 keV. Data were collected in fluorescence mode using a 100-element Ge detector. After applying a dead time correction, the resulting absorption data were reduced and fit in r-space with the Real Space X-ray Absorption Package (RSXAP)[144–146]. A constant pre-edge background was removed from each data set, and the EXAFS function $\chi(k)$ was determined using a 5-knot cubic spline function or a 5th-order Chebychev polynomial to estimate the atomic background absorption. The photoelectron wavevector was estimated by measuring the threshold energy, E_0, as the energy at the half-height of the edge. Backscattering phases and lineshapes were calculated using FEFF 9.6.4[147]. Data errors were estimated by collecting multiple scans, and parameter errors were obtained using a profiling method[15].

5.3.4 Computational Details

Geometry optimizations and frequency calculations of Ln and An complexes with TDA, THTPA, and TPA were done using density functional theory (DFT) with a Perdew-Burke-Ernzerhof (PBE) functional, scalar relativistic ZORA Hamiltonian[121–123] and triple-ξ plus one polarization function (TZP) basis set with a small frozen core approximation[124] in ADF 2019.104[125]. After optimizing the structures, single point energy calculations of the complexes were performed using the aforementioned conditions with a PBE0 functional and no frozen core for further validation. The inclusion of spin-orbit relativistic effects compared to scalar relativistic approximation resulted in negligible changes to the formation energy (ΔE) of the complex and HOMO/LUMO energy levels. In the COSMO solvation model, atomic radii were set to the Allinger radii divided by 1.2[126]. In all the structures, a sufficient number of water molecules were added around the metal center to maintain a coordination number of 9. Cartesian coordinates of the optimized structures can be found in the Appendix B.

5.4 Results and Discussion

The bonding of TDA and TPA with lanthanides and actinides is examined below. The acid dissociation and formation constants are reported along with EXAFS and computational analysis of the resulting complexes. The potential selectivity of these ligands is also examined.

5.4.1 Ligand Acid Dissociation Constants

The acid dissociation constants for TDA and TPA were determined by potentiometric titration, Figure 5.3. With TDA, the pK_{a1} was found to be 3.154 ± 0.002 and the pK_{a2} was 3.983 ± 0.001. For comparison, at a higher ionic strength of 6.60 mol/kg, Thakur *et al*. found the pK_{a1} to be 3.82 ± 0.01 and the pK_{a2} to be 4.47 ± 0.02[148]. The higher pK_a values are to be expected due to the much greater ionic strength changing the activity of the ions[148,149]. In the case of TPA, the pK_{a1} was found to be 2.611 ± 0.007 and the pK_{a2} was 3.456 ± 0.002. The greater error at 1σ of the pK_{a1} value for TPA came from the need to partially neutralize TPA prior to the titration, enabling dissolution of the ligand which is sparingly soluble when fully protonated.

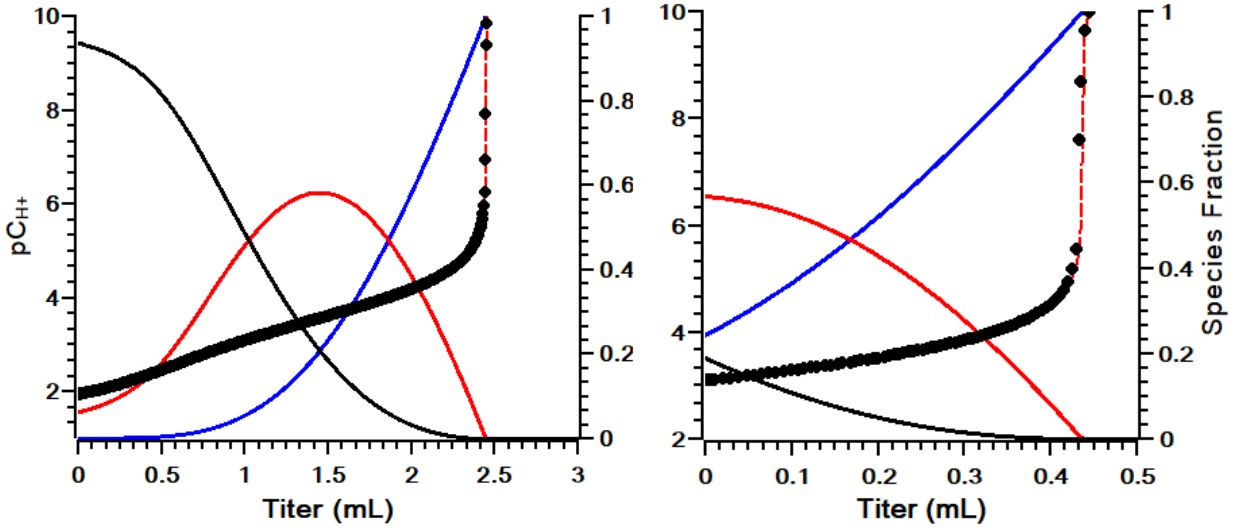

Figure 5.3 Potentiometric titrations of (left) TDA and (right) TPA protonation at 25.0 ± 0.1 °C and ionic strength of 1.00 ± 0.1 M. For the TDA titration , V_{init} = 24.911 mL, C_{TDA} = 19.99 mM, $C_{H+,total}$ = 49.78 mM. For the TPA titration, V_{init} = 24.837 mL, C_{TDA} = 8.56 mM, $C_{H+,total}$ = 8.90 mM. The titrant for both ligands contained 0.507 M NaOH and 0.500 M $NaClO_4$. (•) Experimental pC_{H+}, (dashed red line) calculated pC_{H+}, (black solid line) H_2L, (red solid line) HL^-, and (blue solid line) L^{2-}.

5.4.2 Metal Complex Formation Constants

Formation constants were measured by several different methods. For TDA and TPA, formation constants were found by potentiometric titration (Nd and Eu) and spectrophotometric titration (Nd). The experimental data from the potentiometric titrations is shown in Figure 5.4 and the spectrophotometric data in Figures 5.5 and 5.6. Am and Cm formation constants were calculated from the results of spectrophotometric titrations as ^{243}Am and ^{248}Cm are available in large enough quantities and have sufficiently intense absorption bands to permit these types of experiments. The formation constants are shown in Tables 5.1 and 5.2.

The formation constants for TDA reveal some preference for the actinides over the lanthanides. TDA was observed to form complexes with formulas of $M(TDA)^+$ and $M(TDA)_2^-$. In absolute terms, the $M(TDA)^{2-}$ complex is more selective than the $M(TDA)^+$ complex, but when comparing the spectrophotometric formation constants of Nd and Am, the addition of each TDA adds approximately 0.3 $Log_{10}\beta$ units to the selectivity between these metals. Therefore, the selectivity from each TDA is nearly the same for each TDA with these metals. This is not observed in comparisons with Cm, where the addition of the second TDA enhances the selectivity more than addition of the first TDA ligand. TPA displays a greater selectivity for the actinides among the lanthanides tested than was observed with TDA, as the formation constants for the actinides are significantly higher than for the lanthanides. Due to the poor solubility of TPA under the acidic conditions required to prevent hydrolysis of the metals, the only complex observed was the 1:1 complex of the formula $M(TPA)^+$. Additionally, the lower formation constants of TPA compared to TDA indicate that TPA complexes may have a different structure as both ligands have similar binding sites available.

Table 5.1 Formation constants of trivalent lanthanides and actinides with TDA at 25.0 ± 0.1 °C and 1.00 ± 0.01 M ionic strength.

Lanthanide	$Log_{10}\beta_{101}$	$Log_{10}\beta_{102}$	Actinide	$Log_{10}\beta_{101}$	$Log_{10}\beta_{102}$
Nd[a]	2.639(1)	-	Am[b]	2.85(2)	4.70(3)
Nd[b]	2.55(3)	4.13(3)	Cm[b]	2.89(6)	5.00(9)
Eu[a]	2.796(5)	4.17(3)			

[a]Assessed using potentiometric titration
[b]Assessed using spectrophotometric titration

Table 5.2 Formation constants of trivalent lanthanides and actinides with TPA at 25.0 ± 0.1 °C and 1.00 ± 0.01 M ionic strength.

Lanthanide	$Log_{10}\beta_{101}$	Actinide	$Log_{10}\beta_{101}$
Nd[a]	1.378(9)	Am[a]	1.56(3)
Nd[b]	1.23(2)	Cm[a]	1.53(3)
Eu[a]	1.313(9)		

[a]Assessed using potentiometric titration
[b]Assessed using spectrophotometric titration

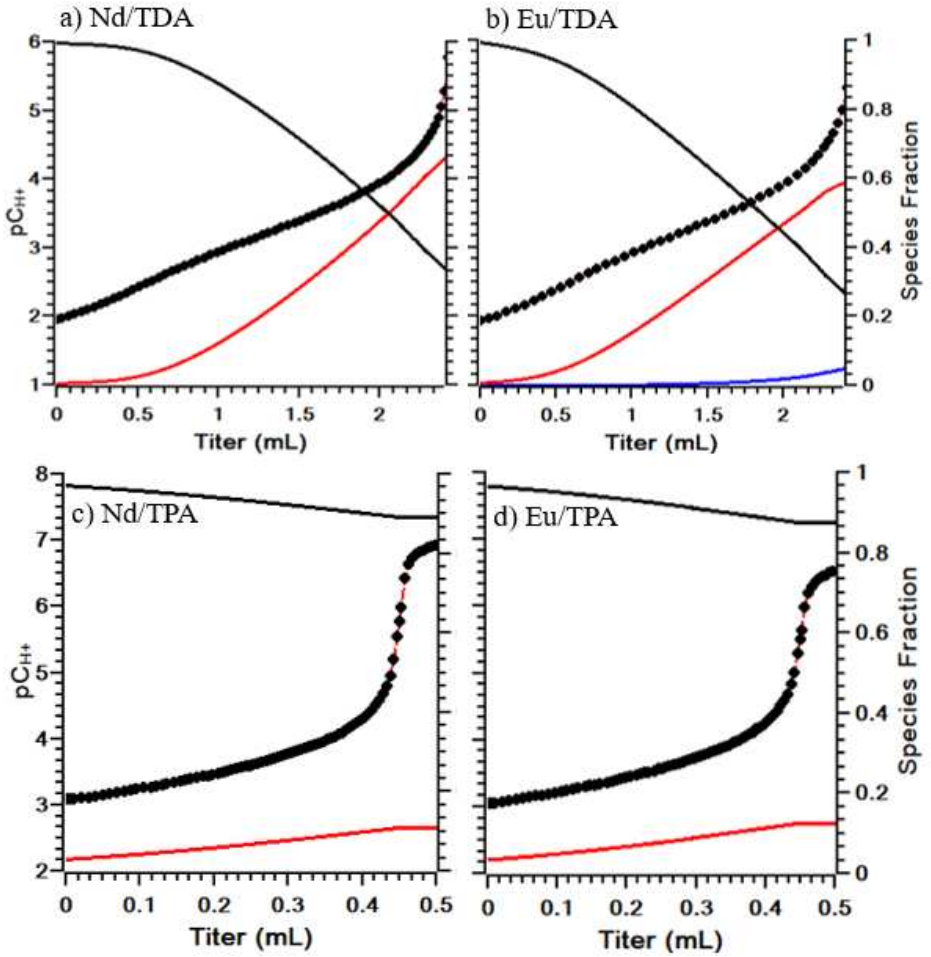

Figure 5.4 Nd and Eu Potentiometric Titrations with TDA and TPA at 1.00 ± 0.01 M $NaClO_4$ and 25 °C. (•) Experimental pC_{H+}, (red dashed line) calculated pC_{H+}, (black solid line) Eu, (red solid line) ML^+ (blue solid line) ML_2^-. a) Nd/TDA. For this titration, Vinit = 25.349 mL, C_{TDA} = 19.25 mM, C_{Nd} = 7.806 mM, and C_{H+},total = 48.73 mM. The titrant contained 0.507 M NaOH and 0.500 M $NaClO_4$. b) Eu/TDA. For this titration, V_{init} = 25.261 mL, C_{TDA} = 19.70 mM, C_{Eu} = 6.634 mM, and $C_{H+,total}$ = 49.03 mM. The titrant contained 0.507 M NaOH and 0.500 M $NaClO_4$. b) Nd/TPA. For this titration, Vinit = 25.447 mL, C_{TPA} = 8.375 mM, C_{Nd} = 10.15 mM, and $C_{H+,}$total = 8.939 mM. The titrant contained 0.507 M NaOH and 0.500 M $NaClO_4$. d) Eu/TPA For this titration, V_{init} = 25.494 mL, C_{TPA} = 8.374 mM, C_{Eu} = 10.18 mM, and $C_{H+,total}$ = 9.021 mM. The titrant contained 0.507 M NaOH and 0.500 M $NaClO_4$.

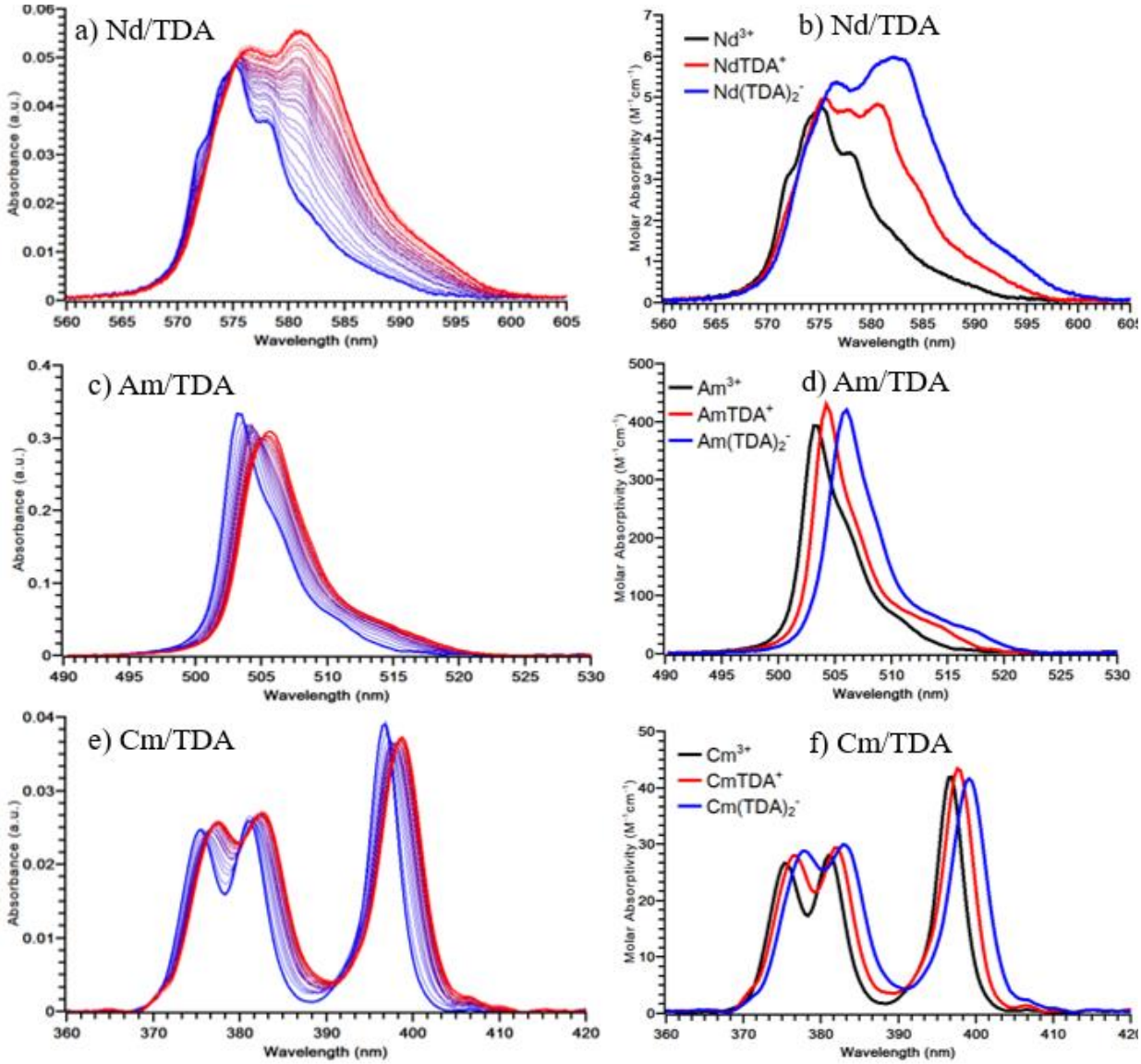

Figure 5.5 Spectrophotometric titrations of Nd, Am, and Cm with TDA and molar absorptivities calculated using HypSpec2014 at room temperature and an ionic strength of 1.00 ± 0.01 M. The spectra changes from blue to red over the course of the titration. a) Nd/TDA titration, V_{init} = 0.803 mL, C_{Nd} = 10.15 mM, and pC_{H+} ,initial = 3.08. The titrant contained C_{TDA} = 150.1 mM, C_{Nd} = 10.12 mM and after the addition of 0.792 mL of titrant, the $pC_{H+,final}$ = 5.17. b) Molar absorptivity of Nd, $NdTDA^+$, and $Nd(TDA)_2^-$. c) Am/TDA titration, V_{init} = 0.795 mL, C_{Am} = 0.844 mM, and $pC_{H+,initial}$ = 2.581. The titrant contained C_{TDA} = 10.03 mM, C_{Am} = 0.832 mM and after the addition of 0.793 mL of titrant, the $pC_{H+,final}$ = 3.676. d) Molar absorptivity of Am, $AmTDA^+$, and $Am(TDA)_2^-$. e) Cm/TDA titration, V_{init} = 0.795 mL, C_{Cm} = 0.937 mM, and $pC_{H+,initial}$ = 3.182. The titrant contained C_{TDA} = 0.137 M, C_{Cm} = 0.939 mM and after the addition of 0.731 mL of titrant, the $pC_{H+,final}$ = 3.707. f) Molar absorptivity of Cm, $CmTDA^+$, and $Cm(TDA)_2^-$.

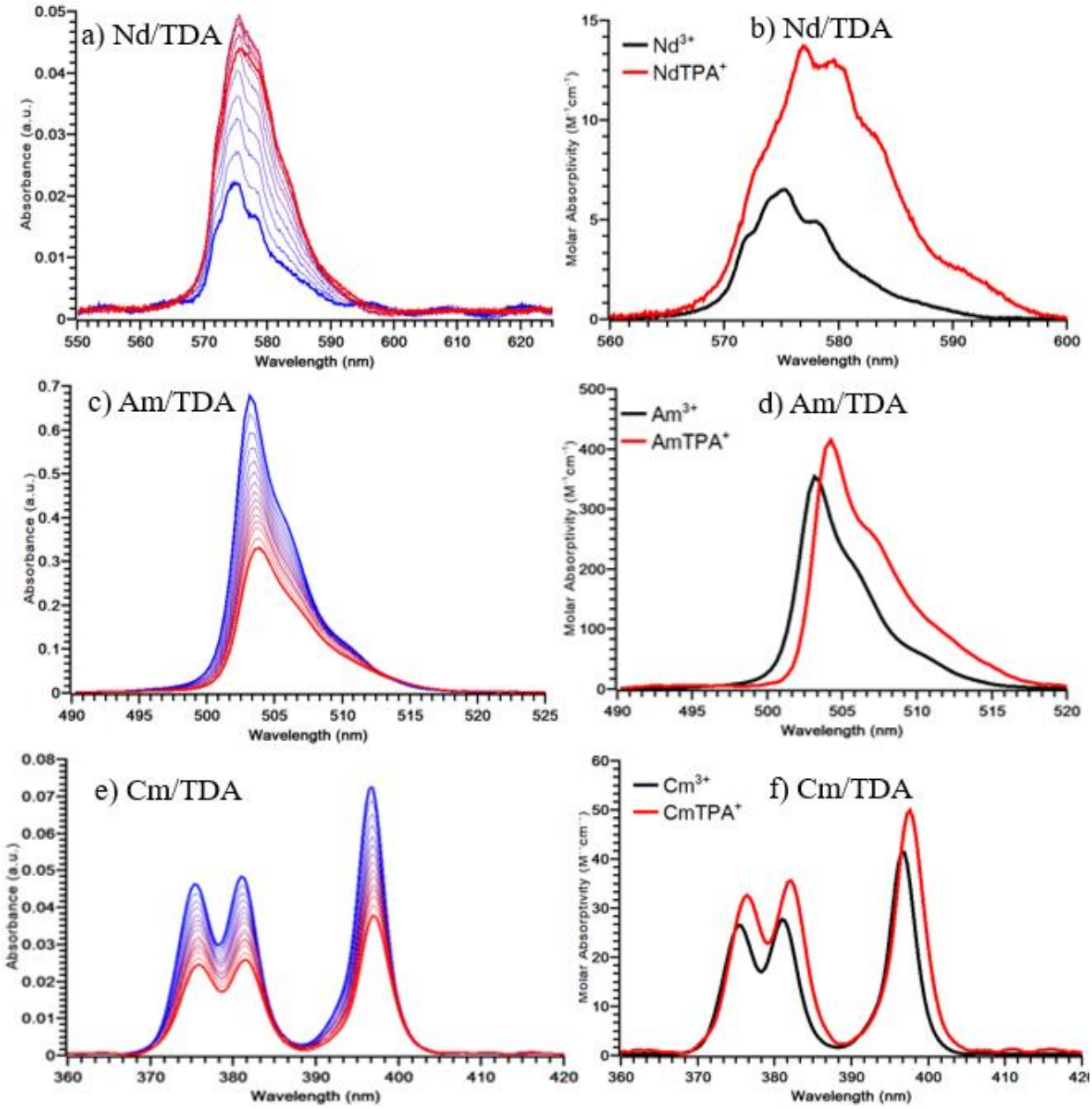

Figure 5.6 Spectrophotometric titrations of Nd, Am, and Cm with TPA and molar absorptivities calculated using HypSpec2014 at room temperature and an ionic strength of 1.00 ± 0.01 M. The spectra changes from blue to red over the course of the titration. a) Nd/TPA titration, V_{init} = 0.803 mL, C_{Nd} = 10.14 mM, and $pC_{H+,initial}$ = 3.12. The titrant contained C_{TPA} = 50.32 mM and after the addition of 0.792 mL of titrant, the $pC_{H+,final}$ = 4.21. b) Molar absorptivity of Nd and $NdTPA^+$. c) Am/TPA titration, V_{init} = 0.795 mL, C_{Am} = 1.914 mM, and $pC_{H+,initial}$ = 2.404. The titrant contained C_{TPA} = 49.79 mM and after the addition of 0.796 mL of titrant, the $pC_{H+,final}$ = 4.007. d) Molar absorptivity of Am and $AmTPA^+$. e) Cm/TPA titration, V_{init} = 0.795 mL, C_{Cm} = 1.746 mM, and $pC_{H+,initial}$ = 3.282. The titrant contained C_{TPA} = 49.79 mM and after the addition of 0.796 mL of titrant, the $pC_{H+,final}$ = 4.296. f) Molar absorptivity of Cm and $CmTPA^+$.

5.4.3 Extended X-ray Absorption Fine Structure

Figure 5.7 shows the EXAFS data and fit for the $Cf(TDA)_x$ sample. Note that the Fourier transform (FT) is plotted as a function r, which includes shifts from the real pair distances, R, due to the complex backscattering function. Detailed fits are therefore necessary to extract metrical parameters. All data and fits for the other samples are reported in the Supplemental Materials. Before reporting the fit results, however, we must first discuss the model used to fit the data. The EXAFS spectra are fit well with 3 or 4 shells around the Ln/An atom. The nearest-neighbor M-O shell is well separated from the M-S and M-C shells (M = Eu, Tb, Cm, Bk, Cf); therefore, the oxide shell fit parameters are well determined. Unfortunately, the combination of a low-amplitude M-S shell at R ≈ 3.05 Å and a broad, or split, even-lower amplitude M-C shell centered near R ≈ 3.5 Å generates very strong correlations between the M-S and M-C shells' fit parameters. In addition, the attempts to fit the M-C coordination resulted in large error estimates that render such estimates too unreliable to be useful. Given the low amplitude of the M-S contribution to the EXAFS and the expected coordination of TDA and TPA, we hypothesize that there are only one or, at most, two S neighbors around the metal. In the case of one S neighbor, the only contribution to the Debye-Waller (pair-distance distribution variance) factor, σ^2, is thermal. Since the thermal contribution to σ^2(M-O) is generally near 0.005 $Å^2$ at similar bond lengths (eg. see Ref. [150–153]) and the M-S bond length is over 0.5 Å longer, and is therefore more weakly bound, we expect σ^2(M-S) to be between 0.005 $Å^2$ and 0.01 $Å^2$. We choose 0.008 $Å^2$ as a reasonable value that could also account for small bond length differences in the event of two S atoms coordinating the metal. Fits using 0.005 $Å^2$ indicate a potential 30% absolute error, but by freezing to 0.008 Å, we can better compare values between samples. In addition, we freeze the M-C coordination to both 4 and 8 in the fits to test for any correlation effect on the M-S parameters. We observe no significant effect on the S shell; these fit comparisons are presented in Appendix B.

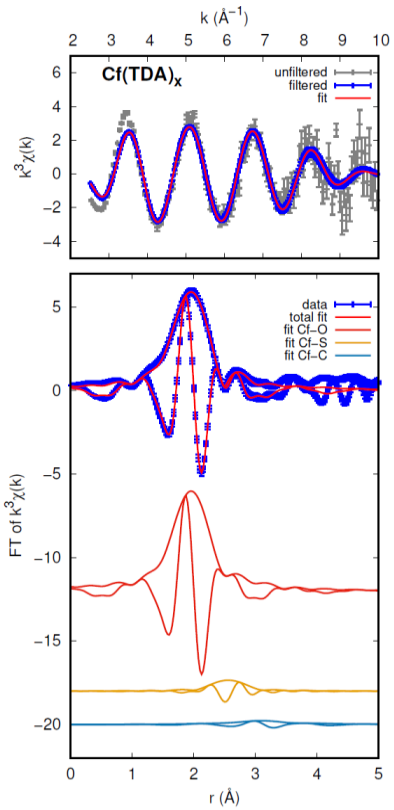

Figure 5.7 Data and fit results for the Cf(TDA)$_x$ sample, assuming N(Cf-C)=4. The left panel shows the data and results in k-space. The right panel shows the Fourier transform (FT), where the outer envelope is the complex transform amplitude and the modulating line is the real part. The data were transformed between 2.5 and 10 Å^{-1}, and narrowed with a Gaussian window with width 0.3 Å^{-1}. The fit range is from 1.5 to 3.5 Å. Individual fit components are arbitrarily offset vertically for display.

The pertinent fit results for all the samples are given in Table 5.3, which shows the coordination numbers, N, and pair distances, R, for the M-O and M-S pairs for all measured samples freezing N(M-C)=4. The coordination number for all M-O pairs is consistent with 8. A slight contraction is measured from Eu to Tb and from Cm to Cf. M-S coordination is clearly observed based on the measured N for the samples, except possibly Eu(TPA) and both Tb samples. For the others, N(M-S) is consistent with a single S coordinating the metal, although Cm(TDA)$_x$ may have 2 S, and therefore is also consistent with Cm(TDA)$_2$. Moreover, the fit to the data from this sample is the only one that clearly improves with 8 Cm-C atoms compared to 4 Cm-C pairs (see Appendix B); however, we emphasize again that allowing this coordination to

be free in the fit produces very large error estimates. Although the estimated errors can encompass no coordinating S in the Eu(TPA) and Tb samples, the data can also accommodate 1 S neighbor.

Table 5.3 Fit results assuming σ^2(M-S) = 0.008 Å^2 and N(M-C) = 4. Note that with these constraints, the absolute error on N(M-S) is estimated to be as large as 30%. For full details and for fits with N(M-C) = 8, see Appendix B.

Pair	Eu	Tb	Cm	Bk	Cf
R(M-O)(Å) TDA	2.404(4)	2.382(7)	2.440(10)	2.410(8)	2.426(7)
R(M-O) (Å) TPA	2.419(9)	2.396(6)	2.467(8)	-	-
R(M-S) (Å) TDA	3.09(2)	3.04(4)	3.05(2)	3.05(1)	3.04(2)
R(M-S) (Å) TPA	3.08(9)	2.86(7)	3.07(2)	-	-
N(M-O) TDA	7.2(4)	7(1)	7(1)	8(1)	8(1)
N(M-O) TPA	9(1)	8(1)	8(1)	-	-
N(M-S) TDA	0.9(2)	0.5(3)	1.6(4)	1.2(2)	0.7(2)
N(M-S) TPA	0.5(4)	0.3(2)	0.8(2)	-	-

EXAFS results from the $Cm(TDA)_2^-$ complex are consistent with each of the TDA ligands binding Cm in a tridentate manner with an average of 1.6 ± 0.4 coordinating sulfur atoms at a distance of 3.05 ± 0.02 Å. Tridentate TDA also accounts for four of the coordinated oxygens and the remaining oxygens come from three coordinated water molecules. For the same Eu and Tb complexes, an average of only 0.9 ± 0.2 and 0.5 ± 0.3 coordinating sulfur atoms was observed at a longer distance of 3.09 ± 0.02 and 3.04 ± 0.04 Å. The greater number of sulfur atoms coordinating Cm at a shorter distance as compared to Eu is indicative of a preferential interaction between Cm and S as is also seen in the formation constants for these two metals. Bk and Cf samples were prepared under conditions that would promote the 1:1 complex and the observed number of coordinating sulfur atoms is consistent with the $M(TDA)^+$ species. The TPA complexes show an average number of 0.8 ± 0.2 sulfur atoms coordinating Cm in the $Cm(TPA)^+$ complex. Less sulfur was observed in the coordination sphere of either Eu or Tb which suggests the possibility of different coordination modes for lanthanides and actinides with TPA. Both TDA and TPA have greater M-S bond lengths with the actinides than has been reported for the dithiocarbamates[54]. This is presumably due to the reduced electrostatic interaction between the metal in and neutral sulfur of TDA or TPA compared to the anionic dithiocarbamate.

5.4.4 Computational results

Computational studies of the Cm, Eu, and Gd complexes with TDA, THTPA, and TPA show the geometry of the optimized complex varies with both the identity of the metal and the ligand. The pertinent bond lengths of the low energy conformers are shown in Table 5.4. The lowest energy complexes with TDA and THTPA have both ligands binding in a tridentate manner with one oxygen from each carboxylic acid group and the sulfur coordinating the metal ion, Figures 5.8A and 5.8B. Conformers in which the sulfur of TDA is not binding with the metal center and other mono- or bidentate conformers were found to be higher in energy than the tridentate complexes. As was seen with the EXAFS experiments with TDA, these complexes both show similar distances between the metal and oxygens of the carboxylic acid groups for the similarly sized Cm (0.97 Å[154]) and Eu (0.947 Å[154]) ions while the smaller Gd (0.938 Å[154]) ion gives a somewhat shorter Gd-O length. This trend may not be seen in the metal sulfur bond length where the Cm-S distance is shorter than the Eu-S distance despite the ionic radii of the two metals being similar, although at 1σ uncertainty, these bond lengths a nearly the same. The shorter Cm-S bond, also seen in the EXAFS experiments, may indicate that the sulfur is capable of interacting more strongly with Cm than Eu, but could also be explained by the slightly larger size of the Cm ion.

Complexation by TPA is more complex as multiple complexation modes exist. Unlike TDA and THTPA, tridentate complexation by TPA is hampered by the rigidity of the ligand. The resulting tridentate TPA complexes are far from the lowest energy conformers. Instead, TPA can bind in two different bidentate modes with a lower energy. The lowest energy mode occurs when TPA is binding with both oxygen atoms from a single carboxylic acid (TPA Bi), Figure 5.8C. In this binding mode, the sulfur is too distant from the metal to form any metal sulfur bond. At an energy 22 to 29 kJ/mol above that of TPA Bi is another conformer in which bidentate TPA binds through one oxygen of one carboxylic acid and the sulfur (TPA OS), Figure 5.8D. Although this TPA OS conformer appears to be higher in energy than TPA Bi, it is close enough that it may form to some extent, as was observed by EXAFS. The formation of this conformer is likely dependent on the solvation of the TPA, which unfortunately was not determined or accounted for in the implicit COSMO solvation used in these DFT studies. In the TPA OS conformer, the Cm-S bond length is shorter than the Eu-S length and even the Gd-S length. As with TDA and

THTPA, this is indicative of the sulfur contributing to actinide selectivity and is consistent with the measured formation constants.

Table 5.4 Bond lengths of the computed Cm, Eu, and Gd complexes with TDA, THTPA, and TPA. Coordinating water molecules were added to maintain a coordination number of nine for all complexes. TPA Bi binds to the metal center using both oxygens from one carboxylate group. TPA OS binds to the metal by one oxygen and the sulfur.

		Bond Length (Å)		
Ligand	Bond	Cm	Eu	Gd
TDA	M-O	2.331 & 2.335	2.326 & 2.371	2.287 & 2.294
	M-S	3.040	3.073	3.039
THTPA	M-O	2.327 & 2.337	2.334 & 2.367	2.282 & 2.295
	M-S	2.993	3.038	2.989
TPA Bi	M-O	2.415 & 2.433	2.443 & 2.457	2.373 & 2.408
	M-S	5.366	5.382	5.318
TPA OS	M-O	2.362	2.404	2.315
	M-S	3.108	3.203	3.124

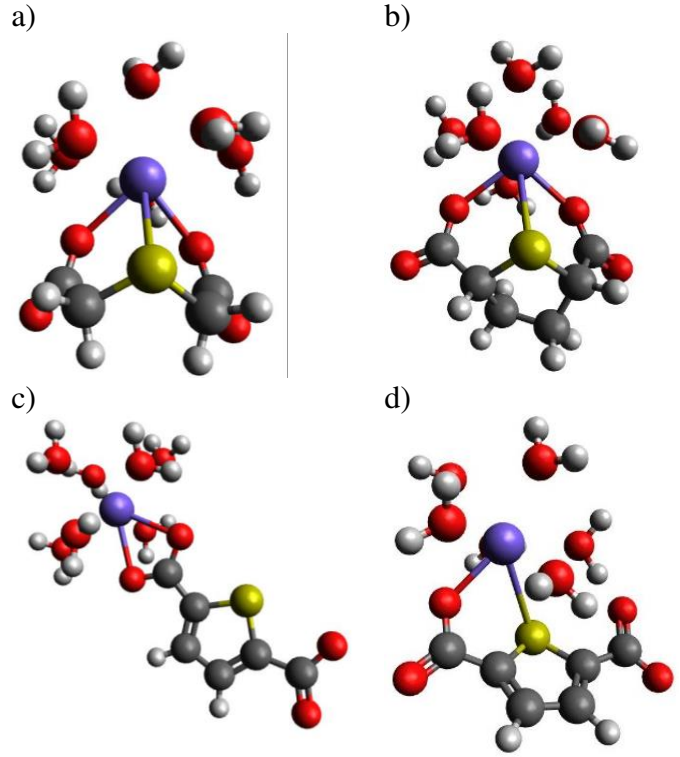

Figure 5.8 The structures of a) TDA, b) THTPA, c) TPA Bi (two coordinating oxygens in one carboxylate group), and d) TPA OS (one oxygen and one sulfur coordinating) complexes. The purple atom represents the metal ion, red represents oxygen, yellow represents sulfur, black represents carbon, and white represents hydrogen.

The energy of formation of the optimized complexes from the hydrated metal ion and free ligand was compared to see if the changes in the geometry of the structure, particularly the metal-sulfur bond length, reveal information regarding the selectivity of the ligands. Table 5.5 shows the energies of the complexes. These energies are calculated by subtracting the sum of the reactant's energies from the sum of the product's energies for Equation 5.1, where *d* represents the denticity of the ligand. The energy of for the tridentate TDA (and THTPA) complexes is considerably lower than either of the bidentate TPA complexes corresponding with the higher formation constants observed for TDA than TPA. The energy of the TDA and TPA OS complexes is slightly lower for Cm than for the slightly smaller Eu, which could be indicative of selectivity. However, since the differences in energies are within the errors expected for these calculations[40,134], conclusions about the better selectivity towards Cm based on these numbers can be ambiguous. The energy of the Gd complex is somewhat lower than for Cm which could be due to greater interactions between the smaller and more charge dense Gd ion or uncertainty. For TPA Bi, in which no sulfur is coordinating the metal ion and no selectivity is expected, the energy for the formation of the Cm and Eu complex is quite similar as would be expected for a non-selective ligand. As was seen with TDA and TPA OS, the formation energy of the Gd complex is slightly lower. The size of the metal ions may also play a role in the formation energy of these complexes as Dellien et al.[155] found that the formation constants of lanthanides with TDA are dependent upon the metal ions size with the highest formation constant for Sm (0.958 Å[154]) and lower formation constants for both larger and smaller lanthanides. As Cm (0.97 Å[154]), is close in ionic radii to Sm, the lower formation energy of the Cm could be due to its size. Therefore, although there are trends in the energy calculations, selectivity cannot be determined with certainty and distinguished from metal size effects from these measurements.

$$M(H_2O)_9^{3+} + L^{2-} \rightleftharpoons ML(H_2O)_{9-d}^{+} + d\ H_2O \qquad (5.1)$$

Table 5.5 Energy of formation (ΔE, kJ/mol) for geometry optimized 1:1 complexes with sufficient coordinated water molecules to maintain a coordination number of nine for Cm, Eu, and Gd with TDA, THTPA, and TPA. The denticity (d) of each ligand is also included.

Ligand	Cm	Eu	Gd	d
TDA	-179	-172	-185	3
THTPA	-187	-193	-189	3
TPA Bi	-120	-119	-129	2
TPA OS	-98	-91	-100	2

5.4.5 Coordination Chemistry & Selectivity Discussion

The determination of formation constants for the lanthanides and actinides enables the calculation of the selectivity of that particular ligand. The further from unity the value of β_{An}/β_{Eu} is, the more selective the ligand will be, Table 5.6.

Table 5.6 Calculated values of β_{An}/β_{Eu}. The upper and lower bounds at 1σ uncertainty of this value are shown in parenthesis.

Ligand	Formation Constants	Actinide	β_{An}/β_{Eu}	Calculated from Ref.
TDA	1:2	Am	3.39 (2.95, 3.89)	
		Cm	6.76 (5.13, 8.91)	
	1:1	Am	1.14 (1.07, 1.20)	
		Cm	1.24 (1.07, 1.44)	
		Am	1.15 (1.00, 1.32)	[148]
		Cm	0.98 (0.81, 1.17)	[148]
TPA	1:1	Am	1.77 (1.61, 1.93)	
		Cm	1.65 (1.50, 1.80)	
IDA	1:1	Am	1.45 (1.12, 1.86)	[148,156]
		Cm	1.20 (0.93, 1.55)	[148,156]
DPA	1:2	Am	1.70 (1.48, 1.95)	[157]
	1:1	Am	1.00 (0.91, 1.10)	[157]

The ratios of formation constants shown in Table 5.6 for TDA and TPA are all greater than one which indicates that a separation of the actinides Am and Cm from Eu is possible. These values are higher for the 1:1 complex of TPA than the 1:1 complex of TDA which indicates that TPA is more selective, but the 1:2 complex of TDA is the most selective. As this suggests that complexes with more sulfur donating ligands are more selective, it may be possible that if the 1:2 complex could be observed with TPA, this complex would have even higher selectivity. Additionally, these calculated selectivities can be compared to the calculated selectivities for other ligands with published acid dissociation and formation constants. Of interest here are iminodiacetic acid (IDA) and 2,6-pyridinedicarboxylic acid (DPA), Figure 5.9. IDA and DPA are both nitrogen donor ligands and have similar physical and electronic structures to TDA and TPA respectively. With IDA, only the formation constants for the 1:1 complex were published by Thakur et al.[148], so to compare IDA with TDA, only the 1:1 complex with TDA was considered. The 1:1 complex of TDA shows less selectivity than IDA with Am, but slightly more with Cm. The 1:1 complex of DPA shows no selectivity as the formation constants were the same for Am and Eu, but moderate selectivity with the 1:2 complex[157]. When comparing the 1:1 complexes of TPA and DPA, it appears that TPA has more selectivity than DPA and it's selectivity for Am and Cm is nearly equal to the selectivity of the DPA 1:2 complex.

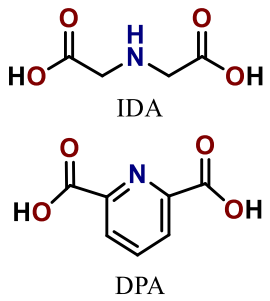

Figure 5.9 Structures of iminodiacetic acid (IDA) and 2,6-pyridinedicarboxylic acid (DPA).

Ultimately, both TDA and TPA show some selectivity between lanthanides and actinides due to the higher formation constants for actinides than lanthanides. TPA is more promising as the formation constants show a greater selectivity for the actinides, when compared to the corresponding 1:1 TDA complex, possibly due to the preferred TPA OS binding conformation for the actinides whereas the lanthanides may tend to form the TPA Bi complex. It may be expected that TDA and TPA would have more similar behavior as they are both thioethers, but

the electronic structure of these ligands is different as TDA is aliphatic whereas TPA is aromatic. A major consequence of the aromatic structure of TPA is being softer than the aliphatic TDA, which could explain the different structures and greater selectivity that was observed with TPA. As it appears that the aromatic thioether is especially selective, the addition of more of these coordinating sulfur sites in the coordination shell of a metal would likely further increase selectivity, as was observed with TDA. This could be achieved by formation of higher complexes than $M(TPA)^+$. However, with TPA, this is limited due to the poor aqueous solubility of the ligand preventing these complexes from forming.

5.5 Conclusions

The ligands TDA, THTPA, and TPA were tested for the ability to selectively bind trivalent actinides and lanthanides. The EXAFS of the TDA complexes suggest a stronger interaction between Cm, Bk and Cf and the sulfur atom than for either the Eu or Tb cations. This finding with Cm and Eu was further supported by the computational results which were also comparable for THTPA. EXAFS experiments of TPA complexes show the presence of more sulfur in the coordination sphere of Cm, than for either Eu or Tb. This suggests that Cm tends to form complexes with TPA OS due to the favorable interaction between Cm and sulfur, while Eu and Tb tend to complex with TPA Bi. The selectivity that TPA has for Cm is seen in the formation constants, where the values for the actinides Am and Cm are higher than either of the lanthanides tested.

The findings here suggest that softer TPA has greater selectivity for the actinides compared to either TDA or THTPA as 1:1 complexes and the related nitrogen donor ligand DPA as a 1:1 complex. Higher complexes of TDA showed even greater selectivity, but the analogous TPA complexes were not observed as the use of TPA is hampered by its poor solubility in acidic aqueous solutions and low formation constants that partially arise due to the inability to bind in a tridentate manner because of its rigid, aromatic structure.

5.6 Acknowledgements

The work at Colorado School of Mines was supported by the U.S. Department of Energy Office of Science, Office of Basic Energy Sciences, Heavy Elements Chemistry Program at Colorado School of Mines under Award Number DE-SC0020189. This work was also based

upon support provided to N.P.B. by the U.S. Department of Energy, Office of Science Graduate Student Research (SCGSR) Program. P.Y. and E.R.B. was sponsored by the US Department of Energy, Chemical Sciences, Geosciences, and Biosciences Division, Separation program, under Award Number DE-SC0000248350. This work was also supported by the US Department of Energy through the Los Alamos National Laboratory. Los Alamos National Laboratory is operated by Triad National Security, LLC, for the National Nuclear Security Administration of U.S. Department of Energy (Contract No. 89233218CNA000001). N.P.B.'s work at Idaho National Laboratory was supported by U.S. Department of Energy Offices of Nuclear Energy and Environmental Management under the Radiochemistry Traineeship program at the Colorado School of Mines. All experimental work at the Idaho National Laboratory was performed under contract DE-AC07-05ID14517. The Bk-249 and Cf-249 used in this and prior research by this PI were supplied by the United States Department of Energy Office of Science by the Isotope Program in the Office of Nuclear Physics. X-ray absorption studies were supported by the U.S. Department of Energy Office of Science, Office of Basic Energy Sciences, Heavy Elements Chemistry Program at the Lawrence Berkeley National Laboratory under Contract No. DE-AC02-05CH11231. Use of the Stanford Synchrotron Radiation Lightsource, SLAC National Accelerator Laboratory, is supported by the U.S. Department of Energy, Office of Science, Office of Basic Energy Sciences under Contract No. DEAC02-76SF00515. I.A.P. acknowledges the support from J. Robert Oppenheimer Distinguished Postdoctoral Fellowship at Los Alamos National Laboratory.

CHAPTER 6

CONCLUDING STATEMENTS

Within this dissertation, research on advancing the separation of trivalent lanthanides and actinides with sulfur donating ligands and extractants has been discussed. Sulfur donor-based separation processes have shown remarkably high selectivities for the actinides but are often complicated by the formation of multiple species and unclear mechanisms for their formation. These complex systems need to be more thoroughly characterized in order to both understand and optimize a potential separation procedure and to provide more insight into the fundamental chemistry of the actinides. To pursue a more complete understanding of these sulfur donor systems, three different studies were completed. A novel method for quickly quantifying the commercially available and widely studied dithiophosphinic acid HC301 within a possible separations process by permanganometry has been discussed as knowing and controlling process conditions is necessary for an efficient and effective separation. The extraction behavior of the transplutonium actinides Am-Es with HC301 was examined to determine what how readily these metals are extracted and what extracted complexes they form. Additionally, a study on thioether based ligands with greater stability than HC301 is reported to see in thioethers can provide similar selectivity to the dithiophosphinic acids while having greater resistance to degradation. Both HC301 and thioethers have selectivity for the actinides and appear to form complexes with different structures for the lanthanides and actinides. The lanthanides tended to have less coordination by sulfur and longer metal-sulfur bonds when present, whereas the actinides generally had more extensive coordination by sulfur and shorter metal-sulfur bonds. Due to these differences, existing sulfur donors show great promise for the separation of actinides and lanthanides which may be further improved by the development of even more selective sulfur donating ligands and extractants.

6.1 Permanganometric Quantification of Cyanex 301

A one-step permanganometric titration with subsequent colorimetric analysis has proven to be an effective method for quickly determining the amount of HC301 in *n*-dodecane. Water, acetone, and a mixture of benzene and 18-crown-6 were tested as possible solvents for this

reaction. Potassium permanganate was found to have the highest stability in water but was unsuitable for colorimetric determination as droplets of insoluble *n*-dodecane and oxidized HC301 scattered light preventing the quantification of the remaining $KMnO_4$. Although $KMnO_4$ had reduced stability in both organic solvents tested, the acetone-based solution was able to accurately quantify the amount of HC301 by setting up the double beam spectrophotometer to automatically account for the degradation of $KMnO_4$. The accuracy of this quantification was assessed by Leave-One-Out Cross-Validation and found to vary by up to 4.03% with an average difference of 1.73%.

6.2 Extraction of Transplutonium Actinides with Cyanex 301

The extraction of the trivalent actinides Am-Es and many of the lanthanides by HC301 was examined to determine if the transcurium actinides are extracted as inner sphere complexes like the lighter actinides and lanthanides or as outer sphere complexes like the heavier lanthanides. The distribution ratios and pH dependence of the transcurium actinides were found to be relatively similar to Am and Cm, but this alone could not prove a continuation of the inner sphere coordination across the actinide series as the change from inner- to outer-sphere coordination was found to have a limited impact on the distribution ratios of the lanthanides. The dependence of the distribution ratio upon the aqueous nitrate concentration was also examined and found to provide support for the formation of inner-sphere complexes with the transcurium actinides. On increasing the aqueous nitrate concentration, the extraction of the lanthanides, particularly the heavier lanthanides, was found to increase while the extraction of the actinides was relatively constant. As the nitrate addition suppresses the extraction of water, it seems that the formation of outer sphere complexes is suppressed leaving the lanthanides only able to form the more extractable inner-sphere complexes. Since the extraction of the actinides remained unchanged, it appears that they were originally extracted as inner sphere complexes and thus unaffected by the suppression of outer sphere complexes.

6.3 Aqueous Sulfur Donor Ligands

The thioether based ligands 2,2'-thiodiacetic acid (TDA), (2R,5S)-tetrahydrothiophene-2,5-dicarboxylic acid (THTPA), and 2,5-thiophenedicarboxylic acid (TPA) were examined for their ability to selectively bond with the actinides. Formation constants were found to be higher for the actinides than for either of the lanthanides tested indicating that these ligands are selective

for the actinides. Extended x-ray absorption fine structure spectroscopy revealed that the actinides are coordinated by more sulfur atoms from these ligands at a closer distance than for the lanthanides. These trends in bond lengths were reproduced computationally where TDA and THTPA were both able to form tridentate complexes while TPA formed two distinct bidentate conformers. In comparing 1:1 complexes, the softer, aromatic TPA was found to have a higher selectivity than the aliphatic TDA, but higher complexes with TDA that could not be replicated with TPA had even greater selectivity for the actinides.

6.4 Future Directions

This work has expanded our knowledge of sulfur donor chemistry for the separation of trivalent actinides and lanthanides, but additional research is needed before these processes could be implemented in the reprocessing of used nuclear fuel. One of the most pressing challenges, that was not addressed here, is the development of wasteforms that are amenable to the containment of sulfur, particularly as sulfate. Future studies more closely related to this work would include testing the ability of permanganometry to quantify other dithiophosphinic acids and oxidizable species. Of particular interest would be the dithiophosphinic acid bis(*o*-trifluoromethylphenyl)dithiophosphinic acid, which has displayed greater selectivity than HC301, but is more resistant to oxidation. More thoroughly examining the extraction of transcurium actinides is also of interest. Although the solvent extraction studies presented here suggest these metals are extracted as inner sphere complexes, more concrete studies, such as extended x-ray absorption fine structure spectroscopy and dynamic light scattering, are needed to conclusively determine what is occurring when transcurium actinides are extracted by HC301. Expanding upon the work with aqueous thioether based ligands may also prove valuable. Examining more metals with these ligands will reveal not only possible separations methods but may uncover more fundamental information about the heavy actinides. Additionally, as reasonable selectivity was observed with these thioether ligands which was increased upon forming higher complexes with more coordinating sulfur, development of new ligands that are more able to displace bound water molecules with sulfur and increase the number of coordinating sulfur sites may further increase the selectivity of this class of ligands.

REFERENCES

(1) Michel-Sendis, F.; Gauld, I.; Martinez, J. S.; Alejano, C.; Bossant, M.; Boulanger, D.; Cabellos, O.; Chrapciak, V.; Conde, J.; Fast, I.; et al. SFCOMPO-2.0: An OECD NEA Database of Spent Nuclear Fuel Isotopic Assays, Reactor Design Specifications, and Operating Data. *Ann. Nucl. Energy* **2017**, *110*, 779–788. https://doi.org/10.1016/j.anucene.2017.07.022.

(2) Gauld, I. C.; Williams, M. L.; Michel-Sendis, F.; Martinez, J. S. Integral Nuclear Data Validation Using Experimental Spent Nuclear Fuel Compositions. *Nucl. Eng. Technol.* **2017**, *49* (6), 1226–1233. https://doi.org/10.1016/j.net.2017.07.002.

(3) Jensen, M. P.; Bond, A. H. Influence of Aggregation on the Extraction of Trivalent Lanthanide and Actinide Cations by Purified Cyanex 272, Cyanex 301, and Cyanex 302. *Radiochim. Acta* **2002**, *90* (4), 205–209. https://doi.org/10.1524/ract.2002.90.4_2002.205.

(4) Matloka, K.; Sah, A. K.; Srinivasan, P.; Scott, M. J. Design , Synthesis and Evaluation of Carbamoylmethylphosphine Sulfide (CMPS) -Based Chelates for Separation of Lanthanides and Actinides. *Comptes Rendus Chim.* **2007**, *10* (10–11), 1026–1033. https://doi.org/10.1016/j.crci.2007.02.006.

(5) Pattee, D.; Musikas, C.; Faure, A.; Chachaty, C. Extraction of Lanthanides and Actinides (III) by Di-2-Ethyl Dithiophosphoric Acid and Di-2-Ethyl Hexyl Monothiophosphoric Acid. Structure of the Complexes in the Organic Phase. In *International Solvent Extraction Conference*; **1986**; pp 1–8.

(6) Tian, G.; Zhu, Y.; Xu, J. Extraction of Am(III) and Ln(III) by Dialkyldithiophosphinic Acid with Different Alkyl Groups. *Solvent Extr. Ion Exch.* **2001**, *19* (6), 993–1005. https://doi.org/10.1081/SEI-100107615.

(7) Klaehn, J. R.; Peterman, D. R.; Harrup, M. K.; Tillotson, R. D.; Luther, T. A.; Law, J. D.; Daniels, L. M. Synthesis of Symmetric Dithiophosphinic Acids for "Minor Actinide" Extraction. *Inorganica Chim. Acta* **2008**, *361* (8), 2522–2532. https://doi.org/10.1016/j.ica.2008.01.007.

(8) Peterman, D. R.; Greenhalgh, M. R.; Tillotson, R. D.; Klaehn, J. R.; Harrup, M. K.; Luther, T. A.; Law, J. D. Selective Extraction of Minor Actinides from Acidic Media Using Symmetric and Asymmetric Dithiophosphinic Acids. *Sep. Sci. Technol.* **2010**, *45* (12–13), 1711–1717. https://doi.org/10.1080/01496395.2010.493787.

(9) Jensen, M. P.; Bond, A. H. Comparison of Covalency in the Complexes of Trivalent Actinide and Lanthanide Cations. *J. Am. Chem. Soc.* **2002**, *124* (33), 9870–9877. https://doi.org/10.1021/ja0178620.

(10) Tian, G.; Zhu, Y.; Xu, J.; Zhang, P.; Hu, T.; Xie, Y.; Zhang, J. Investigation of the Extraction Complexes of Light Lanthanides(III) with Bis(2,4,4-Trimethylpentyl)Dithiophosphinic Acid by EXAFS, IR, and MS in Comparison with the Americium(III) Complex. *Inorg. Chem.* **2003**, *42* (3), 735–741. https://doi.org/10.1021/ic025783z.

(11) Tian, G.; Zhu, Y.; Xu, J.; Hu, T.; Xie, Y. Characterization of Extraction Complexes of Am(III) with Dialkyldithiophosphinic Acids by Extended X-Ray Absorption Fine Structure Spectroscopy. *J. Alloys Compd.* **2002**, *334* (1–2), 86–91. https://doi.org/10.1016/S0925-8388(01)01783-2.

(12) Zhu, Y.; Chen, J.; Jiao, R. Extraction of Am(III) and Eu(III) from Nitrate Solution with Purified Cyanex 301. *Solvent Extr. Ion Exch.* **1996**, *14* (1), 61–68. https://doi.org/10.1080/07366299608918326.

(13) Chen, J.; Jiao, R.; Zhu, Y. A Study on the Radiolytic Stability of Commercial and Purified Cyanex 301. *Solvent Extr. Ion Exch.* **1996**, *14* (4), 555–565. https://doi.org/10.1080/07366299608918356.

(14) Stern, E. A. Number of Relevant Independent Points in X-Ray-Absorption Fine-Structure Spectra. *Phys. Rev. B* **1993**, *48* (13), 9825–9827. https://doi.org/10.1103/PhysRevB.48.9825.

(15) Booth, C. H.; Hu, Y.-J. Confirmation of Standard Error Analysis Techniques Applied to EXAFS Using Simulations. *J. Phys. Conf. Ser.* **2009**, *190*, 012028. https://doi.org/10.1088/1742-6596/190/1/012028.

(16) Broeders, C. H.; Kiefhaber, E.; Wiese, H. Burning Transuranium Isotopes in Thermal and Fast Reactors. *Nucl. Eng. Des.* **2000**, *202* (2–3), 157–172. https://doi.org/10.1016/S0029-5493(00)00341-1.

(17) Ozawa, M.; Koma, Y.; Nomura, K.; Tanaka, Y. Separation of Actinides and Fission Products in High-Level Liquid Wastes by the Improved TRUEX Process. *J. Alloys Compd.* **1998**, *271–273*, 538–543. https://doi.org/10.1016/S0925-8388(98)00147-9.

(18) Pearson, R. G. Hard and Soft Acids and Bases. *J. Am. Chem. Soc.* **1963**, *85* (22), 3533–3539. https://doi.org/10.1021/ja00905a001.

(19) Street, K. J.; Seaborg, G. T. The Separation of Americium and Curium from the Rare Earth Elements. *J. Am. Chem. Soc.* **1950**, *72* (6), 2790–2792. https://doi.org/10.1021/ja01162a530.

(20) Musikas, C.; Le Marois, G.; Fitoussi, R.; Cuillerdier, C. Properties and Uses of Nitrogen and Sulfur Donors Ligands in Actinide Separations. In *Actinide Separations*; **1980**; pp 131–145. https://doi.org/10.1021/bk-1980-0117.ch010.

(21) Choppin, G. R. Comparison of the Solution Chemistry of the Actinides and Lanthanides. *J. Less Common Met.* **1983**, *93*, 323–330.

(22) Casellato, U.; Vidali, M.; Vigato, P. A. Actinide Complexes with Chelating Ligands Containing Sulfur and Amidic Nitrogen Donor Atoms. *Coord. Chem. Rev.* **1979**, *28* (2–3), 231–277. https://doi.org/10.1016/S0010-8545(00)82015-9.

(23) Choppin, G. R.; Thakur, P.; Mathur, J. N. Complexation Thermodynamics and Structural Aspects of Actinide – Aminopolycarboxylates. *Coord. Chem. Rev.* **2006**, *250* (7–8), 936–947. https://doi.org/10.1016/j.ccr.2006.02.003.

(24) Gaunt, A. J.; Reilly, S. D.; Enriquez, A. E.; Scott, B. L.; Ibers, J. A.; Sekar, P.; Ingram, K.

I. M.; Kaltsoyannis, N.; Neu, M. P. Experimental and Theoretical Comparison of Actinide and Lanthanide Bonding in M $[N(EPR_2)_2]_3$ Complexes (M = U , Pu , La , Ce ; E = S , Se , Te ; R = Ph, IPr, H). *Inorg. Chem.* **2008**, *47* (1), 29–41. https://doi.org/10.1021/ic701618a.

(25) Roger, M.; Barros, N.; Arliguie, T.; Thuery, P.; Maron, L.; Ephritikhine, M. Lanthanide (III)/ Actinide(III) Differentiation in Agostic Interactions and an Unprecedented η^3 Ligation Mode of the Arylthiolate Ligand , from X-Ray Diffraction and DFT Analysis. *J. Am. Chem. Soc.* **2006**, *128* (35), 8790–8802. https://doi.org/10.1021/ja0584830.

(26) Cross, J. N.; Macor, J. A.; Bertke, J. A.; Ferrier, M. G.; Girolami, G. S.; Kozimor, S. A.; Maassen, J. R.; Scott, B. L.; Shuh, D. K.; Stein, B. W.; et al. Comparing the 2,2'-Biphenylenedithiophosphinate Binding of Americium with Neodymium and Europium Angewandte. *Angew. Chemie Int. Ed.* **2016**, *55* (41), 12755–12759. https://doi.org/10.1002/anie.201606367.

(27) Klaehn, J. R.; Peterman, D. R.; Harrup, M. K.; Tillotson, R. D.; Luther, T. A.; Law, J. D.; Daniels, L. M. Synthesis of Symmetric Dithiophosphinic Acids for ''Minor Actinide" Extraction. *Inorganica Chim. Acta* **2008**, *361*, 2522–2532. https://doi.org/10.1016/j.ica.2008.01.007.

(28) Bhattacharyya, A.; Mohapatra, P. K.; Manchanda, V. K. Separation of Americium(III) and Europium(III) from Nitrate Medium Using a Binary Mixture of Cyanex-301 with N-donor Ligands. *Solvent Extr. Ion Exch.* **2006**, *24* (1), 1–17. https://doi.org/10.1080/07366290500388459.

(29) Clark, A. E.; Yang, P.; Shafer, J. C. Coordination of Actinides and the Chemistry Behind Solvent Extraction. In *Experimental and Theoretical Approaches to Actinide Chemistry*; **2018**; pp 237–282.

(30) Choppin, G. R. Studies of the Synergistic Effect. *Sep. Sci. Technol.* **1981**, *16* (9), 1113–1126. https://doi.org/10.1080/01496398108057602.

(31) Keith, J. M.; Batista, E. R. Theoretical Examination of the Thermodynamic Factors in the Selective Extraction of Am^{3+} from Eu^{3+} by Dithiophosphinic Acids. *Inorg. Chem.* **2012**, *51* (1), 13–15. https://doi.org/10.1021/ic202061b.

(32) Bhattacharyya, A.; Ghanty, T. K.; Mohapatra, P. K.; Manchanda, V. K. Selective Americium(III) Complexation by Dithiophosphinates: A Density Functional Theoretical Validation for Covalent Interactions Responsible for Unusual Separation Behavior from Trivalent Lanthanides. *Inorg. Chem.* **2011**, *50* (9), 3913–3921. https://doi.org/10.1021/ic102238c.

(33) Kaneko, M.; Miyashita, S.; Nakashima, S. Bonding Study on the Chemical Separation of Am(III) from Eu(III) by S-, N-, and O-Donor Ligands by Means of All-Electron ZORA-DFT Calculation. *Inorg. Chem.* **2015**, *54* (14), 7103–7109. https://doi.org/10.1021/acs.inorgchem.5b01204.

(34) Kaneko, M.; Watanabe, M.; Miyashita, S.; Nakashima, S. Roles of D- and f-Orbital Electrons in the Complexation of Eu(III) and Am(III) Ions with Alkyldithiophosphinic Acid and Alkylphosphinic Acid Using Scalar-Relativistic DFT Calculations. *J. Nucl. Radiochem. Sci.* **2017**, *17* (0), 9–15. https://doi.org/10.14494/jnrs.17.9.

(35) Chandrasekar, A.; Ghanty, T. K. Uncovering Heavy Actinide Covalency: Implications for Minor Actinide Partitioning. *Inorg. Chem.* **2019**, *58* (6), 3744–3753. https://doi.org/10.1021/acs.inorgchem.8b03358.

(36) Gans, P.; Sabatini, A.; Vacca, A. Investigation of Equilibria in Solution. Determination of Equilibrium Constants with the HYPERQUAD Suite of Programs. *Talanta* **1996**, *43* (10), 1739–1753. https://doi.org/10.1016/0039-9140(96)01958-3.

(37) Teo, B. K.; Joy, D. C. *EXAFS Spectroscopy: Technique and Applications*; **1981**.

(38) Drader, J. A.; Luckey, M.; Braley, J. C. Thermodynamic Considerations of Covalency in Trivalent Actinide- (Poly)Aminopolycarboxylate Interactions Thermodynamic Considerations of Covalency in Trivalent. *Solvent Extr. Ion Exch.* **2016**, *34* (2), 114–125. https://doi.org/10.1080/07366299.2016.1140436.

(39) Seaborg, G. T. Place in Periodic System and Electronic Structure of the Heaviest Elements. *Nucleonics* **1949**, *5*, 16–36.

(40) Kelley, M. P.; Su, J.; Urban, M.; Luckey, M.; Batista, E. R.; Yang, P.; Shafer, J. C. On the Origin of Covalent Bonding in Heavy Actinides. *J. Am. Chem. Soc.* **2017**, *139*, 9901–9908. https://doi.org/10.1021/jacs.7b03251.

(41) Cary, S. K.; Vasiliu, M.; Baumbach, R. E.; Stritzinger, J. T.; Green, T. D.; Diefenbach, K.; Cross, J. N.; Knappenberger, K. L.; Liu, G.; Silver, M. A.; et al. Emergence of Californium as the Second Transitional Element in the Actinide Series. *Nat. Commun.* **2015**, *6* (1), 6827. https://doi.org/10.1038/ncomms7827.

(42) Silver, M. A.; Cary, S. K.; Johnson, J. A.; Baumbach, R. E.; Arico, A. A.; Luckey, M.; Urban, M.; Wang, J. C.; Polinski, M. J.; Chemey, A.; et al. Characterization of Berkelium(III) Dipicolinate and Borate Compounds in Solution and the Solid State. *Science (80),* **2016**, *353* (6302), aaf3762–aaf3762. https://doi.org/10.1126/science.aaf3762.

(43) Kelley, M. P.; Bessen, N. P.; Su, J.; Urban, M.; Sinkov, S. I.; Lumetta, G. J.; Batista, E. R.; Yang, P.; Shafer, J. C. Revisiting Complexation Thermodynamics of Transplutonium Elements up to Einsteinium. *Chem. Commun.* **2018**, *54* (75), 10578–10581. https://doi.org/10.1039/c8cc05230a.

(44) Polinski, M. J.; Wang, S.; Alekseev, E. V; Depmeier, W.; Albrecht-Schmitt, T. E. Bonding Changes in Plutonium(III) and Americium(III) Borates. *Angew. Chemie Int. Ed.* **2011**, *50* (38), 8891–8894. https://doi.org/10.1002/anie.201103502.

(45) Polinski, M. J.; Garner, E. B.; Maurice, R.; Planas, N.; Stritzinger, J. T.; Parker, T. G.; Cross, J. N.; Green, T. D.; Alekseev, E. V; Van Cleve, S. M.; et al. Unusual Structure, Bonding and Properties in a Californium Borate. *Nat. Chem.* **2014**, *6* (5), 387–392. https://doi.org/10.1038/nchem.1896.

(46) Polinski, M. J.; Wang, S.; Alekseev, E. V; Depmeier, W.; Liu, G.; Haire, R. G.; Albrecht-Schmitt, T. E. Curium(III) Borate Shows Coordination Environments of Both Plutonium(III) and Americium(III) Borates. *Angew. Chemie Int. Ed.* **2012**, *51* (8), 1869–1872. https://doi.org/10.1002/anie.201107956.

(47) Iversen, B. B.; Larsen, F. K.; Pinkerton, A. A.; Martin, A.; Darovsky, A.; Reynolds, P. A. Characterization of Actinide Bonding in $Th(S_2PMe_2)_4$ by Synchrotron X-Ray Diffraction. *Inorg. Chem.* **1998**, *37* (18), 4559–4566. https://doi.org/10.1021/ic9715613.

(48) Wang, X.; Andrews, L.; Thanthiriwatte, K. S.; Dixon, D. A. Infrared Spectra of H_2ThS and H_2US in Noble Gas Matrixes : Enhanced. *Inorg. Chem.* **2013**, *52* (18), 10275–10285. https://doi.org/10.1021/ic400560k.

(49) Neidig, M. L.; Clark, D. L.; Martin, R. L. Covalency in F-Element Complexes. *Coord. Chem. Rev.* **2013**, *257* (2), 394–406. https://doi.org/10.1016/j.ccr.2012.04.029.

(50) Kaltsoyannis, N. Does Covalency Increase or Decrease across the Actinide Series? Implications for Minor Actinide Partitioning. *Inorg. Chem.* **2013**, *52* (7), 3407–3413. https://doi.org/10.1021/ic3006025.

(51) Ojovan, M. I.; Lee, W. E. Glassy Wasteforms for Nuclear Waste Immobilization. *Metall. Mater. Trans. A* **2011**, *42A* (4), 837–851. https://doi.org/10.1007/s11661-010-0525-7.

(52) Modolo, G.; Odoj, R. Influence of the Purity and Irradiation Stability of Cyanex 301 on the Separation of Trivalent Actinides from Lanthanides by Solvent Extraction. *J. Radioanal. Nucl. Chem.* **1998**, *228* (1–2), 83–89. https://doi.org/10.1007/BF02387304.

(53) Barros, N.; Maynau, D.; Maron, L.; Eisenstein, O.; Zi, G.; Andersen, R. A. Single but Stronger UO, Double but Weaker UNMe Bonds: The Tale Told by Cp_2UO and Cp_2UNR. *Organometallics* **2007**, *26* (20), 5059–5065. https://doi.org/10.1021/om700628e.

(54) Cary, S. K.; Su, J.; Galley, S. S.; Albrecht-Schmitt, T. E.; Batista, E. R.; Ferrier, M. G.; Kozimor, S. A.; Mocko, V.; Scott, B. L.; Van Alstine, C. E.; et al. A Series of Dithiocarbamates for Americium, Curium, and Californium. *Dalt. Trans.* **2018**, *47* (41), 14452–14461. https://doi.org/10.1039/c8dt02658k.

(55) Daly, S. R.; Keith, J. M.; Batista, E. R.; Boland, K. S.; Clark, D. L.; Kozimor, S. A.; Martin, R. L. Sulfur K - Edge X - Ray Absorption Spectroscopy and Time-Dependent Density Functional Theory of Dithiophosphinate Extractants: Minor Actinide Selectivity and Electronic Structure Correlations. *J. Am. Chem. Soc.* **2012**, *134* (35), 14408–14422. https://doi.org/10.1021/ja303999q.

(56) Tsakiridis, P. E.; Agatzini, S. L. Simultaneous Solvent Extraction of Cobalt and Nickel in the Presence of Manganese and Magnesium from Sulfate Solutions by Cyanex 301. *Hydrometallurgy* **2004**, *72*, 269–278. https://doi.org/10.1016/S0304-386X(03)00180-4.

(57) Rydberg, J.; Musikas, C.; Choppin, G. R. *Principles and Practices of Solvent Extraction*; **1992**.

(58) Clark, A. E.; Yang, P.; Braley, J. 7 Coordination of Actinides and the Chemistry Behind Solvent Extraction 7.2 Overview of Separations Processes. 1–44.

(59) Xu, Q.; Wu, J.; Chang, Y.; Zhang, L.; Yang, Y. Extraction of Am(III) and Lanthanides (III) with Organo Dithiophosphinic Acids. *Radiochim. Acta* **2008**, *96* (12), 771–779. https://doi.org/10.1524/ract.2008.1565.

(60) Xu, Q.; Wu, J.; Zhang, L.; Yang, Y. Extraction of Am(III) and Eu(III) with Dialkyldi (or

Mono) Thiophosphinic (or Phosphoric) Acids. *J. Radioanal. Nucl. Chem.* **2007**, *273* (1), 235–245. https://doi.org/10.1007/s10967-007-0742-8.

(61) Gelis, A. V; Lumetta, G. J. Actinide Lanthanide Separation Process—ALSEP. *Ind. Eng. Chem. Res.* **2014**, *53* (4), 1624–1631. https://doi.org/10.1021/ie403569e.

(62) Nash, K. L.; Choppin, G. R. Separations Chemistry for Actinide Elements : Recent Developments and Historical Perspective. *Sep. Sci. Technol.* **1997**, *32* (1–4), 255–274. https://doi.org/10.1080/01496399708003198.

(63) Lumetta, G. J.; Carter, J. C.; Gelis, A. V; Vandegrift, G. F. Combining Octyl(Phenyl)-N,N-Diisobutyl-Carbamoylmethylphosphine Oxide and Bis-(2-Ethylhexyl)Phosphoric Acid Extractants for Recovering Transuranic Elements from Irradiated Nuclear Fuel. In *Nuclear Energy and the Environment*; ACS Publications, **2010**; pp 107–118. https://doi.org/10.1021/bk-2010-1046.ch009.

(64) Aleksenko, V. Y.; Sharova, E. V; Artyushin, O. I.; Aleksanyan, D. V; Klemenkova, Z. S.; Nelyubina, Y. V; Petrovskii, P. V; Kozlov, V. A.; Odinets, I. L. Coordination of P(X)-Modified (X = O, S) N-Aryl-Carbamoylmethylphosphine Oxides and Sulfides with Pd (II) and Re (I) Ions : Facile Formation of 6,6-Membered Pincer Complexes Featuring Atropisomerism. *Polyhedron* **2013**, *51*, 168–179. https://doi.org/10.1016/j.poly.2012.12.025.

(65) Lefferts, J. L.; Molloy, K. C.; Zuckerman, J. J.; Haiduc, I.; Guta, C.; Ruse, D. Oxy and Thio Phosphorus Acid Derivatives of Tin. 1. Triorganotin(IV) Dithiophosphate Esters. *Inorg. Chem.* **1980**, *19* (6), 1662–1670. https://doi.org/10.1021/ic50208a046.

(66) Curtui, M.; Haiduc, I. Synergic Extraction of Dioxouranium(VI) with Di(2-Ethylhexyl)Dithiophosphoric Acid and Triphenylphosphine Oxide in Benzene. *J. Radioanal. Nucl. Chem.* **1993**, *176* (3), 233–242. https://doi.org/10.1021/BF02163674.

(67) Takayama, R.; Ooe, K.; Yahagi, W.; Fujisawa, H.; Komori, Y.; Kikunaga, H.; Yoshimura, T.; Takahashi, N.; Takahisa, K.; Haba, H.; et al. Solvent Extraction of Trivalent Actinides with Di (2-Ethylhexyl) Phosphoric Acid. *Proc. Radiochem.* **2011**, *1* (1), 157–160. https://doi.org/10.1524/rcpr.2011.0029.

(68) Zhu, Y.; Chen, J.; Choppin, G. R. Extraction of Americium and Fission Product Lanthanides with Cyanex 272 and Cyanex 301. *Solvent Extr. Ion Exch.* **1996**, *14* (4), 543–553. https://doi.org/10.1080/07366299608918355.

(69) Pattee, D.; Musikas, C.; Faure, A.; Chachaty, C. Extraction Des Lanthanides et Actinides Trivalents Par l'acide Di-2-Ethylhexyldithiophosphorique: Structure Des Complexes Organiques. *J. Less-Common Met.* **1986**, *122*, 295–302. https://doi.org/10.1016/0022-5088(86)90423-6.

(70) Hidaka, J.; Fujita, J.; Shimura, Y.; Tsuchida, R. Studies on the Cobalt(III) Complexes of Monothiophosphate Ion. *Bull. Chem. Soc. Jpn.* **1959**, *32* (12), 1317–1320. https://doi.org/10.1246/bcsj.32.1317.

(71) Zucal, R. H.; Dean, J. A.; Handley, T. H. Behavior of Dialkyl Phosphorodithioic Acids in Liquid Extraction Systems. *Anal. Chem.* **1963**, *35* (8), 988–991.

https://doi.org/10.1021/ac60201a021.

(72) Ionova, G.; Ionov, S.; Rabbe, C.; Hill, C.; Madic, C.; Guillaumont, R.; Krupa, J. C.; Modolo, G.; Claude Krupa, J. Mechanism of Trivalent Actinide/Lanthanide Separation Using Bis(2,4,4-Trimethylpentyl)Dithiophosphinic Acid (Cyanex 301) and Neutral O-Bearing Co-Extractant Synergistic Mixtures. *Solvent Extr. Ion Exch.* **2001**, *25* (3), 391–414. https://doi.org/10.1081/SEI-100103277.

(73) Higgins, W. M. A.; Vogel, P. W.; Craig, W. G. Aromatic Phosphinic Acids and Derivatives. I. Diphenylphosphinodithoic Acid and Its Derivatives. *J. Am. Chem. Soc.* **1955**, *77* (7), 1864–1866. https://doi.org/10.1021/ja01612a047.

(74) Benson, M. T.; Moser, M. L.; Peterman, D. R.; Dinescu, A. Determination of p K a for Dithiophosphinic Acids Using Density Functional Theory. *J. Mol. Struct. THEOCHEM* **2008**, *867* (1–3), 71–77. https://doi.org/10.1016/j.theochem.2008.07.020.

(75) Hill, C.; Madic, C.; Baron, P.; Ozawa, M.; Tanaka, Y. Trivalent Minor Actinides/Lanthanides Separation, Using Organophosphinic Acids. *J. Alloys Compd.* **1998**, *271–273*, 159–162. https://doi.org/10.1016/S0925-8388(98)00045-0.

(76) Pu, N.; Xu, L.; Sun, T.; Chen, J.; Xu, C. Tremendous Impact of Substituent Group on the Extraction and Selectivity to Am(III) over Eu(III) by Diaryldithiophosphinic Acids: Experimental and DFT Analysis. *J. Radioanal. Nucl. Chem.* **2019**, *320* (1), 219–226. https://doi.org/10.1007/s10967-019-06445-5.

(77) Pu, N.; Su, J.; Xu, L.; Sun, T.; Batista, E. R.; Chen, J.; Yang, P.; Shafer, J. C.; Xu, C. "Sweeping" Ortho Substituents Drive Desolvation and Overwhelm Electronic Effects in Nd^{3+} Chelation: A Case of Three Aryldithiophosphinates . *Inorg. Chem.* **2019**. https://doi.org/10.1021/acs.inorgchem.9b01931.

(78) Modolo, G.; Odoj, R. The Separation of Trivalent Actinides from Lanthanides by Dithiophosphinic Acids from HNO3 Acid Medium. *J. Alloys Compd.* **1998**, *271–273*, 248–251. https://doi.org/10.1016/S0925-8388(98)00064-4.

(79) Modolo, G.; Odoj, R. Synergistic Selective Extraction of Actinides(III) over Lanthanides from Nitric Acid Using New Aromatic Diorganyldithiophosphinic Acids and Neutral Organophosphorous Compounds. *Solvent Extr. Ion Exch.* **1999**, *17* (1), 33–53. https://doi.org/10.1080/07360299908934599.

(80) Grigorieva, N. A.; Pavlenko, N. I.; Pleshkov, M. A.; Pashkov, G. L.; Fleitlikh, I. Y. Investigation of the State of Bis(2,4,4-Trimethylpentyl)Dithiophosphinic Acid in Nonane and Toluene Solutions. *Solvent Extr. Ion Exch.* **2009**, *27* (5–6), 745–760. https://doi.org/10.1080/07366290903113983.

(81) Almela, A.; Elizalde, M. P. Interactions of Metal Extractant Reagents. Part VIII. Comparative Aggregation Equilibria of Cyanex 302 and Cyanex 301 in Heptane. *Anal. Proc. Incl. Anal. Commun.* **1995**, *32* (4), 145. https://doi.org/10.1039/ai9953200145.

(82) Sella, C.; Bauer, D. Diphasic Acido-Basic Properties of Organophosphorus Acids. *Solvent Extr. Ion Exch.* **1988**, *6* (5), 819–833. https://doi.org/10.1080/07366298808917967.

(83) Jensen, M. P.; Chiarizia, R.; Urban, V. Investigation of the Aggregation of the

Neodymium Complexes of Dialkylphosphoric, -Oxothiophosphinic, and -Dithiophosphiic Acids in Toluene. *Solvent Extr. Ion Exch.* **2001**, *19* (5), 865–884. https://doi.org/10.1081/SEI-100107027.

(84) Jensen, M. P.; Bond, A. H.; Rickert, P. G.; Nash, K. L. Solution Phase Coordination Chemistry of Trivalent Lanthanide and Actinide Cations with Bis(2,4,4-Trimethylpentyl)Dithiophosphinic Acid. *J. Nucl. Sci. Technol.* **2002**, *39* (sup3), 255–258. https://doi.org/10.1080/00223131.2002.10875456.

(85) Xu, C.; Sun, T.; Rao, L. Interactions of Bis(2,4,4-Trimethylpentyl)Dithiophosphinate with Trivalent Lanthanides in a Homogeneous Medium: Thermodynamics and Coordination Modes. *Inorg. Chem.* **2017**, *56* (5), 2556–2565. https://doi.org/10.1021/acs.inorgchem.6b02744.

(86) Pinkerton, A. A.; Schwarzenbach, D.; Spiliadis, S. The Preparation and Crystal Structures of $[Ln(S_2PEt_2)_4]$ $[Ph_4As]$ (Ln = La, Er). *Inorganica Chim. Acta* **1987**, *128* (2), 283–287. https://doi.org/10.1016/S0020-1693(00)86559-7.

(87) Boland, K. S.; Hobart, D. E.; Kozimor, S. A.; Macinnes, M. M.; Scott, B. L. The Coordination Chemistry of Trivalent Lanthanides (Ce, Nd, Sm, Eu, Gd, Dy, Yb) with Diphenyldithiophosphinate Anions. *Polyhedron* **2014**, *67*, 540–548. https://doi.org/10.1016/j.poly.2013.09.019.

(88) He, X.; Tian, G.; Chen, J.; Rao, L. Characterization of the Extracted Complexes of Trivalent Lanthanides with Purified Cyanex 301 in Comparison with Trivalent Actinide Complexes. *Dalt. Trans.* **2014**, *43* (46), 17352–17357. https://doi.org/10.1039/c4dt02553a.

(89) Sun, T.; Xu, C.; Xie, X.; Chen, J.; Liu, X. Quantum Chemistry Study on the Extraction of Trivalent Lanthanide Series by Cyanex 301: Insights from Formation of Inner- and Outer-Sphere Complexes. *ACS Omega* **2018**, *3* (4), 4070–4080. https://doi.org/10.1021/acsomega.8b00359.

(90) Sun, T.; Xu, C.; Chen, J. Formation of W/O Microemulsions in the Extraction of Nd(III) by Bis(2,4,4-Trimethylpentyl)Dithiophosphinic Acid and Its Effects on Nd(III) Coordination. *Dalt. Trans.* **2016**, *45* (3), 1078–1084. https://doi.org/10.1039/c5dt03964a.

(91) Sun, T.; Xu, C.; Chen, J.; Duan, W. Formation of W/O Microemulsions in the Extraction of the Lanthanide Series by Purified Cyanex 301. *Solvent Extr. Ion Exch.* **2017**, *35* (3), 199–209. https://doi.org/10.1080/07366299.2017.1326729.

(92) Sole, K. C.; Hiskey, J. B. Solvent Extraction Characteristics of Thiosubstituted Organophosphinic Acid Extractants. *Hydrometallurgy* **1992**, *30* (1–3), 345–365. https://doi.org/10.1016/0304-386X(92)90093-F.

(93) Ionova, G.; Ionov, S.; Rabbe, C.; Hill, C.; Madic, C.; Guillaumont, R.; Modolo, G.; Claude Krupa, J. Mechanism of Trivalent Actinide/Lanthanide Separation Using Synergistic Mixtures of Di(Chlorophenyl)Dithiophosphinic Acid and Neutral O-Bearing Co-Extractants. *New J. Chem.* **2001**, *25* (3), 491–501. https://doi.org/10.1039/b006745h.

(94) Wieszczycka, K.; Tomczyk, W. Degradation of Organothiophosphorous Extractant

Cyanex 301. *J. Hazard. Mater.* **2011**, *192* (2), 530–537. https://doi.org/10.1016/j.jhazmat.2011.05.045.

(95) Modolo, G.; Seekamp, S. Hydrolysis and Radiation Stability of the Alina Solvent for Actinide(III)/Lanthanide(III) Separation During the Partitioning of Minor Actinides. *Solvent Extr. Ion Exch.* **2002**, *20* (2), 195–210. https://doi.org/10.1081/SEI-120003021.

(96) Sole, K. C.; Brent Hiskey, J.; Ferguson, T. L. An Assessment of the Long-Term Stabilities of Cyanex 302 and Cyanex 301 in Sulfuric and Nitric Acids. *Solvent Extr. Ion Exch.* **1993**, *11* (5), 783–796. https://doi.org/10.1080/07366299308918186.

(97) Groenewold, G. S.; Peterman, D. R.; Klaehn, J. R.; Delmau, L. H.; Marc, P.; Custelcean, R. Oxidative Degradation of Bis(2,4,4-Trimethylpentyl)Dithiophosphinic Acid in Nitric Acid Studied by Electrospray Ionization Mass Spectrometry. *Rapid Commun. Mass Spectrom.* **2012**, *26* (19), 2195–2203. https://doi.org/10.1002/rcm.6339.

(98) Marc, P.; Custelcean, R.; Groenewold, G. S.; Klaehn, J. R.; Peterman, D. R.; Delmau, L. H. Degradation of Cyanex 301 in Contact with Nitric Acid Media. *Ind. Eng. Chem. Res.* **2012**, *51* (40), 13238–13244. https://doi.org/10.1021/ie300757r.

(99) Zalupski, P. R.; Chiarizia, R.; Jensen, M. P.; Herlinger, A. W. Metal Extraction by Sulfur-Containing Symmetrically-Substituted Bisphosphonic Acids. Part I. P,P′-di(2-ethylhexyl) Methylenebisthio-Phosphonic Acid. *Solvent Extr. Ion Exch.* **2006**, *24* (3), 331–346. https://doi.org/10.1080/07366290600646988.

(100) Devore, M. A.; Gorden, A. E. V. Copper and Uranyl Extraction from Aqueous Solutions Using Bis-Dithiophosphinate Ligands Have Been Characterized. *Polyhedron* **2012**, *42* (1), 271–275. https://doi.org/10.1016/j.poly.2012.05.026.

(101) Haiduc, I. Reactions of Bis(Thiophosphoryl)Disulfanes and Bis(Thiophosphinyl)Disulfanes with Metal Species: An Alternative, Convenient Route to Metal Complex and Organometallic Dithiophosphates and Dithiophosphinates. *Coord. Chem. Rev.* **2002**, *224* (1–2), 151–170. https://doi.org/10.1016/S0010-8545(01)00402-7.

(102) Shishkov, A. Disulphides of Dithiophosphinic Acids as Analytical Reagents—I Extractive Spectrophotometric Determination of Palladium with Some Bis(Dialkylthiophosphoryl)- and Bis(Diarylthiophosphoryl)Disulphides. *Talanta* **1978**, *25* (9), 533–535. https://doi.org/10.1016/0039-9140(78)80092-7.

(103) Edelmann, F. T.; Rieckhoff, M.; Haiduc, I.; Silaghi-Dumitrescu, I. Ansa-Metallocenderivate Des Samariums Und Ytterbiums Mit 'Weichen' Donorliganden. *J. Organomet. Chem.* **1993**, *447* (2), 203–208. https://doi.org/10.1016/0022-328X(93)80239-8.

(104) Rieckhoff, M.; Noltemeyer, M.; Edelmann, F. T.; Haiduc, I.; Silaghi-Dumitrescu, I. Ein Alter Ligand in Neuer Umgebung: Dreifach Verbrückendes O,Ó- Dimethyldithiophosphat Im Organosamarium-Komplex [(C5Me5)Sm{S2P(OMe)2}2]2. *J. Organomet. Chem.* **1994**, *469* (1), C19–C21. https://doi.org/10.1016/0022-328X(94)80092-8.

(105) Miyasita, S.; Yanaga, M.; Satoh, I.; Suganuma, H. Separation of Americium(III) from Europium(III) by Dioctylammonium Dioctyldithiocarbamate/Nitrobenzene Extraction.

Chem. Lett. **2006**, *35* (2), 236–237. https://doi.org/10.1246/cl.2006.236.

(106) Miyashita, S.; Satoh, I.; Yanaga, M.; Okuno, K.; Suganuma, H. Separation of Am(III) from Eu(III) by Extraction Based on in Situ Extractant Formation of Dithiocarbamate Derivatives. *Prog. Nucl. Energy* **2008**, *50* (2–6), 499–503. https://doi.org/10.1016/j.pnucene.2007.11.035.

(107) Miyashita, S.; Yanaga, M.; Satoh, I.; Suganuma, H. Separation of Americium(III) from Europium(III) by Extraction Based on in Situ Formation of Dioctylammonium Dioctyldithiocarbamate Extractant. *J. Nucl. Sci. Technol.* **2007**, *44* (2), 233–237. https://doi.org/10.1080/18811248.2007.9711277.

(108) Boerrigter, H.; Tomasberger, T.; Verboom, W.; Reinhoudt, D. N. Novel Ligands for the Separation of Trivalent Lanthanides and Actinides - Tetrakis(Phosphane Sulfide) and -(Phosphinic Acid) Cavitands. *European J. Org. Chem.* **1999**, No. 3, 665–674. https://doi.org/10.1002/(SICI)1099-0690(199903)1999:3<665::AID-EJOC665>3.0.CO;2-F.

(109) Yao, J.; Wharf, R. M.; Choppin, G. R. Solvent Extraction of Eu(III) and Am(III) with Thio and Amide Extractants. In *Separations of f Elements*; Nash, K. L., Choppin, G. R., Eds.; Springer US: Boston, MA, **1995**; pp 31–42. https://doi.org/10.1007/978-1-4899-1406-4.

(110) Jakovljevic, B.; Bourget, C.; Nucciarone, D. CYANEX® 301 Binary Extractant Systems in Cobalt/Nickel Recovery from Acidic Chloride Solutions. *Hydrometallurgy* **2004**, *75* (1–4), 25–36. https://doi.org/10.1016/j.hydromet.2004.06.006.

(111) Bessen, N. P.; Jackson, J. A.; Jensen, M. P.; Shafer, J. C. Sulfur Donating Extractants for the Separation of Trivalent Actinides and Lanthanides. *Coord. Chem. Rev.* **2020**, *421*, 213446. https://doi.org/10.1016/j.ccr.2020.213446.

(112) Doheny, A. J.; Ganem, B. Purple Benzene Revisited. *J. Chem. Educ.* **1980**, *57* (4), 308. https://doi.org/10.1021/ed057p308.1.

(113) Gokel, G. W.; Durst, H. D. Crown Ether Chemistry: Principles and Appications. *Aldrichimica Acta* **1976**, *9* (1), 3–12.

(114) Wiberg, K. B.; Geer, R. D. The Kinetics of the Permanganate Oxidation of Acetone. *J. Am. Chem. Soc.* **1965**, *87* (22), 5202–5209. https://doi.org/10.1021/ja00950a039.

(115) Zhengshui, H.; Ying, P.; Wanwu, M.; Xun, F. Purification of Organophosphorus Acid Extractants. *Solvent Extr. Ion Exch.* **1995**, *13* (5), 965–976.

(116) Chen, J.; Jiao, R. Z.; Zhu, Y. J. Purification and Properties of Cyanex 301. *Chinese J. Appl. Chem.* **1996**, *13* (2), 45–48.

(117) Chauhan, M. Permanganate Oxidation Mechanisms of Alkylarenes. *IOSR J. Appl. Chem.* **2014**, *7* (6), 16–27. https://doi.org/10.9790/5736-07611627.

(118) Webb, G. I.; Sammut, C.; Perlich, C.; Horváth, T.; Wrobel, S.; Korb, K. B.; Noble, W. S.; Leslie, C.; Lagoudakis, M. G.; Quadrianto, N.; et al. Leave-One-Out Cross-Validation. In *Encyclopedia of Machine Learning*; Springer US: Boston, MA, **2011**; pp 600–601.

https://doi.org/10.1007/978-0-387-30164-8_469.

(119) He, X.; Tian, G.; Chen, J.; Rao, L. Characterization of the Extracted Complexes of Trivalent Lanthanides with Purified Cyanex 301 in Comparison with Trivalent Actinide Complexes. *Dalt. Trans.* **2014**, *43* (46), 17352–17357. https://doi.org/10.1039/c4dt02553a.

(120) Wang, Y.; Deblonde, G. J. P.; Abergel, R. J. Hydroxypyridinone Derivatives: A Low-PH Alternative to Polyaminocarboxylates for TALSPEAK-like Separation of Trivalent Actinides from Lanthanides. *ACS Omega* **2020**, *5* (22), 12996–13005. https://doi.org/10.1021/acsomega.0c00873.

(121) Van Lenthe, E. Geometry Optimizations in the Zero Order Regular Approximation for Relativistic Effects. *J. Chem. Phys.* **1999**, *110* (18), 8943–8953. https://doi.org/10.1063/1.478813.

(122) Van Lenthe, E.; Baerends, E. J.; Snijders, J. G. Relativistic Total Energy Using Regular Approximations. *J. Chem. Phys.* **1994**, *101* (11), 9783–9792. https://doi.org/10.1063/1.467943.

(123) Van Lenthe, E.; Van Leeuwen, R.; Baerends, E. J.; Snijders, J. G. Relativistic Regular Two-Component Hamiltonians. *Int. J. Quantum Chem.* **1996**, *57* (3), 281–293. https://doi.org/10.1002/(SICI)1097-461X(1996)57:3<281::AID-QUA2>3.0.CO;2-U.

(124) Van Lenthe, E.; Baerends, E. J. Optimized Slater-Type Basis Sets for the Elements 1-118. *J. Comput. Chem.* **2003**, *24* (9), 1142–1156. https://doi.org/10.1002/jcc.10255.

(125) Te Velde, G.; Bickelhaupt, F. M.; Baerends, E. J.; Fonseca Guerra, C.; van Gisbergen, S. J. A.; Snijders, J. G.; Ziegler, T. Chemistry with ADF. *J. Comput. Chem.* **2001**, *22* (9), 931–967. https://doi.org/10.1002/jcc.1056.

(126) Pye, C. C.; Ziegler, T. An Implementation of the Conductor-like Screening Model of Solvation within the Amsterdam Density Functional Package. *Theor. Chem. Acc.* **1999**, *101* (6), 396–408. https://doi.org/10.1007/s002140050457.

(127) Swain, B.; Otu, E. O. Competitive Extraction of Lanthanides by Solvent Extraction Using Cyanex 272: Analysis, Classification and Mechanism. *Sep. Purif. Technol.* **2011**, *83* (1), 82–90. https://doi.org/10.1016/j.seppur.2011.09.015.

(128) Yuan, M.; Luo, A.; Wang, C.; Li, D. Solvent Extraction of Lanthanides in Aqueous Nitrite Media by Cyanex 302. *Acta Metall. Sin.* **1995**, *8* (1), 10–14.

(129) Tchougréeff, A. L.; Dronskowski, R. Nephelauxetic Effect Revisited. *Int. J. Quantum Chem.* **2009**, *109* (11), 2606–2621. https://doi.org/10.1002/qua.21989.

(130) Xu, C.; Rao, L. Interactions of Bis(2,4,4-Trimethylpentyl)Dithiophosphinate with Nd III and Cm III in a Homogeneous Medium: A Comparative Study of Thermodynamics and Coordination Modes. *Chem. - A Eur. J.* **2014**, *20* (45), 14807–14815. https://doi.org/10.1002/chem.201402987.

(131) Rao, L.; Tian, G. Complexation of Lanthanides with Nitrate at Variable Temperatures: Thermodynamics and Coordination Modes. *Inorg. Chem.* **2009**, *48* (3), 964–970.

https://doi.org/10.1021/ic801604f.

(132) Liu, L.; Tian, G.; Rao, L. Effect of Solvation? Complexation of Neodymium(III) with Nitrate in an Ionic Liquid (BumimTf$_2$N) in Comparison with Water. *Solvent Extr. Ion Exch.* **2013**, *31* (4), 384–400. https://doi.org/10.1080/07366299.2013.800410.

(133) Bhattacharyya, A.; Mohapatra, P. K.; Manchanda, V. K. Solvent Extraction and Extraction Chromatographic Separation of Am^{3+} and Eu^{3+} from Nitrate Medium Using Cyanex® 301. *Solvent Extr. Ion Exch.* **2007**, *25* (1), 27–39. https://doi.org/10.1080/07366290601067713.

(134) Kelley, M. P.; Deblonde, G. J.-P.; Su, J.; Booth, C. H.; Abergel, R. J.; Batista, E. R.; Yang, P. Bond Covalency and Oxidation State of Actinide Ions Complexed with Therapeutic Chelating Agent 3,4,3-LI(1,2-HOPO). *Inorg. Chem.* **2018**, *57* (9), 5352–5363. https://doi.org/10.1021/acs.inorgchem.8b00345.

(135) Koch, L. Minor Actinide Transmutation—a Waste Management Option. *J. Less Common Met.* **1986**, *122*, 371–382. https://doi.org/10.1016/0022-5088(86)90432-7.

(136) Nash, K. L.; Braley, J. C. Challenges for Actinide Separations in Advanced Nuclear Fuel Cycles. In *Nuclear Energy and the Environment*; ACS Publications, **2010**; pp 19–38. https://doi.org/10.1021/bk-2010-1046.ch003.

(137) Nash, K. L.; Braley, J. C. Chemistry of Radioactive Materials in the Nuclear Fuel Cycle. In *Advanced Separation Techniques for Nuclear Fuel Reprocessing and Radioactive Waste Treatment*; Woodhead Publishing, **2011**; pp 3–22. https://doi.org/10.1533/9780857092274.1.3.

(138) Braley, J. C.; Grimes, T. S.; Nash, K. L. Alternatives to HDEHP and DTPA for Simplified TALSPEAK Separations. *Ind. Eng. Chem. Res.* **2012**, *51* (2), 629–638. https://doi.org/10.1021/ie200285r.

(139) Wyrzykowski, D.; Pranczk, J.; Jacewicz, D.; Tesmar, A.; Pilarski, B.; Chmurzyński, L. Investigations of Ternary Complexes of Co(II) and Ni(II) with Thiodiacetate Anion and 1,10-Phenanthroline or 2,2'-Bipyridine in Aqueous Solutions. *Open Chem.* **2014**, *13* (1), 369–375. https://doi.org/10.1515/chem-2015-0048.

(140) Oddy, H.; Dodson, V. Thionyldiacetic Acid. *Ohio J. Sci.* **1949**, *49* (4), 149–153.

(141) Hancock, R. D.; Bartolotti, L. J. A DFT Study of the Affinity of Lanthanide and Actinide Ions for Sulfur-Donor and Nitrogen-Donor Ligands in Aqueous Solution. *Inorganica Chim. Acta* **2013**, *396*, 101–107. https://doi.org/10.1016/j.ica.2012.10.010.

(142) Weaver, B.; Kappelmann, F. A. Preferential Extraction of Lanthanides over Trivalent Actinides by Monoacidic Organophosphates from Carboxylic Acids and from Mixtures of Carboxylic and Aminopolyacetic Acids. *J. Inorg. Nucl. Chem.* **1968**, *30* (1), 263–272. https://doi.org/10.1016/0022-1902(68)80089-2.

(143) Rossotti, F. J. C.; Rossotti, H. Potentiometric Titrations Using Gran Plots: A Textbook Omission. *J. Chem. Educ.* **1965**, *42* (7), 375. https://doi.org/10.1021/ed042p375.

(144) Li, G. G.; Bridges, F.; Booth, C. H. X-Ray-Absorption Fine-Structure Standards: A

Comparison of Experiment and Theory. *Phys. Rev. B* **1995**, *52* (9), 6332–6348. https://doi.org/10.1103/PhysRevB.52.6332.

(145) Hayes, T. M.; Boyce, J. B. Extended X-Ray Absorption Fine Structure Spectroscopy. In *Solid State Physics*; Ehrenreich, H., Seitz, F., Turnbull, D., Eds.; Academic Press, Inc.: New York, **1983**; pp 173–351. https://doi.org/10.1016/S0081-1947(08)60667-0.

(146) Booth, C. H. RSXAP EXAFS Analysis Package http://lise.lbl.gov/RSXAP/.

(147) Rehr, J. J.; Kas, J. J.; Vila, F. D.; Prange, M. P.; Jorissen, K. Parameter-Free Calculations of X-Ray Spectra with FEFF9. *Phys. Chem. Chem. Phys.* **2010**, *12* (21), 5503. https://doi.org/10.1039/b926434e.

(148) Thakur, P.; Pathak, P. N.; Gedris, T.; Choppin, G. R. Complexation of Eu(III), Am(III) and Cm(III) with Dicarboxylates: Thermodynamics and Structural Aspects of the Binary and Ternary Complexes. *J. Solution Chem.* **2009**, *38* (3), 265–287. https://doi.org/10.1007/s10953-009-9373-8.

(149) Smith, R. M.; Martell, A. E.; Motekaitis, R. J. NIST Critically Selected Stability Constants of Metal Complexes Database. National Institute of Standards and Technology: Gaithersburg, MD **1999**.

(150) Booth, C. H.; Bridges, F.; Kwei, G. H.; Lawrence, J. M.; Cornelius, A. L.; Neumeier, J. J. Lattice Effects in $La_{1-x}Ca_xMnO_3$ (X=0->1): Relatioships between Distortions, Charge Distribution, and Magnetism. *Phys. Rev. B* **1998**, *57* (17), 10440–10454. https://doi.org/10.1103/PhysRevB.57.10440.

(151) Allen, P. G.; Bucher, J. J.; Shuh, D. K.; Edelstein, N. M.; Reich, T. Investigation of Aquo and Chloro Complexes of UO_2^{2+}, NpO^{2+}, Np^{4+}, and Pu^{3+} by X-Ray Absorption Fine Structure Spectroscopy. *Inorg. Chem.* **1997**, *36* (21), 4676–4683. https://doi.org/10.1021/ic970502m.

(152) Panak, P. J.; Booth, C. H.; Caulder, D. L.; Bucher, J. J.; Shuh, D. K.; Nitsche, H. X-Ray Absorption Fine Structure Spectroscopy of Plutonium Complexes with Bacillus Sphaericus. *Radiochim. Acta* **2002**, *90* (6). https://doi.org/10.1524/ract.2002.90.6.315.

(153) Tobin, J. G.; Booth, C. H.; Siekhaus, W.; Shuh, D. K. EXAFS Investigation of UF_4. *J. Vac. Sci. Technol. A Vacuum, Surfaces, Film.* **2015**, *33* (3), 033001. https://doi.org/10.1116/1.4915893.

(154) Shannon, R. D. Revised Effective Ionic Radii and Systematic Studies of Interatomic Distances in Halides and Chalcogenides. *Acta Crystallogr. Sect. A* **1976**, *32* (5), 751–767. https://doi.org/10.1107/S0567739476001551.

(155) Dellien, I.; Grenthe, I.; Hessler, G.; Liaaen-Jensen, S.; Enzell, C. R.; Swahn, C.-G. Thermodynamic Properties of Rare Earth Complexes. XVIII. Free Energy, Enthalpy, and Entropy Changes for the Formation of Some Lanthanoid Thiodiacetate and Hydrogen Thiodiacetate Complexes. *Acta Chem. Scand.* **1973**, *27*, 2431–2440. https://doi.org/10.3891/acta.chem.scand.27-2431.

(156) Thakur, P.; Mathur, J. N.; Moore, R. C.; Choppin, G. R. Thermodynamics and Dissociation Constants of Carboxylic Acids at High Ionic Strength and Temperature.

Inorganica Chim. Acta **2007**, *360* (12), 3671–3680. https://doi.org/10.1016/j.ica.2007.06.002.

(157) Heathman, C. R.; Nash, K. L. Characterization of Europium and Americium Dipicolinate Complexes. *Sep. Sci. Technol.* **2012**, *47* (14–15), 2029–2037. https://doi.org/10.1080/01496395.2012.704225.

APPENDIX A

CHAPTER FOUR SUPPLEMENTARY INFORMATION

Table A.1 Emission wavelengths of lanthanides used in ICP-OES.

Metal	Wavelength (nm)	Metal	Wavelength (nm)
La	398.852	Dy	353.171
Pr	422.293	Ho	345.600
Nd	430.358	Er	337.271
Sm	443.432	Tm	384.802
Eu	393.048	Yb	328.937
Gd	342.247	Lu	547.669

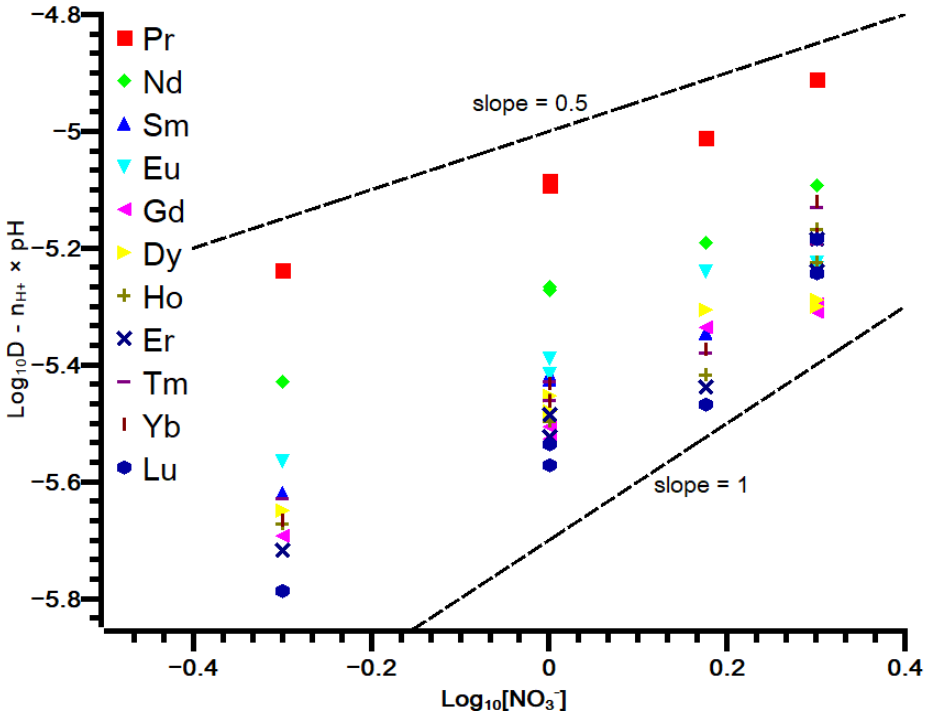

Figure A.1 The pH corrected distribution ratio of the lanthanides Pr, Nd, Sm, Eu, Gd, Dy, Ho, Er, Tm, Yb, and Lu with 0.5024 M HC301 at an average pC_{H+} of 4.46. The value for n_{H+} (1.13) was obtained from radiotracer experiments with Eu.

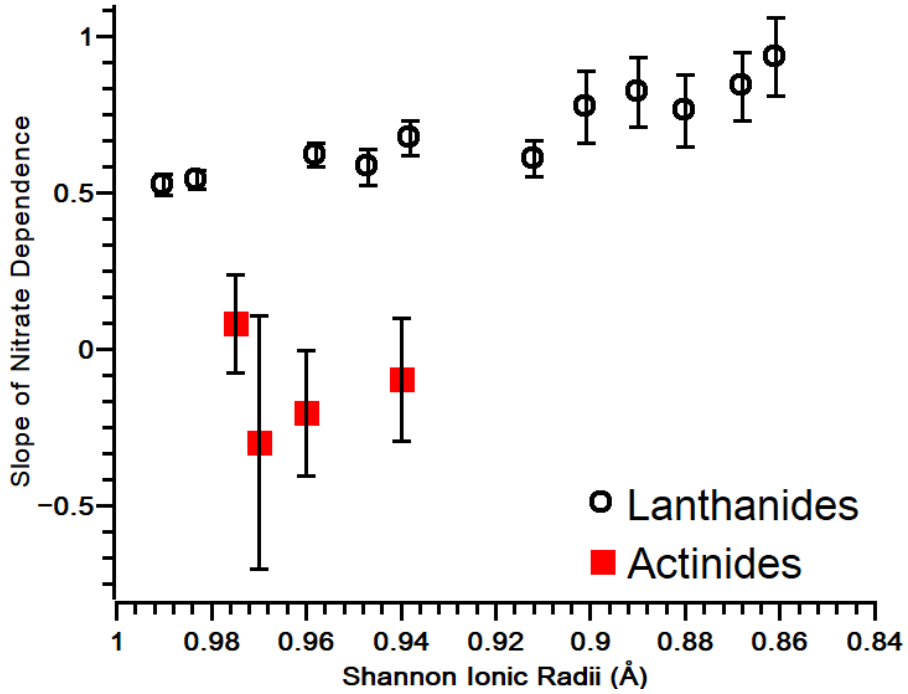

Figure A.2 The slope of the nitrate dependency of the pH corrected distribution ratio vs. $Log_{10}[NO_3^-]$ for the lanthanides and the actinides Am, Cm, Bk, and Es with 0.5024 M HC301 at an average pC_{H+} of 4.46 for lanthanides and 3.07 for actinides.

Optimized geometries of Am extracted complexes. Coordinates are representative of the optimized structures of all lanthanide and actinide complexes modeled.

$Am(C301)_3$

C	-3.34540759	-2.90041902	0.80716076
S	2.44053787	-0.81160548	-1.48082444
Am	0.17554057	-0.00000000	-0.00000000
S	2.44053787	0.81160548	1.48082444
S	-0.27618505	2.42071506	-1.38337778
S	-1.75162280	-1.42866993	-1.48995462
S	-1.75162280	1.42866993	1.48995462
S	-0.27618505	-2.42071506	1.38337778
P	-1.71980314	-2.82918494	-0.00364666
P	-1.71980314	2.82918494	0.00364666
P	3.59035078	-0.00000000	-0.00000000

C	4.68474461	1.27289595	-0.69646039
C	-1.44489696	-4.47974795	-0.71433944
C	-3.34540759	2.90041902	-0.80716076
C	-1.44489696	4.47974795	0.71433944
C	4.68474461	-1.27289595	0.69646039
H	-3.32497382	-3.67550359	1.58562711
H	-4.10999205	-3.14000985	0.05556288
H	-3.56102288	-1.92437908	1.25910754
H	5.31075974	1.68282731	0.10785318
H	4.07270692	2.07017125	-1.13521300
H	5.31654123	0.81759495	-1.47115287
H	-0.47477649	-4.49393937	-1.22550142
H	-2.24814063	-4.69827238	-1.43117171
H	-1.45141463	-5.22076609	0.09693026
H	-3.32497382	3.67550359	-1.58562711
H	-4.10999205	3.14000985	-0.05556288
H	-3.56102288	1.92437908	-1.25910754
H	-0.47477649	4.49393937	1.22550142
H	-2.24814063	4.69827238	1.43117171
H	-1.45141463	5.22076609	-0.09693026
H	5.31075974	-1.68282731	-0.10785318
H	4.07270692	-2.07017125	1.13521300
H	5.31654123	-0.81759495	1.47115287

$Am(C301)_2(NO_3)$

O	-2.08009326	-3.99843583	0.40082905
S	2.18503174	-1.06214484	-1.43257272
Am	-0.22581121	-0.33847483	-0.18537492
S	1.81115292	0.61258194	1.47816941
S	-0.42862827	2.02988095	-1.69289553
O	-2.07550158	-1.98287868	-0.49752654

S	-2.12141053	1.27884741	1.11901539
O	-0.40104486	-2.61139321	0.76577400
N	-1.54344889	-2.90751348	0.22868136
P	-1.61680622	2.75740601	-0.20119486
P	3.12959341	-0.00910651	0.04456802
C	3.97320927	1.43349830	-0.67198059
H	4.94116695	-0.43405572	1.57194302
C	-3.11924119	3.49887800	-0.90255620
C	-0.75991216	4.09689564	0.67904529
C	4.43131120	-1.02668117	0.80018601
H	-3.67090351	2.73459940	-1.46272703
H	0.16662852	3.70022558	1.11260115
H	-1.41284028	4.47829379	1.47587948
H	4.49913692	1.97177275	0.12854954
H	3.22460969	2.08941724	-1.13273979
H	4.69094063	1.09174139	-1.42983871
H	-0.52709858	4.90033821	-0.03287213
H	5.14594848	-1.32513548	0.02091284
H	3.97664751	-1.91690877	1.25133182
H	-2.83074773	4.32038971	-1.57261928
H	-3.73985718	3.88419863	-0.08201920

APPENDIX B

CHAPTER FIVE SUPPLEMENTARY INFORMATION

A 0.1492 M solution of TDA was titrated into a 3 mM solution of the appropriate Nd or Eu solution in a TA instruments SV Affinity ITC. The ionic strength of each solution was adjusted to 1 M with sodium perchlorate and the pC_{H+} was controlled by addition of sodium hydroxide or perchloric acid within a range of 4.00 to 4.04. The resulting data was background corrected using TA Instruments NanoAnalyze software and corrected for the heat of dilution. The enthalpy and entropy of each complex were determined using HypCal from Hyperquad and previously determined formation constants.

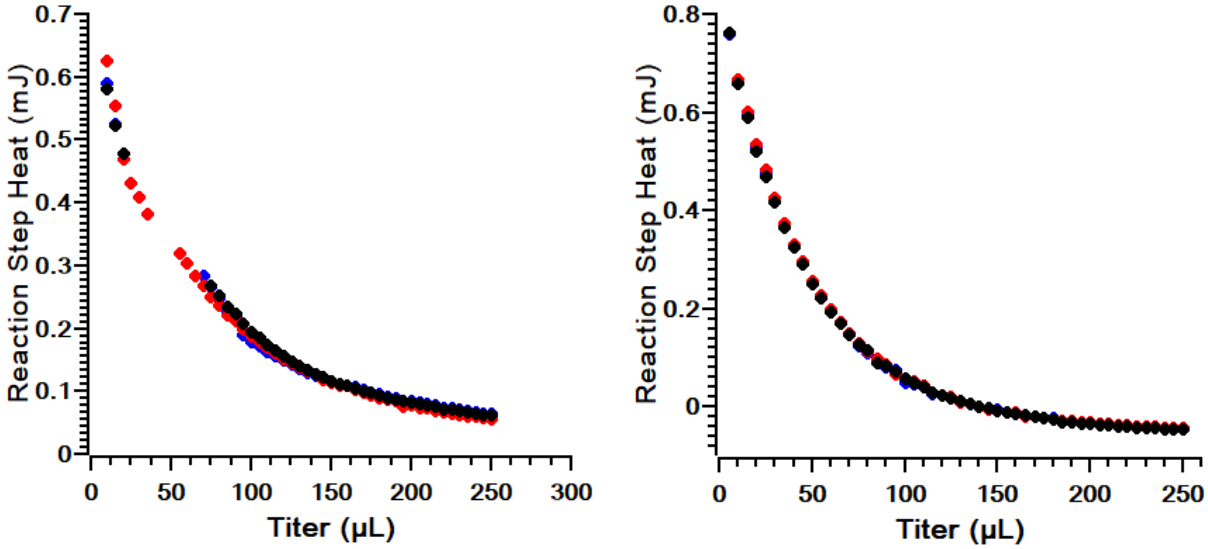

Figure B.1 Nd and Eu Isothermal Titration Calorimetry with TDA. Three TDA isothermal titration calorimetry trials at 1.00 ± 0.01 M $NaClO_4$ and 25 °C. Left) Nd. For this titration, V_{init} = 965 µL, C_{Nd} = 3.00 mM, pC_{H+} = 4.00. The titrant contained 0.1492 M TDA at a pC_{H+} of 4.03. Right) Eu. For this titration, V_{init} = 965 µL, C_{Eu} = 3.00 mM, pC_{H+} = 4.01. The titrant contained 0.1492 M TDA at a pC_{H+} of 4.03.

Table B.1 Thermodynamic parameters for Nd and Eu complexes with TDA as determined by isothermal titration calorimetry.

Lanthanide	ΔH_{101} (kJ/mol)	ΔH_{102} (kJ/mol)	ΔS_{101} (kJ/mol·K)	ΔS_{102} (kJ/mol·K)
Nd	-15(1)	-19(1)	-39(2)	-45(2)
Eu	-8.90(4)	-35.6(8)	24(5)	-40(9)

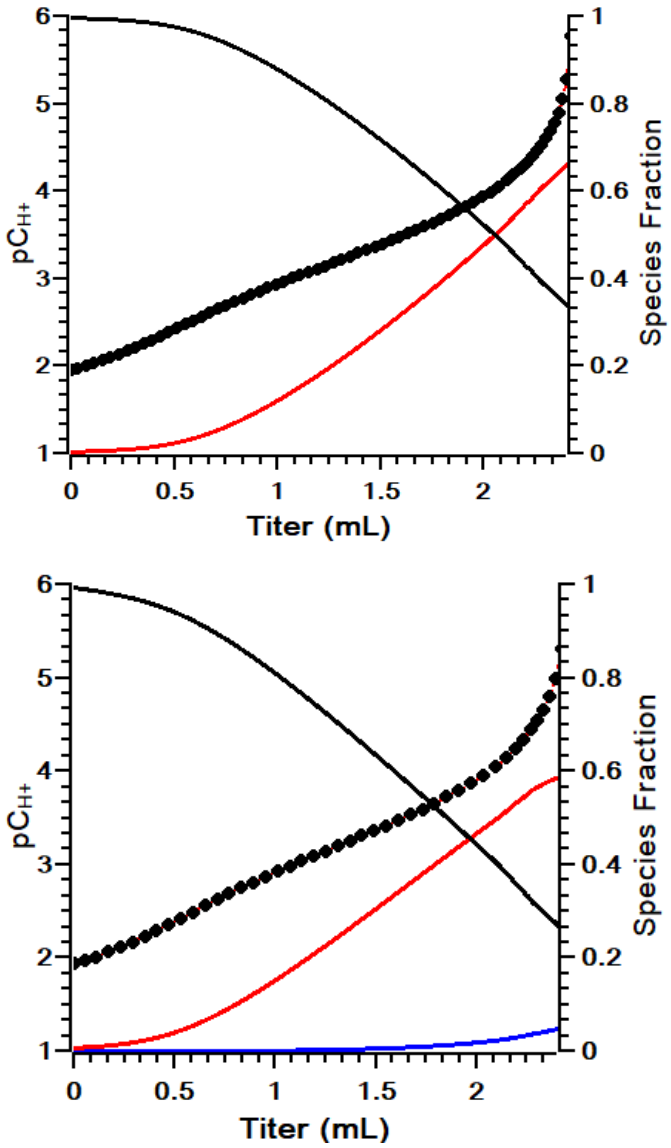

Figure B.2 Nd and Eu Potentiometric Titrations with TDA. TDA potentiometric titrations with Nd or Eu at 1.00 ± 0.01 M $NaClO_4$ and 25 °C. Top) Nd. For this titration, Vinit = 25.349 mL, C_{TDA} = 19.25 mM, C_{Nd} = 7.806 mM, and C_{H+},total = 48.73 mM. The titrant contained 0.507 M NaOH and 0.500 M $NaClO_4$. (•) Experimental pC_{H+}, (red dashed line) calculated pC_{H+}, (black solid line) Nd, (red solid line) NdTDA+. Bottom) Eu. For this titration, V_{init} = 25.261 mL, C_{TDA} = 19.70 mM, C_{Eu} = 6.634 mM, and $C_{H+,total}$ = 49.03 mM. The titrant contained 0.507 M NaOH and 0.500 M $NaClO_4$. (•) Experimental pC_{H+}, (red dashed line) calculated pC_{H+}, (black solid line) Eu, (red solid line) $EuTDA^+$, (blue solid line) $EuTDA_2^-$.

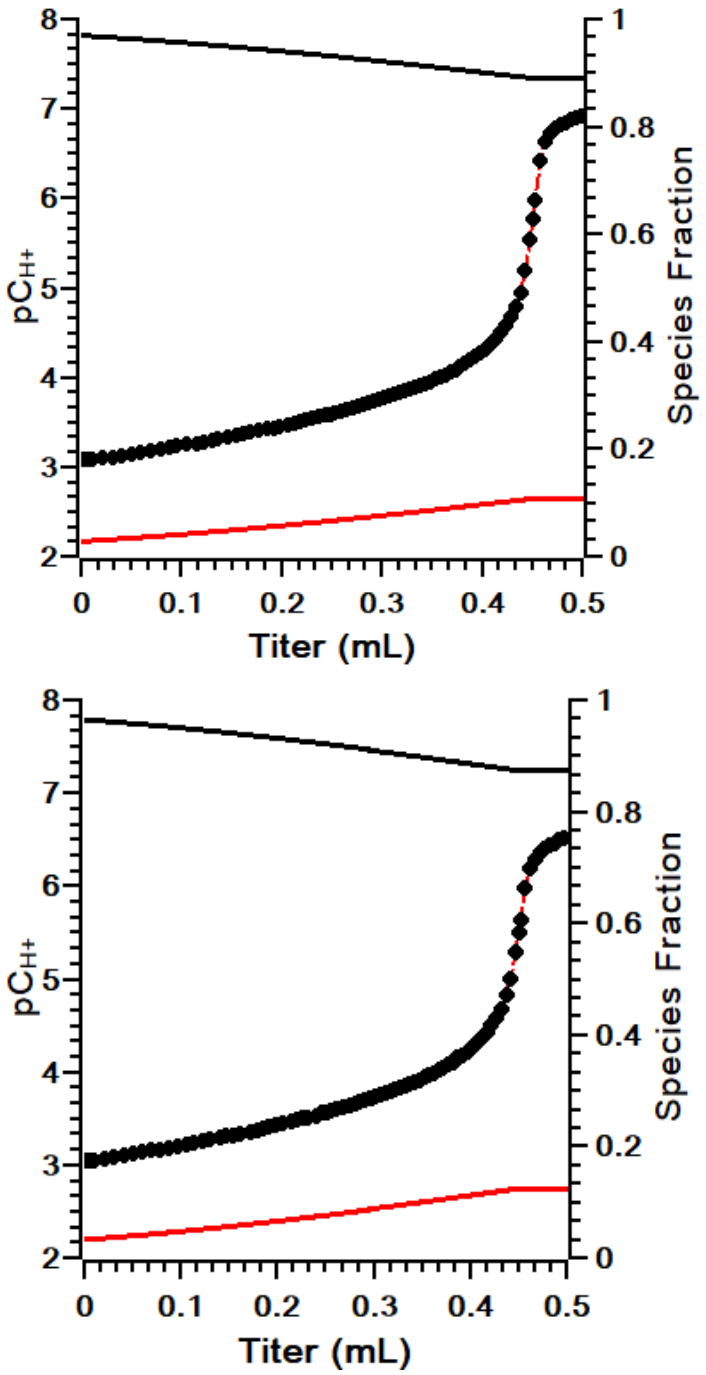

Figure B.3 Nd and Eu Potentiometric Titrations with TPA. TPA potentiometric titrations with Nd or Eu at 1.00 ± 0.01 M $NaClO_4$ and 25 °C. Top) Nd. For this titration, Vinit = 25.447 mL, C_{TPA} = 8.375 mM, C_{Nd} = 10.15 mM, and $C_{H+,}$total = 8.939 mM. The titrant contained 0.507 M NaOH and 0.500 M $NaClO_4$. (•) Experimental $pC_{H+,}$ (red dashed line) calculated $pC_{H+,}$ (black solid line) Nd, (red solid line) Nd_{TPA}^{+}. Bottom) Eu. For this titration, V_{init} = 25.494 mL, C_{TPA} = 8.374 mM, C_{Eu} = 10.18 mM, and $C_{H+,total}$ = 9.021 mM. The titrant contained 0.507 M NaOH and 0.500 M $NaClO_4$. (•) Experimental pC_{H+}, (red dashed line) calculated pC_{H+}, (black solid line) Eu, (red solid line) $EuTPA^{+}$.

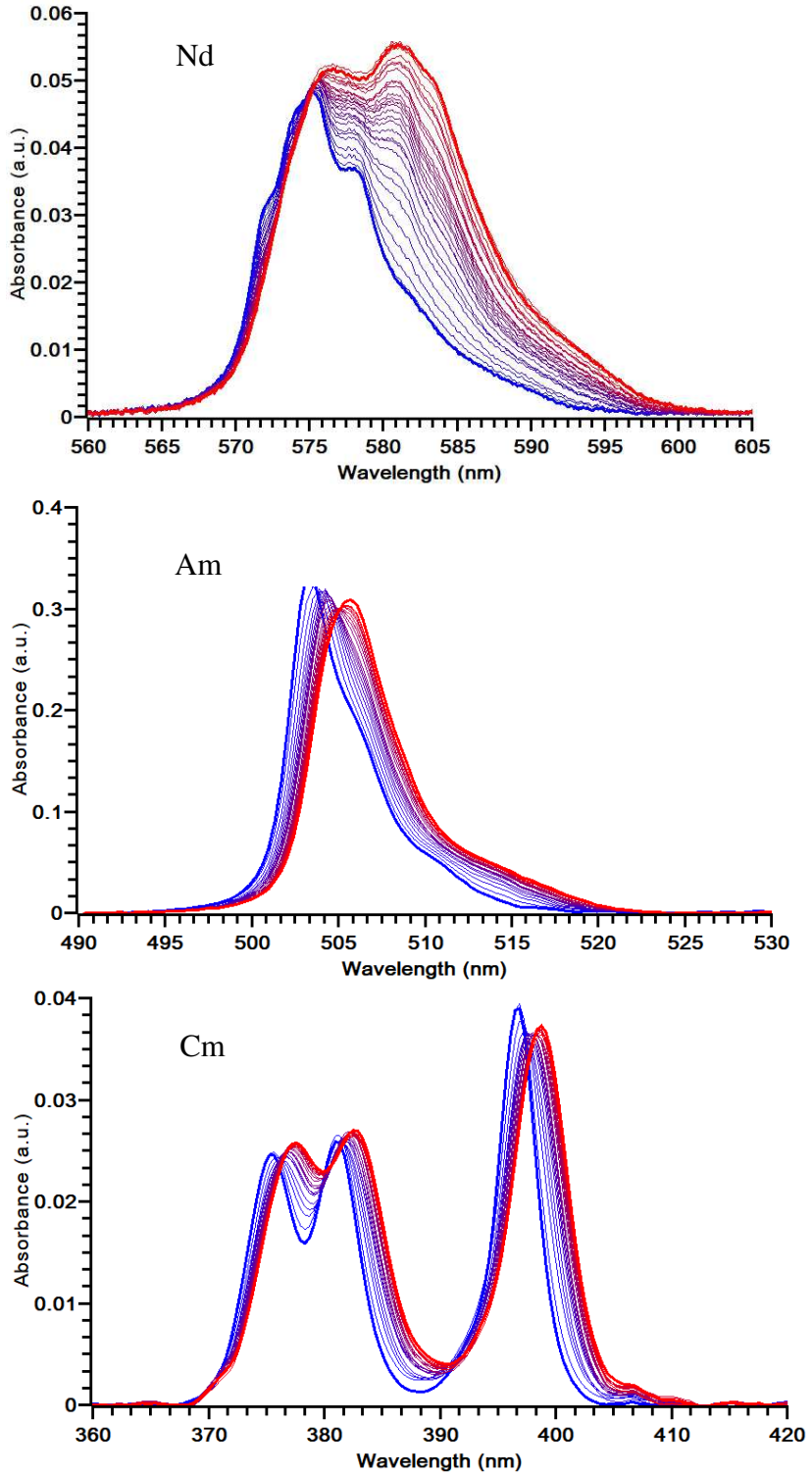

Figure B.4 Spectrophotometric Titrations of Nd, Am, and Cm with TDA. Spectrophotometric titration of a metal and TDA at room temperature and an ionic strength of 1.00 ± 0.01 M. The spectra changes from blue to red over the course of the titration. Top) For the Nd titration, V_{init} = 0.803 mL, C_{Nd} = 10.15 mM, and pC_{H+} ,initial = 3.08. The titrant contained C_{TDA} = 150.1 mM, C_{Nd} = 10.12 mM and after the addition of 0.792 mL of titrant, the $pC_{H+,final}$ = 5.17. Middle) For

the Am titration, V_{init} = 0.795 mL, C_{Am} = 0.844 mM, and $pC_{H+,initial}$ = 2.581. The titrant contained C_{TDA} = 10.03 mM, C_{Am} = 0.832 mM and after the addition of 0.793 mL of titrant, the $pC_{H+,final}$ = 3.676. Bottom) For the Cm titration, V_{init} = 0.795 mL, C_{Cm} = 0.937 mM, and $pC_{H+,initial}$ = 3.182. The titrant contained C_{TDA} = 0.137 M, C_{Cm} = 0.939 mM and after the addition of 0.731 mL of titrant, the $pC_{H+,final}$ = 3.707.

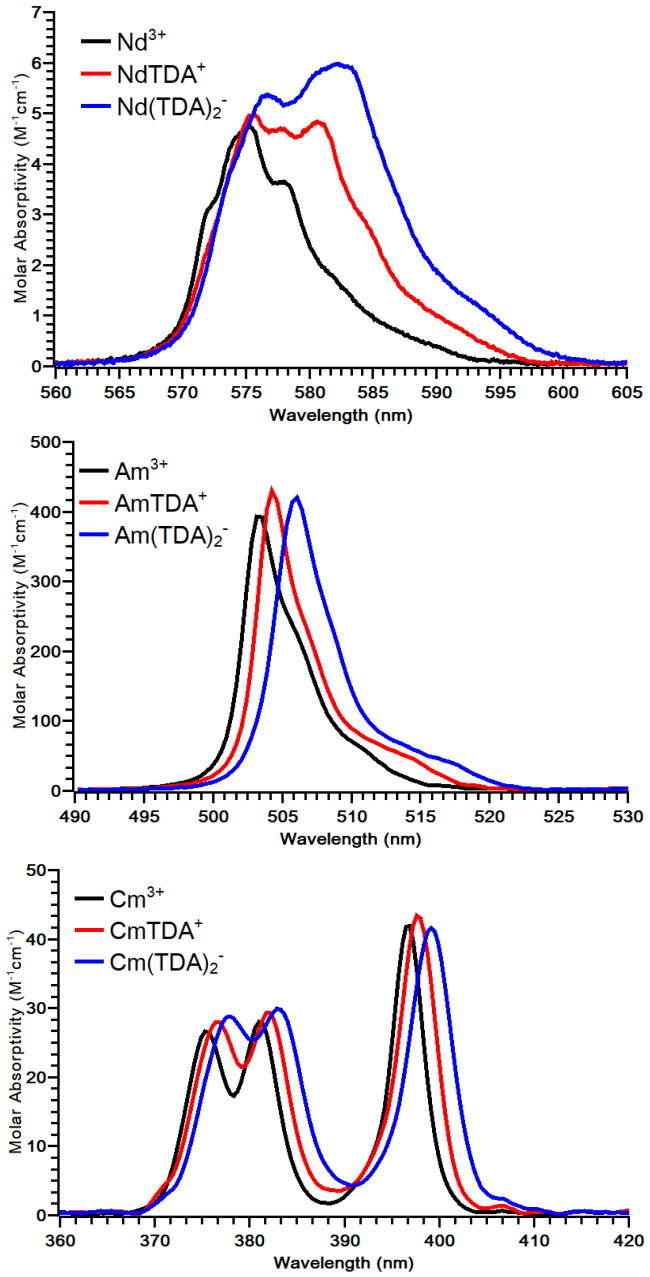

Figure B.5 Molar absorptivity of Nd, Am, and Cm complexes with TDA. Molar absorptivity of Nd (top), Am (middle), and Cm (bottom) complexes with TDA calculated from the spectra shown in Figure B.4 using HypSpec2014. These spectra were collected at room temperature and an ionic strength of 1.00 ± 0.01 M.

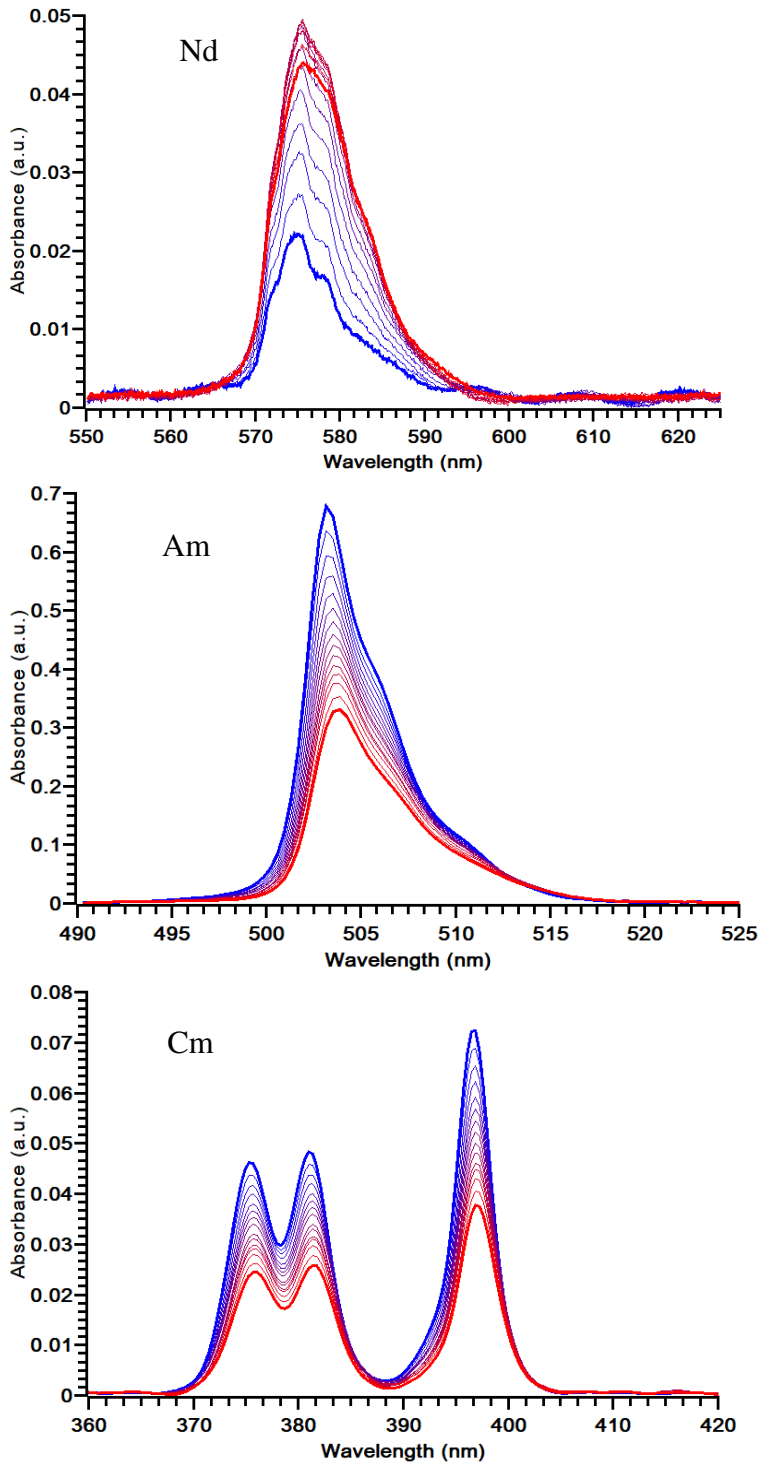

Figure B.6 Spectrophotometric Titrations of Nd, Am, and Cm with TPA. Spectrophotometric titration of a metal and TPA at room temperature and an ionic strength of 1.00 ± 0.01 M. The spectra changes from blue to red over the course of the titration. Top) For the Nd titration, V_{init} = 0.803 mL, C_{Nd} = 10.14 mM, and $pC_{H+,initial}$ = 3.12. The titrant contained C_{TPA} = 50.32 mM and after the addition of 0.792 mL of titrant, the $pC_{H+,final}$ = 4.21. Middle) For the Am titration, V_{init} = 0.795 mL, C_{Am} = 1.914 mM, and $pC_{H+,initial}$ = 2.404. The titrant contained C_{TPA} = 49.79 mM and

after the addition of 0.796 mL of titrant, the $pC_{H+,final}$ = 4.007. Bottom) For the Cm titration, V_{init} = 0.795 mL, C_{Cm} = 1.746 mM, and $pC_{H+,initial}$ = 3.282. The titrant contained C_{TPA} = 49.79 mM and after the addition of 0.796 mL of titrant, the $pC_{H+,final}$ = 4.296.

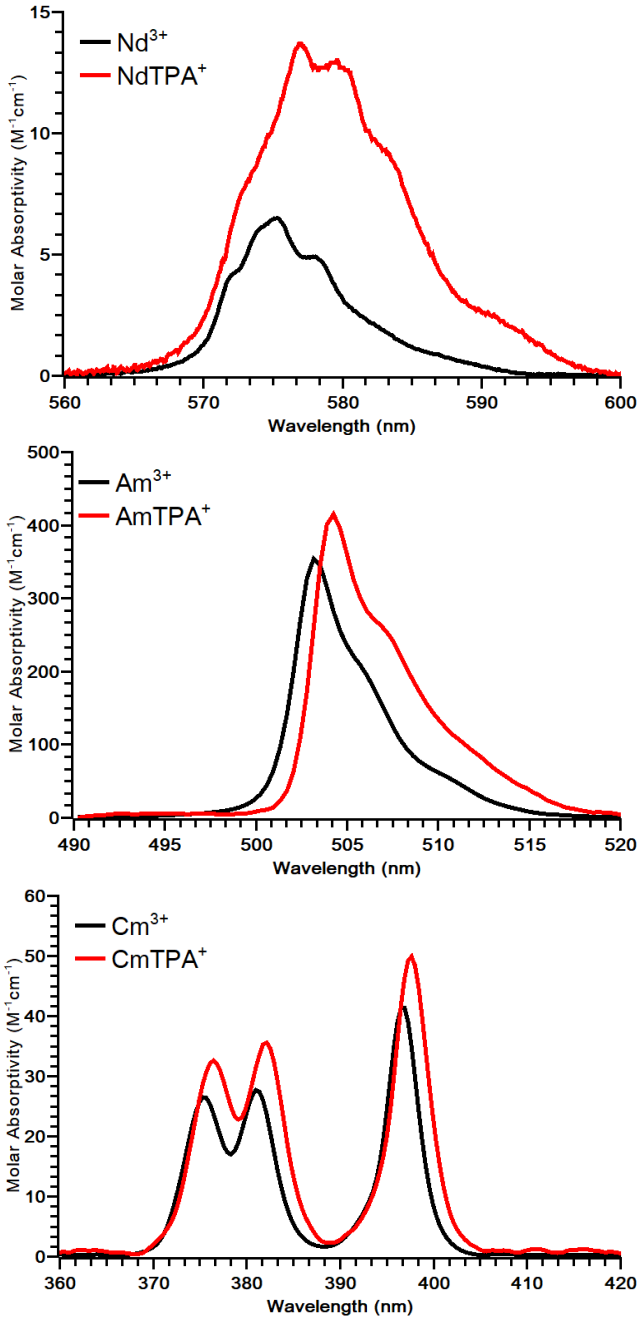

Figure B.7 Molar absorptivity of Nd, Am, and Cm complexes with TPA. Molar absorptivity of Nd (top), Am (middle), and Cm (bottom) complexes with TPA calculated from the spectra shown in Figure B.6 using HypSpec2014. These spectra were collected at room temperature and an ionic strength of 1.00 ± 0.01 M.

Table B.2 Details of EXAFS fitting. Fourier transform and fit ranges, together with the associated number of independent data points, N_{ind}[14,15], and fit degrees of freedom, ν, after fitting. These are followed with the figures and tables for all the fit parameters for each fit, using both N(M-C)=4 and N(M-C)=8. Important! σ^2(M-S) is fixed at 0.008 Å^2 for all fits; therefore, the reported errors on N(M-S) are for comparisons between these samples only. Absolute errors are estimated to be as large as 30% on N(M-S). Note that the M-C shell is included to account for overlap with the M-S shell. Likewise, the M-C shell likely overlaps with further shells, and so the results from the M-C shell should be viewed with skepticism.

Sample	k-range (Å^{-1})	R-range (Å)	N_{ind}	ν
$Eu(TDA)_x$	3-12	1.55-3.6	13.7	5.7
$Eu(TPA)_x$	2.5-12	1.5-3.7	15.3	7.3
$Tb(TDA)_x$	3-11	1.55-3.5	11.9	3.9
$Tb(TPA)_x$	2.5-11	1.5-3.8	14.4	6.4
$Cm(TDA)_x$	2.5-11	1.7-3.8	13.4	3.4
$Cm(TPA)_x$	2.5-12	1.5-3.4	13.5	5.5
$Bk(TDA)_x$	2.5-10	1.5-3.5	11.5	3.5
$Cf(TDA)_x$	2.5-10	1.5-3.5	11.5	3.5

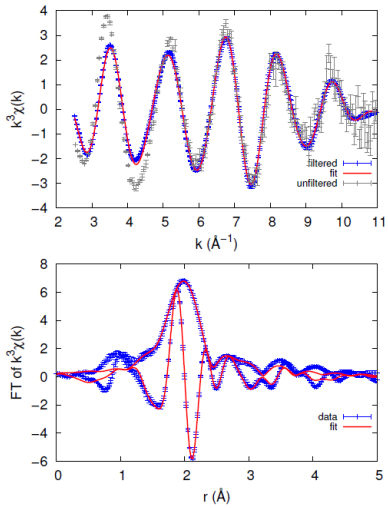

Figure B.8 EXAFS results of $Cm(TDA)_2^-$ complex with N(Cm-C) = 4. EXAFS data for the $Cm(TDA)_2^-$ complex. For this sample, C_{Cm} = 0.79 mM, C_{TDA} = 0.15 M, pH = 3.50, and the ionic strength was adjusted to 1.00 M by addition of sodium perchlorate.

Table B.3 EXAFS results of $Cm(TDA)_2^-$ complex with N(Cm-C) = 4. EXAFS fit for the $Cm(TDA)_2^-$ complex. For this sample, C_{Cm} = 0.79 mM, C_{TDA} = 0.15 M, pH = 3.50, and the ionic strength was adjusted to 1.00 M by addition of sodium perchlorate. Note that the Cm-C shell is split.

Pair	N	R(Å)	σ^2(Å^2)
Cm-O	7(1)	2.440(10)	0.009(1)
Cm-S	1.6(4)	3.05(2)	0.008
Cm-C	2	3.49(4)	0.002(5)
Cm-C	2	3.72(3)	0.000(1)
ΔE_0	-18.7(11)		
R(%)	6.5		

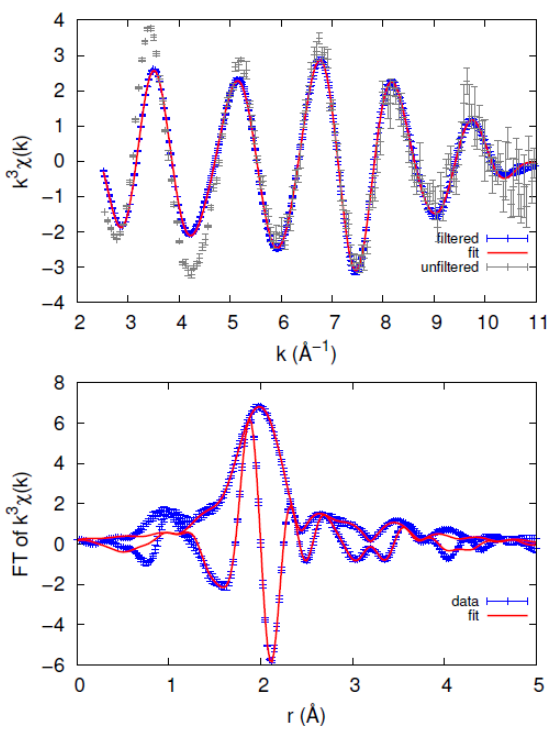

Figure B.9 EXAFS results of $Cm(TDA)_2^-$ complex with N(Cm-C) = 8. EXAFS data for the $Cm(TDA)_2^-$ complex. For this sample, C_{Cm} = 0.79 mM, C_{TDA} = 0.15 M, pH = 3.50, and the ionic strength was adjusted to 1.00 M by addition of sodium perchlorate.

Table B.4 EXAFS results of $Cm(TDA)_2^-$ complex with N(Cm-C) = 8. EXAFS fit for the $Cm(TDA)_2^-$ complex. For this sample, C_{Cm} = 0.79 mM, C_{TDA} = 0.15 M, pH = 3.50, and the ionic strength was adjusted to 1.00 M by addition of sodium perchlorate. Note that the Cm-C shell is split.

Pair	N	R(Å)	σ^2(Å^2)
Cm-O	7(1)	2.396(8)	0.008(1)
Cm-S	1.6(2)	2.85(11)	0.008
Cm-C	4	3.51(2)	0.005(3)
Cm-C	4	3.74(1)	0.002(2)
ΔE_0	-19.2(7)		
R(%)	13.6		

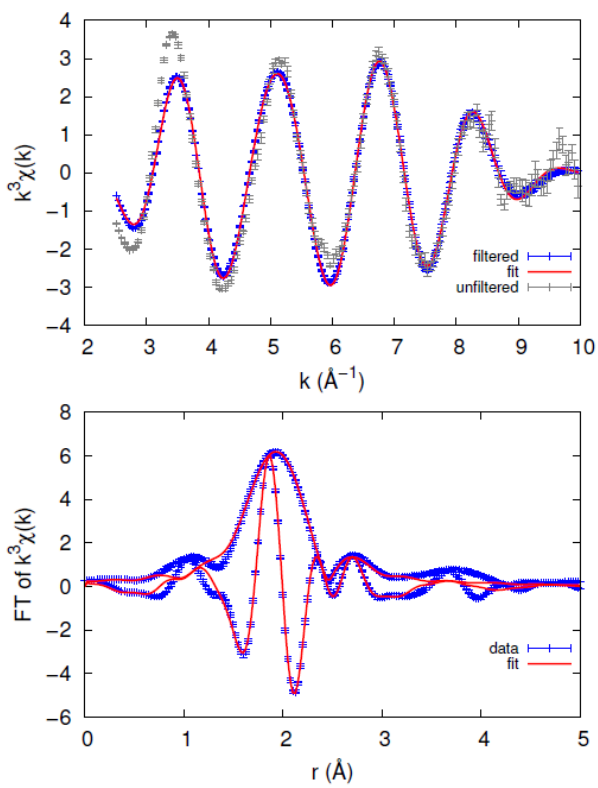

Figure B.10 EXAFS results of $Bk(TDA)_2^-$ complex with N(Bk-C) = 4. EXAFS data for the $Bk(TDA)_2^-$ complex. For this sample, C_{Bk} = 0.79 mM, C_{TDA} = 0.02 M, pH = 3.50, and the ionic strength was adjusted to 1.00 M by addition of sodium perchlorate.

Table B.5 EXAFS results of $Bk(TDA)_2^-$ complex with N(Bk-C) = 4. EXAFS fit for the $Bk(TDA)_2^-$ complex. For this sample, C_{Bk} = 0.79 mM, C_{TDA} = 0.02 M, pH = 3.50, and the ionic strength was adjusted to 1.00 M by addition of sodium perchlorate.

Pair	N	R(Å)	σ^2(Å^2)
Bk-O	8(1)	2.410(8)	0.011(2)
Bk-S	1.2(2)	3.05(1)	0.008
Bk-C	4	3.5(2)	0.05(3)
ΔE_0	-15.5(12)		
R(%)	5.2		

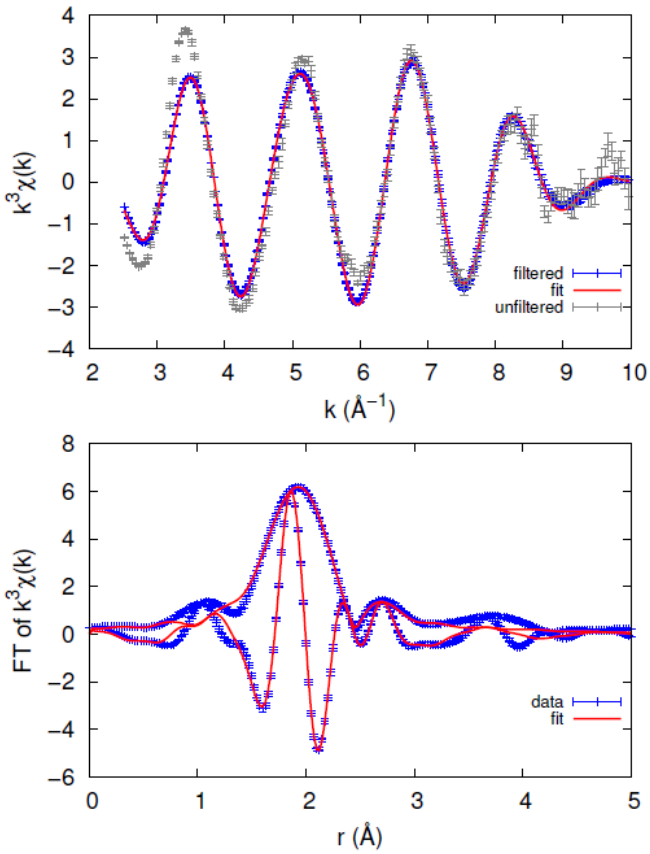

Figure B.11 EXAFS results of $Bk(TDA)_2^-$ complex with N(Bk-C) = 8. EXAFS data for the $Bk(TDA)_2^-$ complex. For this sample, C_{Bk} = 0.79 mM, C_{TDA} = 0.02 M, pH = 3.50, and the ionic strength was adjusted to 1.00 M by addition of sodium perchlorate.

Table B.6 EXAFS results of $Bk(TDA)_2^-$ complex with N(Bk-C) = 8. EXAFS fit for the $Bk(TDA)_2^-$ complex. For this sample, C_{Bk} = 0.79 mM, C_{TDA} = 0.02 M, pH = 3.50, and the ionic strength was adjusted to 1.00 M by addition of sodium perchlorate.

Pair	N	R(Å)	σ^2(Å^2)
Bk-O	8(1)	2.411(7)	0.011(1)
Bk-S	1.1(2)	3.05(1)	0.008
Bk-C	8	3.55(8)	0.05(2)
ΔE_0	-15.5(9)		
R(%)	4.7		

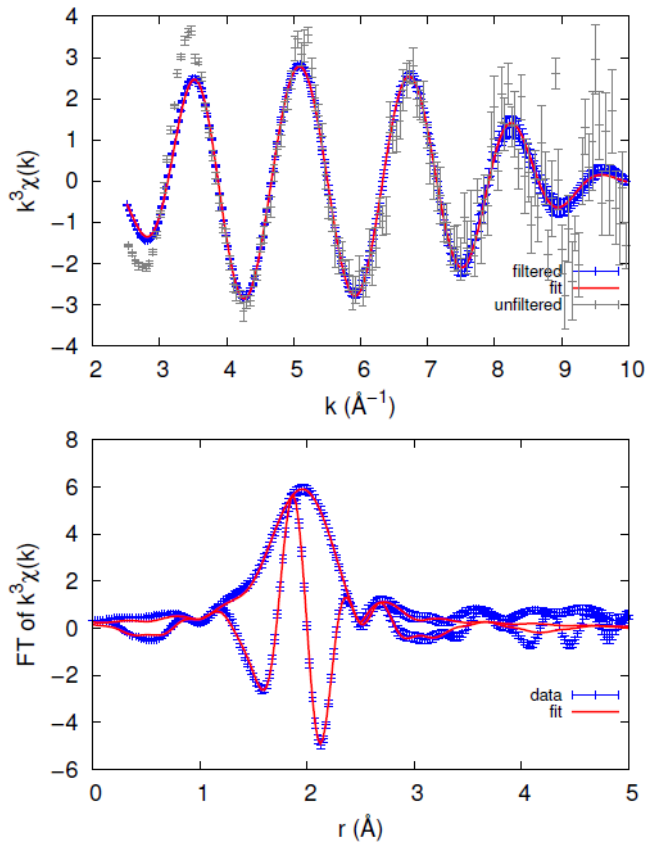

Figure B.12 EXAFS results of $Cf(TDA)_2^-$ complex with N(Cf-C) = 4. EXAFS data for the $Cf(TDA)_2^-$ complex. For this sample, C_{Cf} = 0.79 mM, C_{TDA} = 0.02 M, pH = 3.50, and the ionic strength was adjusted to 1.00 M by addition of sodium perchlorate.

Table B.7 EXAFS results of $Cf(TDA)_2^-$ complex with N(Cf-C) = 4. EXAFS fit for the $Cf(TDA)_2^-$ complex. For this sample, C_{Cf} = 0.79 mM, C_{TDA} = 0.02 M, pH = 3.50, and the ionic strength was adjusted to 1.00 M by addition of sodium perchlorate.

Pair	N	R(Å)	σ^2(Å^2)
Cf-O	8(1)	2.426(7)	0.012(1)
Cf-S	0.7(2)	3.04(2)	0.008
Cf-C	4	3.64(8)	0.03(2)
ΔE_0	-17.0(7)		
R(%)	5.4		

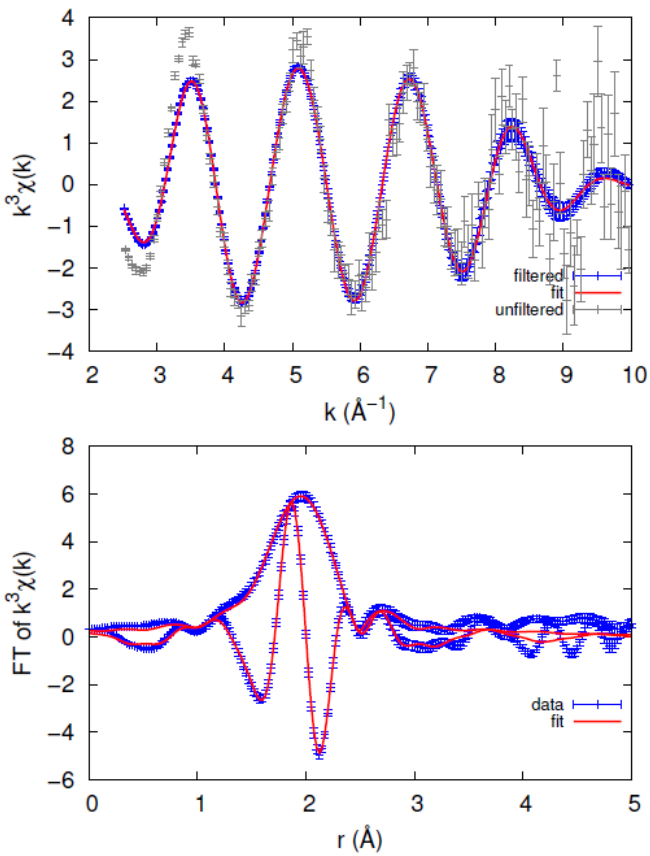

Figure B.13 EXAFS results of $Cf(TDA)_2^-$ complex with N(Cf-C) = 8. EXAFS data for the $Cf(TDA)_2^-$ complex. For this sample, C_{Cf} = 0.79 mM, C_{TDA} = 0.02 M, pH = 3.50, and the ionic strength was adjusted to 1.00 M by addition of sodium perchlorate.

Table B.8 EXAFS results of $Cf(TDA)_2^-$ complex with N(Cf-C) = 8. EXAFS fit for the $Cf(TDA)_2^-$ complex. For this sample, C_{Cf} = 0.79 mM, C_{TDA} = 0.02 M, pH = 3.50, and the ionic strength was adjusted to 1.00 M by addition of sodium perchlorate.

Pair	N	R(Å)	σ^2(Å^2)
Cf-O	8(1)	2.428(6)	0.012(1)
Cf-S	0.7(2)	3.04(2)	0.008
Cf-C	8	3.65(6)	0.04(1)
ΔE_0	-17.0(8)		
R(%)	4.8		

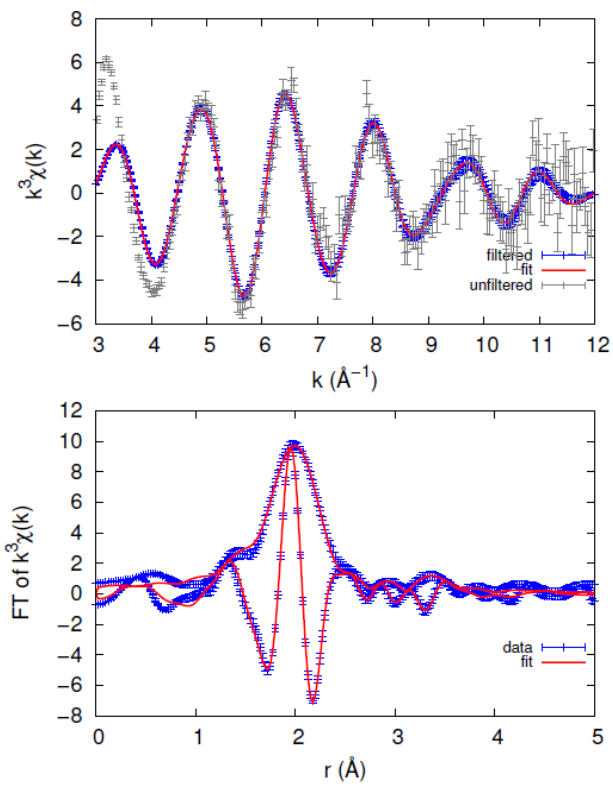

Figure B.14 EXAFS results of $Eu(TDA)_2^-$ complex with N(Eu-C) = 4. EXAFS data for the $Eu(TDA)_2^-$ complex. For this sample, C_{Eu} = 3.00 mM, C_{TDA} = 0.15 M, pH = 3.50, and the ionic strength was adjusted to 1.00 M by addition of sodium perchlorate.

Table B.9 EXAFS results of $Eu(TDA)_2^-$ complex with N(Eu-C) = 4. EXAFS fit for the $Eu(TDA)_2^-$ complex. For this sample, C_{Eu} = 3.00 mM, C_{TDA} = 0.15 M, pH = 3.50, and the ionic strength was adjusted to 1.00 M by addition of sodium perchlorate.

Pair	N	R(Å)	σ^2(Å^2)
Eu-O	7.2(4)	2.404(4)	0.0080(6)
Eu-S	0.9(2)	3.09(2)	0.008
Eu-C	4	3.66(2)	0.010(3)
ΔE_0	-16.8(8)		
R(%)	5.4		

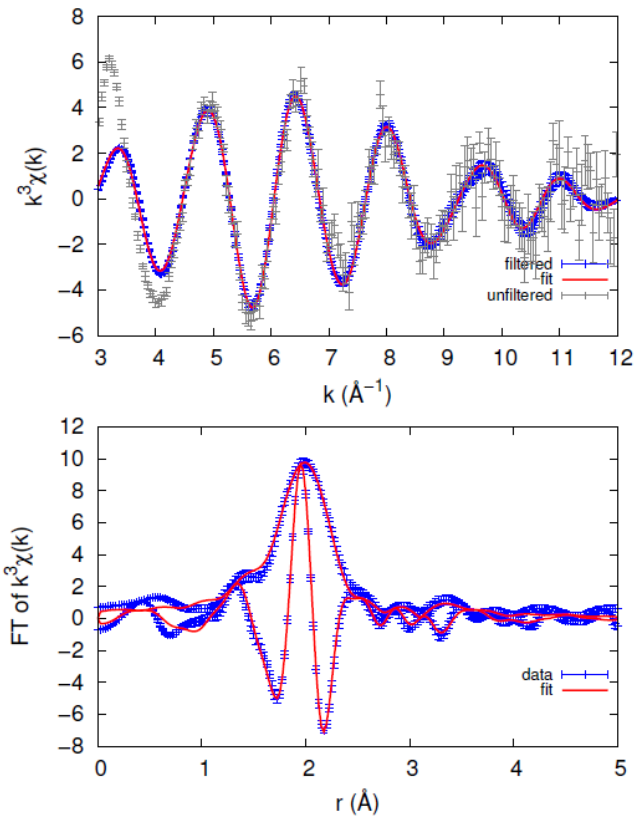

Figure B.15 EXAFS results of $Eu(TDA)_2^-$ complex with N(Eu-C) = 8. EXAFS data for the $Eu(TDA)_2^-$ complex. For this sample, C_{Eu} = 3.00 mM, C_{TDA} = 0.15 M, pH = 3.50, and the ionic strength was adjusted to 1.00 M by addition of sodium perchlorate.

Table B.10 EXAFS results of $Eu(TDA)_2^-$ complex with N(Eu-C) = 8. EXAFS fit for the $Eu(TDA)_2^-$ complex. For this sample, C_{Eu} = 3.00 mM, C_{TDA} = 0.15 M, pH = 3.50, and the ionic strength was adjusted to 1.00 M by addition of sodium perchlorate.

Pair	N	R(Å)	σ^2(Å^2)
Eu-O	7.3(5)	2.405(5)	0.0080(7)
Eu-S	0.8(2)	3.09(2)	0.008
Eu-C	8	3.67(3)	0.021(5)
ΔE_0	-16.8(9)		
R(%)	7.1		

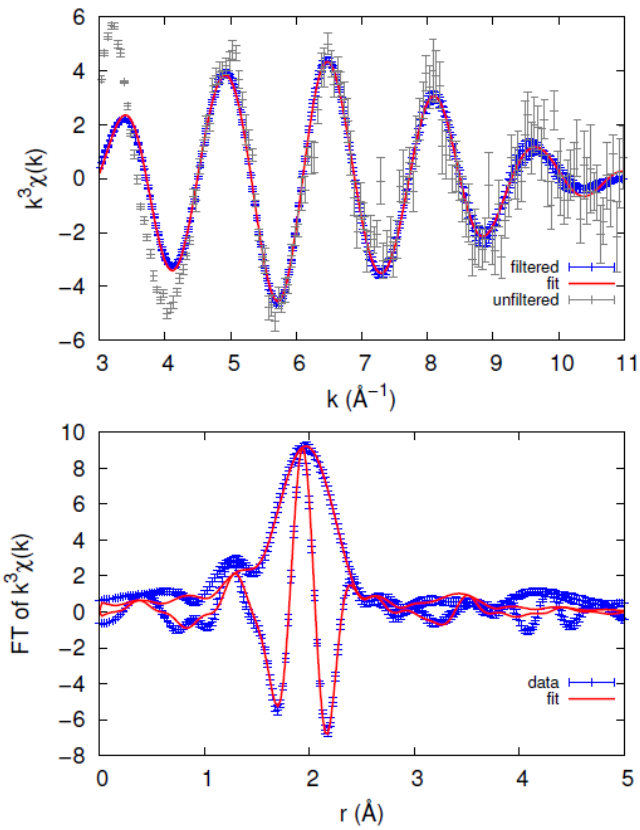

Figure B.16 EXAFS results of $Tb(TDA)_2^-$ complex with N(Tb-C) = 4. EXAFS data for the $Tb(TDA)_2^-$ complex. For this sample, C_{Tb} = 3.00 mM, C_{TDA} = 0.15 M, pH = 3.50, and the ionic strength was adjusted to 1.00 M by addition of sodium perchlorate.

Table B.11 EXAFS results of $Tb(TDA)_2^-$ complex with N(Tb-C) = 4. EXAFS fit for the $Tb(TDA)_2^-$ complex. For this sample, C_{Tb} = 3.00 mM, C_{TDA} = 0.15 M, pH = 3.50, and the ionic strength was adjusted to 1.00 M by addition of sodium perchlorate.

Pair	N	R(Å)	σ^2(Å^2)
Tb-O	7(1)	2.382(7)	0.079(9)
Tb-S	0.5(3)	3.04(4)	0.008
Tb-C	4	3.61(3)	0.011(3)
ΔE_0	-17.3(12)		
R(%)	5.6		

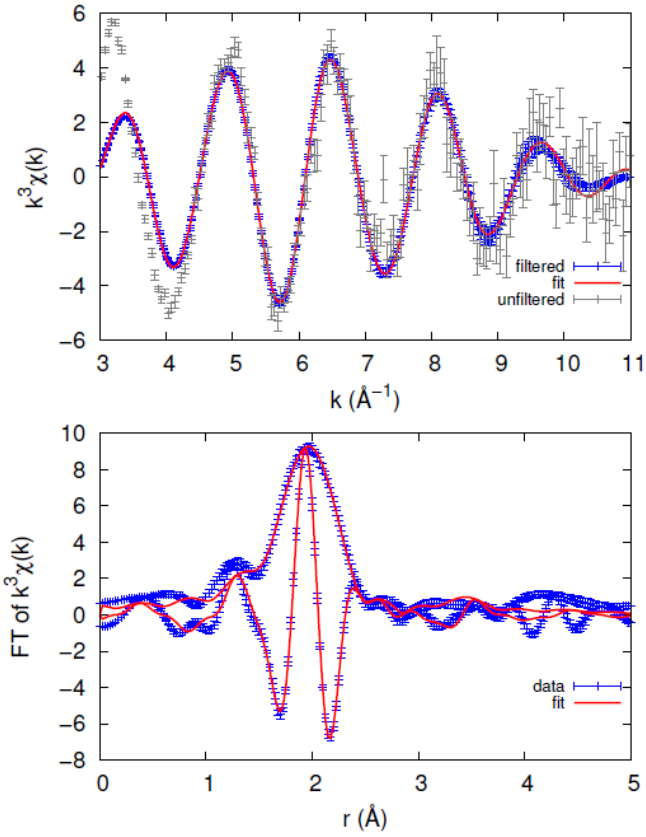

Figure B.17 EXAFS results of $Tb(TDA)_2^-$ complex with N(Tb-C) = 8. EXAFS data for the $Tb(TDA)_2^-$ complex. For this sample, C_{Tb} = 3.00 mM, C_{TDA} = 0.15 M, pH = 3.50, and the ionic strength was adjusted to 1.00 M by addition of sodium perchlorate.

Table B.12 EXAFS results of $Tb(TDA)_2^-$ complex with N(Tb-C) = 8. EXAFS fit for the $Tb(TDA)_2^-$ complex. For this sample, C_{Tb} = 3.00 mM, C_{TDA} = 0.15 M, pH = 3.50, and the ionic strength was adjusted to 1.00 M by addition of sodium perchlorate.

Pair	N	R(Å)	σ^2(Å^2)
Tb-O	7(1)	2.384(6)	0.0081(9)
Tb-S	0.5(2)	3.03(4)	0.008
Tb-C	8	3.63(2)	0.020(4)
ΔE_0	-17.3(9)		
R(%)	5.4		

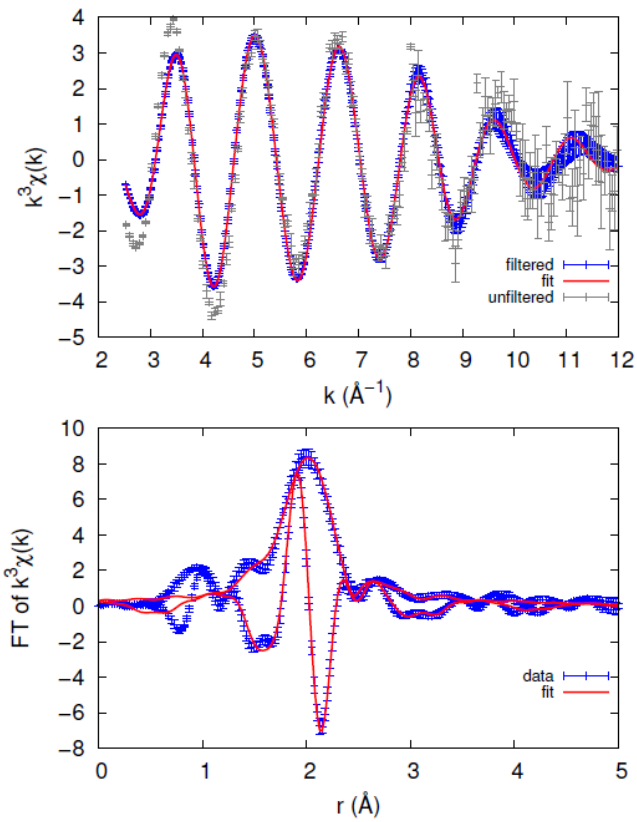

Figure B.18 EXAFS results of $Cm(TPA)^+$ complex with N(Cm-C) = 4. EXAFS data for the $Cm(TPA)^+$ complex. For this sample, C_{Cm} = 0.79 mM, C_{TPA} = 0.05 M, pH = 3.90, and the ionic strength was adjusted to 1.00 M by addition of sodium perchlorate.

Table B.13 EXAFS results of $Cm(TPA)^+$ complex with N(Cm-C) = 4. EXAFS fit for the $Cm(TPA)^+$ complex. For this sample, C_{Cm} = 0.79 mM, C_{TPA} = 0.05 M, pH = 3.90, and the ionic strength was adjusted to 1.00 M by addition of sodium perchlorate.

Pair	N	R(Å)	σ^2(Å^2)
Cm-O	8(1)	2.467(8)	0.009(1)
Cm-S	0.8(2)	3.07(2)	0.008
Cm-C	4	3.67(6)	0.03(1)
ΔE_0	-18.8(9)		
R(%)	7.5		

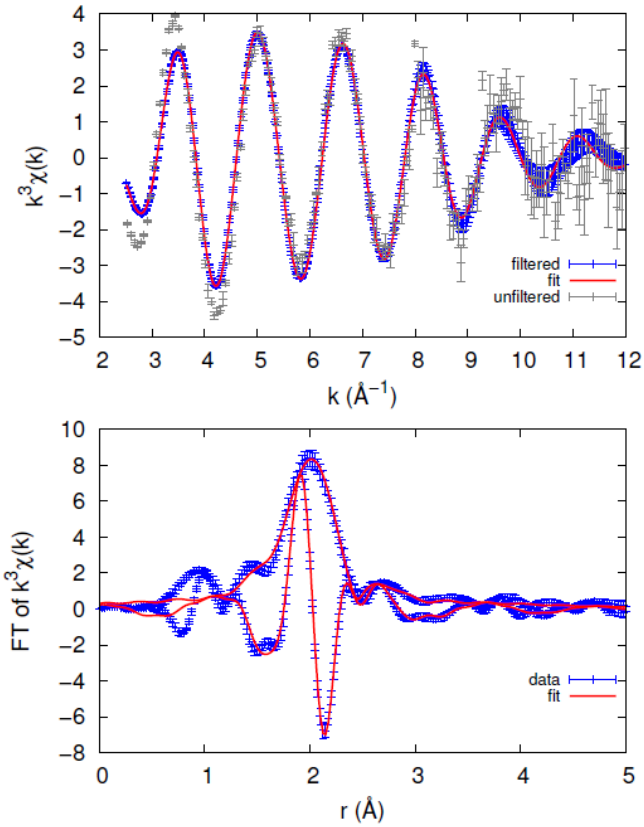

Figure B.19 EXAFS results of $Cm(TPA)^+$ complex with N(Cm-C) = 8. EXAFS data for the $Cm(TPA)^+$ complex. For this sample, C_{Cm} = 0.79 mM, C_{TPA} = 0.05 M, pH = 3.90, and the ionic strength was adjusted to 1.00 M by addition of sodium perchlorate.

Table B.14 EXAFS results of $Cm(TPA)^+$ complex with N(Cm-C) = 8. EXAFS fit for the $Cm(TPA)^+$ complex. For this sample, C_{Cm} = 0.79 mM, C_{TPA} = 0.05 M, pH = 3.90, and the ionic strength was adjusted to 1.00 M by addition of sodium perchlorate.

Pair	N	R(Å)	σ^2(Å^2)
Cm-O	8(1)	2.47(1)	0.008(1)
Cm-S	0.8(3)	3.06(2)	0.008
Cm-C	8	3.7(1)	0.06(4)
ΔE_0	-18.8(12)		
R(%)	7.8		

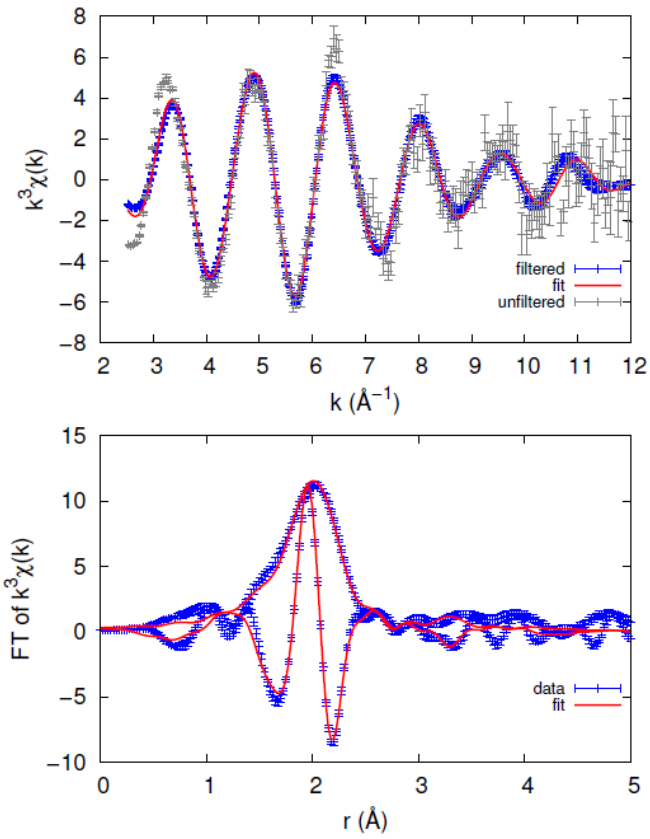

Figure B.20 EXAFS results of $Eu(TPA)^+$ complex with N(Eu-C) = 4. EXAFS data for the $Eu(TPA)^+$ complex. For this sample, C_{Eu} = 3.00 mM, C_{TPA} = 0.05 M, pH = 3.90, and the ionic strength was adjusted to 1.00 M by addition of sodium perchlorate.

Table B.15 EXAFS results of $Eu(TPA)^+$ complex with N(Eu-C) = 4. EXAFS fit for the $Eu(TPA)^+$ complex. For this sample, C_{Eu} = 3.00 mM, C_{TPA} = 0.05 M, pH = 3.90, and the ionic strength was adjusted to 1.00 M by addition of sodium perchlorate.

Pair	N	R(Å)	σ^2(Å^2)
Eu-O	8(1)	2.422(8)	0.009(1)
Eu-S	0.5(4)	3.08(8)	0.008
Eu-C	4	3.61(6)	0.014(9)
ΔE_0	-13.3(12)		
R(%)	11.4		

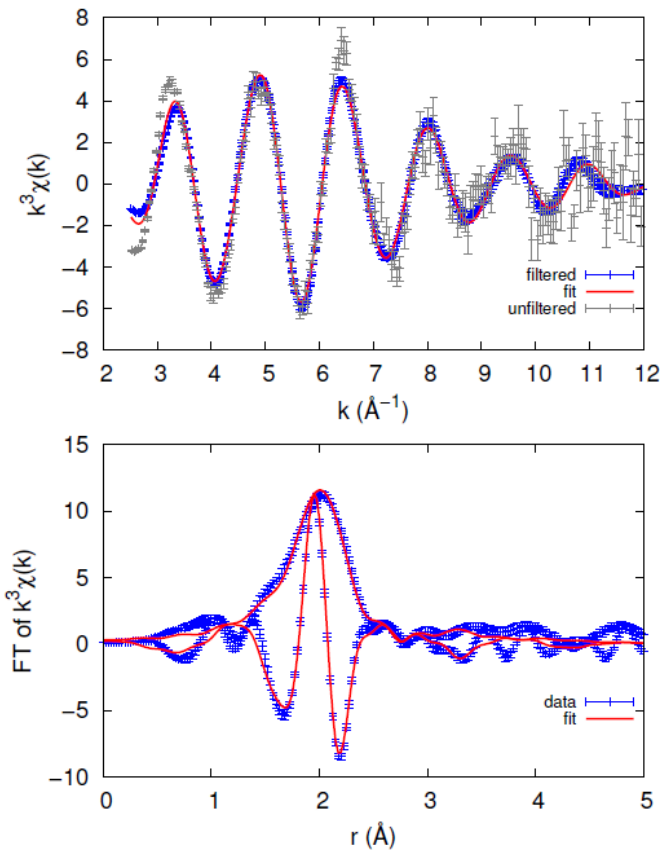

Figure B.21 EXAFS results of $Eu(TPA)^+$ complex with N(Eu-C) = 8. EXAFS data for the $Eu(TPA)^+$ complex. For this sample, C_{Eu} = 3.00 mM, C_{TPA} = 0.05 M, pH = 3.90, and the ionic strength was adjusted to 1.00 M by addition of sodium perchlorate.

Table B.16 EXAFS results of $Eu(TPA)^+$ complex with N(Eu-C) = 8. EXAFS fit for the $Eu(TPA)^+$ complex. For this sample, C_{Eu} = 3.00 mM, C_{TPA} = 0.05 M, pH = 3.90, and the ionic strength was adjusted to 1.00 M by addition of sodium perchlorate.

Pair	N	R(Å)	σ^2(Å^2)
Eu-O	9(1)	2.423(9)	0.009(1)
Eu-S	0.4(4)	3.096(11)	0.008
Eu-C	8	3.61(7)	0.03(2)
ΔE_0	-13.3(16)		
R(%)	12.1		

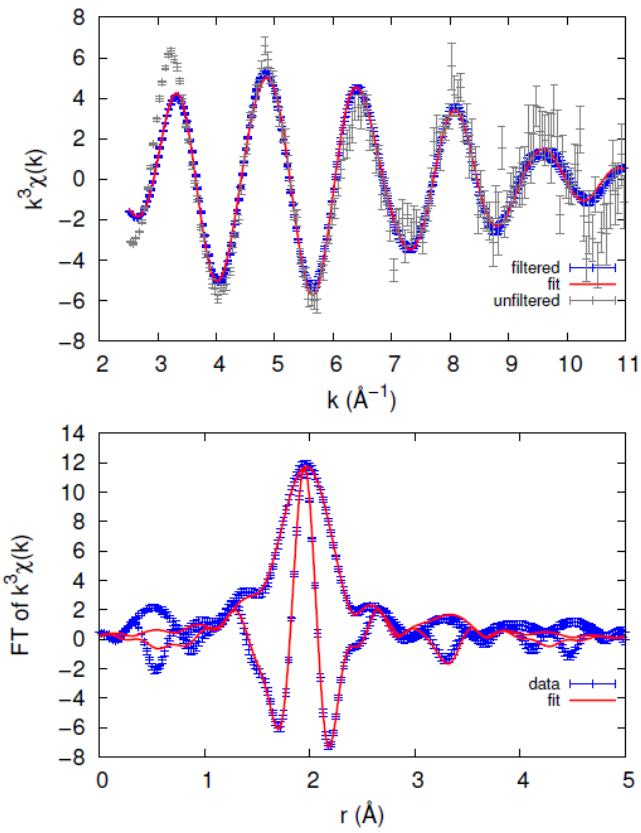

Figure B.22 EXAFS results of $Tb(TPA)^+$ complex with N(Tb-C) = 4. EXAFS data for the $Tb(TPA)^+$ complex. For this sample, C_{Tb} = 3.00 mM, C_{TPA} = 0.05 M, pH = 3.90, and the ionic strength was adjusted to 1.00 M by addition of sodium perchlorate.

Table B.17 EXAFS results of $Tb(TPA)^+$ complex with N(Tb-C) = 4. EXAFS fit for the $Tb(TPA)^+$ complex. For this sample, C_{Tb} = 3.00 mM, C_{TPA} = 0.05 M, pH = 3.90, and the ionic strength was adjusted to 1.00 M by addition of sodium perchlorate.

Pair	N	R(Å)	σ^2(Å^2)
Tb-O	8(1)	2.396(6)	0.008(1)
Tb-S	0.3(2)	2.86(7)	0.008
Tb-C	4	3.64(2)	0.007(3)
ΔE_0	-17.1(7)		
R(%)	7.6		

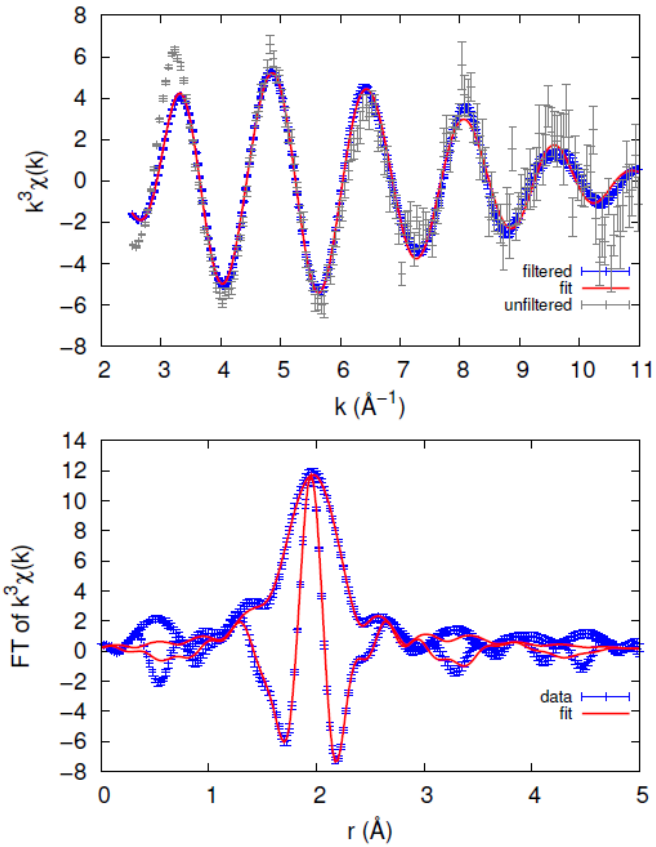

Figure B.23 EXAFS results of $Tb(TPA)^+$ complex with N(Tb-C) = 8. EXAFS data for the $Tb(TPA)^+$ complex. For this sample, C_{Tb} = 3.00 mM, C_{TPA} = 0.05 M, pH = 3.90, and the ionic strength was adjusted to 1.00 M by addition of sodium perchlorate.

Table B.18 EXAFS results of $Tb(TPA)^+$ complex with N(Tb-C) = 8. EXAFS fit for the $Tb(TPA)^+$ complex. For this sample, C_{Tb} = 3.00 mM, C_{TPA} = 0.05 M, pH = 3.90, and the ionic strength was adjusted to 1.00 M by addition of sodium perchlorate.

Pair	N	R(Å)	σ^2(Å^2)
Tb-O	8(1)	2.396(8)	0.008(1)
Tb-S	0.3(3)	2.85(11)	0.008
Tb-C	8	3.7(1)	0.04(3)
ΔE_0	-17.2(9)		
R(%)	10.4		

Cartesian coordinates of selected structures

TDA2-

C	-4.12257528	1.52686661	-0.33149043
C	-2.75136267	0.83955621	-0.47442204
H	-2.63085234	0.49015902	-1.51091636
H	-2.71981683	-0.04251060	0.18209079
C	0.02777623	0.81109486	-0.31747388
C	1.35200574	1.55103903	-0.03261077
H	0.00129683	0.46552512	-1.35959236
H	-0.08553677	-0.04043830	0.36733988
S	-1.37717138	1.96757934	-0.04812863
O	1.93265864	2.09986430	-1.02281757
O	1.75745647	1.56334336	1.17352777
O	-4.14969905	2.74856966	0.01354314
O	-5.12843515	0.79076308	-0.58226323

$THTPA^{2-}$

O	-5.22837414	-1.70947454	-1.93849552
C	-4.60291273	-1.53116478	-0.84131576
C	-3.43298550	-0.51677702	-0.89523260
S	-1.92851083	-1.38954897	-1.56999385

C	-0.73691550	-0.52788128	-0.42130279
C	-0.10460299	-1.57257376	0.53165282
O	-0.38538333	-1.51938024	1.76818584
O	-4.85187953	-2.11276458	0.25892238
C	-1.54913036	0.59412475	0.23049242
O	0.67460606	-2.41846333	-0.02028133
H	-1.55338046	1.47239566	-0.43425884
H	-2.99177835	-0.70410350	1.19622305
H	-1.08162804	0.88565846	1.18138491
C	-2.97641432	0.08327747	0.42977089
H	-3.66182733	0.88617793	0.74432391
H	0.06943534	-0.12847922	-1.05305715
H	-3.69535229	0.27035627	-1.61722087

TPA^{2-}

O	-4.92439456	-2.17931339	-1.80154758
C	-4.84981246	-1.16115654	-1.03640146
C	-3.51099737	-0.87643073	-0.41394929
S	-2.14907121	-1.90032712	-0.75184002
C	-1.10280160	-0.95083189	0.26111000
C	0.34572279	-1.32304816	0.42482624
O	1.05079735	-0.57714608	1.17782742
O	-5.79968179	-0.36366520	-0.75078049
C	-1.79388798	0.10698216	0.82866413
O	0.75012682	-2.35659699	-0.20420785
C	-3.15679303	0.14956084	0.44648485
H	-3.87303674	0.90124933	0.77993126
H	-1.31435559	0.82110843	1.49857318

$Cm(H_2O)_9^{3+}$

Cm	-0.03457035	-0.11145316	0.01617222
O	-0.39903775	1.95511209	-1.36369695
H	0.02131159	2.82386929	-1.21267718
H	-1.18299751	2.12021657	-1.92292236
O	-2.03162068	-1.34025479	0.90950919
H	-2.09862120	-2.30548182	1.04534010
H	-2.76930349	-0.93988107	1.40917143
O	2.28330025	-1.03867949	0.37833370
H	3.03510976	-0.89192932	-0.22823477
H	2.67319295	-1.24904430	1.24927365
O	-1.51252731	1.45867193	1.25774694
H	-1.91679634	2.26787323	0.88941272
H	-1.67474854	1.48689333	2.22047118
O	0.35468221	-0.61623738	2.42235506
H	-0.23723481	-1.16299081	2.97523210
H	0.87802191	-0.07590986	3.04622419
O	1.43156963	1.72474318	0.82972923
H	2.40264651	1.68089849	0.92580916
H	1.13963572	2.48535330	1.36869387
O	-1.77026829	-0.46957897	-1.74073551
H	-2.57073918	-0.98326280	-1.51499405
H	-1.63231739	-0.58951748	-2.70053859
O	0.11336613	-2.55080816	-0.49240837
H	-0.35960525	-3.03450612	-1.19729816
H	0.99219331	-2.97257394	-0.41512451
O	1.27595461	-0.18114519	-2.10139176
H	1.48570824	-0.96327206	-2.64834374
H	1.18980849	0.56809913	-2.72354932

$Eu(H_2O)_9^{3+}$

Eu	-0.17816115	0.05057396	-0.05172489
O	1.59369966	-0.07649955	-1.76161520
O	-1.01354759	1.67219225	1.60462108
O	-1.11165304	1.28571413	-1.96880550
O	1.61891094	0.32052029	1.63186433
O	-0.93632318	-1.32690623	1.82999726
O	-1.08030065	-1.66660642	-1.57507146
O	1.20412259	-2.07060912	0.11037335
O	0.86896323	2.30026856	-0.36371142
O	-2.67537568	0.02031667	-0.08340900
H	2.09057897	-0.91971132	-1.77458037
H	-1.96278238	1.78710091	1.80972858
H	-1.32768520	0.86005027	-2.82294589
H	2.26114151	1.05572682	1.67550935
H	-1.37280745	-1.05234274	2.66003296
H	-2.04303538	-1.83407742	-1.59327171
H	2.00287034	-2.18977036	0.66081434
H	1.75863518	2.46560310	-0.73286727
H	-3.17711710	0.69299789	-0.58571007
H	1.71287778	-0.16192998	2.47669037
H	0.68658397	3.04057680	0.24758229
H	1.56337576	0.22841499	-2.69005657
H	0.94805086	-2.96820404	-0.18000528
H	-0.54432039	1.79309164	2.45434699
H	-0.53091811	-2.19678459	2.01698007
H	-3.28687911	-0.32033374	0.59787085
H	-0.66168719	2.12687505	-2.18944781

H	-0.68544770	-2.27499316	-2.22885175

$Gd(H_2O)_9^{3+}$

Gd	0.00000000	0.00000000	0.00000000
O	1.26871627	0.05952533	-2.19733014
O	-0.96922350	1.57814447	1.52173415
O	-0.94548464	1.68378250	-1.42005080
O	1.26871627	0.05952533	2.19733014
O	-0.81901892	-1.67921746	1.50168097
O	-0.75000808	-1.67981447	-1.53665879
O	1.80787300	-1.57390894	-0.00385349
O	1.60773966	1.77784684	-0.00654270
O	-2.52799929	-0.22508572	0.00000000
H	2.13363791	-0.35992286	-2.37388017
H	-1.37605870	2.42721831	1.25839214
H	-1.81643188	1.67974624	-1.86253862
H	2.10371371	0.53067097	2.38372172
H	-1.78782666	-1.82160777	1.47884294
H	-1.14640694	-2.55354209	-1.35098929
H	2.36093056	-1.67742446	0.79589028
H	2.27651832	1.88673322	-0.71083420
H	-3.03238135	-0.57499469	-0.76048058
H	1.08025705	-0.48043808	2.98990646
H	1.66343068	2.57728732	0.55240868
H	1.07866342	0.62409295	-2.97136416
H	1.84134916	-2.43358908	-0.46841507
H	-0.55329159	1.73263493	2.39326235
H	-0.41685974	-2.54679809	1.70540676
H	-3.12041071	0.41874826	0.43568737

H	-0.50822756	2.51502288	-1.68927690
H	-0.28703837	-1.76085550	-2.39422591

$Cm(TDA)^{+}\bullet 6H_2O$

Cm	0.00086361	-0.09915117	0.05510147
O	0.48590253	-0.01805344	-2.42910493
O	-0.57746707	1.73199934	1.81390674
O	-1.31419981	1.82041362	-1.02276722
O	1.24148924	-0.23542097	2.02418372
O	-2.02160168	-0.62726615	1.47932049
O	-0.13246274	-2.42297702	0.24266529
S	2.69029138	-1.45274731	-0.36425280
O	1.71579362	1.73750997	-0.39802527
O	-1.82928480	-1.17692878	-1.49436612
H	-0.09036878	-0.61511140	-2.94708379
H	-0.48909302	2.68732503	1.62871825
H	-1.42759103	1.82127125	-1.99313671
H	-2.13025487	2.22879913	-0.67432536
H	-2.11395694	-0.07739222	2.28289475
H	-1.83332173	-2.10466150	-1.17793547
H	-2.01908694	-1.55352124	1.79564923
H	1.38781649	2.53743044	-0.85383179
H	-2.76024654	-0.88644613	-1.43341661
H	0.11695006	1.53391125	2.47913093
H	2.25301634	2.08220639	0.34164579
H	1.37237002	-0.08338135	-2.83391323
C	2.33938134	-0.81476196	2.40950861
C	3.34228804	-1.22670022	1.32455533
C	0.69488015	-3.42406624	0.23447568

C	2.10473488	-3.17898080	-0.31737246
O	0.40700724	-4.58049036	0.59296066
O	2.65657915	-1.00567209	3.59682626
H	4.08562008	-0.41907133	1.24140372
H	2.10791889	-3.51194460	-1.36676704
H	2.83958231	-3.79242029	0.21865655
H	3.88243057	-2.13330880	1.62389144

$Cm(THTPA)^{+} \bullet 6H_2O$

Cm	0.00079015	0.02622997	-0.13744729
O	-1.86637402	1.85394949	-0.29631299
H	-1.72867007	2.48857440	-1.02737048
H	-2.78540411	1.53695307	-0.39924766
O	-2.32679104	-0.71548311	0.71998772
H	-2.43369548	-1.68001968	0.59124966
H	-2.56512003	-0.56682622	1.65657044
S	2.84616246	0.41924740	0.70424719
H	-0.11773905	-2.96487274	0.16141154
O	1.52091503	-0.59056493	-1.80135423
O	-0.09508763	1.64937904	1.80728664
H	-0.89963507	2.20583272	1.76528558
H	-0.02663803	1.35502844	2.73631814
O	0.60763208	-1.29998948	1.67566237
H	-0.21412631	-2.88741997	-1.38765941
C	2.81333178	-0.71167996	-1.89386944
O	0.77233434	2.25146208	-1.16838542
H	1.31875270	2.15742340	-1.97376830
H	1.25155599	2.90656034	-0.62314951
O	-1.07347479	-0.11538903	-2.45533059

H	-1.94019684	-0.48656597	-2.71028892
H	-0.41626725	-0.54811534	-3.03887558
O	-0.53603987	-2.46293394	-0.56815482
C	1.66067411	-1.54777644	2.39612145
C	2.98775917	-0.83938977	2.04442978
O	1.67738867	-2.33094565	3.36323290
O	3.42403454	-0.92689219	-2.95710933
C	3.62872460	-0.64599928	-0.59518775
C	4.05765874	-1.82259059	1.53535437
C	3.78455728	-2.03870205	0.04711998
H	4.61095426	-0.21272773	-0.81995956
H	2.85474145	-2.61379159	-0.08606046
H	4.59442042	-2.59171124	-0.44740607
H	4.01105646	-2.75918736	2.10720504
H	5.05435520	-1.38153888	1.67916534
H	3.32939255	-0.31740278	2.94800650

$Cm(TPA\ Bi)^{+} \bullet 7H_2O$

Cm	0.03783811	-0.11482673	0.17142334
O	0.22324133	1.84027994	-1.37420441
H	-0.16884786	2.72836386	-1.26913132
H	0.24481476	1.67363186	-2.33725872
O	-1.66266505	-1.72282584	1.17836842
H	-1.47112929	-2.67907241	1.11286584
H	-2.19643727	-1.61150964	1.98896056
O	2.57610760	0.07098571	0.01204971
H	2.93367049	0.01348769	-0.89655998
H	3.08412340	-0.59179522	0.52138270
O	-1.78623944	1.31425847	1.21439623

H	-2.67382465	1.29154202	0.80631444
H	-1.94291303	1.50493578	2.15953693
O	1.06244689	-0.96290371	2.30935000
H	0.70101529	-1.74377331	2.77246782
H	1.22994612	-0.30238084	3.01112832
O	1.02009796	1.78826412	1.58233718
H	1.93063352	2.02594206	1.31316182
H	0.56101900	2.64098027	1.71203431
O	-2.10870507	-0.22805467	-1.17590105
H	-2.65264237	-1.00046683	-0.92118014
H	-2.03649917	-0.27814602	-2.14977563
H	1.25581478	-1.99522052	-4.51068919
H	1.77072984	-4.29594245	-5.73262382
C	1.57267029	-4.18782762	-4.66719527
O	1.73113189	-7.53611487	-3.12763353
C	1.80068621	-6.73098942	-4.11198803
C	1.56322662	-5.27299076	-3.80302860
S	1.21708308	-4.79235292	-2.17928064
C	1.08144552	-3.12683960	-2.65630201
C	0.75741424	-2.08737932	-1.68529500
O	0.67371883	-0.85507816	-2.05684230
O	2.04436504	-7.02326927	-5.32277081
C	1.29959705	-2.96660898	-4.01887294
O	0.54624668	-2.39330910	-0.44744605

$Cm(TPA\ OS)^{+} \bullet 7H_2O$

Cm	0.08615457	-0.05686397	-0.11924971
O	-1.60765262	-0.25867997	-1.75259558
H	2.07129089	-1.79453083	1.47623410

H	1.83463849	-2.19000050	-1.56152117
H	-2.64068324	-0.87768785	1.22790811
H	0.89032929	0.26116729	2.98178814
H	1.28969545	1.73766017	-2.54806207
H	2.73633497	1.16681486	0.86412044
S	-1.15087500	-2.87225680	-0.56868606
H	-0.75232132	2.79029742	-0.58601060
C	-2.72823114	-0.94245686	-1.76026029
C	-2.69779265	-2.15264971	-0.88423020
C	-3.66918015	-2.69532605	-0.06719540
C	-3.14401184	-3.65186170	0.85017440
C	-1.78030776	-3.82454185	0.73938032
C	-0.82650191	-4.61735874	1.58381704
O	0.41014271	-4.23976577	1.54414120
O	-1.27859382	-5.56366004	2.27087349
O	-3.75215759	-0.62550473	-2.38733563
H	-3.73904413	-4.16915703	1.60192759
H	-4.71117836	-2.37750321	-0.09305388
O	-0.78741566	2.27554061	0.24609990
H	-1.70586300	2.37074992	0.56879247
O	2.38757330	0.92450318	-0.01639065
H	3.13836823	0.53175096	-0.50343059
O	0.45197345	1.46959991	-2.12362184
H	-0.17390573	1.27098827	-2.84928393
O	0.62975755	0.82152528	2.22597039
H	0.39632622	1.69256691	2.60049210
O	-1.92067060	-0.22831770	1.38023251
H	-1.78020475	-0.20595577	2.34715499

O	1.54212595	-1.27976209	-1.76589554
H	1.32794965	-1.29313444	-2.71973645
O	1.13924308	-1.82571619	1.18887699
H	0.82038293	-2.82236660	1.31317947

$Eu(TDA)^{+} \bullet 6H_2O$

Eu	-0.08078337	-0.10910618	-0.02192113
O	0.42059088	-0.41650880	-2.50062496
O	-0.94068724	1.71019503	1.54326597
O	-0.92135570	1.97929916	-1.57812897
O	1.08986570	-0.06819124	2.00939503
O	-1.69095629	-1.24900048	1.68064465
O	-0.05965153	-2.45606002	-0.13194105
S	2.73762274	-1.39123402	-0.11840219
O	1.62560461	1.68665689	-0.59484683
O	-2.43739097	-0.46101417	-0.91292884
H	0.21936257	-1.27728286	-2.91838868
H	-0.99009084	2.66910009	1.36439354
H	-0.91955997	1.82442890	-2.54331769
H	-1.53511683	2.72751739	-1.44713542
H	-1.48107313	-1.10517141	2.62465149
H	-3.06217492	-0.73850227	-0.21332026
H	-1.40404865	-2.17087155	1.49942888
H	1.08484048	2.41035893	-0.97850011
H	-2.85259730	0.32086612	-1.32703559
H	-0.29657438	1.62318705	2.27938166
H	2.18962072	2.11096084	0.08002970
H	1.29441836	-0.16541917	-2.86115195
C	2.11928379	-0.62411101	2.55554513

C	3.19182345	-1.23972366	1.63597797
C	0.77525610	-3.44147051	-0.05856799
C	2.26861482	-3.13841811	-0.26581762
O	0.45098088	-4.62908358	0.12381383
O	2.34038551	-0.66226064	3.78067958
H	4.06805912	-0.57637059	1.66814555
H	2.52420314	-3.42997932	-1.29574297
H	2.88303726	-3.74384501	0.41161381
H	3.50570364	-2.21912809	2.01600987

$Eu(THTPA)^{+} \bullet 6H_2O$

Eu	-0.07364589	0.09137145	-0.12889309
O	-1.93176216	1.92942693	-0.33857892
H	-1.79007582	2.53564800	-1.09213336
H	-2.84504998	1.60000093	-0.44803976
O	-2.39024833	-0.65493180	0.71818532
H	-2.44225382	-1.62619482	0.60806626
H	-2.65052024	-0.49978478	1.64737595
S	2.83718003	0.39789292	0.68894854
H	-0.14456072	-2.87873064	0.23609613
O	1.49652386	-0.55583443	-1.77704804
O	-0.18509162	1.69160939	1.81935327
H	-0.97538621	2.26640172	1.77115913
H	-0.12951554	1.39974347	2.74976936
O	0.60823002	-1.21318151	1.69862795
H	-0.30998004	-2.88589166	-1.30687481
C	2.77574507	-0.72646514	-1.89373194
O	0.75020606	2.31046634	-1.14548603
H	1.36517261	2.19813996	-1.89720530

H	1.17242652	2.99438721	-0.58905068
O	-1.04276603	-0.07503606	-2.48381443
H	-1.85992643	-0.50517365	-2.80138061
H	-0.30437880	-0.51930730	-2.95422378
O	-0.60148471	-2.42014264	-0.49867852
C	1.67259994	-1.56259723	2.34748467
C	3.00836374	-0.85370984	2.02116893
O	1.69042943	-2.43624208	3.23444425
O	3.35625497	-0.99557309	-2.96270643
C	3.62387504	-0.64974478	-0.61274829
C	4.09422759	-1.81740545	1.51635359
C	3.82387011	-2.03870676	0.02811046
H	4.59056369	-0.18908901	-0.85186011
H	2.91031393	-2.63965790	-0.10425861
H	4.64725455	-2.56697132	-0.47042175
H	4.05870608	-2.75403123	2.08902524
H	5.08382893	-1.36225669	1.66250349
H	3.32809435	-0.32385992	2.92864678

$Eu(TPA\ Bi)^{+} \bullet 7H_2O$

Eu	0.19765783	-0.05587680	0.20704031
O	-0.09087465	1.86054188	-1.41731037
H	-0.63630374	2.65535076	-1.25804315
H	-0.30356380	1.58910425	-2.33218996
O	-1.16570912	-1.78450361	1.53585754
H	-0.86224982	-2.70037424	1.37687526
H	-1.45665671	-1.76257265	2.46806114
O	2.67267138	0.17428250	-0.46792754
H	2.86207240	0.04571463	-1.41814709

H	3.29510207	-0.42622627	-0.01226162
O	-1.36264480	1.32565580	1.65232628
H	-2.32600446	1.21611691	1.52981239
H	-1.25242505	1.54347330	2.59803875
O	1.60981985	-0.65106286	2.21492941
H	1.36952780	-1.35103902	2.85225911
H	1.90477351	0.10350499	2.76225991
O	1.42828674	1.99144622	1.23117010
H	2.23518154	2.15056502	0.70019165
H	1.00328482	2.86731043	1.30990688
O	-2.20968651	-0.30098314	-0.58854214
H	-2.57358822	-1.10456850	-0.16262440
H	-2.34937249	-0.43958363	-1.54606993
H	0.46378278	-2.04793442	-4.60889207
H	1.01089395	-4.31475757	-5.87034773
C	1.02983126	-4.18494100	-4.78915878
O	1.63958483	-7.49860417	-3.31915142
C	1.70311254	-6.63218376	-4.24971277
C	1.34897770	-5.21876805	-3.91842840
O	0.69225129	-2.34667341	-0.48200820
C	0.84219589	-3.10196125	-2.73952987
C	0.61729481	-2.05733833	-1.73417566
O	0.35424042	-0.85799128	-2.10982953
O	2.05167476	-6.88721116	-5.44500902
C	0.73917356	-2.98152692	-4.12020102
S	1.28966770	-4.71014330	-2.26423211

$Eu(TPA\ OS)^{+} \bullet 7H_2O$

Eu	0.00000000	0.00000000	0.00000000

O	-1.89743013	0.00000000	-1.46884525
H	1.77886414	-1.74531659	2.34625028
H	2.01490634	-2.15415368	-1.73641942
H	-3.10904718	0.00000000	1.43150398
H	1.77886414	1.74531659	2.34625028
H	2.01490634	2.15415368	-1.73641942
H	3.33475946	0.00000000	0.77120514
S	-1.39000000	-2.40755062	0.00000000
H	-1.08897587	3.22192803	-0.38560257
C	-2.96531910	-0.86470587	-1.26239613
C	-2.77814789	-2.12612331	-0.56887910
C	-3.64558824	-3.10640386	-0.33016718
C	-2.95578481	-4.17558386	0.41375723
C	-1.67669769	-3.83806185	0.62366707
C	-0.67208562	-4.77277863	1.17225611
O	0.59985953	-4.80392983	0.66177793
O	-0.99189782	-5.57890311	2.03143305
O	-4.05378717	-0.59183345	-1.74275876
H	-3.40172289	-5.12648455	0.68832863
H	-4.68415260	-3.11814300	-0.64422046
O	-1.37200000	2.37637371	0.00000000
H	-2.24578358	2.55404479	0.38560257
O	2.74400000	0.00000000	0.00000000
H	3.33475946	0.00000000	-0.77120514
O	1.08490971	1.87911875	-1.67970820
H	0.62205643	2.41319983	-2.34625028
O	1.08490971	1.87911875	1.67970820
H	0.85809863	2.82203692	1.73641942

O	-2.16981943	0.00000000	1.67970820
H	-2.16487838	0.00000000	2.65116571
O	1.08490971	-1.87911875	-1.67970820
H	0.62205643	-2.41319983	-2.34625028
O	1.08490971	-1.87911875	1.67970820
H	0.85809863	-2.82203692	1.73641942

$Gd(TDA)^{+} \bullet 6H_2O$

Gd	0.00977911	-0.07970717	0.04492916
O	0.51139902	0.00781304	-2.38440688
O	-0.52773588	1.74617685	1.77775342
O	-1.23482469	1.83623500	-0.99086303
O	1.21084965	-0.25006590	1.98420137
O	-2.01167718	-0.52931324	1.41191128
O	-0.17609075	-2.36098213	0.19773402
S	2.67135365	-1.48486891	-0.37419780
O	1.73006072	1.68501823	-0.37835193
O	-1.81734050	-1.07248356	-1.49705492
H	-0.06328482	-0.57824313	-2.91740575
H	-0.40389304	2.69994822	1.60602641
H	-1.38506066	1.82686749	-1.95628002
H	-2.04107716	2.24044246	-0.61513462
H	-2.08607815	0.02231149	2.21627896
H	-1.82437306	-1.99920795	-1.17505937
H	-2.05371040	-1.45575593	1.72422796
H	1.40494314	2.50008789	-0.81101875
H	-2.74300333	-0.76965019	-1.41251184
H	0.15675219	1.51256244	2.44279506
H	2.25972478	2.00459799	0.37813045

H	1.40749946	-0.07415412	-2.76453848
C	2.28277688	-0.86337947	2.39188701
C	3.30008196	-1.28703170	1.32567136
C	0.61512362	-3.39172631	0.19717778
C	2.03660486	-3.19287471	-0.34171404
O	0.28235458	-4.53625060	0.55260810
O	2.56206345	-1.07670500	3.58410621
H	4.06049560	-0.49350459	1.26402800
H	2.03745857	-3.52167143	-1.39228356
H	2.74607373	-3.83182287	0.19855720
H	3.81514239	-2.20684764	1.62881206

$Gd(THTPA)^{+} \bullet 6H_2O$

Gd	0.02772700	-0.15248900	0.02208800
O	0.34436200	-0.33692800	-2.44312500
O	-0.92313900	1.56487200	1.59229200
O	-1.02268600	1.85444600	-1.38207800
O	1.26235800	0.09515900	1.94059500
O	-1.39353300	-1.29789600	1.80597900
O	0.02213000	-2.41856700	-0.24765500
S	2.77803800	-1.29364200	-0.23928200
O	1.57352000	1.68762900	-0.63699900
O	-2.31837400	-0.62822800	-0.70872200
H	0.10067700	-1.18051700	-2.87309700
H	-1.12133600	2.50206700	1.40261500
H	-1.07668900	1.68094100	-2.34288800
H	-1.69676300	2.53902200	-1.20751000
H	-1.30581000	-1.02031200	2.73906700
H	-2.81988200	-0.98841300	0.05146300

H	-1.16360300	-2.24909400	1.79807000
H	1.01244700	2.42943500	-0.94890600
H	-2.84061200	0.13848500	-1.01603300
H	-0.18632900	1.58210700	2.24381400
H	2.19121000	2.08022000	0.01039500
H	1.20209700	-0.09035700	-2.84257000
C	2.42106500	-0.29836300	2.38589200
C	3.16499700	-1.36574500	1.57214700
C	0.86421300	-3.38545500	-0.46160300
C	2.37509100	-3.08326100	-0.38710500
O	0.53259400	-4.55765100	-0.71450200
O	2.93563500	0.09864200	3.44592900
C	2.78545400	-2.79122200	2.02393400
C	3.04048600	-3.72748100	0.84299200
H	2.82977000	-3.44762000	-1.31764000
H	2.62988500	-4.73206600	1.01295000
H	4.11984200	-3.82484200	0.65928900
H	1.72102400	-2.81901600	2.30317800
H	3.37210000	-3.07287400	2.90828800
H	4.24356600	-1.19912300	1.67984900

$Gd(TPA\ Bi)^{+} \bullet 7H_2O$

Gd	-0.16062253	0.57747959	-0.19928879
S	3.53138191	-1.38060367	-3.48887880
O	-0.84081631	2.55669794	1.18211662
O	0.28841742	2.74711311	-1.34173909
O	-0.25392832	-0.25428485	2.11358368
C	4.91898162	-3.00250704	-2.03010946
O	-1.13423672	-1.69546427	-0.52633035

O	1.25285097	-0.06841556	-1.99328152
O	1.89998178	1.58578965	0.75348680
O	-2.54434567	0.53851217	0.43467372
H	-3.01729531	1.33254289	0.74900924
H	-0.66537454	3.45819048	0.84796387
H	5.68654467	-3.71576443	-1.73159818
H	0.40089368	-0.92665314	2.38918804
H	3.78348469	-2.77672166	-0.13451970
H	-0.47638837	-2.39548881	-0.33934882
H	-0.88502757	2.63145802	2.15477875
H	2.56115952	0.91671252	1.02306154
H	-3.21974277	-0.14928261	0.28184211
H	-1.11509030	-0.59217621	2.43150686
H	1.83598797	2.20462153	1.50728591
H	-1.49000186	-1.92237284	-1.40837034
C	5.74688931	-2.76559082	-4.49676771
C	4.84943648	-2.48624113	-3.31597881
C	1.93491635	-0.88542386	-1.26336309
C	3.06934654	-1.60665063	-1.82932365
O	6.70492430	-3.57570322	-4.30349523
O	1.60709199	-1.04865952	-0.02508572
C	3.90858834	-2.50497113	-1.18240030
H	1.23421920	2.97593511	-1.44296234
H	-0.07602437	2.76848043	-2.24975508
O	5.46041751	-2.16240631	-5.58095339
O	-1.46135647	0.71641247	-2.29843773
H	-2.43313619	0.75787278	-2.38585697
H	-1.12873765	0.31703895	-3.12649833

$Gd(TPA\ OS)^{+} \bullet 7H_2O$

Gd	0.12918122	-0.04647594	-0.06752271
O	-1.49841889	-0.24150333	-1.70198676
H	2.05324902	-1.76352211	1.50799631
H	1.88169865	-2.14402102	-1.41857549
H	-2.57904370	-0.89168964	1.23407844
H	1.07173280	0.37344262	2.92662104
H	1.36308116	1.63988067	-2.50492106
H	2.74960629	1.44923728	0.71779964
S	-1.10964053	-2.87159707	-0.55854738
H	-0.68210381	2.75927712	-0.56462515
C	-2.63380213	-0.90400416	-1.74791240
C	-2.64105304	-2.13080200	-0.89723848
C	-3.63433695	-2.66491029	-0.10006448
C	-3.13770109	-3.63238943	0.82192519
C	-1.77399752	-3.82122165	0.73253159
C	-0.83818501	-4.61395588	1.59757273
O	0.39725355	-4.22989191	1.58692824
O	-1.30184738	-5.56256435	2.27359272
O	-3.63551786	-0.55259726	-2.39039362
H	-3.75238916	-4.14141755	1.56341402
H	-4.67036162	-2.32910422	-0.13812292
O	-0.73283576	2.24432826	0.26649489
H	-1.65709658	2.33471421	0.57366946
O	2.44524386	0.71202042	0.15436871
H	3.09989487	0.63684370	-0.56697221
O	0.52627704	1.46823803	-2.03130593
H	-0.13115150	1.22466914	-2.71672044

O	0.49957650	0.81259483	2.26845090
H	0.49308270	1.76042340	2.50458286
O	-1.86096761	-0.23551187	1.36255822
H	-1.68491573	-0.20105364	2.32413042
O	1.55810681	-1.25905016	-1.68067379
H	1.29173909	-1.35610154	-2.61645549
O	1.12031558	-1.80641953	1.22403139
H	0.80664165	-2.80361086	1.35407232

APPENDIX C

COPYRIGHT PERMISSIONS

Copyright Clearance Center | RightsLink®

Home | Help | Email Support | Sign in | Create Account

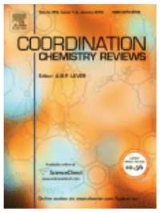

Sulfur donating extractants for the separation of trivalent actinides and lanthanides

Author: N.P. Bessen,J.A. Jackson,M.P. Jensen,J.C. Shafer

Publication: Coordination Chemistry Reviews

Publisher: Elsevier

Date: 15 October 2020

Please note that, as the author of this Elsevier article, you retain the right to include it in a thesis or dissertation, provided it is not published commercially. Permission is not required, but please ensure that you reference the journal as the original source. For more information on this and on your other retained rights, please visit: https://www.elsevier.com/about/our-business/policies/copyright#Author-rights

BACK | CLOSE WINDOW

ELSEVIER

About Elsevier | Products & Solutions | Services

Journal author rights | Government employees | Elsevier's rights | Protecting author rights | Open access

Journal author rights

In order for Elsevier to publish and disseminate research articles, we need publishing rights. This is determined by a publishing agreement between the author and Elsevier. This agreement deals with the transfer or license of the copyright to Elsevier and authors retain significant rights to use and share their own published articles. Elsevier supports the need for authors to share, disseminate and maximize the impact of their research and these rights, in Elsevier proprietary journals* are defined below:

For subscription articles	For open access articles
Authors transfer copyright to the publisher as part of a journal publishing agreement, but have the right to: • Share their article for Personal Use, Internal Institutional Use and Scholarly Sharing purposes, with a DOI link to the version of record on ScienceDirect (and with the Creative Commons CC-BY-NC- ND license for author manuscript versions) • Retain patent, trademark and other intellectual property rights (including research data). • Proper attribution and credit for the published work.	Authors sign an exclusive license agreement, where authors have copyright but license exclusive rights in their article to the publisher**. In this case authors have the right to: • Share their article in the same ways permitted to third parties under the relevant user license (together with Personal Use rights) so long as it contains a CrossMark logo, the end user license, and a DOI link to the version of record on ScienceDirect. • Retain patent, trademark and other intellectual property rights (including research data). • Proper attribution and credit for the published work.

Copyright Permission

Inbox ×

Nathan Bessen <nbessen@mymail.mines.edu> Fri, Oct 16, 7:14 PM (16 hours ago)
to Jessica

Hello Jess,
In order to include the review article we wrote within my dissertation, I must request permission from all co-authors not on my committee to do so. I would appreciate it if you could reply to this email granting permission to include the following review article as a chapter of my dissertation.

> Bessen, N. P.; Jackson, J. A.; Jensen, M. P.; Shafer, J. C. Sulfur Donating Extractants for the Separation of Trivalent Actinides and Lanthanides. *Coord. Chem. Rev.* **2020**, *421*, 213446. https://doi.org/10.1016/j.ccr.2020.213446.

Thank you,
Nathan Bessen

Jessica Jackson <jagjackson@mines.edu> Fri, Oct 16, 8:31 PM (15 hours ago)
to me

Hi Nathan,

You have my permission to include that article in your dissertation.

Best,
Jess

Sent from my iPhone

About Elsevier | Products & Solutions | Services

Journal author rights | Government employees | Elsevier's rights | Protecting author rights | Open access

Journal author rights

In order for Elsevier to publish and disseminate research articles, we need publishing rights. This is determined by a publishing agreement between the author and Elsevier. This agreement deals with the transfer or license of the copyright to Elsevier and authors retain significant rights to use and share their own published articles. Elsevier supports the need for authors to share, disseminate and maximize the impact of their research and these rights, in Elsevier proprietary journals* are defined below:

For subscription articles	For open access articles
Authors transfer copyright to the publisher as part of a journal publishing agreement, but have the right to: • Share their article for Personal Use, Internal Institutional Use and Scholarly Sharing purposes, with a DOI link to the version of record on ScienceDirect (and with the Creative Commons CC-BY-NC- ND license for author manuscript versions) • Retain patent, trademark and other intellectual property rights (including research data). • Proper attribution and credit for the published work.	Authors sign an exclusive license agreement, where authors have copyright but license exclusive rights in their article to the publisher**. In this case authors have the right to: • Share their article in the same ways permitted to third parties under the relevant user license (together with Personal Use rights) so long as it contains a CrossMark logo, the end user license, and a DOI link to the version of record on ScienceDirect. • Retain patent, trademark and other intellectual property rights (including research data). • Proper attribution and credit for the published work.

Copyright Permission

Inbox ×

Nathan Bessen <nbessen@mymail.mines.edu> Fri, Oct 16, 7:11 PM (16 hours ago)
to Erin

Hello Erin,
In order to include the manuscript we submitted within my dissertation, I must request permission from all co-authors not on my committee to do so. I would appreciate it if you could reply to this email granting permission to include the following manuscript as a chapter of my dissertation.

Permanganometric Quantification of Cyanex 301 in *n*-dodecane

Thank you,
Nathan Bessen

Bertelsen, Erin R Fri, Oct 16, 7:19 PM (16 hours ago)
to me

Hi Nathan,

I am pleased to grant you permission to use the manuscript in your dissertation.

Best regards,
Erin R. Bertelsen

Copyright Permission Inbox ×

Nathan Bessen <nbessen@mymail.mines.edu> 11:27 AM (6 hours ago)
to Ning

Hello Ning,
In order to include the Cyanex 301 manuscript we are writing within my dissertation, I must request permission from all co-authors not on my committee to do so. I would appreciate it if you could reply to this email granting permission to include the following manuscript as a chapter of my dissertation.

Extraction of the Trivalent Transplutonium Actinides Americium Through Einsteinium by Purified Cyanex 301

Thank you,
Nathan Bessen

jspuning@126.com 5:41 PM (1 minute ago)
to me

Hello Nathan!
Of course you can include this into your dissertation.
Hopefully you can finish your dissertation successfully!
Best wishes
Ning

Copyright Permission Inbox ×

Nathan Bessen <nbessen@mymail.mines.edu> Sat, Oct 17, 11:27 AM (22 hours ago)
to Chao

Hello Chao,
In order to include the Cyanex 301 manuscript we are writing within my dissertation, I must request permission from all co-authors not on my committee to do so. I would appreciate it if you could reply to this email granting permission to include the following manuscript as a chapter of my dissertation.

Extraction of the Trivalent Transplutonium Actinides Americium Through Einsteinium by Purified Cyanex 301

Thank you,
Nathan Bessen

Chao Xu 10:20 AM (7 minutes ago)
to me

Hi Nathan,

I have fully understood the information of the manuscript entitled "Extraction of the Trivalent Transplutonium Actinides Americium Through Einsteinium by Purified Cyanex 301" we coauthored and it is my pleasure to grant you the permission to include this manuscript as a chapter of your dissertation.

Best regards,

Chao

Copyright Permission Inbox ×

Nathan Bessen <nbessen@mymail.mines.edu> Sat, Oct 17, 11:31 AM (1 day ago)
to Ivan

Hello Ivan,
In order to include the aqueous sulfur donor manuscript we are writing within my dissertation, I must request permission from all co-authors not on my committee to do so. I would appreciate it if you could reply to this email granting permission to include the following manuscript as a chapter of my dissertation.

Lanthanide & Actinide Complexes with Aqueous Sulfur Donating Ligands

Thank you,
Nathan Bessen

Popov, Ivan Aleksandrovich 6:08 PM (22 minutes ago)
to me

Hi Nathan,

sure, I give you permission for that. Good luck with the Ph.D. defense!

Sincerely, Ivan

Copyright Permission

Inbox ×

Nathan Bessen <nbessen@mymail.mines.edu> Sat, Oct 17, 11:32 AM (2 days ago)
to Colt

Hello Colt,
In order to include the aqueous sulfur donor manuscript we are writing within my dissertation, I must request permission from all co-authors not on my committee to do so. I would appreciate it if you could reply to this email granting permission to include the following manuscript as a chapter of my dissertation.

Lanthanide & Actinide Complexes with Aqueous Sulfur Donating Ligands

Thank you,
Nathan Bessen

Colt R. Heathman 7:25 AM (1 hour ago)
to me

Nathan,

I give my permission to include the soft donor manuscript in your dissertation as a chapter.

Colt

Copyright Permission

Inbox ×

Nathan Bessen <nbessen@mymail.mines.edu> Sat, Oct 17, 11:32 AM (2 days ago)
to Travis

Hello Travis,
In order to include the aqueous sulfur donor manuscript we are writing within my dissertation, I must request permission from all co-authors not on my committee to do so. I would appreciate it if you could reply to this email granting permission to include the following manuscript as a chapter of my dissertation.

Lanthanide & Actinide Complexes with Aqueous Sulfur Donating Ligands

Thank you,
Nathan Bessen

Travis S. Grimes 6:30 AM (2 hours ago)
to me

To whom it may concern,

I hereby give Nathan Bessen permission to reproduce any material in Lanthanide & Actinide Complexes with Aqueous Sulfur Donating Ligands co-authored by myself as part of his dissertation.

Best Regards,

Travis S. Grimes, PhD

Copyright Permission

Inbox ×

Nathan Bessen <nbessen@mymail.mines.edu> Sat, Oct 17, 11:33 AM (2 days ago)
to Peter

Hello Peter,
In order to include the aqueous sulfur donor manuscript we are writing within my dissertation, I must request permission from all co-authors not on my committee to do so. I would appreciate it if you could reply to this email granting permission to include the following manuscript as a chapter of my dissertation.

Lanthanide & Actinide Complexes with Aqueous Sulfur Donating Ligands

Thank you,
Nathan Bessen

Peter R. Zalupski 6:34 AM (2 hours ago)
to me

Hi Nathan,

You have my permission.

Thank you,
Peter

Copyright Permission Inbox ×

Nathan Bessen <nbessen@mymail.mines.edu> 11:34 AM (10 hours ago)
to Liane

Hello Liane,
In order to include the aqueous sulfur donor manuscript we are writing within my dissertation, I must request permission from all co-authors not on my committee to do so. I would appreciate it if you could reply to this email granting permission to include the following manuscript as a chapter of my dissertation.

Lanthanide & Actinide Complexes with Aqueous Sulfur Donating Ligands

Thank you,
Nathan Bessen

Moreau, Liane Michelle via emailwsu.onmicrosoft.com 10:31 PM (1 minute ago)
to me

Dear Nathan,

You have my permission to include the manuscript "Lanthanide & Actinide Complexes with Aqueous Sulfur Donating Ligands" on which I am a co-author as a chapter of your dissertation.

Good luck,

Liane

Copyright Permission Inbox ×

Nathan Bessen <nbessen@mymail.mines.edu> 11:35 AM (24 minutes ago)
to Kurt

Hello Kurt,
In order to include the aqueous sulfur donor manuscript we are writing within my dissertation, I must request permission from all co-authors not on my committee to do so. I would appreciate it if you could reply to this email granting permission to include the following manuscript as a chapter of my dissertation.

Lanthanide & Actinide Complexes with Aqueous Sulfur Donating Ligands

Thank you,
Nathan Bessen

Kurt Smith 11:53 AM (6 minutes ago)
to me

Hey Nathan,

Hope all is well.

Of course, I am happy for you to do so.

Best wishes,

Kurt

Copyright Permission Inbox ×

Nathan Bessen <nbessen@mymail.mines.edu> 11:35 AM (1 hour ago)
to Corwin

Hello Corwin,
In order to include the aqueous sulfur donor manuscript we are writing within my dissertation, I must request permission from all co-authors not on my committee to do so. I would appreciate it if you could reply to this email granting permission to include the following manuscript as a chapter of my dissertation.

Lanthanide & Actinide Complexes with Aqueous Sulfur Donating Ligands

Thank you,
Nathan Bessen

Corwin Booth 12:47 PM (7 minutes ago)
to me

Permission granted,

Corwin

Copyright Permission

Inbox ×

Nathan Bessen <nbessen@mymail.mines.edu> 11:36 AM (8 hours ago)
to Rebecca

Hello Rebecca,
In order to include the aqueous sulfur donor manuscript we are writing within my dissertation, I must request permission from all co-authors not on my committee to do so. I would appreciate it if you could reply to this email granting permission to include the following manuscript as a chapter of my dissertation.

Lanthanide & Actinide Complexes with Aqueous Sulfur Donating Ligands

Thank you,
Nathan Bessen

Rebecca Abergel 7:54 PM (2 minutes ago)
to me

Hi Nathan,

Yes, absolutely! Please take this email as confirmation of my "permission" to include the manuscript in your dissertation.

Best,

Rebecca

Copyright Permission

Inbox ×

Nathan Bessen <nbessen@mymail.mines.edu> Sat, Oct 17, 11:36 AM (2 days ago)
to Enrique

Hello Enrique,
In order to include the aqueous sulfur donor manuscript we are writing within my dissertation, I must request permission from all co-authors not on my committee to do so. I would appreciate it if you could reply to this email granting permission to include the following manuscript as a chapter of my dissertation.

Lanthanide & Actinide Complexes with Aqueous Sulfur Donating Ligands

Thank you,
Nathan Bessen

Batista, Enrique Ricardo 10:00 AM (36 minutes ago)
to me

Hi Nathan,
You have my permission. Thanks for checking.
Best,
Enrique

Copyright Permission

Inbox ×

Nathan Bessen <nbessen@mymail.mines.edu> Sat, Oct 17, 11:37 AM (2 days ago)
to Ping

Hello Ping,
In order to include the aqueous sulfur donor manuscript we are writing within my dissertation, I must request permission from all co-authors not on my committee to do so. I would appreciate it if you could reply to this email granting permission to include the following manuscript as a chapter of my dissertation.

Lanthanide & Actinide Complexes with Aqueous Sulfur Donating Ligands

Thank you,
Nathan Bessen

Yang, Ping 8:13 AM (1 hour ago)
to me

Hi Nathan,

Sure, please go ahead to use it for your thesis. Best luck in your defense!

Ping